Pharmacological Therapies for Rhodopsin Retinitis Pigmentosa

Hugo Filipe Chaves Pereira Mendes

A thesis submitted to the University of London for the degree of Doctor of Philosophy

August 2007

UCL, Institute of Ophthalmology

ProQuest LLC
789 East Eisenhower Parkway
P.O. Box 1346
Ann Arbor, MI 48106-1346

Abstract

Mutations in the visual pigment protein rod opsin are the most common cause of autosomal dominant retinitis pigmentosa (ADRP) and the majority of these mutations lead to the misfolding of the protein. Patients with ADRP experience progressive loss of vision leading to blindness and at the moment no effective therapy is available. In this study I have developed a cellular model that can mimic the gain-of function and dominant-negative disease mechanisms in rhodopsin ADRP patients. Whereas wild-type rod opsin translocated to the plasma membrane of the cells, P23H mutant rod opsin misfolded was retained in the ER and accumulated in intracellular inclusions. Several pharmacological compounds were tested in this model. The retinoids 9-*cis*-retinal and 11-*cis*-retinal reduced inclusion incidence, alleviated cell death and promoted the translocation of the mutant protein to the plasma membrane in cells expressing P23H rod opsin. In cells co-expressing wild-type and P23H rod opsin these compounds restored the normal processing of the wild-type protein, indicating an alleviation of the dominant-negative mechanism of cell death. Chemical chaperones reduced inclusion incidence and cell death but, unlike retinoids, did not to promote the translocation of the mutant protein and did not alleviate the dominant-negative interaction between wild-type and P23H rod opsin. Heat shock protein inducers were also used. Some of these drugs reduced inclusion incidence and cell death in P23H cells. In addition, one partially promoted the translocation of the mutant protein and partially suppressed the dominant-negative mechanism of cell death induced by the mutant protein. Treatment with other compounds such as autophagy inducers also reduced inclusion incidence and cell death in cells expressing P23H rod opsin. These data have identified a range of compounds that demonstrate the 'proof of principle' that some of the gain of function and dominant-negative properties of mutant misfolded rod opsin can be manipulated. The efficacy of these compounds must be established in animal models prior to translation into the clinic.

Statement of Originality

I certify that this thesis, and the research to which is referred are the product of my own work, and that any idea or quotations from the work of other people, published or otherwise, are fully acknowledged in accordance with the standard referencing practices of the discipline.

Acknowledgements

I would like to thank Professor Michael Cheetham for his support and guidance which were crucial in the completion of this project. I would also like to thank Dr Paul Chapple and Dr Jacqueline van der Spuy for their initial warm welcome and for putting up with all my questions for the duration of this project. It must have been hard work! I am grateful to Professor Robert Molday (UBC), Dr Linda Greensmith (UCL, Institute of Neurology) and Professor Paula Booth (University of Bristol) for supplying vital reagents which vastly enhanced the depth of this study.

I would like to thank the British Retinitis Pigmentosa Society (BRPS) for funding this project.

I would like to express my gratitude to my parents and paternal grandparents for their unwavering support throughout this project. Finally I would like to thank everyone who made my life so colourful over the last three and a half years. You know who you are!

Table of contents

List of Figures

Figure 7.3.2 Treatment of cells expressing P23H rod opsin with DMSO and TMAO enhances the decrease in inclusion incidence observed when these compounds are used alone.

List of Tables

Abbreviations

17-AAG	17-Allylamino-17-demethoxygeldanamycin
1-DNJ	1-deoxynojirimycin
4-PBA	4-phenylbutyric acid
5-GMP	5'-guanosine monophosphate
Aβ	β-amyloid peptide
ADRP	Autosomal dominant retinitis pigmentosa
ALS	Amyotrophic lateral sclerosis
AR	Androgen receptor
ARF4	Adenosine diphosphate-ribosylation factor 4
CA	Carbonic anhydrase
CFP	Cyan fluorescent protein
CFTR	Cystic fibrosis transmembrane conductance regulator
cGMP	Cyclic guanosine monophosphate
CHIP	Carboxy terminus of Hsp70-interacting protein
CSNB	Congenital stationary night blindness
DAPI	4',6-Diamidino-2-phenylindole dihydrochloride
DGJ	1-deoxygalactonorijimycin
DMEM	Dulbecco's Modified Eagle Medium
DMSO	Dimethyl sulphoxide
DNA	Deoxyribonucleic acid
dNTPs	Deoxynucleotide triphosphates
DTT	Dithiothreitol
EDTA	Ethylenediamine tetraacetic acid
EGTA	Ethylene glycol tetraacetic acid
eIF2α	Eukaryotic translation initiation factor 2 subunit α
EndoH	Endoglycosidase H
ER	Endoplasmic reticulum
ERG	Electroretinogram
FBS	Foetal bovine serum

FRET	Fluorescence resonance energy transfer
GCL	Ganglion cell layer
GDP	Guanosine diphosphate
GFP	Green fluorescent protein
GnRHR	Gonadotropin-releasing hormone receptor
GPCR	G protein-coupled receptor
GTP	Guanosine triphosphate
HEPES	4-(2-hydroxyethyl)-1-piperazineethanesulfonic acid
HRP	Horseradish peroxidase
HSF	Heat shock factor
HSF1	Heat shock factor 1
HSP	Heat shock protein
ILM	Inner limiting membrane
INL	Inner nuclear layer
IPL	Inner plexiform layer
LB	Luria-Bertani broth
LDH	Lactate dehydrogenase
MJD	Machado-Joseph disease
mTOR	Mammalian target of rapamycin
NB-DNJ	N-butyldeoxynojirimycin
NDI	Nephrogenic diabetes insipidus
NPD	Nasal potential difference
OLM	Outer limiting membrane
ONL	Outer nuclear layer
OPL	Outer plexiform layer
OPMD	Oculopharyngeal muscular dystrophy
PaeI-R	Parkin-associated endothelin receptor-like receptor
PBS	Phosphate buffer saline
PCR	Polymerase chain reaction
PDE	Phosphodiesterase
PM	Plasma membrane

PNGaseF	Peptide N-glycosidase F
PPA	Protein phosphatase A
PrP	Prion protein
PrP^{C}	Cellular prion protein
PrP^{Sc}	Prion protein pathogenic isoform
R^{*}	Metarhodopsin II
RIPA	Radio immunoprecipitation assay buffer
RIS	Rod inner segment
RPE	Retinal pigment epithelium
ROS	Rod outer segment
RP	Retinitis Pigmentosa
RP17	Retinitis pigmentosa 17
SBMA	Spinal and bulbar muscular atrophy
SCA3	Spinocerebellar ataxia type 3
SCA7	Spinocerebellar ataxia type 7
SDS	Sodium dodecyl sulfate
SDS-PAGE	Sodium dodecyl sulfate polyacrylamide gel electrophoresis
TAE	Tris-acetate
TMAO	Trimethylamine N-oxide
UPR	Unfolded protein response
UPS	Ubiquitin proteasome system
UV	Ultraviolet
V_2R	Vasopressin receptor
WT	Wild-type
YFP	Yellow fluorescent protein

Chapter 1: Introduction

1.1 Structure of the vertebrate retina

The wall of the eye in higher vertebrates is coated by three different layers (Figure 1.1). The external layer is robust and confers protection to the inner structures. It is opaque in the larger, posterior portion (sclera) and transparent in the smaller, anterior section (cornea), which provides the eye with most of its optical power. Together with the lens, the cornea refracts light, and as a result helps the eye to focus. The intermediate layer, also named choroid, is a vascular layer responsible for providing nutrients to the ocular tissues. Its anterior segment, the ciliary body, is responsible for the process of accommodation carried out by the lens. The retina is localised in the innermost layer and is responsible for converting light to visual signals and conveying them to the brain.

The adult retina consists of alternate layers of cell bodies and synaptic processes which are formed by six major neuronal cell types (Figure 1.2) (reviewed in detail by Bloomfield and Dacheux, 2001). The three layers of neurons present are the outer nuclear layer (ONL), inner nuclear layer (INL) and the ganglion cell layer (GCL). The ONL contains the cell bodies of photoreceptors. Vertebrate retinal photoreceptors are divided into two basic categories: rods and cones. Rods are more light-sensitive and used for vision at low light levels (scotopic vision, night vision). Cones need higher light levels and are used for daylight (photopic) vision. Furthermore, cones also provide colour vision. At intermediate (mesopic) light levels both rods and cones contribute to vision. The different sensitivity of rods and cones originates in their different morphological and biochemical properties such as different amounts of visual pigment and different amplification factors of the phototransduction cascade (see Figure 1.3). The sensitivity of rod vision is further increased by a high convergence of the rods onto their postsynaptic neurons, the rod bipolar cells, which improves the signal-to-noise ratio. As a consequence of these distinct functional properties rod/cone ratios vary considerably across

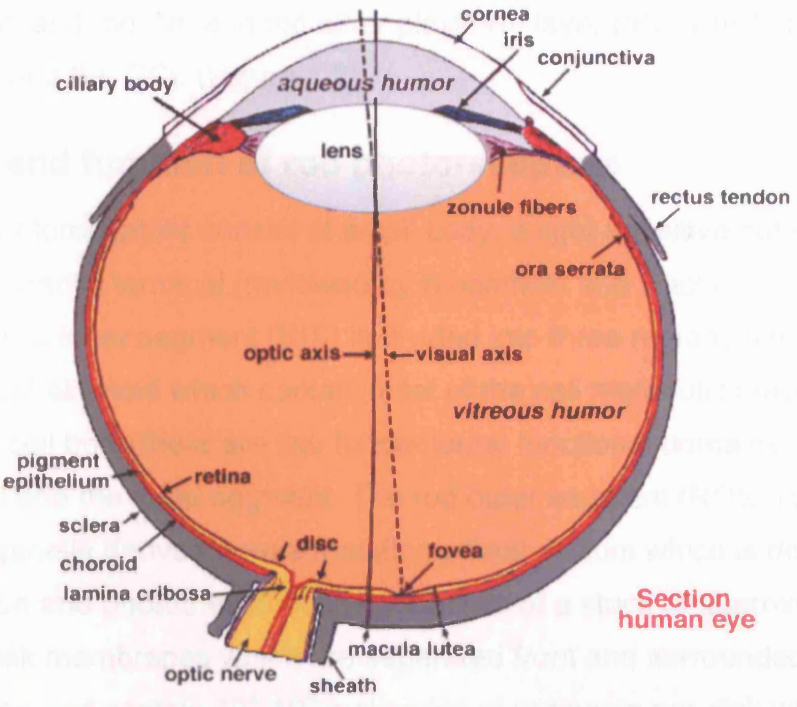

Figure 1.1 Cross section of the human eye.
The retina is the innermost layer of the eye and is responsible for conveying visual signals to the brain. Adapted from Webvision (http://webvision.med.utah.edu/).

mammals roughly correlating with the daily activity pattern (Ahnelt and Kolb, 2000). The INL contains the cell bodies of horizontal cells, bipolar cells and amacrine cells. The GCL contains displaced amacrine cells and ganglion cells which form the output from the retina to the brain via the optic nerve. These layers of cell bodies are separated by synaptic layers which contain most of the fine dendrites and synapses of the retina. These layers are the outer plexiform layer (OPL) which connects the ONL and the INL and the inner plexiform layer (IPL) which lies between the INL and the GCL (Figure 1.2).

1.2 Structure and function of rod photoreceptors

Vertebrate rod photoreceptors consist of a cell body, a light-sensitive outer segment and a synaptic terminal (reviewed by Bloomfield and Dacheux, 2001). The cell body or rod inner segment (RIS) is divided into three regions namely nuclear, myoid and ellipsoid which contain most of the cell metabolic machinery. At either end of the cell body there are two fundamental functional domains, the synaptic terminal and the outer segment. The rod outer segment (ROS) is a membranous organelle derived from a modified primary cilium which is designed for light absorption and phototransduction. It consists of a stack of approximately 1000 flattened disk membranes which are separated from and surrounded by plasma membrane and contain 10^4-10^6 molecules of rod opsin per disk which account for over 80% of the intrinsic membrane protein (Nir and Papermaster, 1983; Hicks and Molday, 1986) . The plasma membrane of the outer segment is connected to the cell body via connecting cilium. Distally, the outer segments of rod photoreceptors are associated with apical processes of the retinal pigment epithelium (RPE). The RPE connects photoreceptors and the choriocapillaris, constitutes one aspect of the blood-retinal barrier and is necessary for photoreceptor development and function. In addition the RPE is responsible for the homeostasis of the photoreceptor environment, recycling and metabolism of vitamin A as part of the visual phototransduction cascade and shedding of photoreceptor disks as part of outer segment turnover (Thompson and Gal, 2003).

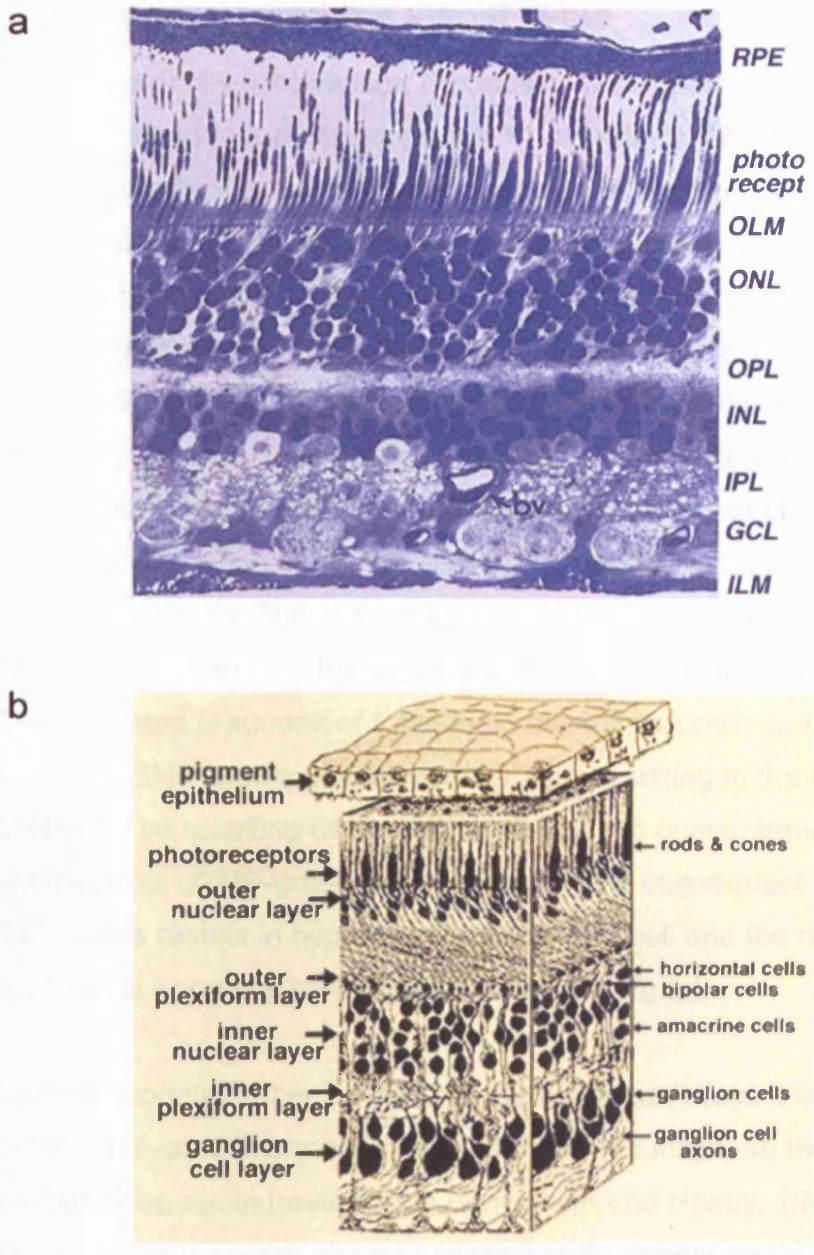

Figure 1.2 Structural organisation of the retina in higher vertebrates.
a) Cross section of the human retina. The structure of the retina is based upon alternate layers of cell bodies and synaptic processes which are formed by six major neuronal cell types. RPE: Retinal pigment epithelium; OLM: Outer limiting membrane; ONL: Outer nuclear layer; OPL: Outer plexiform layer; INL: Inner nuclear layer; IPL: Inner plexiform layer; GCL: Ganglion cell layer; ILM: Inner limiting membrane b) Schematic diagram illustrating the cell types and organisational layers present in the retina of higher vertebrates. Adapted from Webvision (http://webvision.med.utah.edu/).

1.3 Phototransduction and the visual cycle

The rod photoreceptor cell light sensor, rhodopsin, is composed of the rod opsin protein covalently linked to the chromophore, 11-*cis*-retinal. Phototransduction begins when 11-*cis*-retinal is isomerised by a captured photon (Figure 1.3) (reviewed in Park *et al.*, 2006). Upon photoisomerisation from 11-*cis*-retinal to all-*trans*-retinal, rhodopsin undergoes a series of conformational changes resulting in the conversion of rhodopsin to metarhodopsin II (R*). R*, the active form of rhodopsin, interacts with and binds to the photoreceptor-specific heterotrimeric G protein transducin. Transducin activation involves the interaction between R* with the guanosine diphosphate (GDP)-bound form of the transducin αβγ trimer which results in the rapid exchange of bound GDP for guanosine triphosphate (GTP) on the α-subunit of transducin. This is followed by the dissociation of transducin from R* as well as the dissociation of the active α-subunit of transducin from its β and γ subunits. The activated α-subunit of transducin disinhibits cyclic guanosine monophosphate (cGMP) phosphodiesterase (PDE), resulting in the hydrolysis of cGMP to 5'-GMP. The resulting decrease in cytoplasmic concentration of cGMP triggers the closure of cGMP-gated Ca^{2+} channels. The consequent reduction in cytosolic Ca^{2+} levels results in hyperpolarisation of the cell and the modified membrane potential becomes transmitted as a neural signal.

As in all G protein-coupled receptor (GPCR) signalling pathways it is necessary to inactivate all the activated intermediaries of phototransduction, so the pathway can be ready for signalling again (reviewed in Bunemann and Hosey, 1999). A rapid deactivation occurs through the phosphorylation of rhodopsin on multiple serine and threonine residues at the C-terminus region by rhodopsin kinase (Shichi and Somers, 1978). The phosphorylated rhodopsin is then bound by another protein, arrestin, inhibiting the interaction between rhodopsin and transducin and therefore preventing continuous signal transmission (Zuckerman and Cheasty, 1986). Following the binding of arrestin, all-*trans*-retinal is hydrolysed and released allowing a new molecule of the chromophore, 11-*cis*-retinal, to bind.

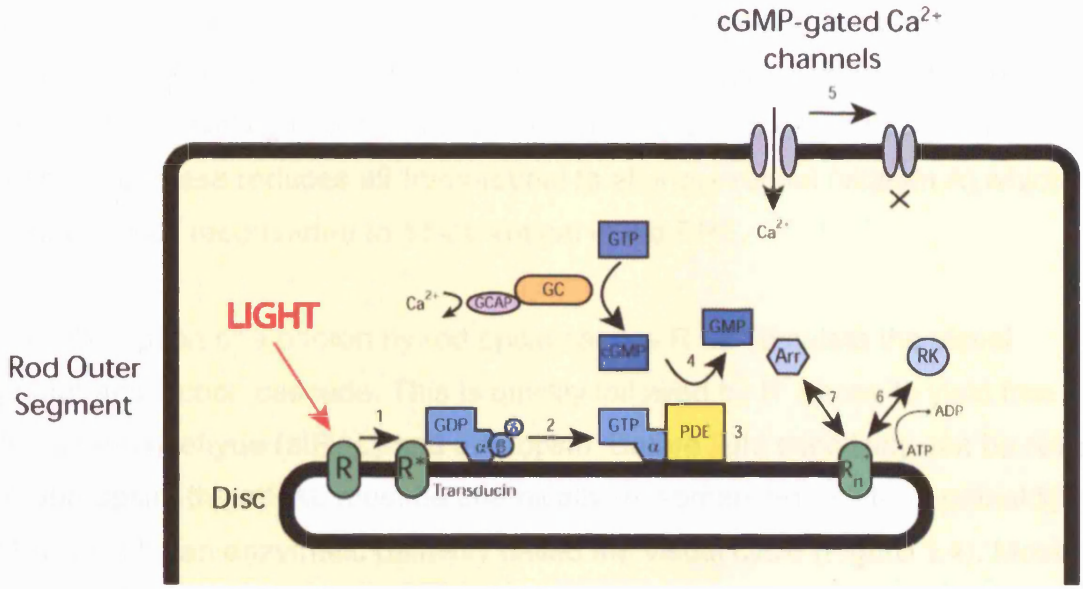

Figure 1.3 Vertebrate phototransduction.
Schematic diagram representing vertebrate phototransduction in the rod opsin segments (ROS) of rod photoreceptors including the mechanisms of activation and inactivation of rhodopsin. When light strikes the retina it activates rhodopsin (R) by causing the isomerization of covalently attached 11-*cis*-retinal at Lys296 to all-trans-retinal (1). Activated rhodopsin (R*) interacts with and activates transducin (2). The activation of transducin involves the exchange of guanosine diphosphate (GDP) for guanosine triphosphate (GTP),which results in the dissociation of the transducin α-subunit GTP from the transducin (βγ-subunit) complex and rhodopsin. The activated transducin (α)-GTP in turn activates cyclic guanosine monophosphate (cGMP) phosphodiesterase (PDE) (3), resulting in the hydrolysis of cGMP to 5'-GMP (4). The decrease in cGMP levels closes the cGMP-gated calcium channels (5) in the plasma membrane of photoreceptors leading to a decrease in calcium influx and the consequent hyperpolarization of the cell. The decrease in intracellular calcium concentration also disinhibits guanylate-cyclase-activating protein (GCAP) which leads to the activation of guanylate cyclase and consequent resynthesis of cGMP, ensuing the continuity of the cycle. The desensitisation of rhodopsin (R*/Rn*) is mediated by the phosphorylation of rhodopsin kinase (RK) (6), which induces the uncoupling of G-protein trimeric complexes and the consequent binding of arrestin (Arr) (7). Adapted from Mendes *et al* (2005).

This results in the completion of the cycle by the release of arrestin and the dephosphorylation of rhodopsin by protein phosphatase A (PPA) (Palczewski *et al.*, 1989). The recycling of the chromophore also occurs at this stage as all-*trans*-retinal reductase reduces all-*trans*-retinal to all-*trans*-retinol (vitamin A) which is consequently reconverted to 11-*cis*-retinal in the RPE.

The absorption of a photon by rod opsin causes R^* to stimulate the visual phototransduction cascade. This is quickly followed by R^* decay to yield free all-*trans*-retinaldehyde (atRAL) and apo-opsin. Before light sensitivity can be restored to apo-opsin, the atRAL must be chemically re-isomerised to 11-*cis*-retinaldehyde (11cRAL) by an enzymatic pathway called the visual cycle (Figure 1.4). Most steps in this pathway take place within the RPE and a key step in this pathway involves the all-*trans* to 11-*cis* re-isomerisation of the retinoid. The isomerase has recently been identified as the Rpe65 (Jin *et al.*, 2005).

1.4 Rod opsin: the prototypical G-protein coupled receptor

1.4.1 Structure of rod opsin

The gene encoding human rod opsin was identified by Nathans and Hogness (1984) and had a length of approximately 7000 base pairs. The coding region of the human rhodopsin gene consisted of five exons which were interrupted by four introns located at positions analogous to those found in the previously characterised bovine rhodopsin gene (Nathans and Hogness, 1983). The amino acid sequence of human rhodopsin deduced from the nucleotide sequence of its gene was 348 residues long which had a molecular mass of ~40 kDa and was 93.4% homologous to that of bovine rod opsin (Nathans and Hogness, 1984). The rod opsin protein, as other GPCR's, is an integral membrane protein which comprises a cytoplasmic (intracellular) domain, an intradiscal (extracellular) domain and seven transmembrane helices whose crystal structure has recently been determined at a resolution of 2.8 Å (Palczewski *et al.*, 2000) (Figure 1.5). This crystal structure suggested that rod opsin had a compact intradiscal area, parts of

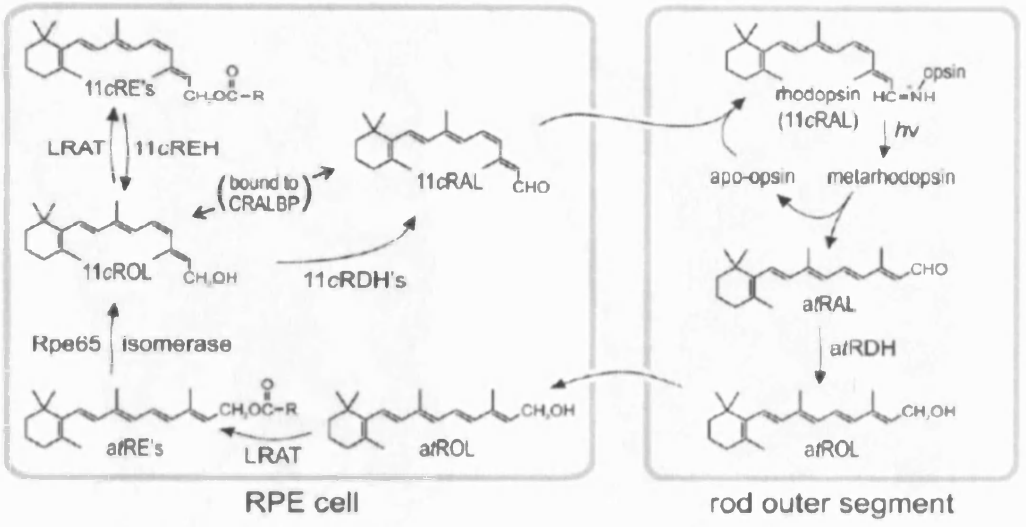

Figure 1.4 Visual cycle for regeneration of rhodopsin.
The light-sensitive protein in rods is rhodopsin, in the membranes of the outer segment. The 11-*cis*-retinaldehyde (11cRAL) chromophore is coupled to rhodopsin through a protonated Schiff-base linkage. Absorption of a photon (hv) induces 11-*cis* to all-*trans* isomerization of retinaldehyde to yield metarhodopsin, which activates the visual transduction cascade. The all-trans-retinaldehyde (atRAL) subsequently dissociates from apo-opsin and is reduced to all-trans-retinol (atROL) by all-*trans*-retinol dehydrogenase (atRDH). The atROL diffuses from the outer segment and is taken up by an RPE cell, where it is transferred to a fatty acid from phosphatidylcholine by lecithin-retinol acyl transferase (LRAT) to yield an all-*trans*-retinyl ester (atRE). The atRE is converted to 11-*cis*-retinol (11cROL) by the Rpe65. The 11cROL is oxidized by one of several 11cROL dehydrogenases (11cRDHs) to yield 11cRAL. 11cROL and 11cRAL are bound to CRALBP. The 11cRAL diffuses back to the outer segment where it combines with apo-opsin to form a new rhodopsin pigment molecule. Modified from Jin *et al* (2005).

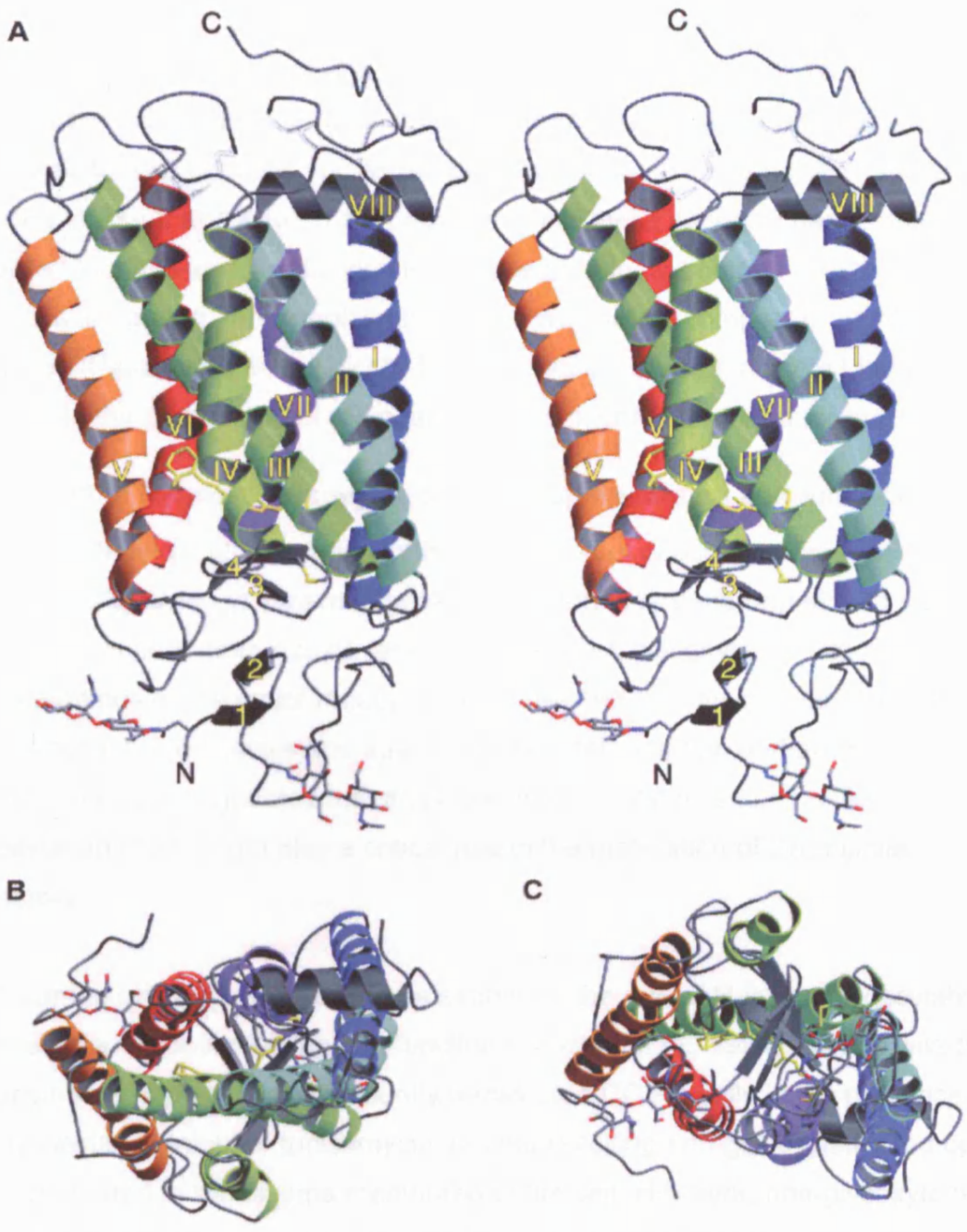

Figure 1.5 Ribbon drawings of the structure of rhodopsin obtained by diffraction data extending to 2.8 angstroms resolution.
A) Parallel to the plane of the membrane (stereoview). A view into the membrane plane is seen from the cytoplasmic (B) and intradiscal side (C) of the membrane. From Palczewski *et al.*, 2000.

which fold inwards to enclose the chromophore. This compact structure involves the second extracellular loop and Cys-187 which forms a disulfide bond with Cys-110 near the extracellular surface of transmembrane helix III. Furthermore, the intradiscal domain contains two asparagine-linked (N-linked) oligosaccharides attached to Asn-2 and Asn-15 although neither of these oligosaccharide chains appeared to make structural contacts with the protein. In contrast with the extracellular domain, the cytoplasmic domain was not as compact or highly organised (Palczewski *et al.*, 2000). These structural studies indicated higher plasticity in the C-terminus of rod opsin and this might be required for function.

1.4.2 Role of N-linked glycosylation in rod opsin folding and function

The role of N-linked glycosylation in the maturation of *Drosophila* rhodopsin was investigated by using *in vitro* mutagenesis and germline transformation to create a *Drosophila* mutant, delta Asn20, lacking the N-linked glycosylation site near the amino terminus of the major rhodopsin (O'Tousa, 1992). This mutation resulted in low rod opsin protein levels and age-dependent deterioration of rhabdomere organisation. This suggested that an N-linked glycosylation site, and likely glycosylation itself, might play a critical role in the maturation of *Drosophila* rhodopsin.

Work carried out in Khorana's lab has examined the role of N-linked glycosylation in vertebrate rod opsin folding and function (Kaushal *et al.*, 1994). Bovine wild-type rod opsin was expressed in transiently transfected COS-1 cells in the presence of the glycosylation inhibitor tunicamycin and the resulting non-glycosylated rod opsin was transported to the plasma membrane of the cell. However, non-glycosylated rhodopsin showed severe reduction of light-dependent activation of transducin when compared to the glycosylated rhodopsin (Kaushal *et al.*, 1994). Furthermore, these authors investigated the role of N-linked glycosylation on rod opsin folding further by introducing amino acid replacements in the region of the two glycosylated sites. Mutations at or near Asn-2 had little effect on cell surface expression, binding to the chromophore or transducin activation (Kaushal *et al.*,

1994). In contrast, mutations at Asn-15 or Lys 16 resulted in rod opsin which was defective in cellular transport and formed little or no chromophore with 11-*cis*-retinal (Kaushal *et al.*, 1994). These data combined suggested that glycosylation of rod opsin was not required for its folding to an apparently correct ground-state structure, but it appeared necessary for full activity in signal transduction.

1.4.3 Role of the intradiscal and cytoplasmic domains on rhodopsin structure and function

The role of the intradiscal domain in rod opsin structure and function was investigated by carrying out deletions in all the intradiscal loops and in the N-terminal tail of rod opsin (Doi *et al.*, 1990). Most of the deletions in the intradiscal loops and the N-terminus were defective proteins which failed to bind the chromophore and showed mannose-rich oligosaccharides characteristic of glycosylation in the ER (Doi *et al.*, 1990). These defective rod opsin structures resulted from relatively short deletions in the intradiscal loops B-C, D-E, F-G (see Figure 1.7 for the secondary structure of rod opsin) or the N-terminal tail and suggested that these segments were all cooperatively involved in forming a specific folding structure in the intradiscal face. In contrast, mutations in the loops C-D and E-F in the cytoplasmic domain did not affect regeneration of the rhodopsin chromophore but resulted in reduced or ablated ability to activate transducin (Franke *et al.*, 1992). These data suggested that the intradiscal domain of rod opsin might have a structural function whereas the cytoplasmic domain might carry out biochemical and regulatory functions.

1.4.4 Synthesis of rod opsin in photoreceptors

Synthesis of rod opsin is initiated in the endoplasmic reticulum (ER) and further modifications occur in the Golgi of the RIS. In order to accomplish the long distance transport of newly synthesised rod opsin on post-Golgi carriers towards the ROS these vesicles fuse with the plasma membrane surrounding the connecting cilium through which rod opsin is delivered to the ROS. The importance of the C-terminus of rod opsin for its transport to the ROS was demonstrated by Tai

and colleagues (1999) which suggested that dynein was responsible for the translocation of rhodopsin-bearing vesicles along microtubules and that this interaction occurred directly between the C-terminal cytoplasmic tail of rhodopsin and Tctex-1, a dynein light chain. Furthermore, transgenic mice showed abnormal accumulation of the Q344ter mutant rod opsin in the plasma membrane of the photoreceptor cell body, indicating that the rod opsin C-terminus is required for efficient transportation to or retention in the outer segment (Sung *et al.*, 1994). More specifically, the C-terminus sorting motif of rod opsin appeared to bind specifically to the small GTPase ARF4, a member of the ARF family of membrane budding and protein sorting regulators (Deretic *et al.*, 2005) which was essential for the generation of post-Golgi carriers targeted to the ROS of retinal photoreceptors.

1.5 Mutations in rod opsin cause autosomal dominant retinitis pigmentosa (ADRP)

Retinitis pigmentosa (RP) is the name given to a heterogeneous group of inherited disorders with an incidence of 1 in 3500 and for which there is currently no cure. RP is a highly variable disorder with some patients developing symptomatic visual loss in childhood whereas others remain asymptomatic until mid-adulthood. The first symptoms in many patients are difficulties with dark adaptation and night blindness in adolescence followed by loss of mid-peripheral visual field in adulthood. As the disease progresses peripheral vision is lost, resulting in tunnel vision, prior to central vision being lost. These visual symptoms are a result of the gradual degeneration of the two photoreceptor types: rods, which mediate achromatic vision in dim conditions; and cones, which are necessary for colour vision and fine acuity in daylight. Ultrastructural studies in the retinas of RP patients obtained at autopsy indicate a reduced density of rods and cones in the affected regions (Flannery *et al.*, 1989; Chapple *et al.*, 2001). Furthermore, the photoreceptors were characterised by shortened and severely distorted outer segments. In addition to photoreceptors, other areas of the retina are also affected by RP, although it is widely accepted that these secondary effects are a result of photoreceptor degeneration and not necessarily a direct consequence of RP. The

rate of retinal degeneration can be measured by the rod electroretinogram (ERG) amplitudes, a measure of retina function. Patients with RP have ERG's which are reduced in amplitude, becoming progressively smaller as the disease evolves. At advanced stages of RP pigmentary deposits can be observed on the surface of the retina (Figure 1.6) hence the name retinitis pigmentosa. Mutations linked non-syndromic to RP have been identified in over 35 genes. The underlying genes for 26 of these loci have been reported (http://www.sph.uth.tmc.edu/RetNet/ provided in the public domain by the University of Texas Houston Health Science Center, Houston, TX). For autosomal dominant RP (ADRP), which accounts for 20% to 40% of all cases, 14 genes have been identified and population surveys of subsets of these genes suggest that the known ADRP genes may account for between one fourth to one half of cases or families screened at the Laboratory for Molecular Diagnosis of Inherited Eye Diseases, Houston (Sullivan *et al.*, 2006).

Mutations in the rhodopsin gene represent the most common single cause of RP. Dryja and colleagues (1990) were the first to associate a mutation in the rhodopsin gene to RP by identifying a point mutation which replaced proline for histidine at position 23 (P23H) in the intradiscal domain of rod opsin. Since then over 120 point mutations (Figure 1.7) and at least 10 small deletions in the rhodopsin gene have been identified in patients with RP (Appendix A). Although some of the mutations in the rhodopsin gene cause recessive RP (E150K, G174S, E249ter and G284S) and congenital stationary night blindness (CSNB) the vast majority is associated with ADRP.

Seminal work by Nathans and Khorana groups showed that several pathological mutations in the rhodopsin gene failed to fold correctly (Sung *et al.*, 1991; Kaushal and Khorana, 1994; Sung *et al.*, 1994). Following the analysis of several mutations in structure-function studies two different classes of ADRP-linked rod opsin mutations were proposed. Class I mutations occurred in the C-terminus of the protein, resembled wild-type protein in their translocation to the plasma membrane and formed a functional chromophore with 11-*cis*-retinal. The vast majority of the

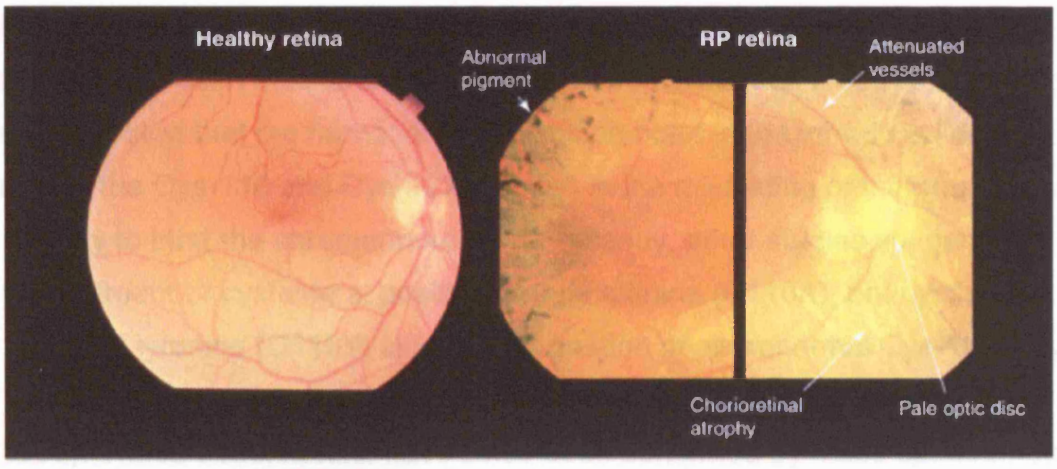

Figure 1.6 A comparison of normal and retinitis pigmentosa (RP) fundus. Retinal dystrophies are classified by ophthalmoscopic findings (fundus examination), psychophysics and electrophysiology, age of onset, and genetics or family history. Fundus examination in RP patients typically shows pigmentation in a 'bone-spicule' pattern in the retina, pallor of the optic nerve and narrowing of retinal blood vessels.

ADRP mutations however were named Class II which resulted in misfolding of the mutant protein defined by the inability to form a functional chromophore with 11-*cis*-retinal and retention in the ER. Recent detailed studies of other rod-opsin mutations have suggested that different biochemical and cellular defects might also arise and this resulted on the proposal of a new expanded classification for rod opsin mutations to encompass these new data (Figure 1.7) (Mendes *et al.*, 2005).

The requirement of a tertiary structure in the intradiscal region with a disulfide bond between Cys-110 and Cys-187 for the correct assembly and/or function of rhodopsin have been elucidated by Davidson and colleagues (1994). Furthermore, it was suggested that the formation of a disulfide bond in the intradiscal domain other than the Cys-110 and Cys-187 resulted in the misfolding of the protein and the inability to bind the chromophore. More recently, other studies suggested that the replacement of cysteine at position 110 by alanine (C110A), phenylalanine (C110F) and tyrosine (C110Y) led to the formation of an abnormal Cys-185 - Cys-187 disulfide bond which resulted in the absence of 11-*cis*-retinal binding (Hwa *et al.*, 1999). These observations have since been confirmed by mass spectrometric analysis and extended to several other misfolded rod opsin mutants which contained the abnormal disulfide bond Cys-185 - Cys-187 in the intradiscal domain (Hwa *et al.*, 2001).

1.6 Potential mechanisms of cell death in rhodopsin RP

An understanding of the mechanisms of cell death initiated by these rod opsin mutations is fundamental in order to delineate future therapeutic strategies. The pharmacological approaches reported in this Thesis represent therapeutic strategies aimed at Class II mutants only. Dominance in ADRP patients could be due to loss-of-function, gain-of function, dominant-negative mutations, or any of the above in combination (Wilson and Wensel, 2003). There are two lines of evidence suggesting that loss-of-function mutations alone are not likely to cause ADRP. Firstly, none of the dominant rod opsin alleles that have been investigated appear to be null mutations. Secondly, heterozygous rhodopsin knockout mice showed

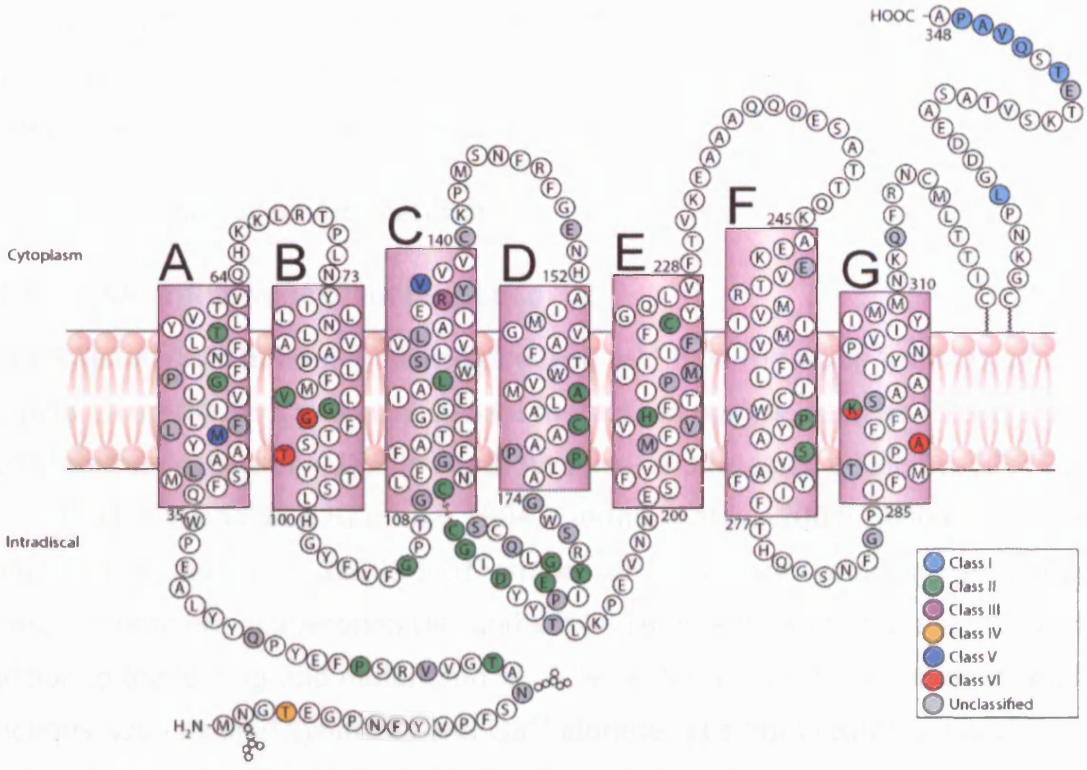

Figure 1.7 Secondary structure of rod opsin.

Secondary structure of rod opsin showing the location of point mutations listed in Appendix A where the transmembrane helices are labelled A-G. Mutated residues are highlighted in colours corresponding to different classifications. Class I mutants (light blue) refer exclusively to rod opsin mutations that fold normally but are not correctly transported to the ROS. Class II (green) refers to mutations that misfold, are retained within the ER and cannot easily reconstitute with 11-*cis*-retinal. Class III mutations correspond to mutations that affect endocytosis (purple). Class IV mutations do not affect folding per se but might affect rod-opsin stability and post-translational modification (orange). Class V (dark blue) mutants have no obvious initial folding defect but show an increased activation rate for transducin. Mutants that appear to fold correctly but lead to the constitutive activation of rod opsin in the absence of chromophore and in the dark constitute Class VI (red). Mutations that have no observed biochemical or cellular defect, or have not been studied in detail, should remain unclassified (grey). The secondary structure of rod opsin is based on the crystal structure by Palczewski *et al* (2000) (Figure 1.4). Modified from Mendes *et al* (2005).

little photoreceptor degeneration (Lem *et al.*, 1999). These observations suggest that haploinsufficiency, or the inadequate expression of rod opsin, in itself is not the cause of ADRP. This leaves the possibility that the dominant alleles might be due to gain-of-function or dominant-negative mutations.

1.6.1 Gain of function mechanisms

1.6.1.1 The unfolded protein response

In transfected cells heterologously expressed wild-type rod opsin translocates to the plasma membrane, whereas class II mutant rod opsins, such as P23H (the most common cause of ADRP in North America) are retained within the ER (Sung *et al.*, 1991; Kaushal and Khorana, 1994; Frederick *et al.*, 2001; Saliba *et al.*, 2002; Chapple and Cheetham, 2003). Furthermore, some mutant rod opsins are bound by the ER-resident chaperones BiP and Grp94 (Anukanth and Khorana, 1994). In addition to the folding and maturation of proteins, the ER performs other essential functions such as lipid synthesis and Ca^{2+} storage. The tight regulation and maintenance of ER homeostasis is vital. Disturbance of Ca^{2+} homeostasis during hypoxia, or imbalance between the demand and capacity of the protein-folding apparatus, initiates an adaptive response of the cell, termed the unfolded protein response (UPR, or ER stress response) (Rutkowski and Kaufman, 2004). The accumulation of misfolded rod opsin within the ER is likely to cause ER stress and could induce the UPR. The UPR is known to alleviate ER stress by reducing the accumulation of misfolded proteins. ER-localized chaperones are induced, protein synthesis is slowed, and protein degradation enhanced. However, if ER stress cannot be alleviated, the UPR can culminate in cell death by apoptosis (Pathway 1, Figure 1.8). Some of the molecules and mechanisms implicated in the transition from adaptive response to pro-apoptotic cascade have been identified; including CHOP, caspase activation, Ca^{2+} release and mitochondrial signalling. Unfortunately, little is understood about how these mechanisms are integrated and able to commit a cell to apoptosis. Nevertheless, the possible overloading of the UPR by Class II mutant rod opsins represents an attractive potential mechanism for the induction of cell death in RP (Frederick *et al.*, 2001).

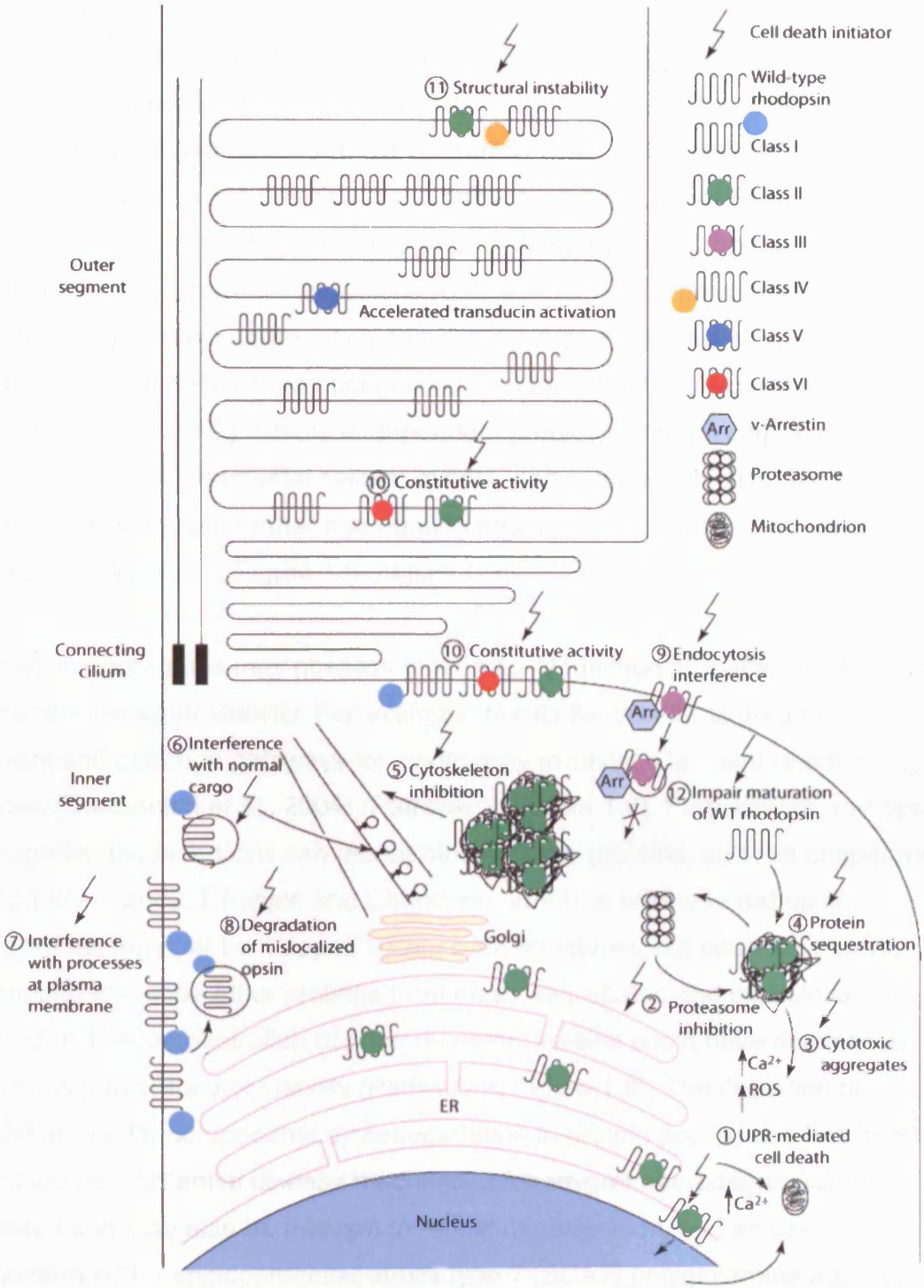
Cell death initiator
Wild-type rhodopsin
Class I
Class II
Class III
Class IV
Class V
Class VI
Arr
v-Arrestin
Proteasome
Mitochondrion
⑪ Structural instability
Outer segment
Accelerated transducin activation
⑩ Constitutive activity
Connecting cilium
⑩ Constitutive activity
⑨ Endocytosis interference
Arr
⑥ Interference with normal cargo
Inner segment
⑤ Cytoskeleton inhibition
Arr
⑫ Impair maturation of WT rhodopsin
④ Protein sequestration
⑦ Interference with processes at plasma membrane
⑧ Degradation of mislocalized opsin
Golgi
② Proteasome inhibition
③ Cytotoxic aggregates
Ca^{2+}
ROS
ER
① UPR-mediated cell death
Ca^{2+}
Nucleus

1.6.1.2 Aggregation and inclusion formation

The retention of Class II mutant rod opsins in the ER by the cellular quality control machinery is followed by their retro-translocation from the ER and degradation by the ubiquitin proteasome system (UPS) (Saliba *et al.*, 2002; Illing *et al.*, 2002). Like other aggregation prone proteins, if the mutant rod opsin is not degraded by the UPS it aggregates in the cytosol. These protein aggregates then coalesce into ubiquitinated proteinaceous inclusions (Saliba *et al.*, 2002; Illing *et al.*, 2002; Kopito, 2000). Protein aggregation can directly impair the function of the UPS (Bence, 2001) and P23H rod opsin expression inhibited UPS activity in HEK-293 cells (Illing *et al.*, 2002). Ubiquitin-dependent proteolysis has a central role in regulating many fundamental cellular events, and such an inhibition by mutant rod opsins could stimulate further aggregation and initiate a cascade that would lead to apoptosis (Pathway 2, Figure 1.8; Figure 1.9).

Rod opsin aggregates may possess other gain of function properties that could affect photoreceptor viability. For example, prefibrillar protein aggregates may have inherent and common pathways for cytotoxicity involving Ca^{2+} and reactive oxygen species (Bucciantini *et al.*, 2004) (Pathway 3, Figure 1.8). Furthermore, rod opsin aggregates and inclusions can recruit other cellular proteins, such as chaperones (Saliba *et al.*, 2002; Chapple and Cheetham, 2003) or wild-type rod opsin. Chaperones may not be 'trapped' within such structures, but could be actively attempting to rescue other proteins from these aggregates and inclusions (Kim *et al.*, 2002). The sequestration of photoreceptor proteins could have deleterious effects on photoreceptor viability (Pathway 4, Figure 1.8). The depletion of essential cellular components by sequestration in protein aggregates has been proposed as a potential disease mechanism for several neurodegenerative diseases and may also be relevant to retinal degeneration, as has been demonstrated for spinocerebellar ataxia type 7 (SCA7) polyglutamine aggregates and CRX, a homeodomain transcription factor which contains a glutamine rich region (Chen *et al.*, 2004).

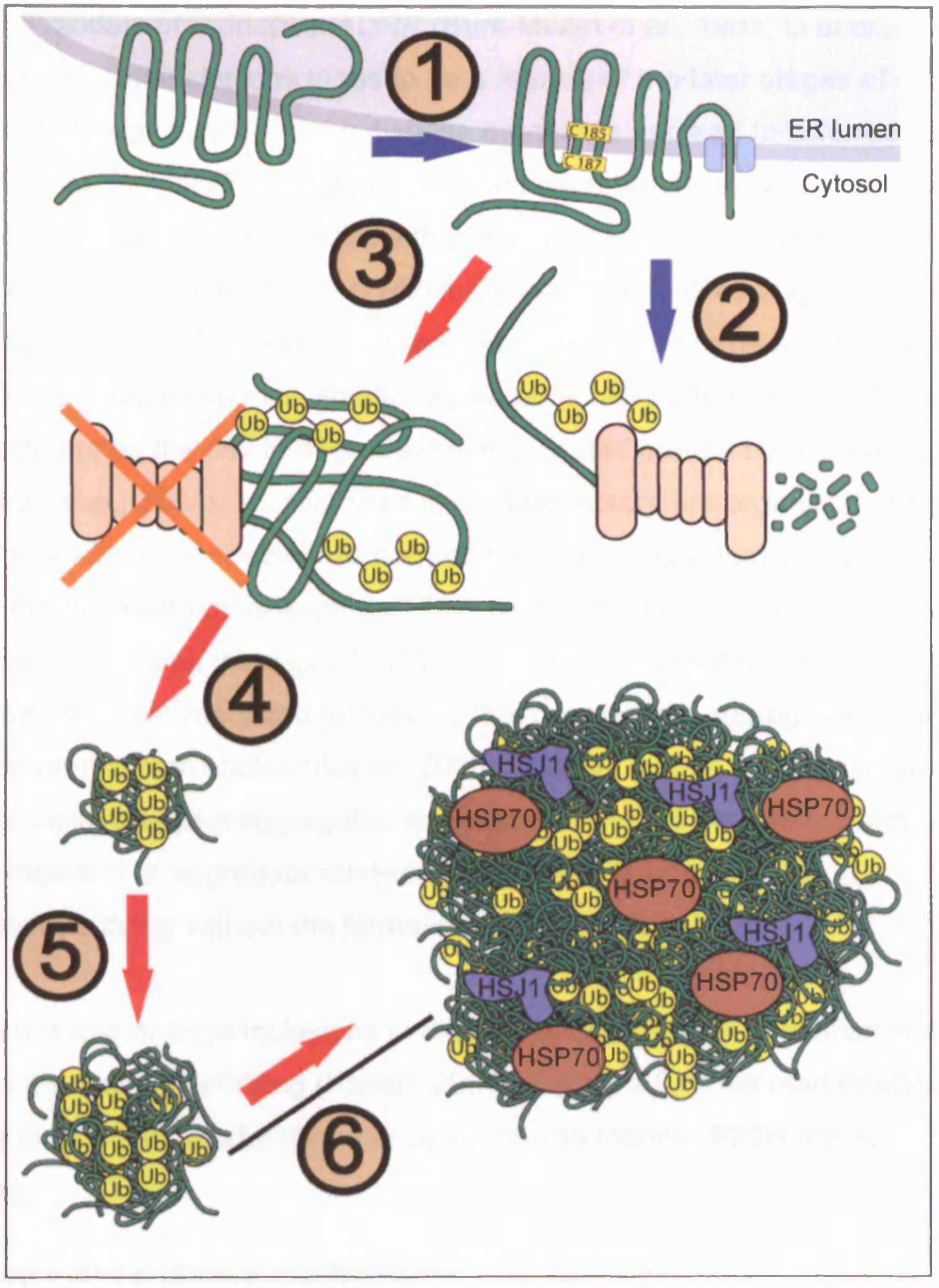

Figure 1.9 Schematic diagram illustrating the process of inclusion formation in the cell.
Misfolded rod opsin (1) can be retrotranslocated from the ER and be ubiquitinated and rapidly degraded by proteasome (2) or aggregate and inhibit the proteasome (3). Small aggregates (4 and 5) can transported to the microtubule organising center (MTOC) and coalesce into large intracellular inclusions where they co-localise with molecular chaperones (6).

Electron dense inclusions of rhodopsin have been observed in both human ADRP and animal models of rhodopsin ADRP (Bunt-Milam *et al.*, 1983; Li *et al.*, 1998), but the presence of inclusions tends to be a feature of the later stages of disease. Therefore, their significance to the disease process is unclear. In cultured cells the formation of these inclusions requires an intact microtubule network (Saliba *et al.*, 2002; Illing *et al.*, 2002) and is it likely that their presence would interfere with the normal function of the cytoskeleton within photoreceptors (Pathway 5, Figure 1.8). Alternatively, intracellular inclusions have been suggested to be a protective mechanism against more toxic smaller aggregates (Arrasate *et al.*, 2004), or another attempt by the cell to degrade the aggregated protein by autophagy (Ravikumar *et al.*, 2004). Microtubules in photoreceptors are organized around the basal bodies within the specialized non-motile connecting cilium at the junction between the outer and inner segment. This highly specialized microtubule organization could limit the capacity of photoreceptors to clear protein aggregates by the type of dynein-mediated processes that concentrate aggregated proteins in pericentriolar inclusion bodies (Kopito, 2000). Without such a mechanism to sequester toxic rod opsin aggregates into inclusion bodies the photoreceptor could be more exposed to aggregate related toxicity and this could lead to photoreceptors dying without the formation of visible inclusions.

Although the role of large inclusions in disease is unclear their formation is a surrogate marker of misfolding (Kopito, 2000) (Figure 1.9). This marker was exploited in a cellular model (Chapter 3) in order to monitor P23H rod opsin misfolding.

1.6.2 Dominant-negative mechanisms

Although the mechanisms discussed so far point towards ADRP being caused by gain-of-function mutations in the rod opsin gene, other studies suggest that a dominant-negative pathogenesis could be equally plausible. Studies of some Class II mutants of *Drosophila* rhodopsin, NinaE (e.g. ninaE^{D1}; S137F), showed that the misfolded mutant rod opsin had a dominant effect on the post-translational

maturation of the normal rod opsin protein (Kurada *et al.*, 1998). Such a potential dominant-negative effect has been confirmed by recent studies in mammalian cells (Saliba *et al.*, 2002). Co-expression of a Class II mutant rod opsin with wild-type rod opsin in COS-7 cells led to the formation of intracellular proteinaceous inclusions that contained the wild-type protein (Saliba *et al.*, 2002). This suggested that when both wild-type and mutant rod opsin were co-expressed, as in heterozygous ADRP patients, the mutant rod opsin could affect the processing of the wild-type protein. More recently, these observations have been extended to show that Class II mutants can impair the delivery of the wild-type protein to the plasma membrane in HEK-293 cells (Rajan and Kopito, 2005). Furthermore, the mutant and wild-type rod opsin appeared to form high molecular weight, detergent-insoluble complexes, in which the two proteins were in close (<70 Å) proximity. Co-expression of Class II mutants also resulted in the enhanced proteasome-mediated degradation and steady-state ubiquitination of the wild-type protein (Rajan and Kopito, 2005).

Mice lacking rod opsin fail to form rod outer segments and develop progressive retinal degeneration, indicating that rhodopsin plays an important role in assembling or stabilizing outer segments (Humphries *et al.*, 1997; Lem *et al.*, 1999). As heterozygous rhodopsin knock-out mice show very mild retinal degeneration (Lem *et al.*, 1999), there must be a rhodopsin 'threshold' between zero and one copy for photoreceptor integrity. In the absence of wild-type rod opsin a Class II mutant rod opsin also will not elaborate outer segments (Frederick *et al.*, 2001), suggesting that these mutants cannot contribute to the stabilization of the outer segment. Curiously, when wild-type protein is present, the bulk of the mutant protein is in the outer segment, hinting that the interplay between the mutant and wild-type protein may work both ways (Li *et al.*, 1996; Frederick *et al.*, 2001). A dominant effect of misfolding mutant rod opsins on the biosynthesis and/or maturation of the wild-type protein could reduce the amount of newly synthesized wild-type rod opsin that matures beyond the ER in photoreceptors. This would reduce the amount of rod opsin that gets to the outer segment possibly leading to

outer segment shortening and ultimately photoreceptor instability (Pathway 12, Figure 1.8).

1.7 Protein misfolding and aggregation underlie the pathogenesis of a variety of neurodegenerative diseases

In order to become functionally active, a newly synthesised polypeptide chain must fold into a unique three-dimensional structure. In the cell protein folding may fail as a result of mutations, posttranslational modifications, or environmental stresses such as changes in pH or temperature. Many misfolded proteins inappropriately expose hydrophobic domains which are normally buried in the protein or at the interface with other subunits. Furthermore, integral membrane proteins such as rod opsin have extensive hydrophobic stretches which are normally embedded in the lipid bilayer (Palczewski *et al.*, 2000). In either case failure to translocate or integrate such proteins renders these hydrophobic domains exposed to the aqueous environment of the cytosol which can lead to protein aggregation.

Protein folding is facilitated by molecular chaperones that are recruited to assist in the folding of newly synthesised nascent chains, but are also involved in the assembly and disassembly of supramolecular protein structures. Many molecular chaperones also named heat shock proteins (Hsp's) are synthesised in response to environmental stresses and comprise several classes of proteins (e.g Hsp90, Hsp70, Hsp60, and small Hsp's). Molecular chaperones such as Hsp70 transiently interact with unfolded or partially folded intermediates and prevent their hydrophobic surfaces from forming incorrect intermolecular and intramolecular interactions, therefore promoting the folding of polypeptide chains (reviewed in Barral *et al.*, 2004).

Aggregation of mutant proteins in the brain is a widely characterised and well accepted phenomenon in a variety of neurodegenerative diseases: such as tau and β-amyloid in Alzheimer's disease (reviewed by Selkoe, 2001); α-synuclein in Parkinson's disease (reviewed by Paleologou *et al.*, 2005); polyglutamine

expansions in Huntington's disease (Trottier *et al.*, 1995); and accumulation of prion protein in prion protein diseases (Grenier *et al.*, 2006). Far less established is whether the formation of these inclusions is related to toxicity or cytoprotection. Some studies suggested a link between inclusion formation and toxicity. For example, expression of pathological polyglutamine repeats in 293 Tet-Off cell lines resulted in the formation of toxic intracellular inclusions determined by nuclear observations (Waelter *et al.*, 2001). In addition, there was a redistribution of the ER-resident chaperone BiP and the heat-shock proteins Hsp40 and Hsp70 suggesting a cellular response to stress. Furthermore, inclusions appeared to be encircled by the intermediate filament vimentin and contain several proteasomal subcomplexes which might inhibit proteasomal activity and disrupt the UPR pathway of the cell leading to further aggregation (Waelter *et al.*, 2001). Different studies, however, indicated that inclusion formation can be dissociated from toxicity and might represent a cellular protective response to aggregation. In order to investigate the relationship between inclusions and toxicity in a cell model of Parkinson's disease, Tanaka and colleagues (2004) over-expressed α-synuclein and its interacting partner synphilin-1 using engineered 293T cells, followed by the manipulation of inclusion incidence using proteasome inhibitors and microtubule disrupting agents. These authors suggested that α-synuclein-induced apoptosis was not coupled with increased prevalence of inclusion-bearing cells and that the caspase inhibitor z-VAD-fmk while significantly reducing the number of apoptotic cells had no impact on the percentage of aggresome-positive cells. Consequently, this data indicated a disconnection between inclusion formation and apoptosis, and supported a protective role for these inclusions from the toxicity associated with the combined over-expression of alpha-synuclein and synphilin-1 (Tanaka *et al.*, 2004).

Although it is unclear whether large intracellular inclusions are toxic *per se* or represent a cytoprotective response to aggregation, the accumulation of misfolded proteins is increasingly recognized as a key pathogenic feature of degenerative diseases. Furthermore the inhibition of early misfolding steps and consequent

aggregation of mutant huntingtin exon 1 protein prevented photoreceptor degeneration and improved motor function in a fly model of Huntington's disease (Ehrnhoefer *et al.*, 2006). In terms of delineating therapeutic strategies for rhodopsin RP it would be important to assess if the pharmacological manipulation of misfolded rod opsin can be achieved and whether it has beneficial effects.

1.8 Aims of this thesis

Previous studies investigating the Class II misfolding rod opsin mutants suggested that the mutant protein misfolded, was retained in the ER and coalesced in intracellular inclusions. The main aim of this thesis was to develop a cellular model using wild-type and P23H rod opsin which mimics the disease process in ADRP patients and allows the analysis of both the gain of function and the dominant-negative mechanisms of cell death induced by these mutations. Futhermore, the model could be used to test and characterise novel rod opsin mutations identified in patients.

This model was used to determine if pharmacological compounds can alleviate the gain of function mechanism of cell death in cells expressing P23H rod opsin either by reducing inclusion incidence, promoting the folding of mutant protein, or reducing cell death.

The model was also used to assess if the interaction between wild-type and P23H rod opsin in a cell model of rhodopsin RP could be suppressed by pharmacological agents and consequently be beneficial in a potential dominant-negative mechanism of cell death occurring in ADRP patients.

Chapter 2: Materials and methods

2.1 Reagents

1-deoxynojirimycin (1-DNJ), 17-Allylamino-17-demethoxygeldanamycin (17-AAG), 4',6-Diamidino-2-phenylindole dihydrochloride (DAPI), 9-*cis*-retinal, dimethyl sulphoxide (DMSO), geldanamycin, N-butyldeoxynojirimycin (NB-DNJ), radicicol, rapamycin, resveratrol, trehalose, trimethylamine N-oxide (TMAO) were purchased from Sigma (Poole, UK). 11-*cis*-retinal was a kind gift from Prof Paula Booth (University of Bristol). Arimoclomol was a kind gift from Dr Linda Greensmith (UCL, Institute of Neurology) Celastrol was from Cayman Chemical Company (Tallinn, Estonia). Salubrinal was purchased from Calbiochem (Darmstadt, Germany). Lipofectamine and plus reagent were from Invitrogen (Paisley, UK). EndoH and PNGaseF were from New England Biolabs (Hitchin, UK). The primary antibody 1D4 to rhodopsin was obtained from Professor Robert Molday (UBC) via the National Cell Culture Centre, (Minneapolis, MN). Cy3 goat anti-mouse Cy3 conjugated secondary antibody was from Jackson Immuno Research Laboratories (West Grove, PA) and the goat anti-mouse antibody conjugated to horseradish peroxidase was from Pierce (Rockford, IL). Bovine WT opsin in pMT3 was a gift from Prof Daniel Oprian (Brandeis). Wild-type and mutant untagged and GFP-tagged rod opsins were obtained from Richard Saliba (Saliba *et al.*, 2002).

2.2 Site-directed mutagenesis (SDM) of rod opsin constructs

G90V-GFP was constructed by using the QuikChange II site-directed mutagenesis (SDM) kit purchased from Stratagene (La Jolla, CA) using WT-GFP as a template. The conditions for PCR are listed below:

5 µl of 10× reaction buffer (Stratagene)
5 ng of WT-GFP
125 ng of forward primer: 5' CATGGTCTTCGGTGTCTTCACCACCACCC 3'
125 ng of reverse primer: 5' GGGTGGTGGTGAAGACACCGAAGACCATG 3'

0.2 mM of dNTPs (Stratagene)
1 µl 50x polymerase mix (Stratagene)
ddH_2O to a final volume of 50 µl

Cycling parameters:

1)	95°C	30 seconds
2)	95°C	30 seconds
	55°C	1 minute
	68°C	5 minutes and 45 seconds

2.2.1 Transformation and purification of SDM products

Following the thermal cycling the digestion of the amplification products was carried out by adding 1 µl of the Dpn I restriction enzyme (10 U/µl). Each reaction mixture was mixed by pipetting the solution up and down several times prior to centrifugation for 1 minute and incubation at 37°C for 1 hour in order to digest the parental, non-mutated, supercoiled dsDNA. The transformation of XL1-Blue supercompetent cells was carried out on ice. 50 µl of the supercompetent cells were added to a 14 ml Falcon tube prior to the transfer of 1 µl of the Dpn I-treated DNA. This mixture was heat-shocked at 42°C for 45 seconds and placed on ice for 2 minutes. 0.5 ml of Luria-Bertani (LB) broth pre-heated to 42°C was added and the transformation reactions were incubated at 37°C for 1 hour shaking at 225 rpm. 100 µl of transformation reactions were then plated on agar plates containing 30 µg/ml kanamycin and incubated at 37°C for 16 hours.

5 ml of LB broth containing 30 µg/ml kanamycin were inoculated with a single colony and incubated for 16 hours at 37°C. Plasmid DNA was purified from the overnight culture using a GFX Micro Plasmid Prep Kit purchased from Amersham Pharmacia Biotech (Little Chalfont, UK) according to the manufacturers instructions. 1.5 ml of inoculated LB broth were placed into 1.5 ml microcentrifuge tubes and centrifuged for 30 seconds to pellet the cells. The supernatant was

removed and the pellets wee resuspended in 150 µl of solution I (100 mM Tris-HCL, 10 mM EDTA, 400 µg/ml Rnase I), followed by the addition of 150 µl solution II (1 M NaOH, 5.3% SDS) and incubated at 22°C for 2 minutes. Then 300 µl of solution III were added to the cell lysates and mixed by inverting the 1.5 ml tubes 10 times. The lysates were centrifuged at 17500g for 5 minutes at 22°C. The supernatant was transferred to a GFX column (containing a glass fibre matrix) and incubated for 1 minute at 22°C. The GFX columns were centrifuged for 30 seconds at 17500g and then washed by adding 400 µl of wash buffer (10 mM Tris-HCL pH 8.0, 1 mM EDTA, 80% ethanol). The GFX columns were then centrifuged for 60 seconds at 17500g to remove the wash buffer. The DNA was eluted from the columns by the addition of 50 µl of sterile ddH_2O and then the columns were centrifuged for 1 minute to collect the DNA solution in sterile 1.5 ml microcentrifuge tubes. The resulting purified DNA was then analysed for the presence of the correct insert by restriction enzyme digests. The DNA was then sequenced to ensure that the plasmid contained the correct mutation.

2.3 Cell culture

2.3.1 Transfection of SK-N-SH cells

SK-N-SH human Caucasian neuroblastoma cells were obtained from the European Collection of Cell Cultures (ECACC) (Salisbury, UK), and grown in DMEM/NUT.MIX.F12 with Glutamax-I, 10% v/v heat inactivated foetal bovine serum (FBS), 50 U/ml penicillin and 50 µg/ml streptomycin in an humidified atmosphere of 6% CO_2 at 37°C. For fluorescence, permanox 8-well chamber slides were seeded at a concentration of $2.5x10^4$ cells per chamber. 24 hours after seeding cells were transfected using 0.5 µl of lipofectamine enhanced with 1 µl of plus reagent per chamber in 100 µl of serum-free media for 3 hours according to the manufacturer instructions. The total amount of plasmid DNA used was 200 ng/chamber. For single plasmid studies 100 ng of the plasmid were added together with 100 ng of pcmvTag3a. For co-transfection studies 100 ng of each plasmid

were added. Following this period, 20% v/v FBS media was added in equal volume in order to restore a 10% v/v FBS solution.

For biochemical assays, 6-well plates or 96-well plates were used and both the cell density and the transfection conditions were adjusted to the size of the surface area. 6-well plates were seeded with $5x10^5$ cells per well with each well being transfected 24 hours later using 4 µl of lipofectamine, 8 µl of plus reagent and a total amount of plasmid DNA of 1.6 µg per well in 800 µl of serum-free media for 3 hours. 96-well plates were seeded at $5x10^3$ per well and each well was transfected using 0.1 µl of lipofectamine, 0.2 µl of plus reagent and a total of 40 ng of plasmid DNA in 50 µl of serum-free media for 3 hours. In both cases, following the 3 hour period, 20% v/v FBS media was added in equal volume in order to restore a 10% v/v FBS solution.

2.3.2 Drug treatments

All drug treatments were carried out upon the re-establishment of the 10% v/v FBS concentration following the 3 hours serum-free period unless otherwise stated. The list of compounds used in this study is shown in Table 2.1.

2.4 Fluorescence and immunofluorescence microscopy

2.4.1 Fluorescence

SK-N-SH cells transfected with GFP-tagged opsin were washed three times with 4°C phosphate buffer saline (PBS: 137 mM NaCl, 2.7 mM KCl, 8.1 mM Na_2HPO_4, 1.5 mM KH_2PO_4, pH 7.3 at 25 °C) 24 hours after transfection, followed by fixation with 3.7% v/v paraformaldehyde for 15 minutes at 22°C. Cells were then washed four times in PBS and incubated with 2 µg/ml DAPI (stock 10 mg/ml of 4',6-Diamidino-2-phenylindole dihydrochloride in DMSO) in PBS for 5 minutes in the third wash.

Compound	Stock	Supplier
9-*cis*-retinal	50 mM in ethanol	Sigma
11-*cis*-retinal	1.8 mg in ethanol	Prof Paula Booth
DMSO	>99%	Sigma
TMAO	1 M in dH_2O	Sigma
4-PBA	Powder	Fluka
Trehalose	Powder	Fluka
Arimoclomol	100 mM in dH_2O	Prof Linda Greensmith
Celastrol	100 mM in DMSO	Cayman
Geldanamycin	10 mM in DMSO	Sigma
Radicicol	5 mM in ethanol	Sigma
17-AAG	10 mM in methanol	Sigma
Rapamycin	5 mM in chloroform	Sigma
Salubrinal	100 mM in DMSO	Calbiochem
Resveratrol	10 mM in ethanol	Sigma
1-DNJ	5 mM in dH_2O	Sigma
NB-DNJ	5 mM in dH_2O	Sigma

Table 2.1 List of pharmacological agents used in this study.
All compounds were added immediately after the serum-free transfection period and were diluted in a 20% FBS media unless otherwise stated.

2.4.2 Immunofluorescence

24 hours after transfection cells were washed three times with 4°C PBS and fixed using 3.7% v/v paraformaldehyde for 15 minutes followed by two washes with PBS. Permeabilisation was carried out using 0.1% v/v Triton X-100 for 5 minutes, followed by two washes in PBS. Prior to the incubation with antibodies cells were blocked for 30 minutes at 22°C with a blocking solution consisting of 3% w/v albumin and 10% v/v normal donkey serum in PBS. Cells were incubated with 1D4 rhodopsin antibody (0.5 µg/ml) in blocking solution for 1 hour at 22°C followed by three washes in PBS and incubation for 1 hour at 22°C with donkey anti-mouse Cy3 conjugated secondary antibody (1:100) in blocking solution. Cells were consequently washed four times in PBS and DAPI was used at a concentration of 2 µg/ml in PBS for 5 minutes in the third wash. Inclusion incidence and cellular morphology counts were carried out using a 40x objective in a Leica DMRBE epifluorescence microscope. Fluorescence and immunofluorescence were visualised using a Zeiss LSM 520 laser scanning confocal microscope. The following excitation/emission conditions were used in separate channels with the 63x oil immersion objective: DAPI 364/475-525 nm, GFP 488/505-530 nm, Cy3 543/560 nm.

2.5 Assessment of the cellular localisation of rod opsin

Inclusion incidence was carried out by scoring the percentage of transfected cells which contained inclusions. Cellular morphology studies were carried out by scoring the predominant localisation of rod opsin in transfected cells: plasma membrane (PM), ER, and inclusions as a percentage of transfected cells. The data presented in the dominant-negative studies represents the predominant cellular localisation of untagged wild-type rod opsin in co-transfected cells. Before initiating these experiments I have carried out extensive training which comprised counting, analysing and discussing cellular morphology in parallel with Professor Michael Cheetham in order to gain proficiency and standardise results. The data presented in this Thesis represent experiments which were carried out double blind with

Professor Michael Cheetham loading unknown samples randomly in 8-chamber slides and Hugo Mendes analysing cellular morphology and counting inclusions unaware of the respective treatments. For each condition 400 cells were counted and each experiment was repeated at least four times.

2.6 Preparation of cell extracts for Western blotting

24 hours after transfection cells were washed twice with 4°C PBS and lysed using 190 µl 1% v/v Triton X-100 in PBS + 10 µl protease inhibitor cocktail for use with mammalian cell and tissue extracts (Sigma). Cells lysates were scraped from wells and collected in 1.5 ml microcentrifuge tubes on ice prior to centrifugation at 17500g for 30 minutes at 4°C. The amount of protein in the soluble cell lysates was calculated by a protein assay based on the method of Bradford and 10 µg of cell lysate protein were mixed with an equal volume of 2x modified Laemmli sample buffer (1x sample buffer: 50 mM Tris-HCL pH 6.8, 2% w/v SDS, 10% v/v Glycerol, 2.5% v/v 2-mercaptoethanol, 0.1% w/v bromophenol blue) and run on a 10% v/v polyacrylamide gel. The stacking gel was made up of 4% v/v polyacrylamide in 0.375 M Tris-HCL (pH 6.8) with 0.1% w/v SDS. The resolving gel was made up of 10% v/v polyacrylamide in 0.125 M Tris-HCL (pH 8.8) containing acrylamide:bisacrylamide in a ratio of 30:1. The Tris-glycine running buffer contained 25 mM Tris-HCL, 250 mM Glycine and 0.1% SDS. Bio-Rad (Hercules, CA) low range molecular weight markers were used as molecular weight standards.

Proteins were transferred from 10% v/v polyacrylamide gels to nitrocellulose using a semi dry electrophoretic transfer cell (Bio-Rad). The electrotransfer buffer was made up of 25 mM Tris, 192 mM glycine and 20% v/v methanol. Electrotransfer of proteins was carried out for 15 minutes at 15 V. For immunodetection of rod opsin on the mitrocellulose blots, 1D4 was used at a concentration of 1.33 µg/ml in PBS plus 5% w/v Marvel^{TM} plus 0.1% v/v Tween-20 for 1 hour followed by three 5 minute washes in PBS + 0.1% v/v Tween 20. The blot was then incubated with

goat anti-mouse HRP 1:30000 in PBS plus 1% w/v Marvel^{TM} plus 0.1% v/v Tween-20 followed by three 5 minute washes in PBS + 0.1% v/v Tween 20.

The ECL plus chemiluminescent detection reagent was purchased from GE Healthcare (Amersham, UK) and used according to the manufacturer's instructions. The mobility of different opsin glycoforms were determined by digesting 10 µg of soluble cell lysates using Endoglycosidase H (EndoH) and Peptide N-glycosidase F (PNGaseF) for 2 hours at 37°C. The deglycosylation reactions were as follows:

EndoH reaction:

EndoH cloned from *Streptomyces plicatus* and over expressed in E.*coli* was supplied in 20 mM Tris-HCL (pH 7.5), 50 mM NaCl, 5 mM Na_2EDTA. 10x G5 buffer: 0.5 M sodium citrate (pH 5.5).

Triton-X soluble lysate	10 µg
10x G5 buffer	2 µl
EndoH (500 U/µl)	1 µl (500 U)
ddH_2O	to 20 µl
Total reaction volume	20 µl

Reaction was incubated for 2 hours at 37 °C

PNGaseF reaction:

PNGaseF purified from Flavobacterium meningosepticum was supplied in 20 mM Tris-HCL (pH 7.5 at 25°C), 50 mM NaCl, 5 mM Na_2EDTA and 50% glycerol. 10x G7 buffer: 0.5 M sodium phosphate (pH 7.5 at 25 °C).

Triton-X soluble lysate	10 µg
10x G7 buffer	2 µl

PNGaseF (500 U/µl)	1 µl (500 U)
ddH_2O	to 20 µl
Total reaction volume	20 µl

Reaction was incubated for 2 hours at 37 °C

2.7 Rod opsin fractionation assay

SK-N-SH cells were seeded on 6-well dishes and transfected with GFP-tagged rod opsin as described above. Total, soluble and insoluble fractions were obtained 24 hours after transfection. Total fractions were obtained by lysing cells with 190 µl of RIPA buffer + 10 µl of protease inhibitor cocktail (RIPA buffer: 50 mM Tris-HCL pH 8.0, 150 mM w/v NaCl, 1 mM EDTA, 1% v/v NP-40, 0.1% w/v SDS, 0.05% w/v sodium deoxycholate). Soluble fractions were obtained by lysing cells with 190 µl of RIPA buffer + 10 µl of protease inhibitor cocktail followed by centrifugation at 17500g for 30 minutes at 4°C and removal of the supernatant. Insoluble fractions were obtained by re-suspension of the pellet in 190 µl of RIPA buffer + 10 µl protease inhibitor cocktail. Protein concentration was measured by a protein assay based on the Bradford method. 50 µg of the total and soluble fractions were loaded onto a 96-well dish. The amount of insoluble fraction loaded was based on the volume corresponding to 50 µg of soluble fraction. Each condition was then normalised to 200 µl with RIPA buffer. Fluorescence was measured by using a Tecan Safire microplate reader with 488/509 nm emission/excitation wavelengths with a bandwidth of ± 2.5 nm and optimal gain. Experiments were carried out at least three times in triplicates (n=3) and the data shown is representative of one experiment.

2.8 Lactate dehydrogenase (LDH) cell death assay

SK-N-SH cells were seeded on a 96-well dish at a concentration of $5x10^3$ cells/well. 24 hours later cells were transfected with GFP-tagged opsin and the LDH assay obtained from Roche (Basel, Switzerland) was carried out 24 hours and 48 hours after transfection. 96-well dishes were centrifuged at 250g for 15 minutes at 22°C. 100 µl of supernatant was removed and placed in another 96-well dish.

100 µl of reaction mixture (250 µl of diaphorase/NAD^+ mixture plus 11.25 ml of dye solution containing iodotetrazolium chloride and sodium lactate) per well, prepared according to the manufacturers instructions, were added to the supernatants and incubated at 22°C for 30 minutes protected from light. Absorbance was then measured at 492 nm using a Tecan Safire microplate reader. Experiments were carried out at least three times in triplicates (n=3) and the data shown is representative of one experiment.

The LDH activity was determined in an enzymatic test: In the first step NAD^+ was reduced to $NADH/H^+$ by the LDH-catalyzed conversion of lactate to pyruvate. In the second step the catalyst (diaphorase) transferred H/H^+ from $NADH/H^+$ to the tetrazolium salt INT (2-[4-iodophenyl]-3-[4-nitrophenyl]-5-phenyltetrazolium chloride) which was reduced to formazan.

An increase in the amount of dead or plasma membrane-damaged cells resulted in an increase of the LDH enzyme activity in the culture supernatant. This increase in the amount of enzyme activity in the supernatant directly correlated to the amount of formazan formed during a limited time period. Therefore, the amount of color formed in the assay was proportional to the number of lysed cells. The formazan dye formed is water-soluble and showed a broad absorption maximum at about 500 nm, whereas the tetra-zolium salt INT showed no significant absorption at these wavelengths.

2.9 Caspase-3 activity assay

A colorimetric caspase-3 activity assay was used based on the protocol of Novoselova TV *et al* (2005). SK-N-SH cells were seeded in a 6-well dish at a concentration of $5x10^5$ cells/well followed by transfection with GFP-tagged opsin 24 hours later. 24 hours or 48 hours after transfection cells were washed twice with 4°C PBS followed by lysis with 190 µl buffer A (25 mM HEPES pH 7.5, 1 mM EDTA, 5 mM EGTA, 50 mM NaCl) + 10 µl protease inhibitor cocktail. 100 µl of buffer B (50 mM HEPES pH 7.5, 20% v/v glycerol, 1 mM EDTA, 5 mM DTT

containing 200 µM DEVD-pNA caspase-3 substrate (Calbiochem) was added to 50 µg of total protein followed by incubation for 4 hours at 37°C. Absorbance was measured at 405 nm using a Tecan Safire microplate reader. Experiments were carried out at least three times in triplicates (n=3) and the data shown is representative of one experiment.

2.10 Fluorescence resonance energy transfer (FRET)

2.10.1 Cloning of WT and P23H rod opsin into CFP and YFP vectors

WT-GFP rod opsin was digested with AgeI and Bam HI using the multicore restriction enzyme buffer (Promega): 1x buffer is 25 mM Tris-Acetate (pH 7.5 at 37°C), 100 mM potassium acetate, 10 mM magnesium acetate, 1 mM DTT. DNA samples were mixed with 6x blue orange loading dye (orange G, bromophenol blue and xylene cyanol) and were loaded onto a 1% w/v agarose gel made up in 1x Tris-acetate (TAE) buffer: 40 mM TAE and 1 mM EDTA. DNA was visualised on a UV transilluminator and the band corresponding to rod opsin was excised using a scalpel. DNA was recovered using a gel purification kit purchased from Qiagen (Crawley, UK).

Ligation reactions of rod opsin to pECFP-N1 and pEYFP-N1 were carried out by using a ratio of vector DNA to insert DNA of 1:4 in the presence of 1x T4 DNA ligase and 1x T4 DNA ligase buffer (10x T4 ligase buffer: 300 mM Tris-HCL (pH 7.8), 100 mM $MgCl_2$, 100 mM DTT and 10 mM ATP) in a total volume of 10 µl. The reaction mixtures were incubated at 4 °C for 16 hours. 5 µl of the ligation reaction was added to 50 µl of competent JM109 E.*coli* cells and incubated for on ice for 20 minutes prior to heat shock at 42 °C for 120 seconds. Cells were then added to pre-warmed (42°C) LB broth and incubated at 37 °C for 60 minutes. 50 µl and 200 µl of cell suspension were plated onto agar plates containing 30 µg/ml of kanamycin which were then incubated for 16 hours at 37 °C. CFP and YFP plasmid purification was carried out as described in Chapter 2.2.1.

2.10.2 Cell culture and FRET measurements

24 hours before transfection SK-N-SH cells were seeded on Matek dishes at a concentration of $5x10^4$ cells/dish. Cells were transfected using lipofectamine and plus reagent as described above. The total amount of plasmid DNA used was 400 ng/dish and cells were transfected as follows: 200 ng WT-CFP + 200 ng WT-YFP; 200 ng WT-CFP + 200 ng P23-YFP and 200 ng P23H-CFP + 200 ng P23H-YFP in a serum-free media for 3 hours prior to reconstitution to a 10% FBS media. After 24 hours FRET acceptor bleaching was carried out on live cells maintained in a humidified atmosphere of 6% CO_2 at 37°C using a Leica TCS SP2 AOBS.

2.11 Statistical analysis

Paired and unpaired Student's t-tests were carried out where appropriate. The sets of values were considered statistically significant the $p \leq 0.05$.

Chapter 3: Development and characterisation of a cellular model for rhodopsin RP

3.1 Introduction

Despite the wealth of genetic data originating from several research groups the precise mechanisms by which mutations in rod opsin induce rod cell death remain largely unknown. Dominance and consequent rod photoreceptor cell death in ADRP patients can either be attributed to loss-of-function mutations, gain-of-function mutations, or dominant-negative mutations (Wilson and Wensel, 2003). However, the interpretation of several studies suggested that loss-of-function mutations were unlikely to be the causative factor of ADRP in humans. Firstly, none of the dominant rod opsin alleles that have been investigated appears to be a null mutation. Secondly, hemizygous mice with a single copy of rod opsin (+/-) showed mild photoreceptor degeneration when compared to the homozygous (-/-) counterparts (Frederick *et al.*, 2001). Consequently these observations suggest that dominant alleles in ADRP are either due to gain-of-function or dominant-negative mutations.

The development of therapeutic strategies for late onset neurodegenerative diseases is a major challenge and this is only partially associated with the poor understanding of the mechanisms of cell death. The late onset of these diseases makes the creation of relevant *in vivo* models costly and time consuming with each experimental cycle taking several weeks, months or years. In order to test a variety of pharmacological compounds with the potential to be of use for patients with these conditions it is paramount to develop rapid and less expensive *in vitro* assays which mimic the disease process in a shorter period of time.

Soon after the identification of rod opsin mutations in early nineties several research groups heterologously expressed rod opsin molecules in mammalian cell

culture in order to investigate the relationship between those mutations and the potential mechanisms of rod cell death (Sung *et al.,* 1991; Sung *et al* 1993; Kaushal and Khorana 1994). The expression of wild-type rod opsin in cell culture revealed properties which related to its *in vivo* function in photoreceptors such as correct folding, translocation from the ER to the plasma membrane and reconstitution with the chromophore, 11-*cis*-retinal. On the other hand the majority of mutants characterised (Class II) misfolded, were retained in the ER, accumulated in large intracellular inclusions and failed to reconstitute with the chromophore.

Mammalian cell culture has been used to investigate the mechanisms associated with a variety of other neurodegenerative diseases. For example, *in vitro* model systems were used to demonstrate that the formation of huntingtin protein inclusions was dependent on the polyglutamine repeat length (Scherzinger *et al.*, 1997), although it remained unclear if inclusion formation was the cause of Huntington's disease or merely a consequence of disease progression. Other laboratories used truncated fragments of the huntingtin protein in NG108-15 mouse-rat neuroblastoma-glioma hybrid cells and associated inclusion formation to cell death (Lunkes and Mandel, 1998) although these data were contradicted by Saudou *et al* (1998) who indicated that aggregation of a mutant huntingtin fragment in striatal neurons in culture *per se* was not required to induce cell death.

Cell models were also used to investigate cell death mechanisms in Parkinson's disease. Following the identification of mutations in α-synuclein as the cause of some rare forms of familial Parkinson's disease, cell culture models using human neuroblastoma SH-SY5Y demonstrated that human wild-type and mutant α-synuclein self-aggregated and induced apoptotic cell death suggesting that the accumulation of α-synuclein and its degradation products may play a role in the development of the pathogenesis of this disease (El-Agnaf *et al.*, 1998).

Other studies have investigated the mechanisms associated with Alzheimer's disease where its neuropathology involved the accumulation of β-amyloid peptide (Aβ) in senile plaques. For example, experiments in primary neuronal cultures have indicated that Alzheimer's disease-linked mutated forms of Aβ precursor protein caused aggregation of Aβ and consequent neuronal loss (Loo *et al.*, 1993). Importantly, cell culture models have been widely used to study not only the mechanisms of disease but also potential therapeutic interventions in neurodegenerative diseases as it will be discussed in later Chapters.

The characterisation of a cell model for rhodopsin RP is described in this chapter using SK-N-SH human neuroblastoma cells. This model has several benefits compared to other previously published rhodopsin RP cell culture models. Firstly, both the gain-of-function and the dominant-negative mechanisms of cell death for any potential rod opsin mutation can be investigated. Secondly, due to its high transfection efficiency the efficacy of drugs which might be of benefit for rhodopsin RP patients can not only be qualitatively but also quantitatively assessed against possible mechanisms of photoreceptor cell death

3.2 Results

3.2.1 Localisation of WT and P23H rod opsin in SK-N-SH cells

The green fluorescent protein (GFP) from the jelly fish *Aequorea victoria* has become a widely used molecular reporter which facilitates the investigation of a variety of processes from gene reporting to intercellular trafficking both *in vivo* and *in vitro*. A variety of proteins fused with GFP including rod opsin (Saliba *et al.*, 2002) mostly maintain similar biological properties and intracellular trafficking patterns of their untagged counterparts. GFP-tagged rod opsin constructs described in Saliba *et al* (2002) were expressed in SK-N-SH cells in order to determine the localisation of wild-type and P23H rod opsin, a prototypical Class II rod opsin mutant. 24 hours after transfection the SK-N-SH cells were fixed and visualised using fluorescence microscopy.

When GFP was transfected into SK-N-SH cells it showed a cytoplasmic staining pattern. In contrast, wild-type rod opsin (Figure 3.1b) was predominantly present on the plasma membrane of SK-N-SH cells. This was in agreement with previously reported cell based models (Sung *et* al., 1991; Kaushal and Khorana, 1994; Saliba *et al.*, 2002) which investigated rod opsin and was the result of correct folding and consequent translocation through the secretory pathway from the ER to the plasma membrane of the cells.

P23H rod opsin (Figure 3.1c), on the other hand, was retained in the ER and no predominant plasma membrane staining was observed. Furthermore, in a proportion of the cells mutant rod opsin accumulated in large intracellular inclusions. Intracellular inclusions are a common feature of a variety of neurodegenerative diseases where the mutant protein misfolds and aggregates (Chapter 1). In addition to a different cellular localisation pattern, the levels of P23H rod opsin fluorescence were reduced when compared to the wild-type rod opsin.

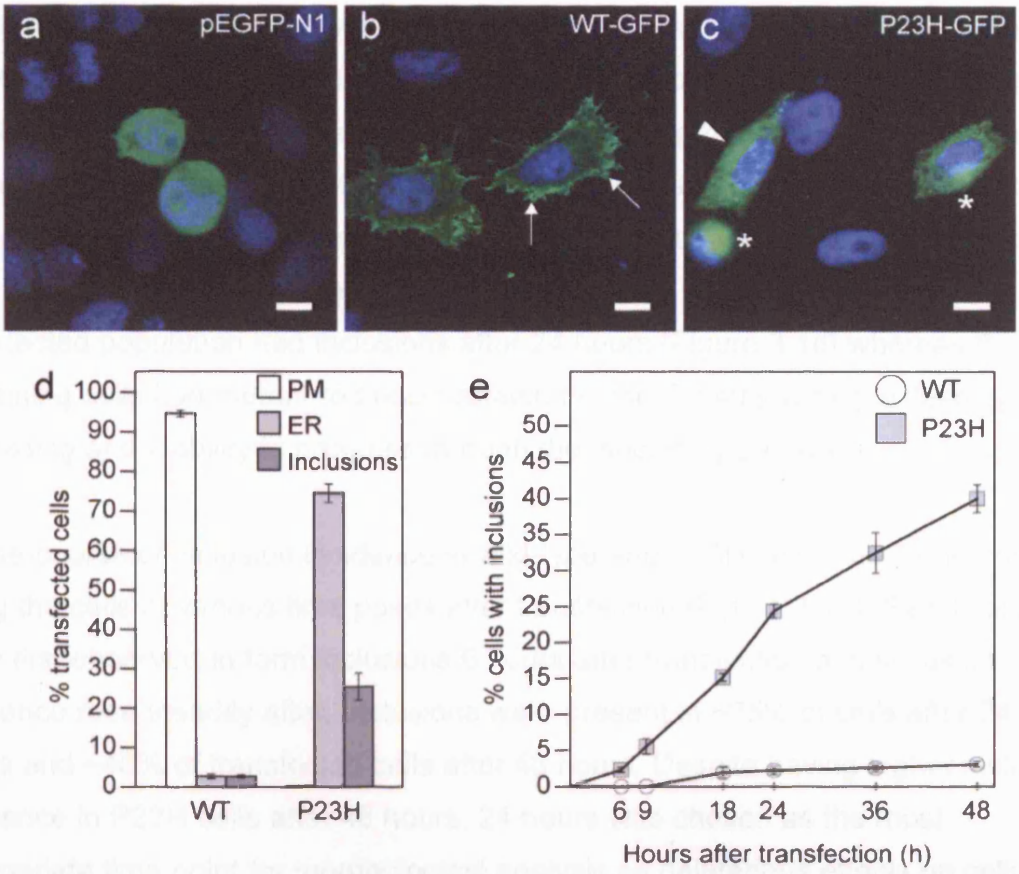

Figure 3.1 Characterisation of cellular morphology and inclusion incidence in cells transfected with WT and P23H rod opsin.

SK-N-SH cells were transfected with pEGFP-N1 (a), WT-GFP (b) and P23H-GFP (c) and fixed after 24 hours. GFP fluorescence was represented in green and DAPI-stained nuclei represented in blue. a) Cells expressing the empty GFP vector showed a general cytoplasmic staining. b) Expression of WT rod opsin resulted in a predominantly plasma membrane (PM) staining pattern (arrow). c) P23H rod opsin expression led to retention of the mutant protein in the ER (arrowhead) or accumulation in large intracellular inclusions (*). Scale bar = 10 μm. d) Quantification of cellular morphology in cells expressing WT and P23H rod opsin after 24 hours. e) Time course of inclusion incidence in WT and P23H cells. Error bars represent ± 2x standard error (2SE).

The incidence of inclusions observed in the controls was relatively consistent throughout the range of experiments performed. Inclusions were in present in ~2-3% of cells expressing wild-type rod opsin after 24 hours (Figure 3.1d) possibly due to the property that when transiently transfecting cells it is impossible to control the amount of rod opsin expressed in each cell and high amounts of any protein might lead to the saturation of the cellular machinery and consequent misfolding. In cells expressing P23H rod opsin, however, the inclusion incidence varied between 20% and 30% although in the vast majority of studies ~25% of the cells in the transfected population had inclusions after 24 hours (Figure 3.1d) whereas the remaining cells had mutant rod opsin retained in the ER suggesting widespread misfolding and inability to progress through the secretory pathway.

A time-course of inclusion incidence in wild-type and P23H cells was carried out by fixing the cells at various time points after transfection (Figure 3.1e). P23H cells were first observed to form inclusions 6 hours after transfection and inclusion incidence rose steadily after. Inclusions were present in ~25% of cells after 24 hours and ~40% of transfected cells after 48 hours. Despite having higher inclusion incidence in P23H cells after 48 hours, 24 hours was chosen as the most appropriate time point for morphological analysis as deleterious effects on cellular morphology started appearing in P23H-transfected cells subjected to longer incubation periods probably due to cell death (Figure 3.5). On the other hand, low levels of inclusions appeared after 18 hours in WT cells and the inclusion incidence remained at the 2-3% basal levels independent of the incubation period (Figure 3.1e).

By using the human neuroblastoma cell line SK-N-SH it was possible to differentiate wild-type and P23H rod opsin on the basis of morphology and inclusion incidence. The quantitative analysis of inclusion incidence could therefore serve as a surrogate marker of protein misfolding and allow the investigation of the extent to which a mutation causes rod opsin misfolding. Moreover, this quantitative

approach could be used to test the effect of drugs on the rod opsin misfolding itself or on the consequences of misfolding (see later Chapters).

3.2.2 Morphological assessment of the rod opsin mutants K296E, G90D, G90V and F276V

3.2.2.1 K296E

Keen and colleagues (1991) identified a severe form of RP associated with a mutation in rhodopsin which involved a base substitution at codon 296. This altered the lysine residue which functions as the attachment site for the chromophore, 11-*cis*-retinal, mutating it to glutamic acid (K296E). This mutation rendered K296E rod opsin unable to bind 11-*cis*-retinal and resulted in the mutant protein being constitutively active (Zhukovsky *et al.*, 1991). K296E-GFP plasmid DNA produced by Saliba *et al* (2002) was expressed in SK-N-SH cells and showed morphological properties associated with Class II mutants such as inability to translocate to the plasma membrane, retention in the ER, and accumulation in large intracellular inclusions (Figure 3.2a-b) which was in agreement with previous studies (Saliba *et al.*, 2002).

3.2.2.2 G90D

The mutation glycine to aspartic acid at position 90 (G90D) of rod opsin is a Class VI mutation which causes congenital night blindness and constitutively activates rod opsin (Rao *et al.*, 1994). When expressed in SK-N-SH cells G90D rod opsin translocated to the plasma membrane (Figure 3.2c-d) and exhibited a phenotype similar to that of wild-type rod opsin. This was in contrast with the K296E mutation which, while also constitutively activating rod opsin, showed morphological properties of a Class II mutant.

3.2.2.3 G90V

We were approached by Dr Andrew Webster (Institute of Ophthalmology, Moorfields Eye Hospital) and asked to characterise a novel mutation which involved the substitution of glycine for valine at codon 90 of rod opsin (G90V). This

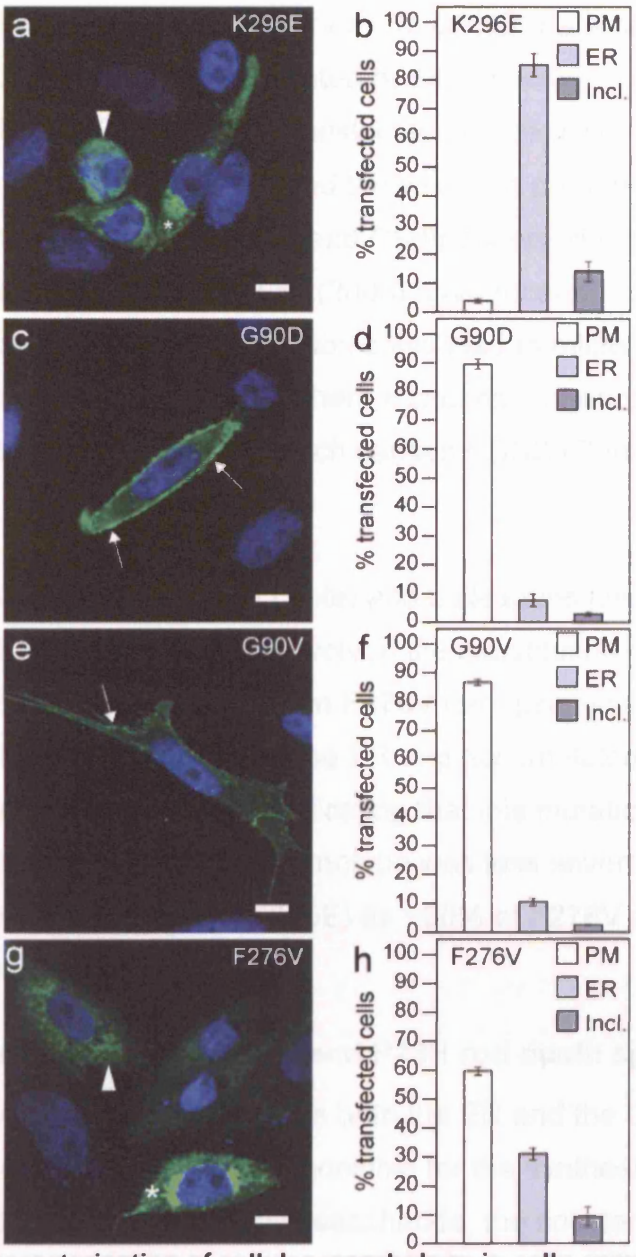

Figure 3.2 Characterisation of cellular morphology in cells expressing K296E, G90D, G90V and F276V rod opsin.

SK-N-SH cells were transfected with K296E-GFP (a-b), G90D-GFP (c-d), G90V-GFP (e-f) and F276V-GFP (g-h) and fixed after 24 hours. a) Expression of K296E rod opsin resulted in retention of the protein in the ER (arrowhead) and accumulation in intracellular inclusions (*). Expression of both G90D (c) and G90V (e) rod opsin led to a phenotype similar to WT with the majority of cells showing a predominant PM staining (arrows). g) Cells expressing F276V rod opsin showed retention in the ER (arrowhead) and accumulation in intracellular inclusions (*) albeit to a lesser extent than K296E cells. Scale bar = 10 μm. Error bars represent ± 2SE.

amino acid change was identified in a family with CSNB (Kabaranou *et al.*, 2004). A G90V-GFP rod opsin plasmid was created by site directed mutagenesis (see Chapter 2 for details). G90V rod opsin translocated to the plasma membrane and exhibited a phenotype similar to G90D and the wild-type protein (Figure 3.2e-f). Despite the similar phenotypes of G90D and G90V observed in this cell model for rhodopsin RP, Neidhardt and colleagues (2006) have recently suggested by homology modelling that the G90V mutation could lead to misfolding. They identified this change in a Swiss family where it caused a phenotype compatible with ADRP unlike the G90D mutation which caused CSNB (Rao *et al.*, 1994).

3.2.2.4 F276V

Dr Smaragda Kamakari (University of Crete) and colleagues identified a mutation in a family of Greek RP patients which involved the substitution of phenylalanine for valine at codon 276 of rod opsin. When F276V rod opsin was expressed in SK-N-SH cells it misfolded, was retained in the ER and accumulated in large intracellular inclusions (Figure 3.2g-h) indicating that this mutation could be classified as a Class II. However, the phenotype was less severe than other misfolding mutations (e.g P23H and K296E) as ~60% of F276V cells showed plasma membrane staining (Figure 3.2h).

3.2.3 Characterisation of soluble WT and P23H rod opsin species

The biosynthesis of glycoproteins involves both the ER and the Golgi of the cell. Cotranslational insertion in the ER is responsible for the synthesis of the polypeptide and addition of the core oligosaccharide, the covalent coupling of glycan and polypeptide, and for the initial modification of the glycans. Once the glycoproteins have folded and oligomerised properly they are trafficked to the Golgi where this process is continued by further trimming and modification of N-linked glycans. Bovine rod opsin is N-linked glycosylated at asparagine residues 2 and 15 (Hargrave *et al.*, 1977) and the oligosaccharides are modified as the protein translocates through the secretory pathway prior to reaching the plasma membrane in cell culture.

In order to investigate the degree of N-linked glycosylation and consequent maturity of wild-type and P23H rod opsin species, SK-N-SH cells were seeded on 6-well dishes as described in Chapter 2 and transfected with untagged wild-type or P23H rod-opsin prior to lysis after 24 hours with 190 µl of 1% Triton-X + 10 µl of protease inhibitor cocktail. Untagged rod opsin species were used as GFP-tagged opsins were retained in the stacking gel and failed to enter a 10% SDS-PAGE gel. 100 µl of total protein fraction was removed at this stage (T) and the remainder was separated into soluble (S) and insoluble (P) fractions by centrifugation at 17500g for 15 minutes at 4°C. Wild-type and P23H transfections had a similar transfection efficiency (~40%) as observed by immunofluorescence microscopy and 10 µg of total protein was loaded and resolved in a 10% SDS-PAGE gel followed by immunoblotting with anti-rhodopsin antibody 1D4 which was targeted to the C-terminus of rod opsin.

Total and soluble fractions of wild-type rod opsin expressed in SK-N-SH cells displayed a similar band pattern with various opsin species migrating from ~36 kDa to ~60 kDa (Figure 3.3a). Rod opsin species residing in the ER can be distinguished from Golgi and post Golgi species by digestion with the enzyme endoglycosidaseH (EndoH). This enzyme exclusively cleaves high mannose oligosaccharides or hybrid structures from N-linked glycoproteins and, therefore, will only digest ER resident rod opsin species (which are high mannose glycoforms) to the core peptide. Most of the wild-type rod opsin species showed resistance to digestion with EndoH (Figure 3.3b) suggesting that they had already progressed in the secretory pathway from the ER to the Golgi and the plasma membrane. Peptide N-glycosidase F (PNGaseF) is an amidase which cleaves between the innermost N-acetyglucoseamine and asparagine residue of high mannose, hybrid and complex oligosaccharides from N-linked glycoprotein, essentially cleaving all N-linked oligosaccharides from glycoproteins. Digestion with PNGaseF caused a mobility shift of wild-type rod opsin species as a single ~32 kDa band (Figure 3.3b - arrowhead) suggesting that this corresponded to deglycosylated species. These data were in agreement with previously published

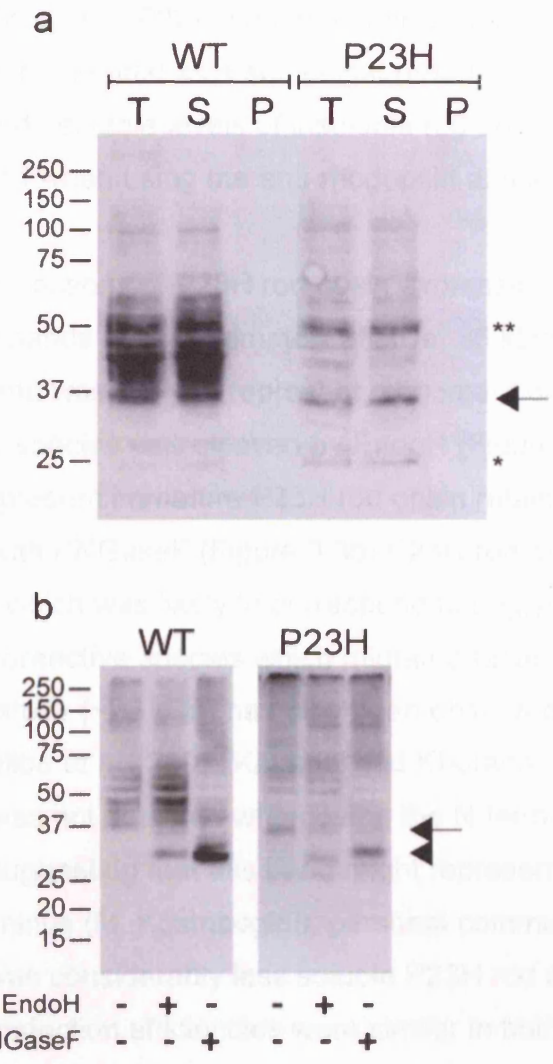

Figure 3.3 Characterisation of soluble WT and P23H rod opsin species. SK-N-SH cells were transfected with untagged WT or P23H rod opsin and lysed with 1% Triton-X 100 after 24 hours. a) 10 μg protein (T), 10 μg 1% Triton-X soluble protein (S) and an equal volume of insoluble (P) fraction were resolved on a 10% SDS-PAGE gel followed by immunoblotting with 1D4 anti-rhodopsin antibody. The 36 kDa band (arrow) is likely to represent glycosylated rod opsin. The 25 kDa band (*) and its dimer (**) might represent rod opsin species with a truncated N-terminus. b) Triton-X soluble WT species resisted digestion with EndoH whereas Triton-X soluble P23H rod opsin (arrow) was mostly cleaved by EndoH. Digestion with PNGaseF resulted in one major band migrating to ~32 kDa in both WT and P23H-expressing cell lysates (arrowhead). The position of molecular weight markers in kDa is shown on the left.

data by our lab (Saliba *et al.*, 2002) and others (Illing *et al.*, 2002) which suggested that wild-type rod opsin migrated as a somewhat broad species bearing complex oligosaccharides. No detectable levels of insoluble rod opsin species in the pellet fraction were observed when using the anti-rhodopsin antibody 1D4.

The total and soluble fractions of P23H rod opsin expressing cell lysates showed three major resolved bands at approximately 25 kDa, 36 kDa and 50 kDa (Figure 3.3a). The 36 kDa band was likely to represent monomers of glycosylated forms of P23H rod opsin. This species was cleaved by EndoH (Figure 3.3b) suggesting that they were likely to represent immature P23H rod opsin retained in the ER. Following digestion with PNGaseF (Figure 3.3b) P23H rod opsin migrated as a major ~32 kDa band which was likely to correspond to deglycosylated rod opsin species. The immunoreactive species which migrated faster than the ~32 kDa band present in this study (~25 kDa) has also been observed in published blots of mutant rod opsin (Saliba *et al.*, 2002; Kaushal and Khorana, 1994). This band and its dimer (~50 kDa) was not detected when using the N-terminal-specific 4D2 rhodopsin antibody suggesting that this band might represent rod opsin species with a cleaved N-terminus (M. Kosmaoglou, personal communication). Furthermore, there was considerably less soluble P23H rod opsin than wild-type rod opsin. As the transfection efficiencies were similar in both sets of cell lysates it is likely that a proportion of P23H rod opsin was either being degraded by the cell or aggregating into insoluble forms, as previously shown (Saliba *et al.*, 2002; Illing *et al.*, 2002).

Despite various optimisation attempts using different lysis buffers and SDS sample buffers the immunoblotting of detectable amounts of the insoluble fractions of wild-type and P23H rod opsin was not achieved with most, if not all, the rod opsin species not being able to enter the resolving gel. In order to investigate the insoluble rod opsin species, a rod opsin fractionation assay was developed which was based on the fluorimetric quantification of GFP-tagged rod opsin expressed in SK-N-SH cells. While not allowing a qualitative assessment of the insoluble rod

opsin species this assay provided a quantitative measurement of the extent of insoluble rod opsin present in cells expressing the wild-type and P23H proteins.

3.2.4 Development of a rod opsin fractionation assay

The rod opsin fractionation assay was carried by expressing the control GFP-vector pEGFP-N1, WT-GFP and P23H-GFP in SK-N-SH cells followed by lysis after 24 hours. This assay was optimised by testing a variety of lysis buffers with different centrifugation g forces for varied amounts of time. The combination that resulted in the highest difference between insoluble amounts of wild-type and P23H rod opsin used RIPA as the lysis buffer and the insoluble fraction was obtained by centrifugation at 17500g for 30 minutes at 4°C.

The results of this assay are shown in Figure 3.4 and represent the fluorescence levels of 50 µg of total protein. The GFP control (Figure 3.4a) was present at a higher level in the soluble than in the insoluble fraction (~20:1) which was expected as it has been widely documented as a soluble protein and fluorescence microscopy observations indicated a generalised cytoplasmic staining and absence of inclusions in SK-N-SH cells (Figure 3.1a). Similarly WT-GFP showed a higher ratio of soluble to insoluble fraction fluorescence (~8:1) which was predicted based on the cellular localisation and morphology observed (Figure 3.4b). In complete contrast with wild-type rod opsin, the ratio of soluble and insoluble fluorescence in P23H rod opsin transfected cells was roughly 1:2 (Figure 3.4c). Furthermore, the soluble and the total levels of P23H rod opsin were considerably lower than those of wild-type rod opsin which confirmed the morphological observations and the soluble fraction steady state levels obtained by Western blots.

This assay enabled the quantification of the soluble and insoluble rod opsin species present in transfected SK-N-SH cell lysates. It could, therefore, be used to complement the morphological and biochemical data obtained with immunoblotting in identifying useful pharmacological therapies in the cell model of rhodopsin RP.

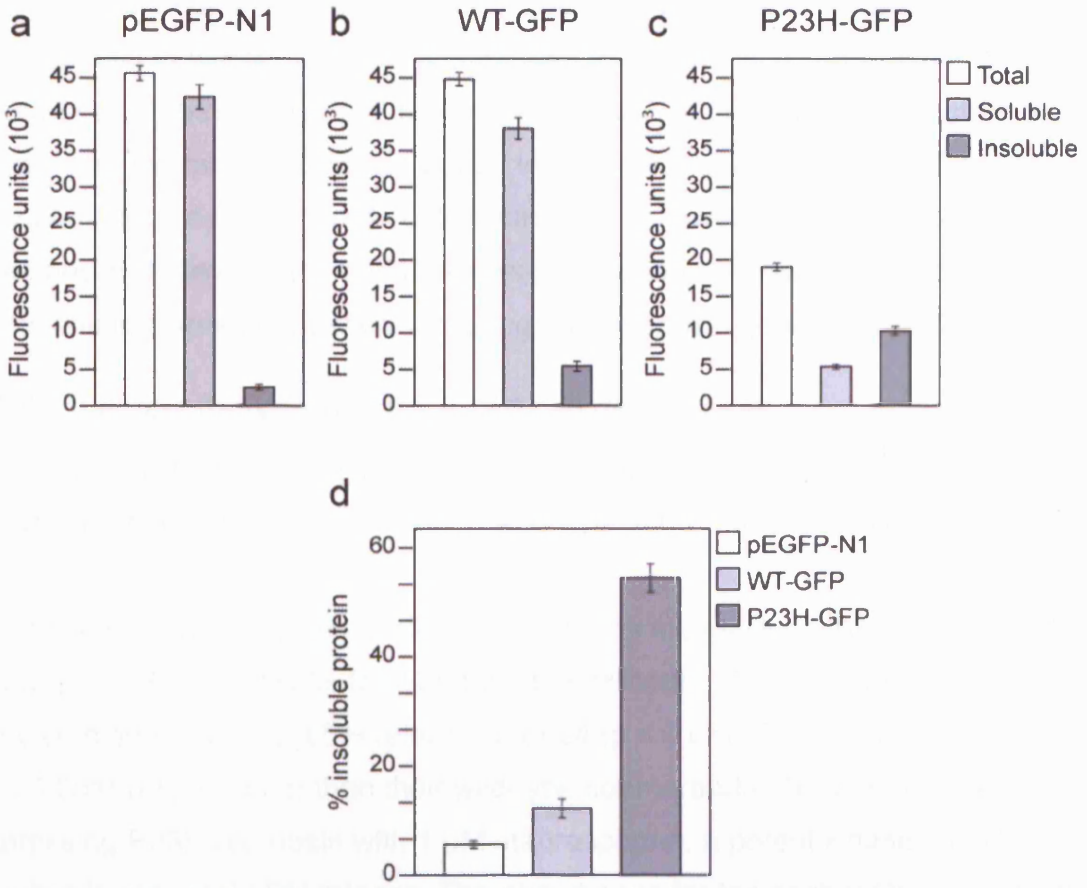

Figure 3.4 Rod opsin fractionation assay.

SK-N-SH cells were transfected with pEGFP-N1, WT-GFP and P23H-GFP and lysed with 190 μl RIPA buffer and 10 μl of protease inhibitor cocktail after 24 hours. 100 μl were removed and corresponded to the total fraction. The remaining cell lysate was separated into soluble and insoluble fractions by centrifugation. a) Cells expressing GFP showed a ratio of soluble to insoluble protein of ~20:1. b) WT cells showed a ratio of soluble to insoluble fraction of ~8:1. c) P23H cells had ratio of soluble to insoluble protein of ~1:2 and the total rod opsin levels were~40% of the WT levels. d) P23H-GFP had the highest levels of insoluble rod opsin shown as percentage of total protein when compared to the WT or GFP. Error bars represent ± 2SE.

3.2.5 Effect of WT and P23H rod opsin on cell death and apoptosis

Cell death is a common and necessary process during the nervous system development in general and the photoreceptors in particular (reviewed in detail by Stone *et al.*, 1999). The retina is highly stable and can maintain its structure and function for the full life of the individual, in humans for many decades. Despite this, in healthy adult eyes hundreds of thousands of photoreceptors die throughout life (Gao and Hollyfield, 1992) and these processes can be greatly accelerated by mutations in a variety of genes, including the rhodopsin gene (Pierce, 2001).

3.2.5.1 Lactate dehydrogenase (LDH) cell death assay

A commercially available lactate dehydrogenase (LDH) assay was used in order to assess the effect of the expression of wild-type and P23H rod opsin on cell death.

The optimisation of this assay was carried out by expressing wild-type and P23H rod opsin in SK-N-SH cells for 24 hours and 48 hours. P23H rod opsin cells showed higher levels of LDH release after 24 ($p \leq 0.05$) (Figure 3.5a) and 48 hours ($p \leq 0.001$) (Figure 3.5c) than their wild-type counterparts. Treatment of cells expressing P23H rod opsin with 1 µM staurosporine, a potent kinase inhibitor, resulted in maximal LDH release. The absorbance for the control GFP transfection was removed from the raw absorbance values and these data are shown in Figure 3.5b and Figure 3.5d for 24 and 48 hours respectively in order to better show any rod opsin specific effects. The results of this assay were more robust after 48 hours than after 24 hours, therefore, 48 hours was used as the standard time point in subsequent experiments.

3.2.5.2 Caspase-3 apoptotic assay

Since the identification of mutations in rod opsin as the cause of ADRP there has been a widespread debate on the mechanisms leading to photoreceptor cell death

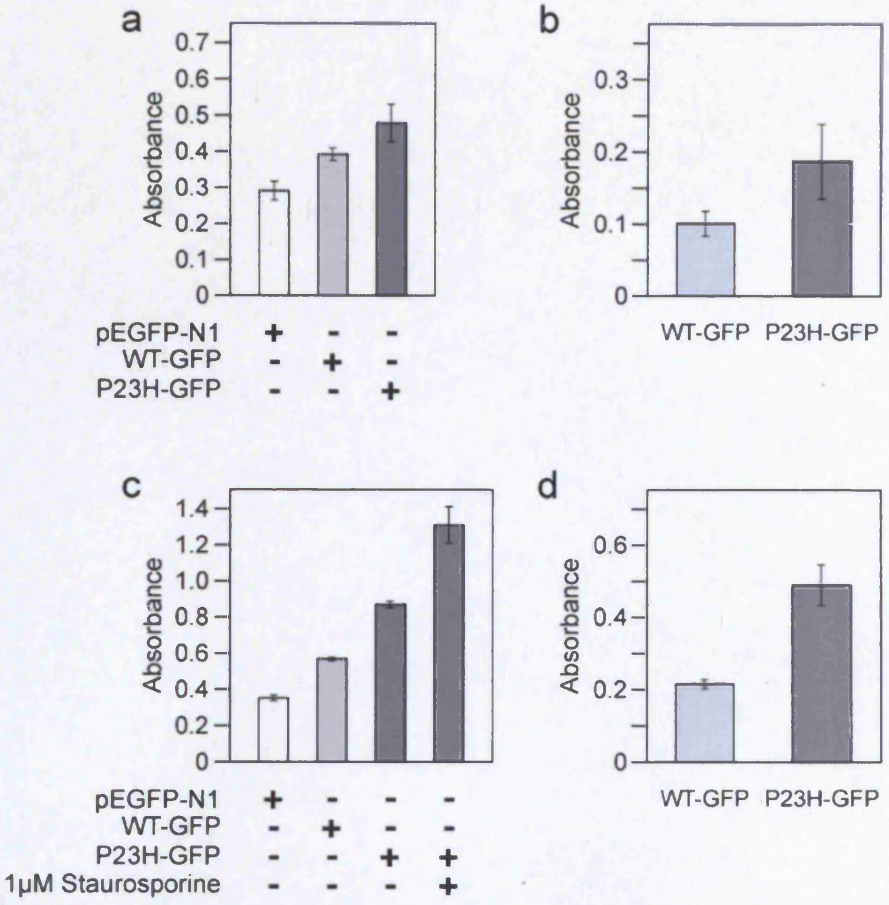

Figure 3.5 Lactate dehydrogenase (LDH) cell death assay.
LDH levels were measured in SK-N-SH cells 24 (a-b) and 48 hours (c-d) after transfection. a) Cells expressing P23H rod opsin had higher levels of LDH release ($p \leq 0.05$) than their WT counterparts. b) LDH release levels in WT and P23H cells after 24 hours following subtraction of the GFP background levels. c) LDH assay carried out in cells expressing pEGFP-N1, WT-GFP and P23H-GFP after 48 hours showed increased LDH release levels in cells expressing P23H ($p \leq 0.001$) then compared to the WT cells. Treatment of P23H cells with 1 μM staurosporine led to maximal LDH release. d) LDH release in WT and P23H cells after 48 hours following subtraction of the baseline GFP background levels. Error bars represent ± 2SE.

with some research groups suggesting that this is a consequence of caspase-dependent apoptotic pathways (Samardzija *et al.*, 2006) while others suggested that photoreceptor degeneration occurred by a mechanism not involving of caspase activation (Zeiss *et al.*, 2004). Several studies which characterised the mechanisms of cell death in a variety of animal models favoured the apoptotic-dependent photoreceptor degeneration and these include Royal College of Surgeons rats (RCS) (Tso *et al.*, 1994) and light-induced photoreceptor degeneration in albino rats (Abler *et al.*, 1996). On the other hand, other research groups have suggested that light-induced photoreceptor apoptosis in Balb/c mice was independent of the activation of several caspases, including caspase-3, which is a key regulator of apoptosis (Donovan and Cotter, 2002). Furthermore, photoreceptor degeneration could not be inhibited by using the broad range caspase inhibitor zVAD-fmk (Donovan and Cotter, 2002).

It was, therefore, important to establish if there were caspase-dependent apoptotic pathways induced by the wild-type or P23H rod opsin in a cell model of rhodopsin RP. For that purpose a colorimetric caspase activation assay was used based on Novoselova *et al* (2005). The assay was carried out using a commercially available caspase-3 substrate. This colorimetric substrate for caspase-3 and related caspases was designed so it would assess the amino acid sequence DEVD which was based on the caspase-3 cleavage site in poly (ADP-ribose) polymerase (PARP). Caspase-3 and related caspase activity can be quantified by spectrophotometric detection of free pNA (λ = 400 nm) after cleavage from the peptide substrate Ac-DEVD-pNA, using a multi-well plate reader and absorbance.

Caspase-3 activity was measured after 24 hours (Figure 3.6a) and 48 hours (Figure 3.6c). P23H rod opsin showed higher levels of caspase-3 activity when compared to wild-type rod opsin both after 24 ($p \leq 0.005$) and 48 hours ($p \leq 0.001$). The absorbance levels of GFP alone were removed from the raw values and these data are shown in Figure 3.5b and Figure 3.5d for 24 and 48 hours respectively.

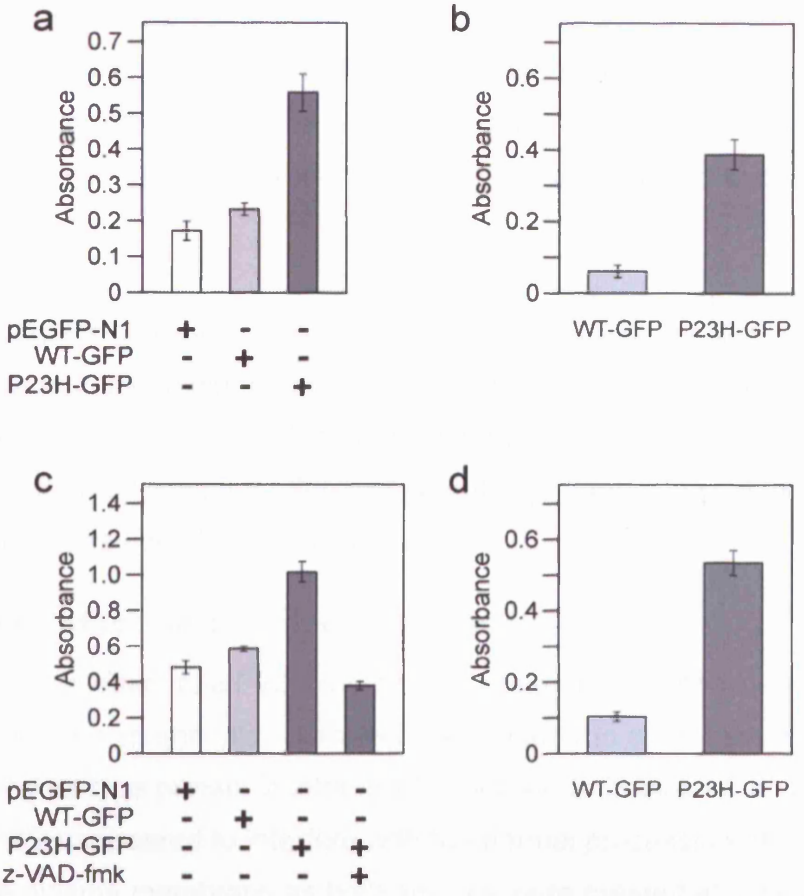

Figure 3.6 Caspase-3 activity assay.
Caspase-3 activity levels were measured in SK-N-SH cells 24 (a-b) and 48 hours (c-d) after transfection. a) Measurement of caspase-3 activity in cells expressing pEGFP-N1, WT-GFP and P23H-GFP after 24 hours. There were increased caspase-3 activity levels in P23H cells ($p \leq 0.005$) when compared to their WT counterparts. b) Levels of caspase-3 activity in WT and P23H cells after 24 hours following subtraction of the GFP background levels. c) Caspase-3 activity assay carried out in cells expressing pEGFP-N1, WT-GFP and P23H-GFP after 48 hours. Increased caspase-3 activity levels were observed in P23H cells ($p \leq 0.001$) when compared with WT cells and treatment of P23H cell lysates with 1 μM z-VAD-fmk inhibited caspase-3 activity. d) Caspase-3 activity in WT and P23H cells after 48 hours following subtraction of the GFP background levels. Error bars represent ± 2SE.

The differences between rod opsin species were more robust after 48 hours so this was adopted as the standard time point for the caspase-3 activity assay in all subsequent experiments. When z-VAD-fmk was added to the assay after lysis, absorbance levels in P23H cells were reduced to levels lower than those of the wild-type protein showing that the absorbance signal corresponded to caspase-3 activity.

The LDH and caspase-3 activity assays suggested that the expression of mutant rod opsin in cells resulted in higher levels of LDH release and caspase-3 activity when compared to the expression of their wild-type counterparts and gave this model the scope for analysing the effects of potential pharmacological treatments for rhodopsin RP on cell death and apoptosis.

3.2.6 WT and P23H rod opsin co-localise in SK-N-SH cells

A dominant-negative effect of a P23H mutant rod opsin on the wild-type rod opsin has been suggested in mammalian cells with the mutant rod opsin leading to the accumulation of wild-type protein in intracellular inclusions (Saliba *et al.*, 2002). Furthermore, P23H appeared to interfere with the normal processing of wild-type rod opsin to the plasma membrane as both species were present at a close proximity (<70 Å) suggesting an interaction between the two rod opsin species (Rajan and Kopito, 2005).

In order to test the potential dominant-negative effects of the mutant rod opsin on the wild-type protein, equal amounts of WT-pMT3 and WT-GFP or WT-pMT3 and P23H-GFP were expressed in SK-N-SH cells. Cells were fixed 24 hours later and immunostained with the anti-rhodopsin antibody 1D4. This antibody only detected the untagged rod opsin species as the GFP-tagged rod opsins had GFP fused to the antibody recognition sequence in the C-terminus of rod opsin.

When cells expressed untagged and GFP-tagged wild-type rod opsin the vast majority of the cells showed predominantly plasma membrane staining (Figure

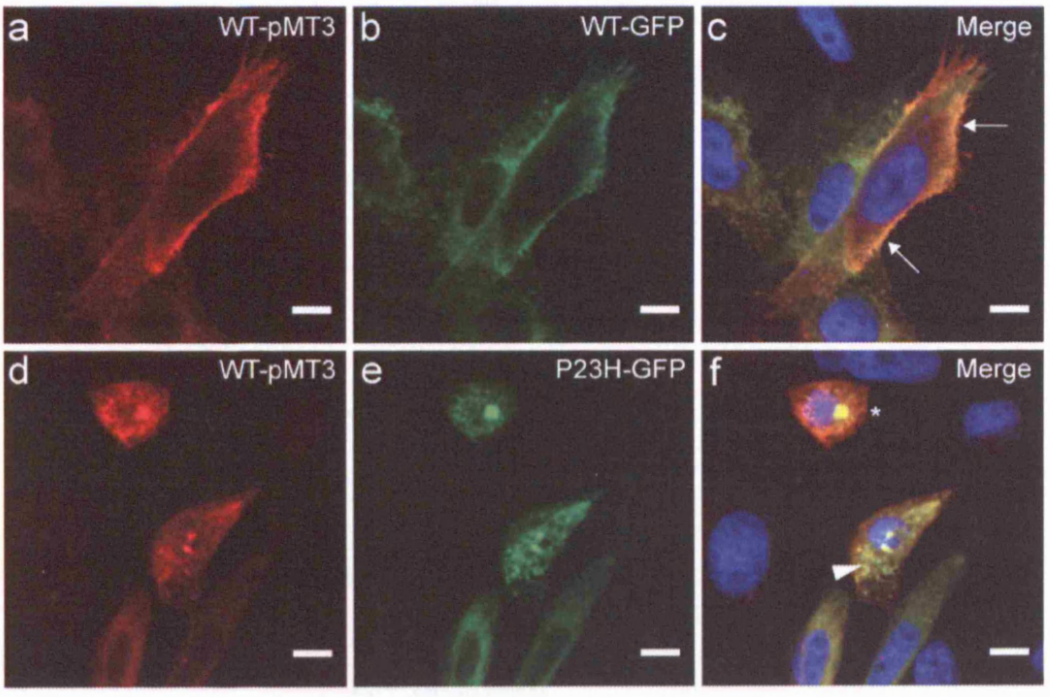

Figure 3.7 Co-expression of WT and P23H rod opsin results in the co-localisation of both opsin species in intracellular inclusions.
Confocal microscopy of SK-N-SH cells. a-c) Co-expression of untagged WT and WT-GFP rod opsin resulted in the normal translocation of both opsin species to the plasma membrane of cells (arrows): a) 1D4 immunostaining (red); b) GFP fluorescence (green); c) merge with DAPI (blue). d-f) Co-expression of untagged WT and P23H-GFP resulted in the disruption of the normal translocation of the WT protein to the plasma membrane and led to its retention in the ER (arrowhead) and intracellular inclusions where it co-localised with the mutant protein (*): d) ID4 immunostaining (red); e) GFP fluorescence (green); f) merge with DAPI (blue). Scale bar = 10 μm.

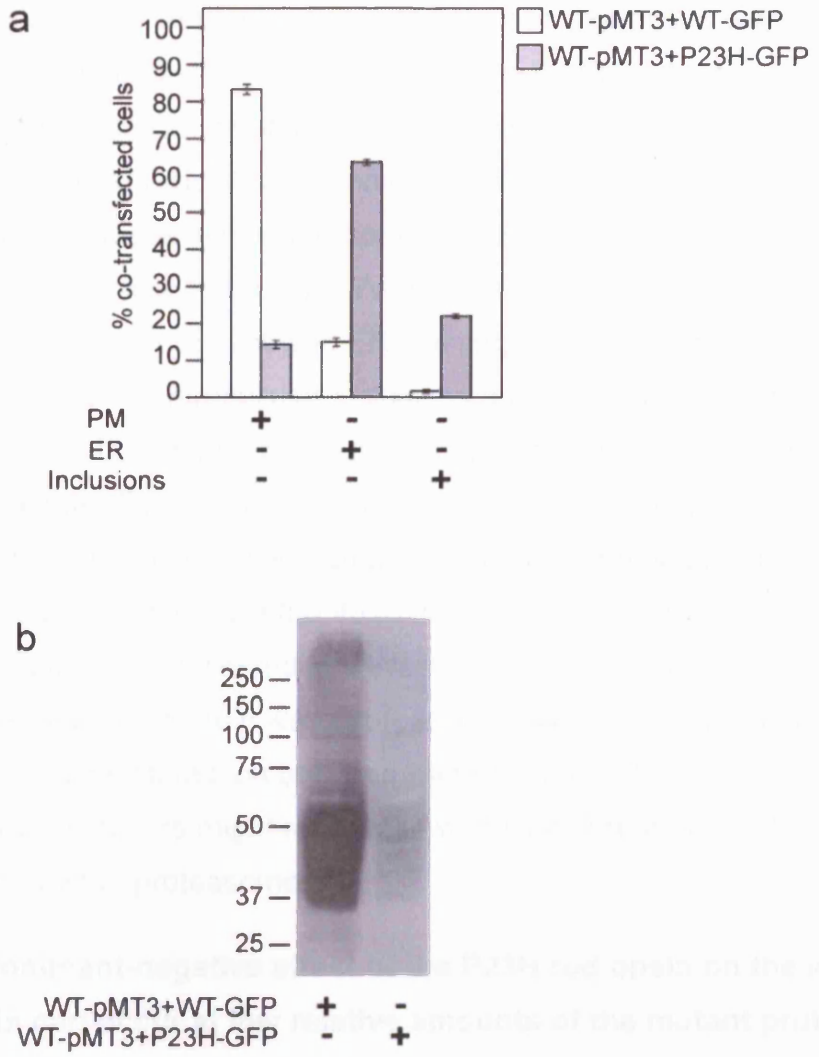

Figure 3.8 Morphological and biochemical assessment of the dominant-negative effect of P23H rod opsin on the WT protein.

a) Morphological characterisation of the effect of P23H rod opsin on the trafficking of the WT protein. This assessment was carried out by scoring the cellular localisation of untagged WT rod opsin, immunodetected by the anti-rhodopsin antibody 1D4, in co-transfected cells. Co-expression of untagged WT and WT-GFP rod opsin resulted in the co-localisation of both rod opsin species in the plasma membrane (PM) of the cells. Co-transfection with untagged WT and P23H-GFP rod opsin led to retention of the WT protein in the ER and the accumulation of WT protein in intracellular inclusions. Error bars represent ± 2SE. b) 10 μg of soluble protein were loaded onto a 10% SDS-PAGE gel. Co-expression of untagged WT and P23H-GFP reduced the amount of soluble WT rod opsin detected by the anti-rhodopsin antibody 1D4. The position of molecular weight markers in kDa is shown on the left.

3.7a-c, Figure 3.8a). In contrast, when wild-type was expressed with P23H rod opsin there was a change in the localisation of the wild-type protein. Co-transfected cells showed a co-localisation of the two rod opsin species in the ER (arrowhead) or in large intracellular inclusions (asterisk) (Figure 3.7d-f) suggesting that the mutant rod opsin was preventing the normal translocation of the wild-type protein to the plasma membrane of the cells. When the cellular morphology was quantified in co-transfected cells ~65% showed ER staining and ~15% had both opsin species accumulated in intracellular inclusions (Figure 3.8a). However, some co-transfected cells (~15%) had a predominantly plasma membrane staining suggesting that the effect of P23H rod opsin on wild-type rod opsin, while significant was not absolute. This recruitment of the wild-type protein to the large intracellular inclusions might contribute to the reduction in the levels of soluble wild-type rod opsin that were observed in a Western blot using the rhodopsin antibody 1D4 when the wild-type protein was expressed with P23H (Figure 3.8b). Furthermore, a close interaction between wild-type and P23H rod opsin or the formation of hybrid dimers might render the wild-type protein unstable and prompt its degradation by the proteasome.

3.2.7 The dominant-negative effect of the P23H rod opsin on the wild-type protein can occur at low relative amounts of the mutant protein

The effect of different relative concentrations of P23H and wild-type rod opsin on the cellular localisation of the wild-type protein in co-transfected cells was analysed (Figure 3.9). When the relative amount of P23H-GFP and WT-GFP plasmid DNA was 1:10, there was a reduction in the percentage of co-transfected cells showing a normal translocation of the wild-type protein when compared to co-transfected cells expressing untagged and GFP-tagged wild-type rod opsin (Figure 3.8a). The interference of the mutant protein on the wild-type localisation increased at ratios of 1:5 and 1:2 and was almost maximal at the ratio of 1:1 where the majority of co-transfected cells had wild-type protein retained in the ER. These data indicate that the dominant-negative effect of the P23H rod opsin on the mutant protein can occur at low relative amounts of P23H rod opsin.

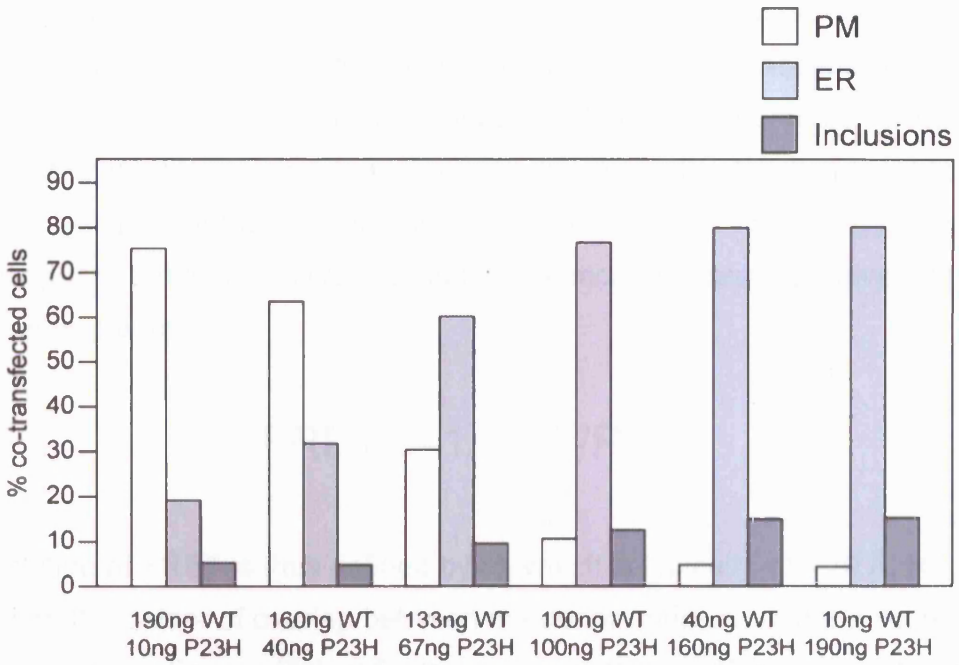

Figure 3.9 The dominant-negative effect of the P23H rod opsin on the wild-type protein can be observed at low levels of P23H plasmid DNA relatively to WT rod opsin.

SK-N-SH cells were co-transfected with various relative ratios of untagged WT and P23H-GFP rod opsin. After 24 hours immunocytochemistry was carried out using the rhodopsin antibody 1D4. The cellular localisation of WT rod opsin in co-transfected cells was assessed and scored as plasma membrane (PM), ER, and inclusions.

3.2.8 Measurement of the interaction between WT and P23H rod opsin by fluorescence resonance energy transfer (FRET)

An interesting application of fluorescent proteins is their use in fluorescence resonance energy transfer (FRET) which is a quantum physical process in which energy is transferred from one fluorophore (donor) to another (acceptor). The sensitivity to distance and orientation makes FRET an ideal method to identify protein-protein interactions, such as any potential interactions between wild-type and P23H rod opsin or the aggregation of mutant rod opsin. The energy transfer efficiency (FRETeff) is directly related to the distance *r* separating a given donor and acceptor pair by:

$$FRET_{eff}=1/[1+(r/R_0)^6]$$

The resolution of FRET is thus defined by R_0 which is typically <10-70 Å. R_0 depends on the extent of overlap between the donor emission and the acceptor spectra, the absorption coefficient for the acceptor, the quantum yield of the donor, and the relative orientation of the donor and acceptor. In any case, when distances separating donor and acceptor are superior to $2R_0$, no FRET can occur. From this, it is possible to distinguish between two proteins being present in the same cellular compartment for instance, from those undergoing specific protein-protein interactions. FRET acceptor bleaching involves measuring the donor "de-quenching" in the presence of an acceptor. This can be done by comparing donor fluorescence intensity in the same sample before and after destroying the acceptor by photobleaching. If FRET was initially present, a resultant increase in donor fluorescence will occur on photo bleaching of the acceptor. The energy transferred efficiency can be quantified as:

$$FRETeff= (Dpost-Dpre)/Dpost$$

where Dpost is the fluorescence intensity of the donor after acceptor photobleaching, and Dpre the fluorescence intensity of the donor before acceptor photobleaching. The FRETeff is considered positive when Dpost > Dpre.

Rajan and Kopito (2005) have reported that co-expression of wild-type (YFP) and P23H (CFP) rod opsin in HEK-293 cells resulted in FRET in solution indicating a close interaction between the rod opsin species. However, a major unresolved question of that study was where within the cell the interaction between the P23H and the wild-type protein was occurring. It could either happen in the ER leading to wild-type rod opsin misfolding and the arrest of processing or is the processing inhibited as a result of subsequent aggregation possibly leading to co-aggregation in the cytoplasm and in inclusions.

In order to address these questions and test if FRET could be used to monitor aggregation wild-type and P23H rod opsin were inserted into pECFP-N1 and pEYFP-N1 vectors as described in Chapter 2. In preparation for the FRET assay, cells were seeded on Matek dishes and transfected with WT-CFP + WT-YFP, WT-CFP + P23H-YFP and P23H-CFP + P23H-YFP for 24 hours prior to bleaching. FRET measurements were carried out by comparing donor fluorescence intensity (CFP) in the same sample before and after destroying the acceptor (YFP) by photo bleaching. Importantly, FRET was detected in inclusions of SK-H-SH cells expressing P23H-CFP and P23H-YFP (Figure 3.10e). However, the FRET signal was too weak to be detected outside the inclusions possibly due to low CFP expression/detection levels. Although is was not clear why this was the case, CFP expression levels were consistently lower than the YFP counterparts even when using the CFP vector alone suggesting that there might have been a malfunction or an incorrect alignment of the CFP laser in the confocal microscope set up. A solution-based FRET assay was also attempted but low signal to noise ratio resulted in poor reproducibility.

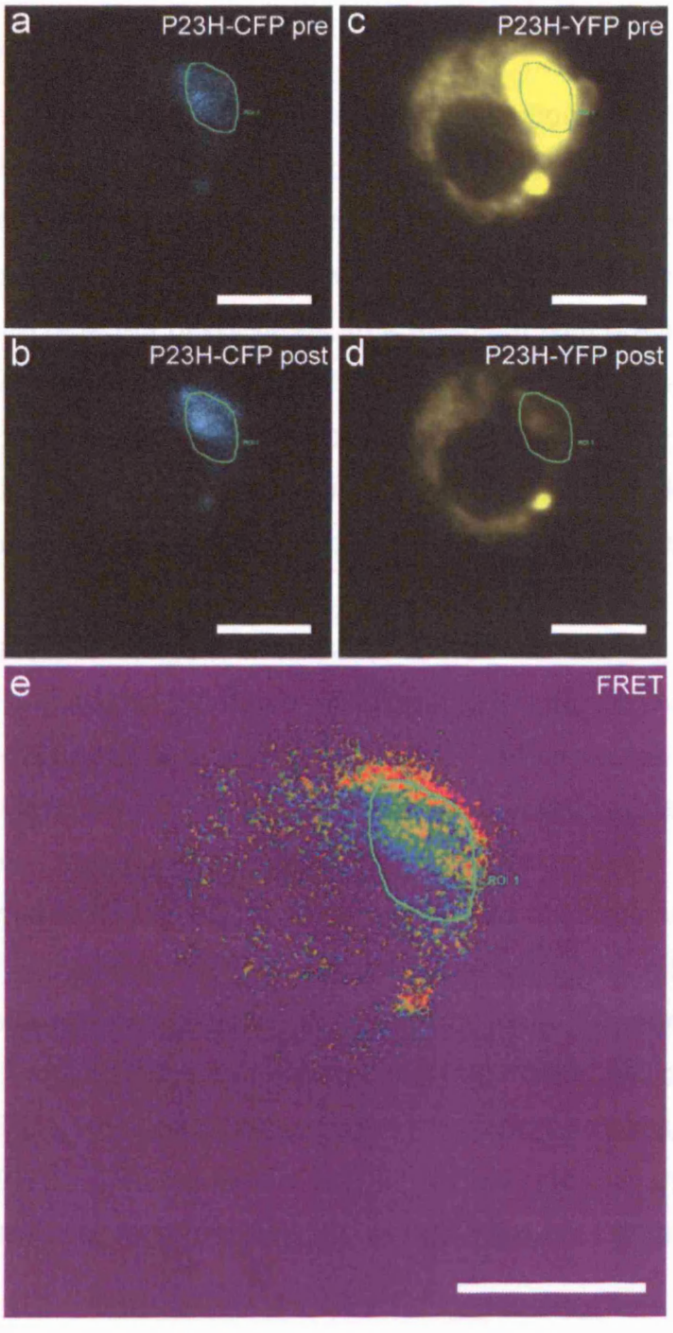

Figure 3.10 Fluorescence resonance energy transfer (FRET) was detected in P23H rod opsin inclusions.

SK-N-SH cells co-expressing with P23H-CFP and P23H-YFP were bleached in highlighted region of interest (ROI) at a wavelength of 525 nm in live cells 24 hours after transfection (c-d) and resulted in energy transfer detected at 425 nm (a-b). e) FRET was detected in intracellular inclusions suggesting that both P23H opsin species were in close proximity (<70 Å). A thermal colour scale was used and 'hot' colours illustrate areas where FRET was measured. Scale bar = 10 μm.

3.3 Discussion

The detailed characterisation of the intracellular distribution of rod opsin in both cell and animal models is important as it can be used to characterise potential pathological mechanisms. The data described in this chapter have continued these studies and demonstrated that when expressed into SK-N-SH cells, wild-type and P23H rod opsin had different phenotypes. In agreement with previously published cell culture models (Saliba *et al.*, 2002; Illing *et al.*, 2002) wild-type rod opsin appeared to fold correctly and was translocated through the secretory pathway to the plasma membrane of the cell whereas P23H rod opsin most likely misfolded, was retained in the ER and coalesced into large intracellular inclusions.

Previous animal and cell culture models support the observations from the data presented here which suggested that misfolding and the possible cytotoxicity of the mutant protein could be major cause of cell death. Studies carried out in transgenic *Xenopus Laevis* expressing the P23H rod opsin have demonstrated that P23H rod opsin induced retinal degeneration whereas the expression of the wild-type rod opsin did not (Tam and Moritz, 2006). Moreover, P23H rod opsin was misfolded and predominantly present in the RIS, a pattern consistent with retention in the ER. The detrimental effect of mutant rod opsin on photoreceptor degeneration was also observed when transgenic mice expressed three N-terminus rod opsin mutations (V20G, P23H, P27L – VPP) on a homozygous rod opsin (-/-) background (Frederick *et al.*, 2001). This resulted in mutant protein retention in the ER and consequent inability to transport and support outer segment formation, leading to rod cell death.

The data presented in this chapter suggest that P23H rod opsin expression in SK-N-SH cells resulted in increased LDH release and caspase-3 activity when compared to the wild-type protein. Following fluorescent microscopy observations P23H rod opsin transfected cells always appeared less healthy even though the cell density and transfection efficiency were similar to that of wild-type rod opsin.

Furthermore, cells transfected with P23H rod opsin would start to die and 'float off' after 48 hours whereas wild-type transfected cells remained attached to the cell culture plastic.

There are several lines of evidence suggesting that Class II rod opsin mutants such as P23H might exert a dominant-negative effect on the processing and transport of WT rod opsin. Work carried out on the *Drosophila* NinaE-encoded Rh1 rhodopsin suggested that Class II mutants exerted a dominant-negative effect on wild-type rod opsin (Kurada *et al.*, 1998). A dominant-negative effect has recently been demonstrated in mammalian cells (Saliba *et al.*, 2002; Rajan and Kopito, 2005) and was confirmed in our model with P23H rod opsin affecting the normal processing of wild-type rod opsin to the secretory pathway. The presence of this dominant-negative effect of the P23H rod opsin on the wild-type suggested that when attempting to manipulate mutant rod opsin using pharmacological agents it might be required to restrict this interaction between wild-type and Class II mutants, and as well as reversing misfolding of the mutant protein or the consequences of misfolding.

The fact that FRET could only be measured in inclusions prevented the investigation of protein-protein interactions outside the inclusions and consequently prevented the biophysical assessment of where within the cell was the interaction between the P23H and the wild-type protein occurring. Consequently FRET could not be used to test drugs for a potential suppression of the dominant-negative interaction between the P23H and the wild-type protein.

The following chapters describe the effects of different classes of pharmacological compounds on the morphology, biochemistry and cell death of wild-type and P23H, and K296E rod opsin. This was achieved exploring the two potential mechanisms of cell death in photoreceptor degeneration which result in misfolding, aggregation and toxicity associated to Class II mutations: gain-of-function and dominant-negative effects on wild-type protein. The next chapter describes the effects of

retinoids, which are pharmacological chaperones for rod opsin, on the wild-type and P23H protein.

Chapter 4: Pharmacological chaperones

4.1 Introduction

As many of the misfolding disease-causing proteins may not be inherently non-functional, several therapeutic strategies have involved assisting their folding and consequent trafficking though the secretory pathway. One of these strategies uses a group of compounds named pharmacological chaperones and aims to overcome folding defects in processing mutants by binding to substrate molecules. Impaired trafficking of lysosomal hydrolases to late endosomes causes lysosomal storage diseases in humans. Fabry disease, for example, is caused by the lysosomal deficiency of α-galactosidase (α-Gal A) which results in lysosomal accumulation of glycosphingolipid globotriosylceramide Gb3 (Brady *et al.*, 1967). Pharmacological chaperone treatment with 1-deoxygalactonorijimycin (1-DGJ), which acts as a competitive inhibitor of α-Gal A, stabilised and corrected the trafficking defect of misfolded α-Gal mutants (Yam *et al.*, 2005).

It has been suggested that pharmacological selective compounds can rescue cell surface expression and function of GPCR misfolding mutants. Vitamin A supplementation reduced the course of photoreceptor degeneration in transgenic mice carrying the dominant rod opsin mutation T17M (Li *et al.*, 1998). Other studies investigated V2 vasopressin receptor (V_2R) mutants which failed to fold properly and therefore were not routed to the cell surface (Morello *et al.*, 2000). These mutants are responsible for nephrogenic diabetes insipidus (NDI), a rare X-linked disease characterised by a loss of anti-diuretic response to the hormone arginin-vasopressin resulting in the inability of affected patients to concentrate their urine, leading to large urinary output. Treatment of HEK-293 cells expressing V_2R with the non-peptidic V2R antagonists SR121463A and VPA-985 increased cell-surface expression and rescued the function of V_2R mutants by promoting their proper folding and consequent maturation (Morello *et al.*, 2000). Pharmacological chaperones were also used to rescue ER-retained gonadotropin-releasing

hormone receptor (GnRHR) mutants responsible for hypogonadotropic hypogonadism (Janovick *et al.*, 2002). As with the V_2R mutants, treatment with a receptor antagonist restored cell-surface expression and signalling activity in a variety of GnRHR mutants tested.

Vitamin A has long been known to be fundamental for several important functions such as vision, embryonic growth and development and immune competence (reviewed in Blomhoff and Blomhoff, 2006). 11-*cis*-retinal, an aldehyde form of vitamin A, initiates phototransduction by a photochemical reaction where opsin-bound 11-*cis*-retinal is isomerised to all-*trans*-retinal. Retinoids are a class of compounds which encompass retinoid analogs, with or without biological activity, and other compounds which are not closely related to retinol but elicit biological vitamin A or retinoid activity.

A potential therapeutic strategy for Class II ADRP patients is to use retinoids as pharmacological chaperones which would correct the misfolding of mutant rod opsin by binding specifically to its non-native and native forms. Previous studies suggested that a vitamin A supplemented diet reduced the rate of decline of both ERG's a-wave and b-wave in the Class II T17M transgenic mice but had no effect on the ERG amplitude in the Class I P347S mice (Li *et al.*, 1998). Furthermore, treatment of COS-7 cells with 9-*cis*-retinal increased the amount of P23H rod opsin reaching the plasma membrane of the cells (Saliba *et al.*, 2002). Addition of 11-*cis*-7-ring retinal, a 7-membered ring analogue of 11-*cis*-retinal, in stable cell lines expressing P23H rod opsin also resulted in the folding of mutant opsin and consequent translocation through the secretory pathway (Noorwez *et al.*, 2003). These data suggested that the addition of some retinoids during the course of protein biosynthesis might induce a more native-like folding of the mutant protein. A similar effect was observed when 9-*cis*-retinal and 11-*cis*-retinal were added to stable cell lines during rod opsin synthesis which resulted in increased folding and consequent translocation to the plasma membrane (Noorwez *et al., 2004)*. In this chapter the effects of retinoids on the cell model of rhodopsin RP are assessed.

The retinoids used were the chromophore, 11-*cis*-retinal, and its functional geometric isomer, 9-*cis*-retinal whose structures are shown in Figure 4.1.

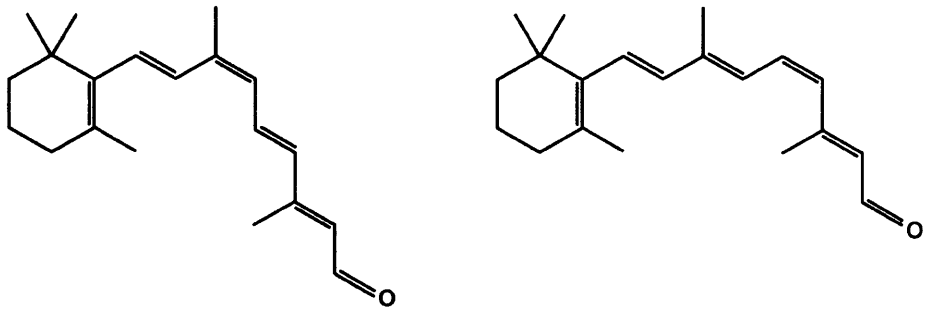

9-*cis*-retinal 11-*cis*-retinal

Figure 4.1 Representation of the molecular structure of 9-*cis*-retinal and 11-*cis*-retinal.

4.2 Results

4.2.1 Retinoids reduce inclusion incidence and promote the trafficking of P23H rod opsin through the secretory pathway

The effect of 9-*cis*-retinal and 11-*cis*-retinal on P23H rod opsin folding was analysed in the cell model of rhodopsin RP. The addition of retinoids and consequent incubation period were carried out in the dark in order to prevent the isomerisation of the compounds. SK-N-SH cells expressing P23H rod opsin were treated with different concentrations of 9-*cis*-retinal and 11-*cis*-retinal ranging from 2 μM to 20 μM which were determined based on previously published studies. The optimal concentration, determined in terms of reduction of inclusion incidence, was 10 μM for both 9-*cis*-retinal and 11-*cis* retinal. Treatment with both 9-*cis*-retinal and 11-*cis*-retinal had no effect in cells expressing wild-type rod opsin with the majority of cells showing plasma membrane staining (Figure 4.2a-c). In P23H cells, however, retinoids reduced inclusion incidence and promoted the trafficking of P23H rod opsin to the plasma membrane of the cells (Figure 4.2d-f). This effect was not seen in cells expressing K296E rod opsin where no morphological changes were observed as a result of treatment with retinoids (Figure 4.2g-i). This suggested that retinoids lost their efficacy when the site of retinal attachment was disrupted and their effect on inclusion incidence required binding to rod opsin.

In cells expressing P23H rod opsin treatment with 9-*cis*-retinal reduced inclusion incidence from 26.92% ± 5.18 in the controls to 10.07% ± 7.48 ($p \leq 0.005$) suggesting an alleviation of the gain-of-function mechanism in this Class II mutation (Figure 4.3a). Treatment with 11-*cis*-retinal reduced the inclusion incidence to 9.63% ± 2.03 ($p \leq 0.001$) of transfected cells (Figure 4.3a). In addition to a reduction in inclusion incidence there was a significant change in cellular morphology as 58.29% ± 9.99 ($p \leq 0.001$) of P23H cells treated with 9-*cis*-retinal (Figure 4.3b) and 42.29% ± 10.50 ($p \leq 0.001$) of cells treated with 11-cis-retinal (Figure 4.3b) showed plasma membrane staining in contrast with the vehicle-treated controls where no cells showed predominant plasma membrane staining.

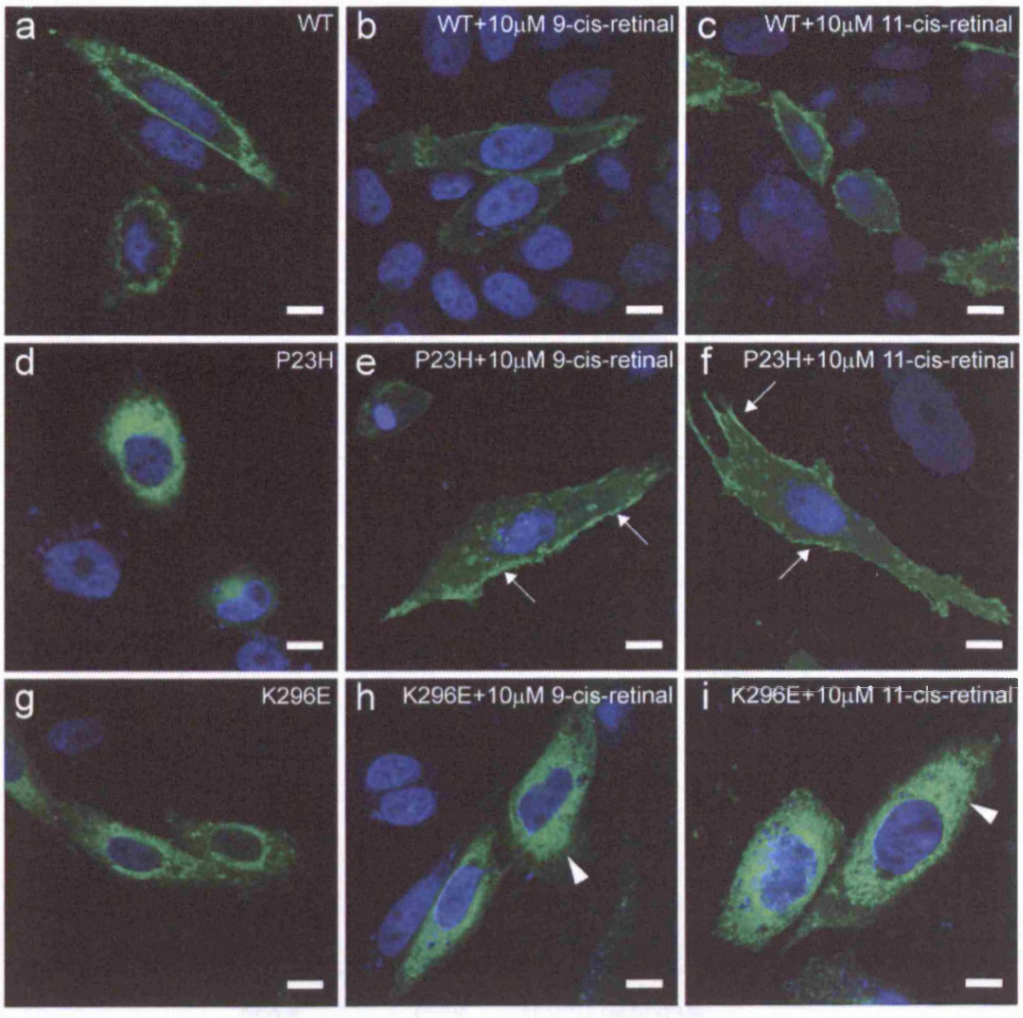

Figure 4.2 Retinoids promote translocation of P23H rod opsin to the plasma membrane of the cell.

Morphological assessment of SK-N-SH cells expressing WT-GFP (a-c), P23H-GFP (d-f), and K296E-GFP (g-i) and treated with retinoids as indicated for 24 hours post transfection and then fixed with 3.7% paraformaldehyde. All controls were vehicle-treated and this resulted in no observable phenotypical change. Treatment with either 10 μM 9-*cis*-retinal or 10 μM 11-*cis*-retinal resulted in no morphological change in cells expressing the WT protein with the majority showing plasma membrane staining. In P23H cells 9-*cis*-retinal and 11-*cis*-retinal reduced inclusion incidence and facilitated the processing of the mutant opsin to the plasma membrane (arrows). Treatment with retinoids resulted in no morphological changes in cells expressing K296E rod opsin where the protein was either retained in the ER (arrowheads) or accumulated in large intracellular inclusions. GFP fluorescence is represented in green and DAPI staining is represented in blue. Scale bar = 10 μm.

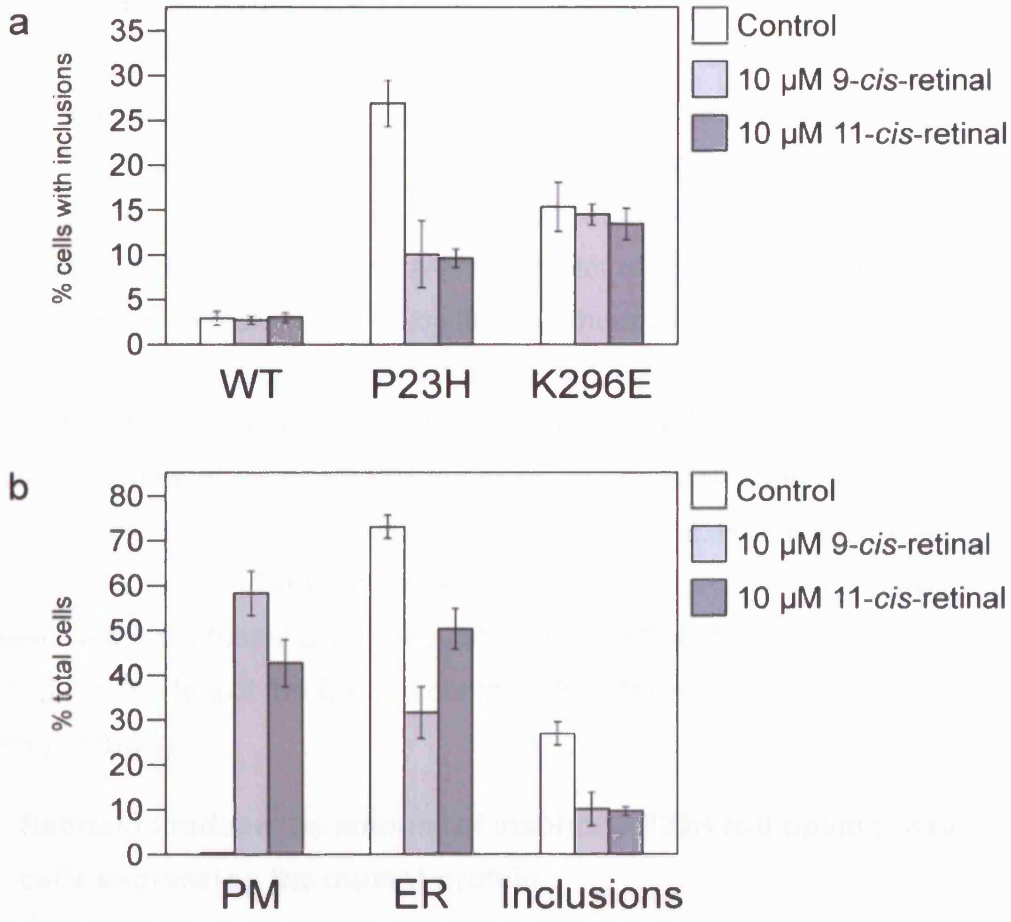

Figure 4.3 9-*cis*-retinal and 11-*cis*-retinal reduce inclusion incidence in P23H cells and promote the translocation of P23H rod opsin to the plasma membrane.

a) The inclusion incidence in SK-N-SH cells expressing WT-GFP, P23H-GFP and K296E-GFP rod opsin was assessed following treatment with retinoids as indicated for 24 hours. Retinoids had no effect in the incidence of inclusions in cells expressing WT or K296E. 10 µM 9-*cis*-retinal ($p \leq 0.005$) and 10 µM 11-*cis*-retinal ($p \leq 0.001$) reduced inclusion incidence in P23H cells. b) Morphological assessment of P23H cells following treatment with retinoids. 10 µM 9-*cis*-retinal ($p \leq 0.001$) and 10 µM 11-*cis*-retinal ($p \leq 0.001$) promoted the translocation of P23H rod opsin to the plasma membrane of the cells. Error bars represent ± 2SE.

4.2.2 Treatment with 9-*cis*-retinal and 11-*cis*-retinal increase the amount of soluble rod opsin in P23H cells

A biochemical characterisation of soluble rod opsin species present following the treatment with retinoids was carried out. SK-N-SH cells expressing untagged wild-type and P23H rod opsin were treated with 10 μM 9-*cis*-retinal or 10 μM 11-*cis*-retinal for 24 hours prior to lysis using 4°C 1% Triton X-100 in PBS plus protease inhibitor cocktail. Figure 4.4 shows a Western blot of soluble wild-type and P23H rod opsin species immunodetected by the anti-rhodopsin antibody 1D4. Treatment with retinoids failed to increase the amount of soluble wild-type rod opsin and the majority of these species were EndoH resistant (Figure 4.4a). In contrast, increased amounts of soluble P23H rod opsin were detected following treatment with 9-*cis*-retinal and 11-*cis*-retinal (Figure 4.4b). The P23H rod opsin species which migrated to ~36 kDa were rendered EndoH resistant (arrow) following treatment with 9-*cis*-retinal and 11-*cis*-retinal suggesting that these species were sufficiently folded to exit the ER and continue their translocation through the secretory pathway.

4.2.3 Retinoids reduce the amount of insoluble P23H rod opsin present in cells expressing the mutant protein

The effect of retinoids on the amount of insoluble rod opsin species was analysed by carrying out a rod opsin fractionation assay as described in Chapter 3. The total rod opsin levels were ~50% lower in P23H cells than in wild-type cells and the treatment with 9-*cis*-retinal and 11-*cis*-retinal did not affect the overall levels of wild-type or mutant rod opsin (Figure 4.5a). However, when the insoluble rod opsin was assessed (Figure 4.5b), retinoids reduced the percentage of insoluble protein from 60.57% ± 3.92 in the vehicle-treated controls to 38.73% ± 2.41 ($p \leq 0.005$) following treatment with 9-*cis*-retinal and 32.44% ± 1.91 ($p \leq 0.005$) following treatment with 11-*cis*-retinal. These reduced levels of insoluble P23H rod opsin were in agreement with the reduction in inclusion incidence observed following retinoid treatment.

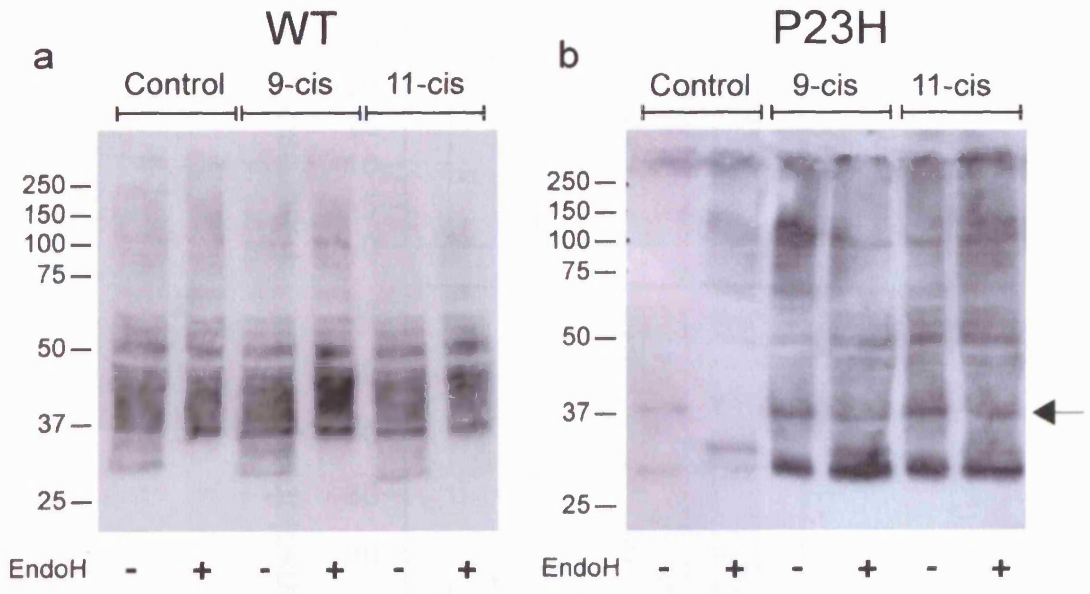

Figure 4.4 Treatment with retinoids results in an increase of soluble P23H rod opsin species which are EndoH resistant.

SK-N-SH cells expressing WT-pMT3 (a) or P23H-pMT3 (b) were treated with 10 μM 9-*cis*-retinal or 10 μM 11-*cis*-retinal as indicated for 24 hours prior to lysis with 1% Triton-X 100. 10 μg of protein from Triton-X soluble fractions were resolved on a 10% SDS-PAGE gel followed by immunoblotting with 1D4 anti-rhodopsin antibody. a) Soluble WT rod opsin levels were unchanged following treatment with 9-*cis* retinal or 11-*cis*-retinal. b) Retinoids increased the levels of soluble P23H rod opsin and resulted in the detection of EndoH resistant species (arrow). The position of molecular markers in kDa is shown on the left.

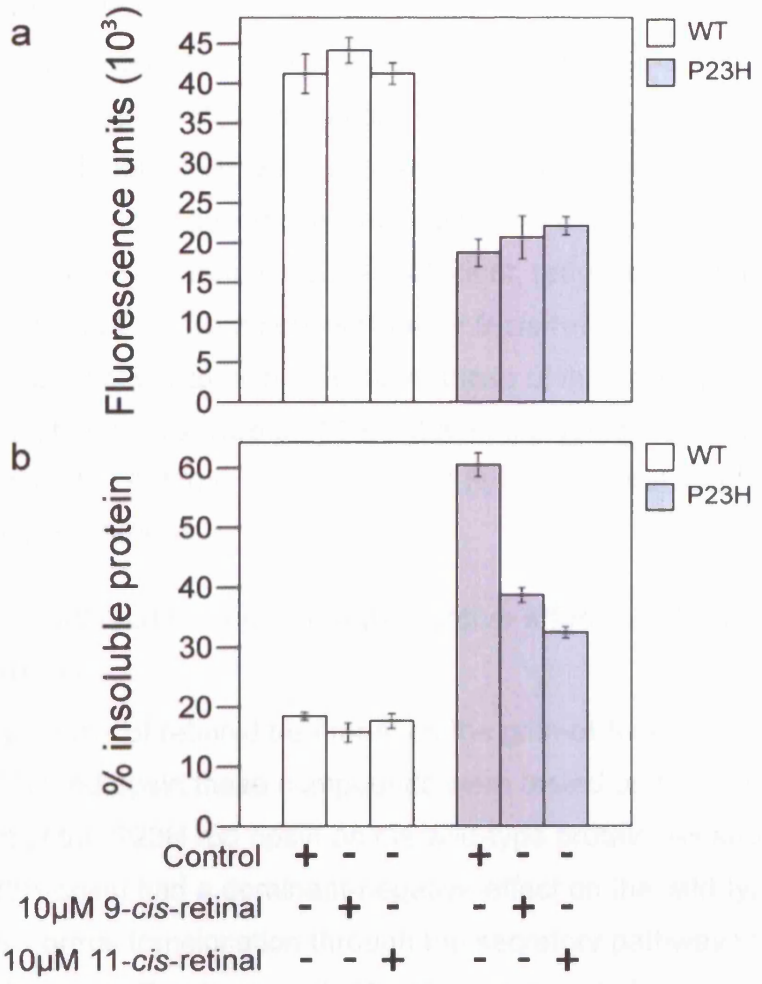

Figure 4.5 Treatment with retinoids decreases the amount of insoluble P23H rod opsin.

SK-N-SH cells expressing WT-GFP or P23H-GFP were treated with retinoids for 24 hours prior to lysis with 190 μl of RIPA buffer + 10 μl protease inhibitor cocktail and spectro-fluorometric analysis. a) 10 μM 9-*cis*-retinal and 10 μM 11-*cis*-retinal did not significantly alter the total levels of either the WT or the P23H cells. b) 9-*cis*-retinal ($p \leq 0.005$) and 11-*cis*-retinal ($p \leq 0.005$) reduced the amount of insoluble P23H rod opsin. Retinoids had no effect in the insoluble levels of the WT protein. Error bars represent ± 2SE.

4.2.4 9-*cis*-retinal and 11-*cis*-retinal reduce LDH release and caspase-3 activity in cells expressing P23H rod opsin

In order to assess if retinoids had a positive effect on the gain-of-function mechanism induced by the P23H mutation, LDH release (Figure 4.6a) and caspase-3 activity (Figure 4.6b) were assessed in cells treated with these compounds. 9-*cis*-retinal reduced LDH release from 0.515 ± 0.037 to 0.172 ± 0.014 ($p \leq 0.001$) whereas 11-*cis*-retinal was less efficient, reducing LDH release to 0.322 ± 0.032 ($p \leq 0.005$). Treatment with either 9-*cis*-retinal or 11-*cis*-retinal reduced caspase-3 activity to levels similar to those of the wild-type protein. Caspase-3 activation levels were 0.967 ± 0.226 in the vehicle-treated controls and those were reduced to 0.370 ± 0.137 ($p \leq 0.01$) by 9-cis-retinal and 0.265 ± 0.102 by 11-*cis*-retinal ($p \leq 0.005$).

4.2.5 Retinoids alleviate the dominant-negative effect of P23H on the wild-type protein

Following the analysis of retinoid treatment on the gain-of-function mechanism induced by P23H rod opsin these compounds were tested on the dominant-negative effect of the P23H rod opsin on the wild-type protein. As shown in Chapter 3, P23H opsin had a dominant-negative effect on the wild-type protein as it prevented its normal translocation through the secretory pathway to the plasma membrane of the cells. Treatment with 10 µM 9-*cis*-retinal (Figure 4.7d-f) or 10 µM 11-*cis*-retinal (Figure 4.7g-i) appeared to suppress this effect as an increased number of co-transfected cells had the wild-type protein present on the plasma membrane. The morphological assessment of the effect of retinoids on the cellular morphology of cells expressing wild-type and P23H rod opsin is shown in Figure 4.8. Treatment with 9-*cis*-retinal resulted in an increase in the percentage of co-transfected cells showing the wild-type protein on the plasma membrane from 15.28% ± 3.86 in the vehicle-treated controls to 57.44 ± 5.44 ($p \leq 0.001$). 11-*cis*-retinal also alleviated the dominant-negative effect of the P23H rod opsin on the

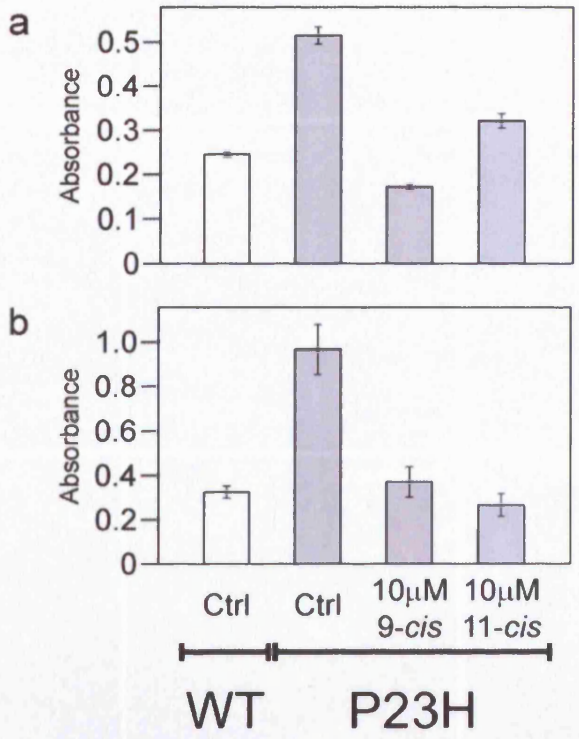

Figure 4.6 9-*cis*-retinal and 11-*cis*-retinal reduce LDH release and caspase-3 activity in cells expressing P23H rod opsin.

a) SK-N-SH cells expressing P23H rod opsin had higher LDH release levels when compared to WT cells. Treatment with 10 μM 9-*cis*-retinal ($p \leq 0.001$) reduced LDH release in P23H cells to WT levels and 10 μM 11-*cis*-retinal was less efficient, reducing LDH release by ~35% ($p \leq 0.005$). b) P23H cells had increased levels of caspase-3 activity when compared to WT. Treatment with 10 μM 9-*cis*-retinal ($p \leq 0.01$) and 10 μM 11-*cis*-retinal ($p \leq 0.005$) reduced caspase-3 activity to levels similar to WT. Error bars represent ± 2SE.

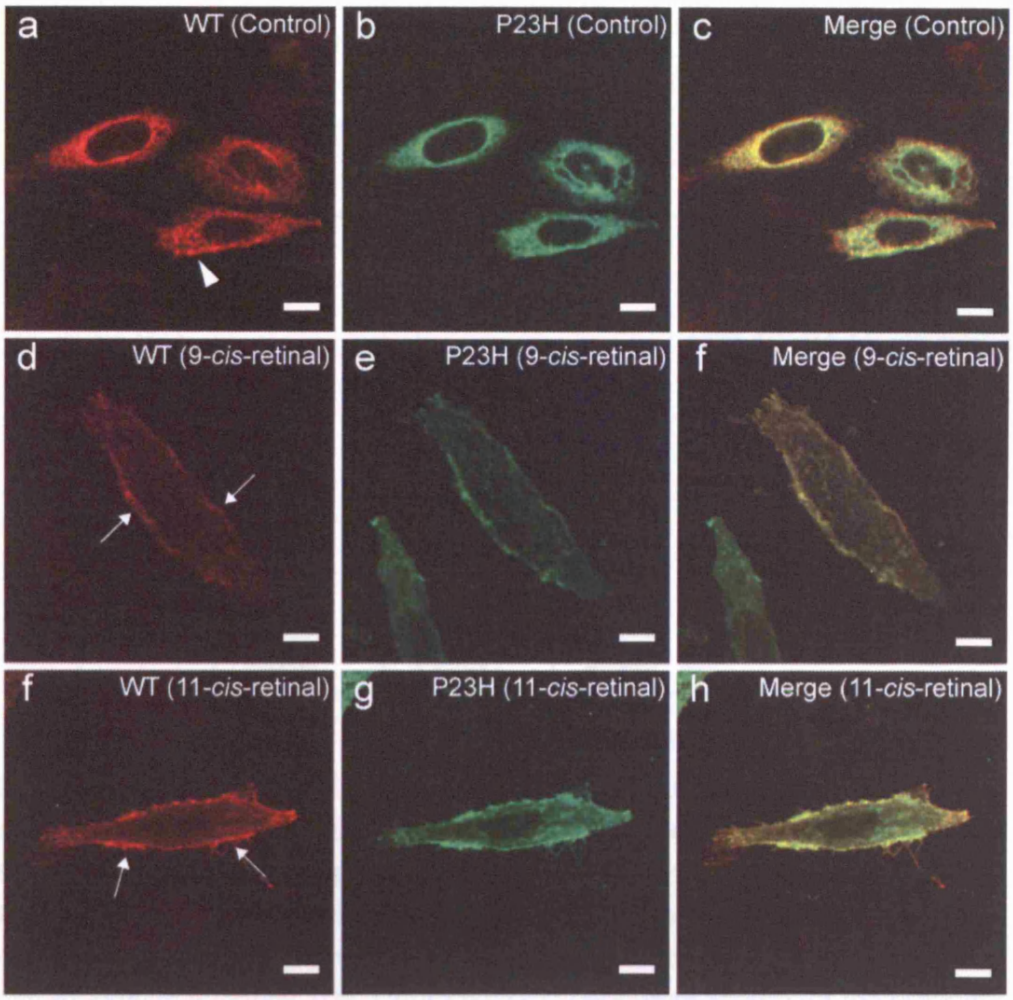

Figure 4.7 Retinoids suppress the dominant-negative effect of the P23H mutant on the WT protein and promote the translocation of the WT rod opsin to the plasma membrane.

Confocal imaging of SK-N-SH cells co-transfected with untagged WT rod opsin and GFP-tagged P23H opsin and treated with retinoids as indicated for 24 hours. The red channel represents 1D4 immunostaining and the green channel represents GFP staining. Co-transfection of WT and P23H opsin resulted in an impairment of the normal trafficking of the WT opsin through the secretory pathway towards the plasma membrane of the cell (arrowhead) (a-c). Treatment with 10 μM 9-*cis*-retinal (d-f) and 10 μM 11-*cis*-retinal (g-i) appeared to supress the dominant-negative effect of the mutant protein on the WT rod opsin resulting in WT plasma membrane staining (arrows). Scale bar = 10 μm.

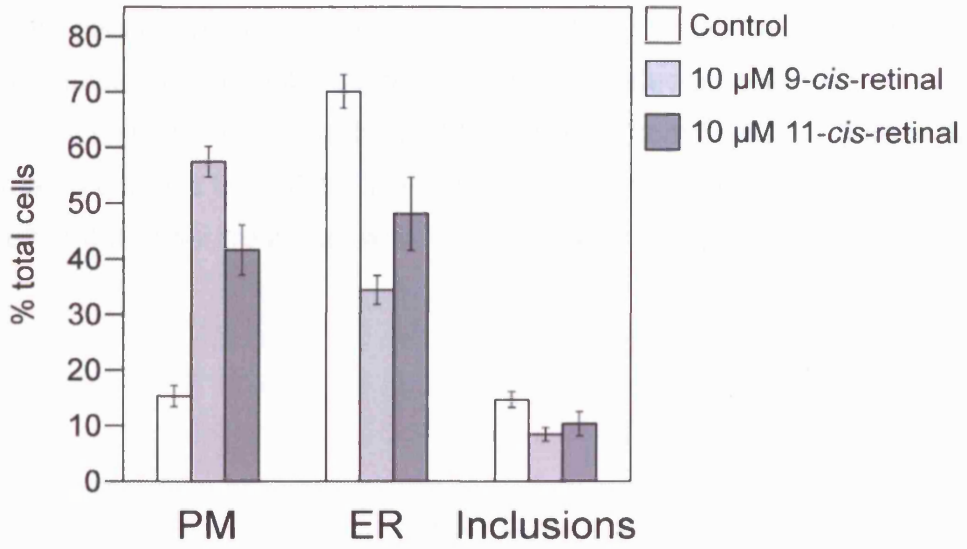

Figure 4.8 Morphological assessment of the effect of retinoids on the dominant-negative effect of P23H rod opsin on the WT protein.
SK-N-SH cells were transfected with equal amounts of WT-pMT3 and P23H-GFP plasmids followed by treatment with 10 µM 9-*cis*-retinal or 10 µM 11-*cis*-retinal as indicated for 24 hours prior to fixation and immunostaining with the anti-rhodopsin antibody 1D4. Co-transfected cells were scored for the predominant cellular localisation of the WT protein. 10 µM 9-*cis*-retinal ($p \leq 0.001$) and 10 µM 11-*cis*-retinal ($p \leq 0.005$) promoted the translocation of the WT protein to the plasma membrane of the cells. Furthermore, 10 µM 9-*cis*-retinal ($p \leq 0.01$) and 10 µM 11-*cis*-retinal reduced the incidence of inclusions containing the WT protein. Error bars represent ± 2SE.

wild-type protein, albeit not to the extent of 9-*cis*-retinal, as 41.59% ± 8.96 ($p \leq 0.005$) of the co-transfected cells had wild-type rod opsin on the plasma membrane. These results correlate with the effect of retinoids on P23H rod opsin alone where 9-*cis*-retinal and 11-*cis*-retinal promoted the translocation of the P23H protein to the plasma membrane of 58.29% and 42.29% of the cells respectively. In addition retinoids reduced the percentage of co-transfected cells with intracellular inclusions containing the wild-type protein from 14.63% ± 2.88 in the vehicle-treated controls to 8.40% ± 2.44 ($p \leq 0.01$) after treatment with 9-*cis*-retinal and 10.30% ± 4.35 after treatment with 11-*cis*-retinal (not significant).

4.3 Discussion

The data presented here indicate that 9-*cis*-retinal and 11-*cis*-retinal can act as pharmacological chaperones by increasing the amount of correctly folded P23H rod opsin that can exit the ER. This had a positive effect in both the gain-of-function and dominant-negative mechanisms induced by the P23H rod opsin. For the gain-of function mechanism of P23H rod opsin this was demonstrated by the reduction in inclusion incidence, the presence of mature glycosylated rod opsin species in soluble cell lysates, and protective effects against LDH release and caspase-3 activity. In the dominant-negative mechanism the interaction between wild-type and P23H rod opsin was suppressed resulting in the increased presence of wild-type protein in the plasma membrane of co-transfected cells and reduction in inclusions which contained the wild-type protein. Saliba *et al* (2002) added 9-*cis*-retinal to cells expressing P23H rod opsin 16 hours after transfection and observed increased levels mature rod opsin in the soluble fraction measured by Western blotting and increased P23H rod opsin present in the plasma membrane of COS-7 cells. However, these authors did not observe a decrease of inclusion incidence following the incubation with 9-*cis*-retinal. This suggested that although the ligand can be used to promote mutant rod opsin folding and prevent its degradation, once a rod opsin inclusion has formed treatment with ligand cannot disaggregate it.

9-*cis*-retinal, an isomer of 11-*cis*-retinal, has been widely used for vision experiments due to its ease of synthesis *in vitro* and consequent ready availability. The rod pigment formed with 9-*cis*-retinal, isorhodopsin, is photosensitive and appears to be very similar to rhodopsin as determined by both *in vitro* studies and *in vivo* studies using isolated photoreceptors (Corson *et al.*, 1990). One of the most abundant proteins in the RPE is RPE65 and when this protein is mutated or lacking, as in the RPE65 knockout ($Rpe65^{-/-}$) mouse the synthesis of 11-*cis*-retinal did not occur, however, a minimal photoreceptor response from rod photoreceptors was observed which appeared to be mediated by isorhodopsin (Fan *et al.*, 2003). Furthermore, $Rpe65^{-/-}$ mice kept in prolonged darkness had increased isorhodopsin

suggesting that there might be a pathway in the eye for the regeneration of this retinoid that is independent of the RPE and light (Fan *et al.*, 2003). The data presented in this Chapter suggested that both 9-*cis*-retinal and 11-*cis*-retinal had equal positive effects on both the gain of function and dominant-negative mechanisms induced by the P23H rod opsin. Consequently these data did not provide conclusive evidence on which of these compounds might be more beneficial for cells expressing the mutant rod opsin.

The data presented here correlates with previously published studies which suggested that the biosynthesis of P23H rod opsin and its incorporation into the plasma membrane could be rescued through the addition of 11-*cis*-retinal, or its analogues, such as 9-*cis*-retinal or 11-*cis*-7-ring retinal (Noorwez *et al.*, 2003; Noorwez *et al.*, 2004). These authors showed that all these three retinoids bind to P23H rod opsin via a Schiff base linkage to the chromophore binding site at Lys296 and allow for proper folding of the mutant protein. In addition, P23H rod opsin with 11-*cis*-retinal or 9-*cis*-retinal as chromophore responded to photon absorption albeit with a decrease in absorption at 500 nm and formation of intermediates absorbing at shorter wavelengths whereas 11-*cis*-7-ring retinal formed locked, non-photoisomerisable and non-bleachable form of P23H rhodopsin in cell membranes (Noorwez *et al.*, 2004). These *in vitro* studies also suggested that the binding of P23H rod opsin to all these ligands was very weak and resulted in poor thermal stability. In structural terms Pro^{23} is located in the intradiscal domain of rod opsin in close proximity to the retinal plug and it is likely that its replacement with a different amino acid might disrupt the retinal plug and alter its structure resulting in thermal instability. The data presented here suggests that retinoids might bind P23H rod opsin thereby stabilising it or they may bind non-native folding intermediaries acting as a scaffold for subsequent folding. These actions combined result in a shift in the folding equilibrium of P23H species towards a folded state which appeared to be beneficial to the cells.

Based on these *in vitro* data one can speculate that the susceptibility of P23H patients or VPP mice (Naash *et al.*, 1996) to light-induced retinal degeneration might be related to poor thermal stability of the P23H rod opsin and the release of 11-*cis*-retinal which could potentially have phototoxic effects. The poor thermal stability of P23H rod opsin suggests that it might be necessary to develop novel 11-*cis*-retinal analogues which allow the formation of a stable protein in the dark and functional phototransduction.

Chapter 5: Chemical Chaperones/Kosmotropes

5.1 Introduction

A variety of studies in the past 12 years have described the use of a group of low molecular weight compounds which reversed the mislocalisation or aggregation of proteins involved in a variety of human diseases associated with protein misfolding. These compounds have been named kosmotropes or chemical chaperones and include: polyols such as glycerol; solvents such as dimethyl sulfoxide (DMSO); methylamines such as trimethylamine-N-oxide (TMAO); fatty acids such as 4-phenylbutyric acid (4-PBA); and sugars such as trehalose among others. There are two mechanisms of action associated with these compounds. Firstly, these compounds might increase the hydration of proteins and consequently promote their stabilisation by enhancing the free-energy difference between a partially folded protein, which has a higher surface area, and a more compact native structure (Back *et al.*, 1979). Secondly, chemical chaperones might reduce the free movement of proteins to prevent aggregation of partially folded molecules (Singer and Lindquist, 1998).

The potential use of kosmotropes as a therapy for protein misfolding disorders initially involved the most common mutation in the gene encoding the cystic fibrosis transmembrane conductance regulator (CFTR) protein (ΔF508 CFTR) of cystic fibrosis patients (White *et al.*, 1990). Newly synthesised ΔF508 CFTR protein failed to fold correctly, was retained in the ER and did not translocate to the cell surface where it normally functioned as a cAMP-regulated chloride channel (Cheng *et al.*, 1990). Treatment of cells expressing the ΔF508 CFTR mutant with a number of chemical chaperones such as glycerol and TMAO resulted in the correct processing of the mutant CFTR protein and its appearance at the plasma membrane (Brown *et al.*, 1996).

This folding defect was temperature-dependent as the processing of ΔF508 CFTR reverted towards that of wild-type as the incubation temperature was reduced from 37°C to 30°C (Denning *et al.*, 1992). This led to appearance of cAMP-regulated chloride channels in the plasma membrane resulting in the cells acquiring competence for cAMP-stimulated chloride exchange, indicating a functional CFTR protein. This recovery was mimicked when cells were cultured in the presence of chemical chaperones such as glycerol, DMSO, and TMAO at 37°C (Powell and Zeitlin, 2002) suggesting the possibility of a therapeutic strategy based on these compounds.

Chemical chaperones have also been reported to reverse intracellular retention of several other misfolded proteins such as α-antitrypsin (Burrows *et al.*, 2000), aquaporin-2 (Tamarappoo and Verkman, 1999), α-galactosidase A (Yam *et al.*, 2005), and P-glycoprotein (Loo and Clarke, 1997).

In addition, chemical chaperones have reduced aggregate formation in a model of Machado-Joseph disease/spinocerebellar ataxia-3 (MJD/SCA3) (Yoshida *et al.*, 2002) and in a model of autosomal dominant oculopharyngeal muscular dystrophy (OPMD) (Bao *et al.*, 2002). Furthermore, trehalose reduced polyglutamine aggregation in a mouse model of Huntington's disease (Tanaka *et al.*, 2004).

Kosmotropes were not effective in all experimental models, however, as a study by Yang and colleagues (1999) demonstrated that treatment with glycerol and TMAO resulted in a rapid acceleration of the Aβ peptide assembly into fibrillar structures, which are a central feature of Alzheimer's disease. An overall assessment of these data, however, suggested that chemical chaperones could potentially rescue a variety of nuclear, cytoplasmic, cell surface and secreted proteins from protein misfolding events. These compounds could therefore be useful in rescuing misfolded P23H rod opsin. This Chapter describes the effect of DMSO, TMAO, 4-PBA and trehalose in the cellular model for rhodopsin RP. The molecular structures of these chemical chaperones are shown in Figure 5.1.

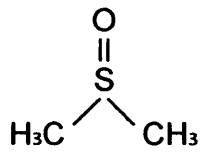

Dimethyl sulphoxide (DMSO)

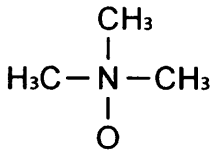

Trimethylamine-N-oxide (TMAO)

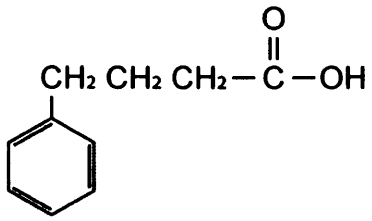

4-Phenylbutyric acid (4-PBA)

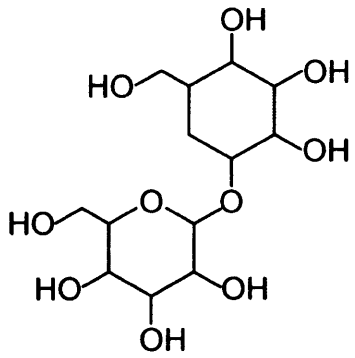

Trehalose

Figure 5.1 Representation of the molecular structures of the chemical chaperones dimethyl sulphoxide (DMSO), trimethylamine-N-oxide (TMAO), 4-phenylbutyric acid (4-PBA) and trehalose.

5.2 Results

5.2.1 Effect of chemical chaperones on inclusion incidence and cellular morphology in P23H-transfected cells

5.2.1.1 Dimethyl sulphoxide (DMSO)

Prior to treatment with chemical chaperones, SK-N-SH cells were transfected with WT-GFP or P23H-GFP rod opsin as described in Chapter 2. DMSO had a positive effect on P23H rod opsin inclusion incidence after 24 hours. Treatment with DMSO led to a dose-dependent decrease in inclusion incidence. The lowest concentration of DMSO to have an effect on inclusion incidence was 0.025%. The largest decrease in inclusion incidence was achieved using 0.25% DMSO which reduced inclusion incidence from 27.44% ± 5.58 in the untreated controls to 6.63% ± 1.05 ($p \leq 0.001$) (Figure 5.2). Using concentrations higher than 0.25% DMSO failed to reduce the incidence of inclusions further. The same DMSO dose-response curve was carried out in cells expressing wild-type rod opsin and no differences were observed in the cellular morphology at concentrations lower than 0.25% (Figure 5.2c). When cells were treated with concentrations of DMSO higher than 0.25% and observed before fixation, increased levels of rounded cells detached from the culture surface which appeared to be in osmotic shock were seen. This effect appeared to be non-specific as it was observed in both the wild-type and P23H cells. Treatment with 0.25% DMSO, however, did not appear to promote the translocation of P23H rod opsin to the plasma membrane of the cells (Figure 5.2e).

5.2.1.2 Trimethylamine-N-oxide (TMAO)

Treatment with TMAO for 24 hours resulted in a dose-dependent decrease in inclusion incidence in cells expressing P23H rod opsin. The lowest concentration of TMAO to have a positive effect on inclusion incidence was 50 μM. The most effective concentration was 5 mM which resulted in the largest decrease in inclusion incidence from 27.35% ± 2.56 in the untreated controls to 6.52% ± 1.21 ($p \leq 0.001$)

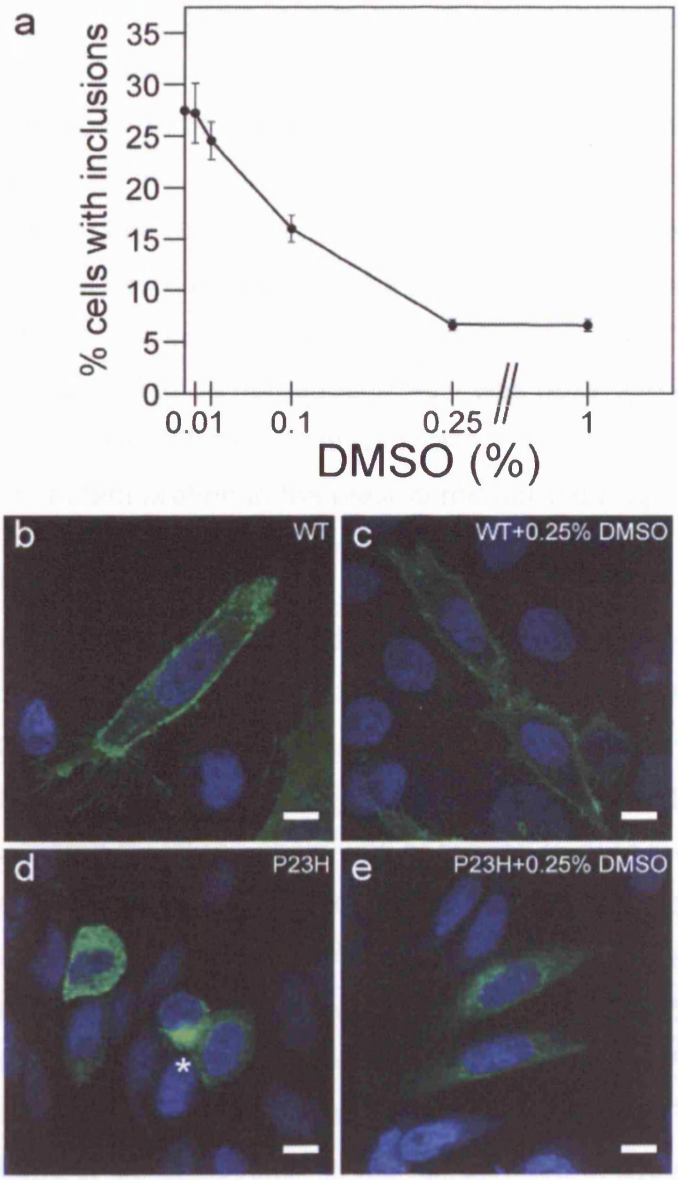

Figure 5.2 Dimethyl sulphoxide (DMSO) reduces inclusion incidence in cells expressing P23H rod opsin.

a) SK-N-SH cells expressing P23H-GFP rod opsin were treated with different concentrations of DMSO (percentage of w/v) for 24 hours. The most effective concentration was 0.25% DMSO which reduced inclusion incidence from 27.44% ± 5.58 in the untreated controls to 6.63% ± 1.05 ($p \leq 0.001$). Error bars represent ± 2SE. b-e) DMSO reduced inclusion incidence in P23H cells but did not promote the translocation of the mutant protein to the plasma membrane of the cells. Asterisks highlight inclusions. Scale bar = 10 μm.

(Figure 5.3a). TMAO treatment had no effect on inclusion incidence in cells expressing wild-type rod opsin when used at a concentration lower than 5 mM (Figure 5.3c). Higher concentrations of TMAO did not appear to decrease the incidence of inclusions further. When cells treated with higher doses of TMAO were observed after 24 hours before fixation, increased levels of rounded cells detached from the culture surface which appeared to be in osmotic shock were seen although this effect was less severe than the one seen with DMSO. This detrimental effect appeared to be non-specific as it was observed in both wild-type and P23H cells. As with DMSO, treatment with TMAO did not appear to elicit the translocation of the mutant protein to the plasma membrane (Figure 5.3e).

5.2.1.3 4-Phenylbutyric acid (4-PBA)

4-PBA is a low molecular weight fatty acid which has been reported to act as a chemical chaperone that reduced the amount of mutant proteins retained in the ER in conditions associated with cystic fibrosis (Rubenstein and Zeitlin, 1998) and liver injury (Vilatoba *et al.*, 2005). The effect of 4-PBA on inclusion incidence after 24 hours in cells expressing P23H rod opsin was assessed (Figure 5.4a). The lowest concentration of 4-PBA to have an effect on inclusion incidence was 1 mM and the concentration which resulted in the largest decrease in inclusion incidence was 10 mM. This led to a reduction in inclusion incidence from 24.52% ± 2.23 in the untreated controls to 5.95% ± 1.78 ($p \leq 0.001$). Treatment with 4-PBA showed no effect on wild-type cells at doses lower than 10 mM (Figure 5.4c).Treatment with higher concentrations of 4-PBA resulted in the appearance of dysmorphic cells, but not rounded and in osmotic shock as seen with high doses of DMAO and TMAO. This effect appeared to be non-specific as it was observed in both wild-type and P23H cells Treatment with 10 mM 4-PBA did not appear to promote the translocation of mutant protein to the plasma membrane (Figure 5.4e).

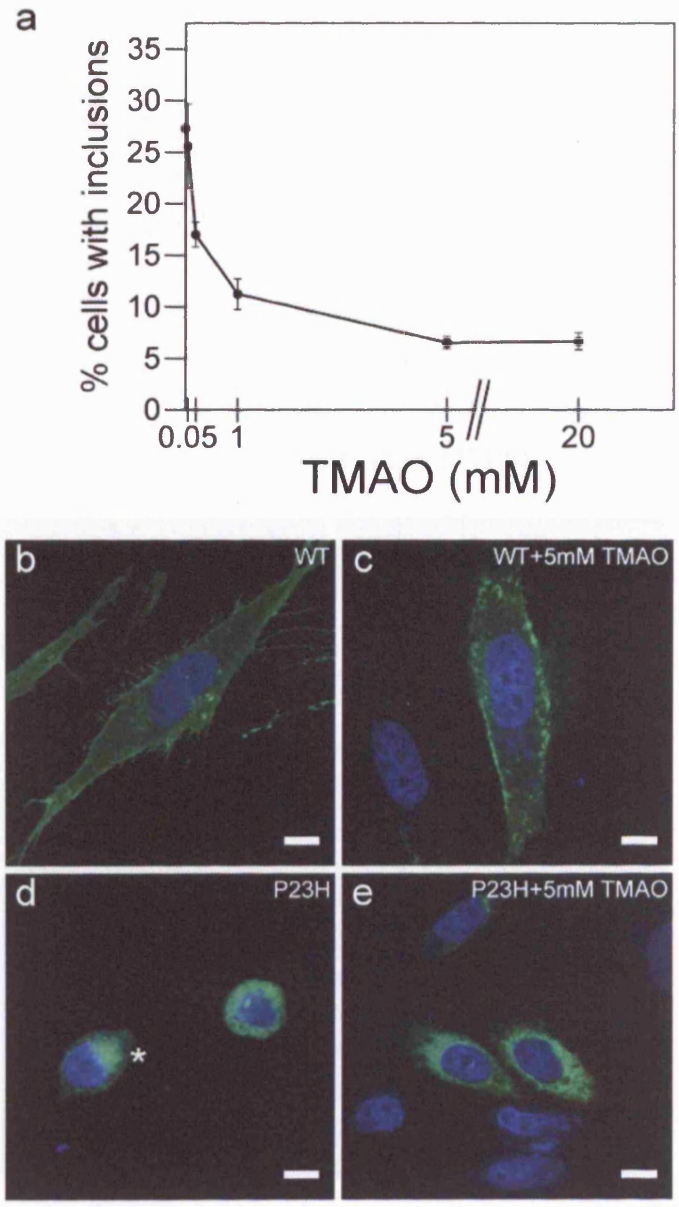

Figure 5.3 Treatment with trimethylamine-N-oxide (TMAO) reduces inclusion incidence in cells expressing P23H rod opsin.

a) SK-N-SH cells were transfected with P23H-GFP rod opsin and treated with different concentrations of TMAO for 24 hours. The most effective concentration was 5 mM TMAO which reduced inclusion incidence from 27.32% ± 2.56 in the untreated controls to 6.52% ± 1.21 ($p \leq 0.001$). Error bars represent ± 2SE. b-e) Treatment with TMAO reduced inclusion incidence in P23H cells but did not promote the translocation of the mutant protein to the plasma membrane of the cells. Asterisks highlight inclusions. Scale bar = 10μm.

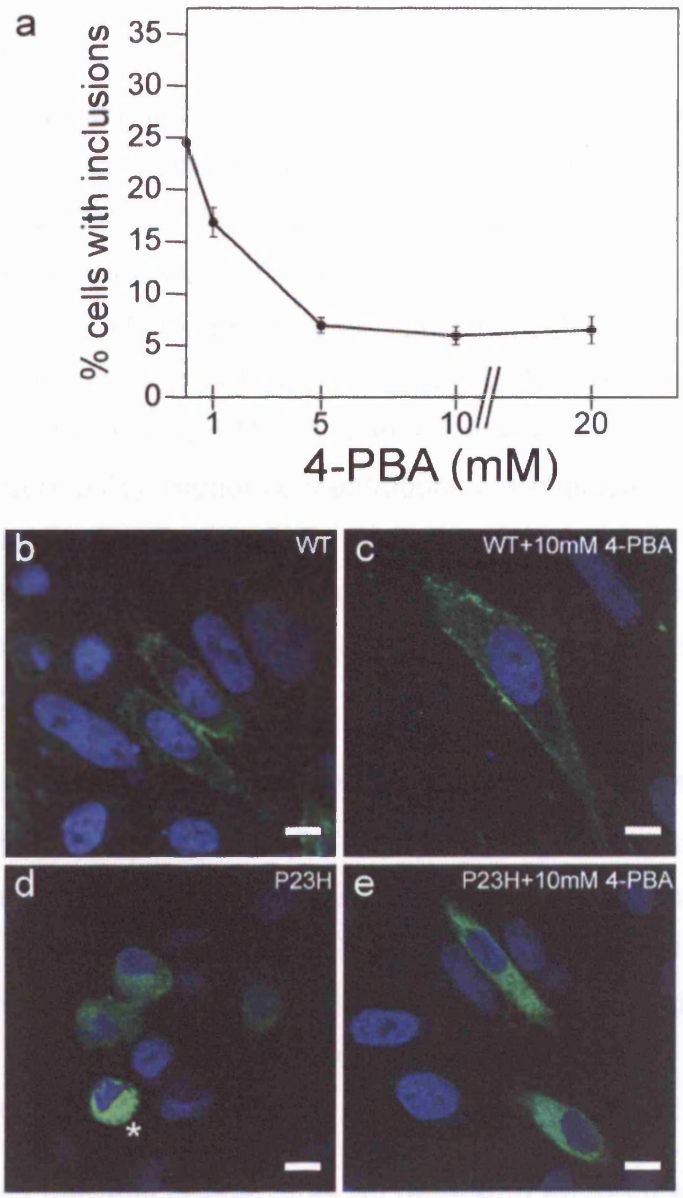

Figure 5.4 Inclusion incidence is reduced in cells expressing P23H rod opsin following treatment with 4-phenylbutyric acid (4-PBA).

a) SK-N-SH cells were transfected with P23H-GFP rod opsin and treated with different concentrations of 4-PBA for 24 hours (a). The most effective concentration was 10 mM 4-PBA which reduced inclusion incidence from 24.52% ± 2.23 in the untreated controls to 5.95% ± 1.78 ($p \leq 0.001$). Error bars represent ± 2SE. b-e) Treatment with 4-PBA reduced inclusion incidence but did not promote the translocation of mutant rod opsin to the plasma membrane of the cell. Asterisks highlight inclusions. Scale bar = 10 μm.

5.2.1.4 Trehalose

Treatment with trehalose resulted in a milder decrease in inclusion incidence in cells expressing P23H rod opsin (Figure 5.5a), when compared to the other chemical chaperones DMSO, TMAO and 4-PBA. The lowest concentration to have an effect on inclusion incidence was 1 mM and the most effective concentration was 50 mM which resulted in a decrease of inclusion incidence from 22.38% ± 3.36 in the untreated controls to 10.37 ± 2.51 ($p \leq 0.001$). Treatment with trehalose at concentrations lower than 50 mM had no effect on the cellular morphology of wild-type cells (Figure 5.5c). Higher concentrations of trehalose resulted in deleterious effects on cellular morphology, including rounded cells detached from the culture surface. Although trehalose reduced inclusion incidence, it did not appear to promote the translocation of P23H rod opsin to the plasma membrane of the cells (Figure 5.5e).

5.2.2 Influence of chemical chaperones on P23H opsin species

The effect of chemical chaperones on the levels of soluble and EndoH resistant P23H opsin species was analysed by SDS-PAGE followed by immunoblotting with 1D4 (Figure 5.6). Treatment with DMSO, TMAO, 4-PBA and trehalose failed to promote EndoH resistance of mature opsin species (arrow) indicating that these compounds were unable to assist the folding of the mutant protein so it would exit from ER to the Golgi.

5.2.3 Efficacy of chemical chaperones on inclusion incidence decreases once inclusion are formed

In order to assess if chemical chaperones were effective in reducing inclusion incidence once the inclusions had formed SK-N-SH cells expressing P23H-GFP rod opsin were treated with 0.25% DMSO or 5 mM TMAO immediately after transfection (0h), 6 hours after transfection (6h) and 12 hours after transfection (12h) then fixed 24 hours after transfection (Figure 5.7). 0.25% DMSO reduced inclusion incidence from 26.15% ± 4.18 in the untreated controls to 5.68% ± 1.74 ($p \leq 0.001$) at

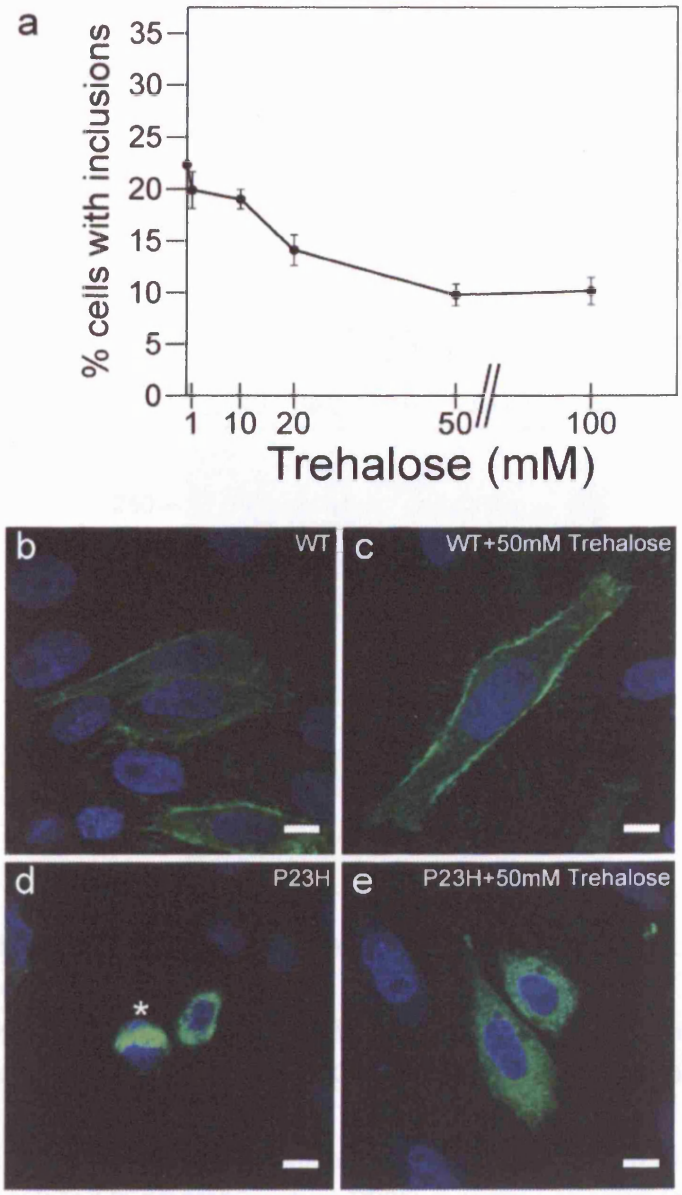

Figure 5.5 Trehalose reduces inclusion incidence in cells expressing P23H rod opsin.

a) SK-N-SH cells were transfected with P23H-GFP rod opsin and treated with different concentrations of trehalose for 24 hours. The most effective concentration was 50 mM trehalose which reduced inclusion incidence from 22.38% ± 3.36 in the untreated controls to 10.37% ± 2.51 ($p \leq 0.001$). Error bars represent ± 2SE. b-e) Trehalose reduced inclusion incidence in P23H cells but no increase in plasma membrane staining was observed. Asterisks highlight inclusions. Scale bar = 10 μm.

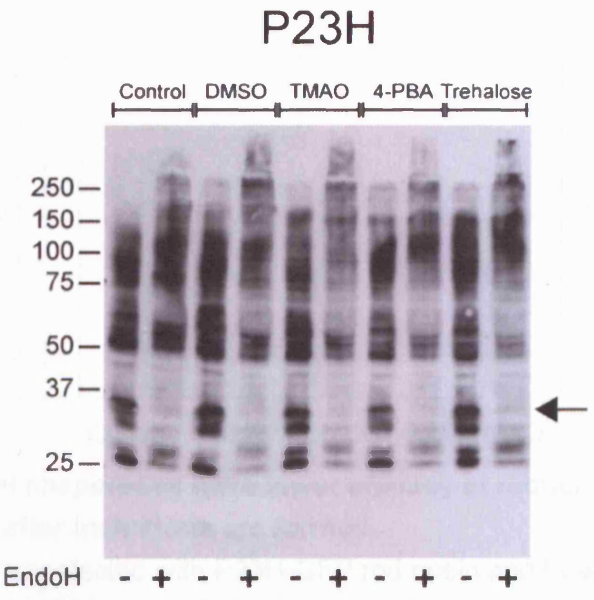

Figure 5.6 Chemical chaperones fail to elicit EndoH resistance in soluble P23H rod opsin.

SK-N-SH cells expressing untagged P23H rod opsin were treated with chemical chaperones, as indicated, for 24 hours. Cells were lysed and the soluble fraction was obtained as described in Chapter 3. 10µg of soluble cell lysate protein were resolved on a 10% SDS-PAGE gel followed by immunoblotting with 1D4. Chemical chaperones failed to promote mature P23H rod opsin species (arrow). The position of molecular weight markers in kDa are shown on the left.

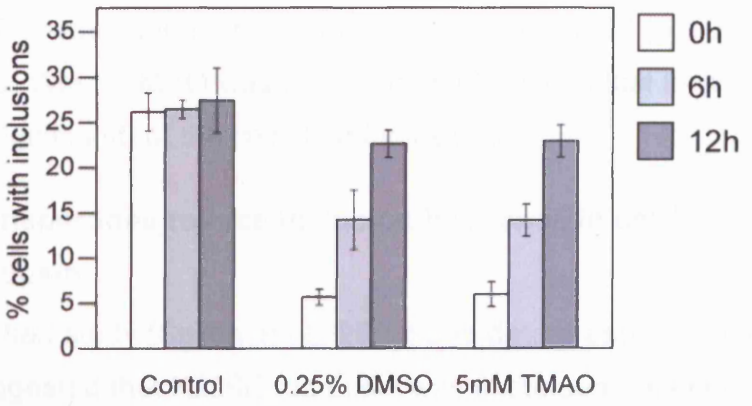

Figure 5.7 Chemical chaperones have lower efficacy at reducing inclusion incidence if added after inclusions are formed.

SK-N-SH cells were transfected with P23H-GFP rod opsin and treated with 0.25% DMSO or 5 mM TMAO as indicated which were added immediately after transfection (0h), 6 hours after transfection (6h) and 12 hours after transfection (12h). Serum media in the controls was added at 0h, 6h, and 12h to mimic the conditions of drug treatments at different time points. Both DMSO ($p \leq 0.001$) and TMAO ($p \leq 0.001$) reduced inclusion incidence in P23H cells when added at 0h. DMSO ($p \leq 0.01$) and TMAO ($p \leq 0.005$) showed lower efficacy if added 6 hours after transfection. DMSO (not significant) and TMAO (not significant) failed to reduce inclusion incidence if added after 12 hours. Error bars represent ± 2SE.

24 hours. DMSO was less efficient at reducing inclusion incidence when it was added after 6 hours which resulted in the presence of inclusions in 14.24% ± 6.58 ($p \leq 0.01$) of the cells, and DMSO lost its efficacy at reducing inclusion incidence when it was added after 12 hours as inclusions were present in 22.63% ± 3.00 (not significant) of the cells. When cells were treated with 5 mM TMAO immediately after transfection it resulted in a decrease in inclusion incidence from 26.15% ± 4.18 in the untreated controls to 6.01% ± 2.74 ($p \leq 0.001$). However, this effect was reduced when TMAO was added after 6 hours as 14.17% ± 2.86 ($p \leq 0.005$) of the cells had inclusions. When TMAO was added after 12 hours it lost its efficacy as 22.94 ± 5.54 (not significant) of the cells had inclusions.

5.2.4 Chemical chaperones reduce inclusion incidence in cells expressing K296E rod opsin

A previously published study (Saliba *et* al., 2002) and data presented in this study (Figure 3.2a-b) suggested that K296E rod opsin was misfolded, retained in the ER and accumulated in intracellular inclusions. As described in Figure 4.3a the specific pharmacological chaperone action of retinoids did not reduce inclusion incidence in K296E cells due to the disruption of the chromophore binding site. It was, therefore, important to assess if the non-specific effects of chemical chaperones on protein stabilisation and prevention of aggregation could have a positive effect on cells expressing K296E mutant rod opsin. SK-N-SH cells expressing K296E-GFP rod opsin were treated with 0.25% DMSO or 5 mM TMAO for 24 hours prior to fixation. Treatment with DMSO resulted in a decrease in inclusion incidence in K296E cells from 15.64% ± 3.55 in the untreated controls to 6.25% ± 0.42 ($p \leq 0.001$) (Figure 5.8). A similar reduction in inclusion incidence in K296E cells was observed with TMAO as it resulted in a decrease in inclusion incidence to 6.20% ± 2.42 ($p \leq 0.001$) (Figure 5.8).

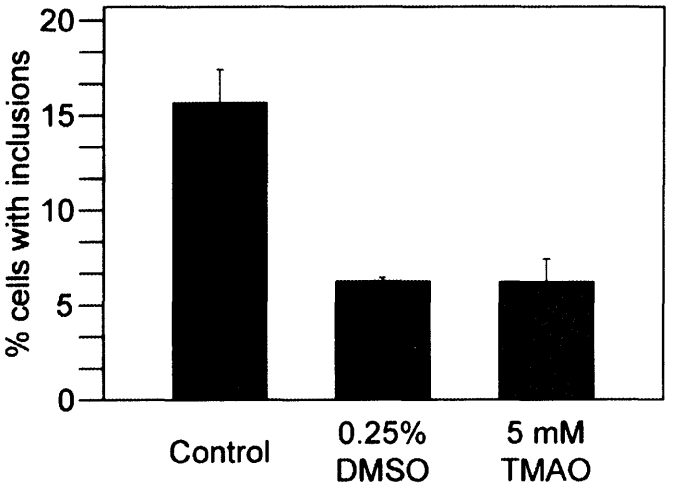

Figure 5.8 Chemical chaperones reduce inclusion incidence in cells expressing K296E rod opsin.

SK-N-SH cells expressing K296E-GFP rod opsin were treated with 0.25% (w/v) DMSO and 5 mM TMAO as indicated for 24 hours. DMSO reduced inclusion incidence from 15.64 ± 3.55 in the untreated controls to 6.25 ± 0.42 ($p \leq 0.001$) whereas TMAO reduced inclusion incidence to 6.20 ± 2.42 ($p \leq 0.001$). Error bars represent ± 2SE.

5.2.5 Treatment with chemical chaperone reduces the amount of insoluble rod opsin in cell lysates of P23H cells

In order to assess the effect of chemical chaperones on the levels of total and insoluble rod opsin a rod opsin fractionation assay was carried out as described in Chapter 2. Treatment with DMSO, TMAO, 4-PBA and trehalose did not affect the total levels of either wild-type or P23H rod opsin expressed in SK-N-SH cells (Figure 5.9a). Treatment with 0.25% DMSO and 5 mM TMAO reduced the percentage of insoluble P23H opsin from 59.57% ± 5.04 in the untreated controls to 40.60% ± 2.89 ($p \leq 0.01$) and 37.96% ± 4.14 ($p \leq 0.01$) respectively (Figure 5.9b). 10 mM 4-PBA and 50 mM trehalose appeared slightly more effective reducing the percentage of insoluble mutant opsin to 26.32% ± 1.36 ($p \leq 0.005$) and 26.32% ±1.52 respectively ($p \leq 0.005$) (Figure 5.9b).

5.2.6 Chemical chaperones reduce LDH release and caspase-3 activity induced by P23H rod opsin

Following the observed decrease in inclusion incidence in P23H cells treated with chemical chaperones it was important to investigate if these compounds had a positive effect on cell death measured by LDH release and caspase-3 activity. For that purpose SK-N-SH cells expressing wild-type or P23H rod opsin were treated with the most effective concentrations of chemical chaperones: 0.25% DMSO; 5 mM TMAO; 10 mM 4-PBA and 50 mM trehalose for 48 hours. The effect of these compounds on LDH release (Figure 5.10a) and caspase-3 activity (Figure 5.10b) were assessed. All chemical chaperones reduced LDH release in P23H cells with DMSO ($p \leq 0.01$) and TMAO ($p \leq 0.01$) reducing LDH release by ~60% when compared to the untreated P23H controls whereas 4-PBA ($p \leq 0.05$) and trehalose ($p \leq 0.05$) were slightly less effective reducing LDH release by ~40% (Figure 5.10a). Chemical chaperones also had a positive effect in protecting P23H cells against caspase-3 activity as DMSO ($p \leq 0.05$), TMAO ($p \leq 0.05$), 4-PBA ($p \leq 0.001$) and trehalose ($p \leq 0.05$) all reduced caspase-3 activity by ~30% when compared to the untreated P23H controls (Figure 5.10b).

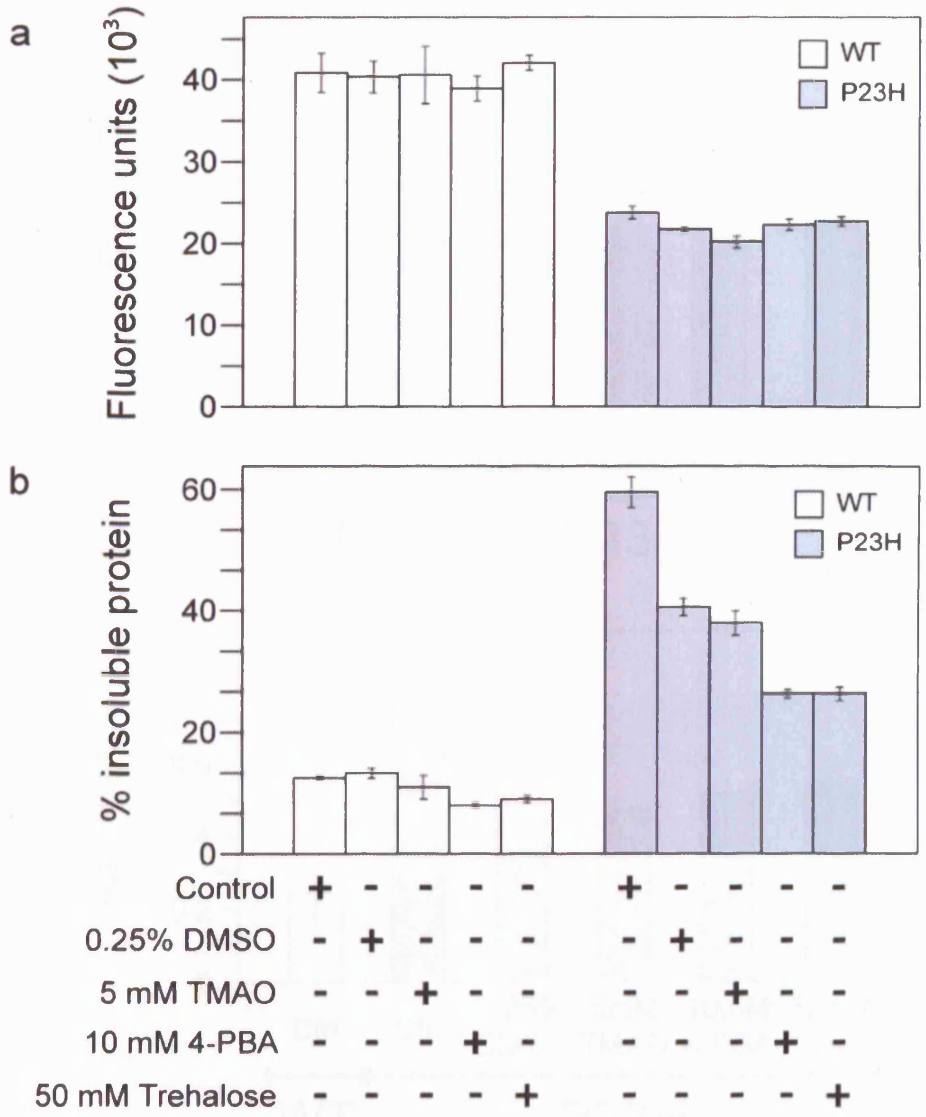

Figure 5.9 Chemical chaperones reduce the amount of insoluble P23H rod opsin.

A rod opsin fractionation assay was carried out in SK-N-SH cells expressing WT-GFP or P23H-GFP and treated with chemical chaperones as indicated for 24 hours. a) The amount of total P23H rod opsin was ~45% lower than WT and chemical chaperones had no effect on the amount of total WT or P23H opsin. b) When insoluble P23H rod opsin was quantified as percentage of total protein DMSO ($p \leq 0.01$) and TMAO ($p \leq 0.01$) reduced the percentage of insoluble opsin from ~60% to ~40%. 4-PBA ($p \leq 0.005$) and trehalose ($p \leq 0.005$) reduced the percentage of insoluble opsin from ~60% to ~25%. Error bars represent ± 2SE.

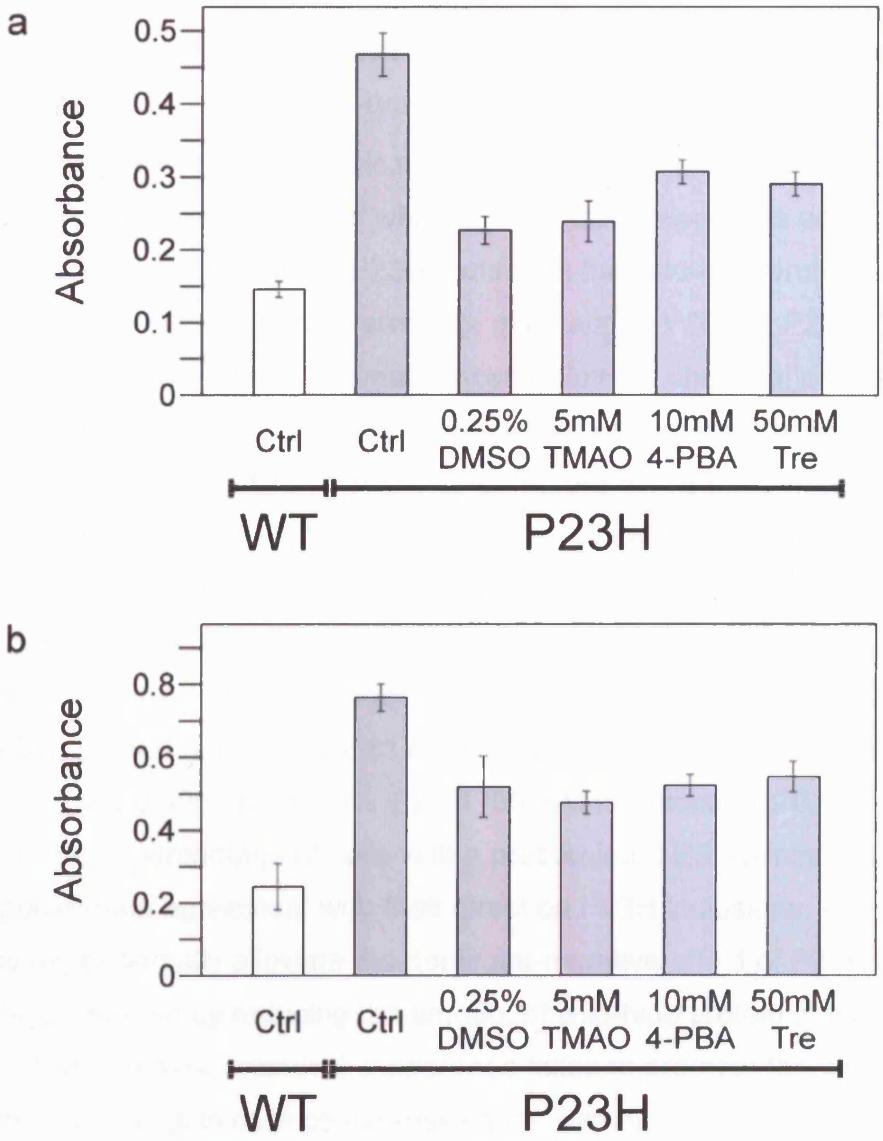

Figure 5.10 Chemical chaperones reduce LDH release and caspase-3 activity in cells expressing P23H rod opsin.

SK-N-SH cells were transfected with GFP-tagged WT or P23H rod opsin and treated with chemical chaperones as indicated for 48 hours before LDH (a) and caspase-3 activity (b) assays were carried out. P23H cells showed increased levels of LDH release when compared to the WT. DMSO ($p \leq 0.01$) and TMAO ($p \leq 0.01$) reduced LDH release in P23H cells by ~60% while 4-PBA ($p \leq 0.05$) and trehalose ($p \leq 0.05$) reduced LDH release by ~40%. Caspase-3 activity levels were higher in P23H cells than in WT cells and DMSO ($p \leq 0.05$), TMAO ($p \leq 0.05$), 4-PBA ($p \leq 0.001$) and trehalose ($p \leq 0.05$) reduced those levels by ~30%. Error bars represent ± 2SE.

5.2.7 Chemical chaperones do not alleviate the dominant-negative effect of P23H rod opsin on the wild-type protein

After investigating the effect of chemical chaperones in the P23H rod opsin gain of function mechanism it was assessed whether chemical chaperones could alleviate the dominant-negative effect of the P23H mutant on the wild-type protein. SK-N-SH cells were co-transfected with equal amounts of untagged WT and P23H-GFP rod opsin followed by treatment with optimal concentrations of chemical chaperones for 24 hours prior to immunocytochemistry being carried out as described in Chapter 2. 0.25% DMSO (Figure 5.11d-f), 5 mM TMAO (Figure 5.11g-i), 10 mM 4-PBA (Figure 5.11j-l) and 50 mM trehalose (Figure 5.11m-o) did not appear to promote the normal translocation of wild-type rod opsin to the plasma membrane. However, chemical chaperones reduced the incidence of rod opsin inclusions in co-transfected cells from 14.40% ± 3.81 in the untreated controls to 6.50% ± 4.72 (0.25% DMSO; $p \leq 0.05$), 6.80% ± 2.81 (5 mM TMAO; $p \leq 0.001$), 6.90% ± 3.01 (10 mM 4-PBA; $p \leq 0.005$) and 8.80% ± 2.24 (50 mM trehalose; $p \leq 0.05$) and led to a increase in the percentage of cells with a predominant ER staining (Figure 5.12). In approximate agreement with their effect on P23H inclusions, chemical chaperones might partially alleviate the dominant-negative effect of P23H rod opsin on the wild-type protein by reducing the amount of wild-type protein in inclusions. However, unlike retinoids, chemical chaperones failed to promote the exit of wild-type protein to the Golgi in cells co-expressing the wild-type and the P23H rod opsin.

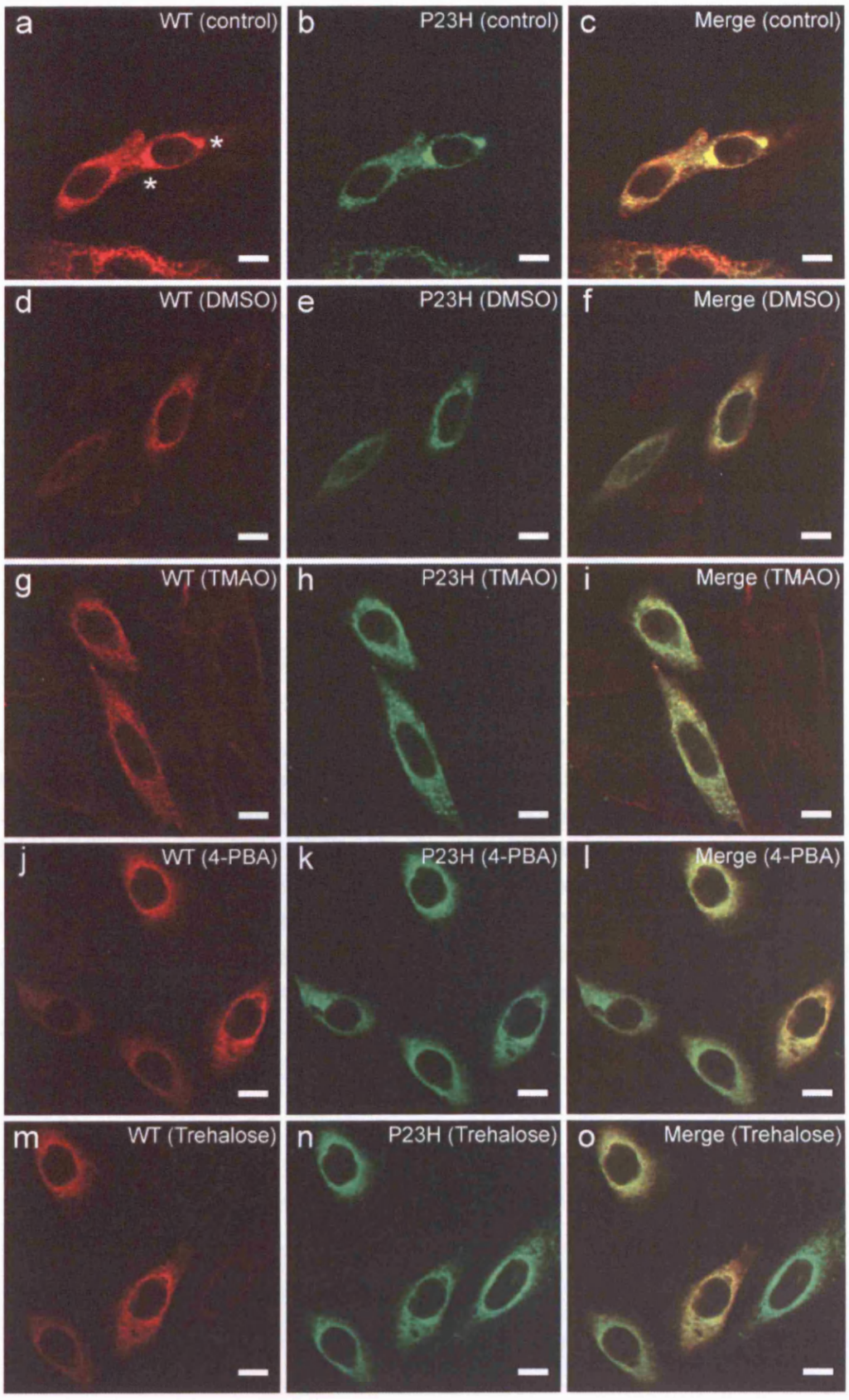
a
WT (control)
b
P23H (control)
c
Merge (control)
d
WT (DMSO)
e
P23H (DMSO)
f
Merge (DMSO)
g
WT (TMAO)
h
P23H (TMAO)
i
Merge (TMAO)
j
WT (4-PBA)
k
P23H (4-PBA)
l
Merge (4-PBA)
m
WT (Trehalose)
n
P23H (Trehalose)
o
Merge (Trehalose)

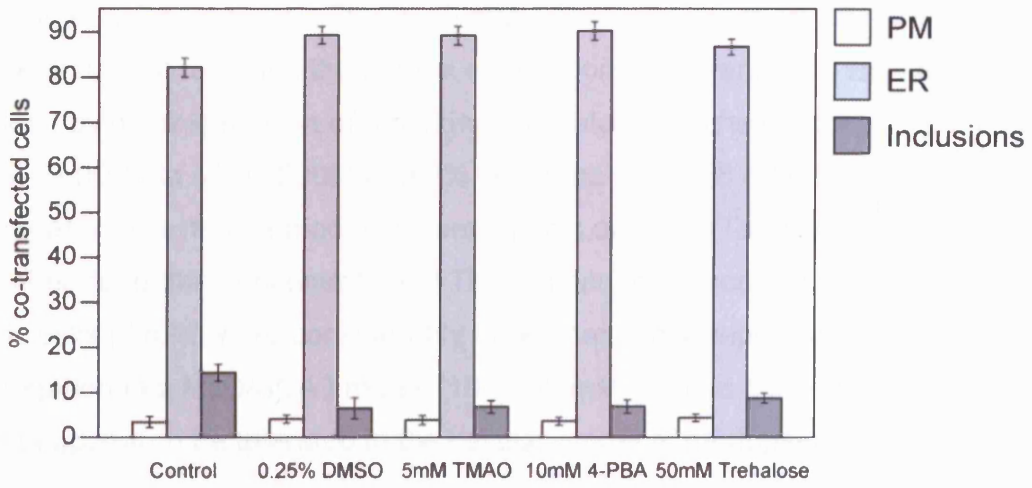

Figure 5.12 Chemical chaperones reduce the recruitment of WT rod opsin to inclusions in cells co-expressing WT and P23H rod opsin.
SK-N-SH cells were co-transfected with equal amounts of untagged WT and P23H-GFP rod opsin and treated with chemical chaperones as indicated for 24 hours. The localisation of WT rod opsin in co-transfected cells was assessed and DMSO ($p \leq 0.05$) , TMAO ($p \leq 0.001$) , 4-PBA ($p \leq 0.005$) and trehalose ($p \leq 0.05$) reduced the incidence of inclusions containing the WT protein. None of these compounds promoted the translocation of WT opsin the plasma membrane. Error bars represent ± 2SE.

5.3 Discussion

The chemical chaperones DMSO, TMAO, 4-PBA and trehalose appeared to reduce inclusion incidence in SK-N-SH cells expressing the P23H rod opsin to a greater extent than retinoids. The most effective concentrations of DMSO, 4-PBA and trehalose at reducing inclusion incidence in P23H cells were similar to other previously published studies. 0.5% v/v DMSO reduced aggregation in a model of MJD/SCA3 (Yoshida *et al.*, 2002), 10 mM 4-PBA was the most effective concentration at restoring the normal expression and attenuating ER stress induced by overexpression of a parkin-associated endothelin receptor-like receptor (Pael-R) (Kubota *et al.*, 2006) and 2% w/v trehalose (~58 mM) reduced aggregation in a mouse model of Huntington's disease (Tanaka *et al.*, 2004). On the other hand, the concentration of TMAO used to reduce inclusion incidence in P23H cells (5 mM) were considerably lower than those reported for the reduction of aggregation in a MJD/SCA3 model (100-150 mM). These concentrations of TMAO did not appear to be tolerated in the cellular model of rhodopsin RP.

In addition, treatment with kosmotropes reduced the amount of insoluble P23H rod opsin as assessed by a rod opsin fractionation assay. DMSO and TMAO reduced insoluble rod opsin to the same extent as retinoids, whereas 4-PBA and trehalose were less effective. However, there were slight discrepancies between the two sets of data. For example trehalose was less effective than DMSO and TMAO in reducing inclusion incidence as determined by morphological observations in a fluorescence microscope but had lower levels of insoluble P23H rod opsin than DMSO and TMAO as determined by the fractionation assay. This might be due to some P23H aggregates which were scored as inclusions being soluble following RIPA buffer lysis. Alternatively some rod opsin aggregation might have occurred post-lysis during the experimental protocol of the rod opsin fractionation assay.

Soluble P23H rod opsin protein did not appear to acquire EndoH resistance following chemical chaperone treatment suggesting that these compounds were

unable to assist the folding of the mutant protein and promote its exit from the ER to the Golgi. It is important to mention that, unlike retinoids, kosmotropes not only failed to produce EndoH resistant species but also did not increase the amount of soluble P23H rod opsin resolved in a 10% SDS-PAGE gel and immunodetected by 1D4. The rod opsin fractionation assay following chemical chaperone treatment suggested that the total levels of P23H protein were unchanged following treatment with these compounds but the insoluble levels decreased. Consequently, an increase in the soluble P23H levels was expected which was not observed following the Western blotting of the soluble P23H rod opsin. One explanation for this might be that some of the misfolded P23H rod opsin might have aggregated during the course of the experiment preventing it from being immunodetected using 1D4. Another possibility is that even though Triton-X soluble protein was used these proteins might not enter or resolve in a SDS-PAGE gel.

The data presented here suggest that DMSO and TMAO lost their efficacy in reducing inclusion incidence in P23H cells if added once the inclusions were formed. These data correlate with a study by Tatzelt and colleagues (1996) which investigated the role of chemical chaperones on a prion protein disease model. A crucial conformational change in prion diseases occurs in one or more of the α-helices of cellular prion protein (PrP^{C}) which are converted into β-sheets during the formation of the pathogenic isoform (PrP^{Sc}). Scrapie-infected mouse neuroblastoma ScN2a cells were treated with DMSO and TMAO and these compounds prevented the conversion to the detergent-insoluble PrP^{Sc} from newly synthesised PrP^{C} but failed to affect the existing population of PrP^{Sc} molecules in the cells. Furthermore, studies which involved the incubation of P23H rod opsin cells with 9-*cis*-retinal once the inclusions were formed suggested that the ligand did not reduce inclusion incidence. Both these studies are in agreement with the data presented here in which chemical chaperones appeared to lose their efficacy at reducing inclusion incidence in P23H cells once the inclusions had formed. This data suggests that chemical chaperones reduce aggregation by acting before inclusions are formed.

Importantly, chemical chaperones, unlike retinoids, reduced inclusion incidence in cells expressing K296E rod opsin. It appeared that the non-specific effect of kosmotropes on protein stabilisation might be beneficial for this misfolding mutation which disrupted the binding site for retinoids. It remains to be seen if this could be extrapolated to other protein misfolding diseases where mutations in the binding site of pharmacological chaperones render them ineffective.

Chemical chaperones protected cells expressing P23H rod opsin against LDH release and caspase-3 activity suggesting that they might alleviate the gain of function mechanism induced by the P23H rod opsin. This was in agreement with previously published studies which found chemical chaperones to be protective against cell death and apoptosis in protein misfolding disease models.
For example, the role of chemical chaperones in cell death of a model of MJD/SCA-3, which is an inherited neurodegenerative disorder caused by expansion of the polyglutamine stretch in the MJD gene-encoded protein ataxin-3, was assessed by Yoshida and colleagues (2002). In this model treatment with DMSO and TMAO reduced cell death in BHK-21 and Neuro2a cells expressing the N-terminal truncated ataxin-3 with an expanded polyglutamine stretch. Another study was carried out to investigate the role of kosmotropes on apoptosis in a model of the RP17 form of ADRP (Bonapace *et al.*, 2004). The R14W mutation in the signal sequence of carbonic anhydrase (CA) IV was identified in patients with the RP 17 form of ADRP. R14W CA IV expressed in COS-7 cells misfolded and accumulated in the ER leading to increased apoptosis. Treatment with 4-PBA was effective at reducing apoptosis in these R14W CA IV expressing cells (Bonapace *et al.*, 2004).

When tested in the dominant-negative context chemical chaperones reduced the incidence of inclusions containing wild-type rod opsin in co-transfected cells. However there was no evidence that chemical chaperones prevented the interaction between the wild-type and the mutant protein as demonstrated by the

inability of the wild-type rod opsin to exit the ER and re-establish its normal translocation through the secretory pathway when co-transfected with P23H rod opsin. This was in contrast with retinoids suggesting that 9-*cis*-retinal and 11-*cis* retinal might affect the folding of P23H rod opsin in order to suppress the dominant-negative interaction between P23H rod opsin and the wild-type protein.

The analysis of the data presented in this Chapter suggested that chemical chaperones might exert their effects in this cellular model of rhodopsin RP by stabilising misfolded P23H protein resulting in the prevention of aggregation, however, this did not result in the facilitation of folding of the mutant rod opsin. Most studies involving other misfolded mutants such as the ΔF508 CFTR (Denning *et al.*, 1992) and others have demonstrated that chemical chaperones when used in their models promoted folding of the respective proteins. It remains to be seen if the anti-aggregation effects of chemical chaperones on the misfolding of Class II mutant rod opsin are sufficient *per se* to prevent or delay the onset of blindness in rhodopsin RP patients.

Chapter 6: HSP inducers and co-inducers

6.1 Introduction

Misfolded or aggregated proteins are thought to be responsible for a variety of neurodegenerative conditions and accumulate in inclusions of similar fibrillar structure despite being structurally unrelated. As a result it has been widely suggested that misfolding is the consequence of hydrophobic regions or other domains that are normally buried in the normal protein becoming exposed as consequence of mutations, leading to impaired interactions with the lipid membrane and other cellular components (Barral *et al.*, 2004). Molecular chaperones in general and HSPs in particular recognise these hydrophobic residues or unstructured backbone regions in misfolded proteins and promote the folding process through cycles of substrate binding and release regulated by their nucleotide binding, hydrolysis and facilitated by cofactor proteins.

As a result of their actions as promoters of the folding process it has been suggested that inducing the expression of molecular chaperones is likely to alleviate toxicity associated with misfolded protein disorders. Cummings and colleagues (1998) carried out work on cellular models of spinocerebellar ataxia type 1 (SCA1), which is an autosomal dominant neurodegenerative disorder caused by expansion of a polyglutamine tract in ataxin-1. These authors showed that the overexpression of a human DnaJ homologue, HDJ-2/HSDJ, in HeLa cells decreased the frequency of ataxin-1 aggregation. Consequently, these data indicate that protein misfolding was responsible for the nuclear aggregates seen in SCA1, and that overexpression of a DnaJ chaperone promoted the recognition of a misfolded polyglutamine repeat protein, allowing its refolding and/or ubiquitin-dependent degradation. Furthermore, overexpression of Hsp70 protected against neurodegeneration in a mouse model of SCA1 (Cummings *et al.*, 2001). Other studies showed that overexpression of Hsp70 in a *Drosophila melanogaster* model of polyglutamine disease resulted in the maintenance of normal retinal structure

suggesting suppression of polyglutamine-induced neurodegeneration, although there was no reduction of inclusion incidence in this study (Warrick *et al.*, 1999).

A pharmacological approach has been attempted in several models of neurodegenerative diseases using inducers and co-inducers of HSPs. An inducer of HSPs is a compound which can activate heat-shock transcription factors (HSFs) and consequently induce HSP expression by itself. On the other hand, a co-inducer is a compound that does not induce HSPs *per se*, but can enhance HSP induction in conjunction with other mild stresses.

In this chapter, the effect of a variety of HSP inducers and co-inducers were assessed in a cell model of rhodopsin RP. Arimoclomol is a derivative of bimoclomol, a hydroxylamine derivative which acts as a co-inducer of HSPs, and was found to improve muscle function and neuronal survival in a mouse model of amyotrophic lateral sclerosis (ALS) (Kieran *et al.*, 2004).

Celastrol, a quinone methide triterpene which is an active component from Chinese herbal medicine has potent anti-inflammatory and anti-oxidative effects in addition to activating heat shock factor 1 (HSF1) (Westerheide *et al.*, 2004). Furthermore, it was recently found to extend the life span of transgenic mice in a model of ALS (Kiaei *et al.*, 2005).

In addition to these compounds, three Hsp90 inhibitors were tested which included the benzoquinone ansamycin geldanamycin, the fungal antibiotic radicicol, and a geldanamycin-derivative 17-allylamino-17-demethoxygeldanamycin (17-AAG) whose molecular structures are shown in Figure 6.1. The rationale for using these Hsp90 inhibitors at low doses to induce HSPs is based on the HSF1 cycle model where HSF1 is usually bound to a molecular chaperone complex containing Hsp90, Hsp70, Hsp40 and other co-chaperones and is usually in an inactive state unless a stress signal is detected. Geldanamycin, radicicol and 17-AAG bind Hsp90 thereby disrupting the chaperone complex and resulting in the release of

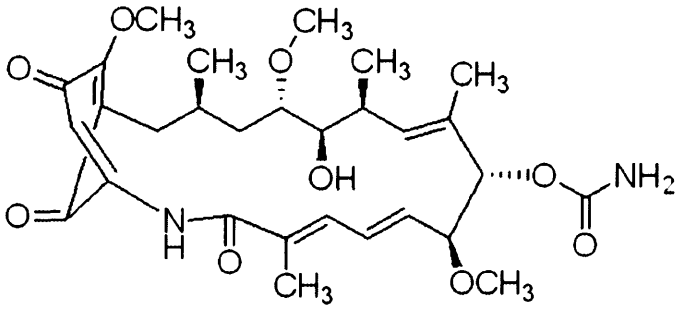

Geldanamycin

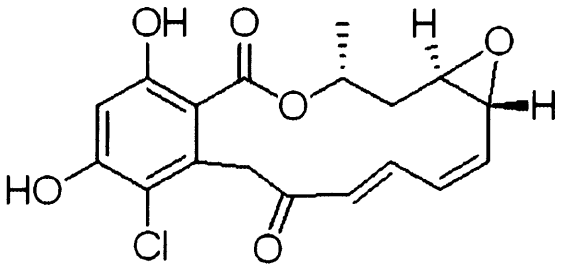

Radicicol

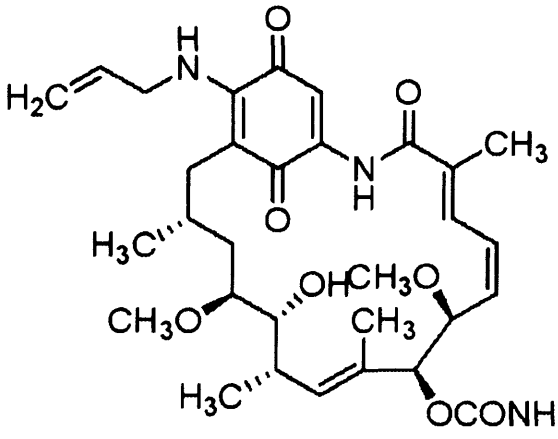

17-AAG

Figure 6.1 Representation of the molecular structures of the Heat shock protein 90 (Hsp90) inhibitors Geldanamycin, Radicicol and 17-allylamino-17-demethoxygeldanamycin (17-AAG).

the inactive HSF1, which in turn leads to the activation of HSF1 and consequent expression of HSPs. This approach has been used in a cell model of Huntington's disease (HD) where treatment of COS-1 cells with geldanamycin induced the expression of Hsp40, Hsp70 and Hsp90 and inhibited the HD exon 1 protein aggregation in a dose-dependent manner (Sittler *et al.*, 2001). The administration of 17-AAG markedly ameliorated motor impairments in the spinal and bulbar muscular atrophy (SBMA) transgenic mouse model without detectable toxicity, by reducing amounts of monomeric and aggregated mutant androgen receptor (AR) (Waza *et al.*, 2005). Furthermore, the mutant AR showed a higher affinity for Hsp90-p23 and preferentially formed an Hsp90 chaperone complex as compared to wild-type AR. In addition, mutant AR was preferentially degraded in the presence of 17-AAG as compared to wild-type AR. 17-AAG also mildly induced Hsp70 and Hsp40 (Waza *et al.*, 2005).

6.2 Results

6.2.1 HSP inducers and co-inducers reduce inclusion incidence in cells expressing P23H rod opsin

6.2.1.1 Arimoclomol

Treatment with arimoclomol reduced inclusion incidence in cells expressing P23H rod opsin in a dose-dependent manner (Figure 6.2a). The lowest concentration to have an effect on inclusion incidence was 0.05 μM and the most effective dose was 1 μM arimoclomol which resulted in the inclusion incidence decreasing from 27.19% ± 5.97 in the untreated controls to 4.23% ± 0.65 ($p \leq 0.001$). Arimoclomol had no effect on the wild-type rod opsin at concentrations lower than 1 μM (Figure 6.2c).Higher concentrations of arimoclomol failed to decrease inclusion incidence further. Furthermore, deleterious effects on cellular morphology were observed in both the wild-type and P23H cells when concentrations higher than 20 μM were used. Treatment with 1 μM arimoclomol appeared to partially promote the translocation of P23H rod opsin to the plasma membrane of the cells (Figure 6.2e).

6.2.1.2 Celastrol

Celastrol caused a moderate decrease in inclusion incidence in P23H-transfected cells (Figure 6.3a). The most efficient concentration at reducing inclusion incidence was 2 μM which led to a reduction of inclusion incidence from 28.24% ± 5.46 in the untreated controls to 17.65% ± 5.89 ($p \leq 0.05$). However, despite this moderate reduction in inclusion incidence treatment with 2 μM celastrol appeared to have a detrimental rather than a beneficial effect on the P23H cells as observations using fluorescent and confocal microscopy indicated a high level of dead or abnormally shaped cells when compared to the untreated controls (Figure 6.3e). Celastrol when used at concentrations lower than 2 μM had no effect on cells expressing the wild-type protein (Figure 6.3c). It has been suggested that P23H rod opsin might make cells more sensitive to toxicity (M.E.Cheetham, personal communication),

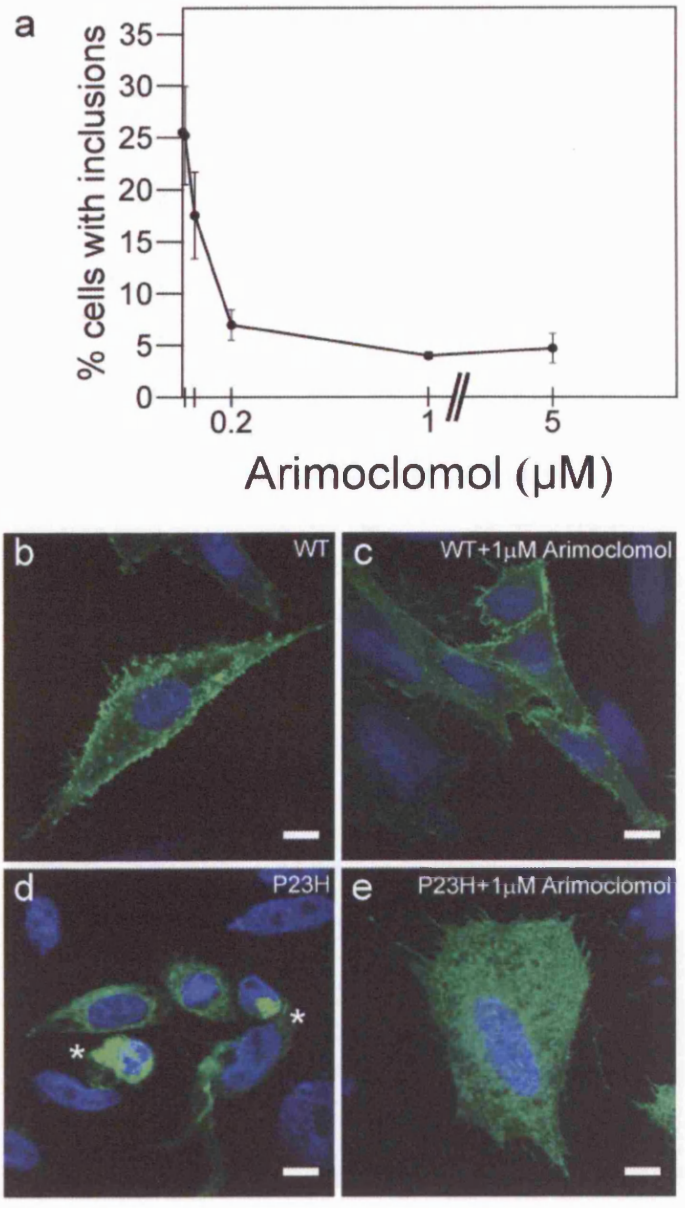

Figure 6.2 Arimoclomol reduces inclusion incidence in cells expressing P23H rod opsin.

a) SK-N-SH cells were transfected with P23H-GFP rod opsin and treated with different concentrations of arimoclomol for 24 hours. The most effective concentration was 1 μM arimoclomol which reduced inclusion incidence from 27.19% ± 5.97 in the untreated controls to 4.23% ± 0.65 ($p \leq 0.001$). Error bars represent ± 2SE. b-e) Arimoclomol reduced inclusion incidence and partially promoted the translocation of mutant rod opsin to the plasma membrane of the cell. Asterisks highlight inclusions. Scale bar = 10 μm.

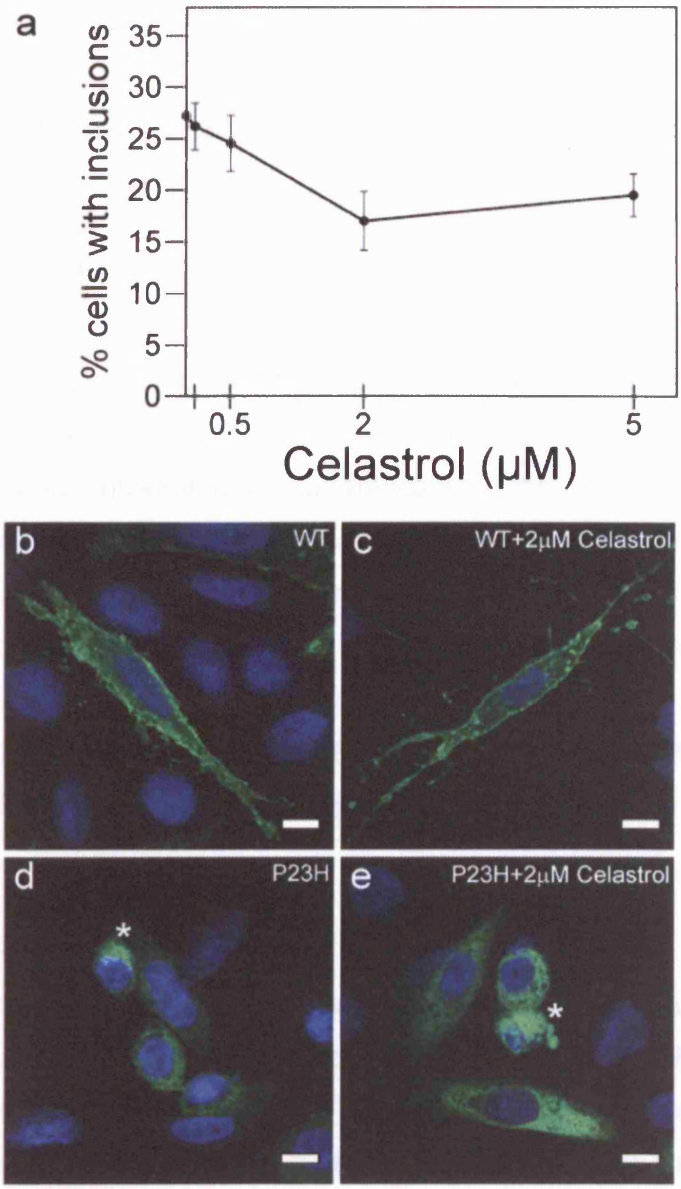

Figure 6.3 Treatment with celastrol results in a moderate reduction of inclusion incidence in cells expressing P23H rod opsin.

a) SK-N-SH cells were transfected with P23H-GFP rod opsin and treated with different concentrations of celastrol for 24 hours. The concentration of celastrol which reduced inclusion incidence the most was 2 μM and resulted in a decrease of inclusion incidence from 28.24% ± 5.46 in the untreated controls to 17.65% ± 5.89 ($p \leq 0.05$). Error bars represent ± 2SE. b-e) Despite its moderate effect on inclusion incidence celastrol failed to promote the translocation of mutant rod opsin to the plasma membrane of the cell. Asterisks highlight inclusions. Scale bar = 10 μm.

and this might account for the different observations as a result of celastrol treatment in wild-type and P23H cells. The levels of abnormal cells were reduced when lower concentrations of celastrol were used, however, these doses did not appear to reduce inclusion incidence.

6.2.1.3 Geldanamycin

The use of the prototypical Hsp90 inhibitor geldanamycin in a cell model of rhodopsin RP resulted in reduction of inclusion incidence in cells expressing P23H rod opsin (Figure 6.4a), although the effect was not as pronounced as with arimoclomol. The concentration of geldanamycin with the greatest effect on inclusion incidence was 2 μM which resulted in a decrease in inclusion incidence from 19.40% ± 6.04 in the untreated controls to 8.84% ± 5.11 ($p \leq 0.05$). Geldanamycin concentrations lower than 2 μM had no effect on the wild-type protein (Figure 6.4c). Geldanamycin treatment resulted in an increase in the percentage of cells with a predominantly ER staining pattern and did not lead to the translocation of the mutant protein to the plasma membrane of the cells (Figure 6.4e).

6.2.1.4 Radicicol

Treatment with the Hsp90 inhibitor radicicol resulted in a reduction of inclusion incidence in cells expressing P23H rod opsin (Figure 6.5a) to levels similar to those achieved with geldanamycin. The largest decrease in inclusion incidence was observed when using 5 μM radicicol which caused the inclusion incidence to decrease from 27.49% ± 4.76 in the untreated controls to 10.16 ± 2.68 ($p \leq 0.001$). When used at concentrations lower than 5 μM radicicol had no effect on the cellular morphology of the wild-type protein (Figure 6.5c). This decrease in inclusion incidence, however, was not accompanied by an increase in the number of cells in the population showing a plasma membrane staining (Figure 6.5e). Treatment with higher concentrations of radicicol resulted in the appearance of cells with an abnormal morphology in both the wild-type and P23H cells.

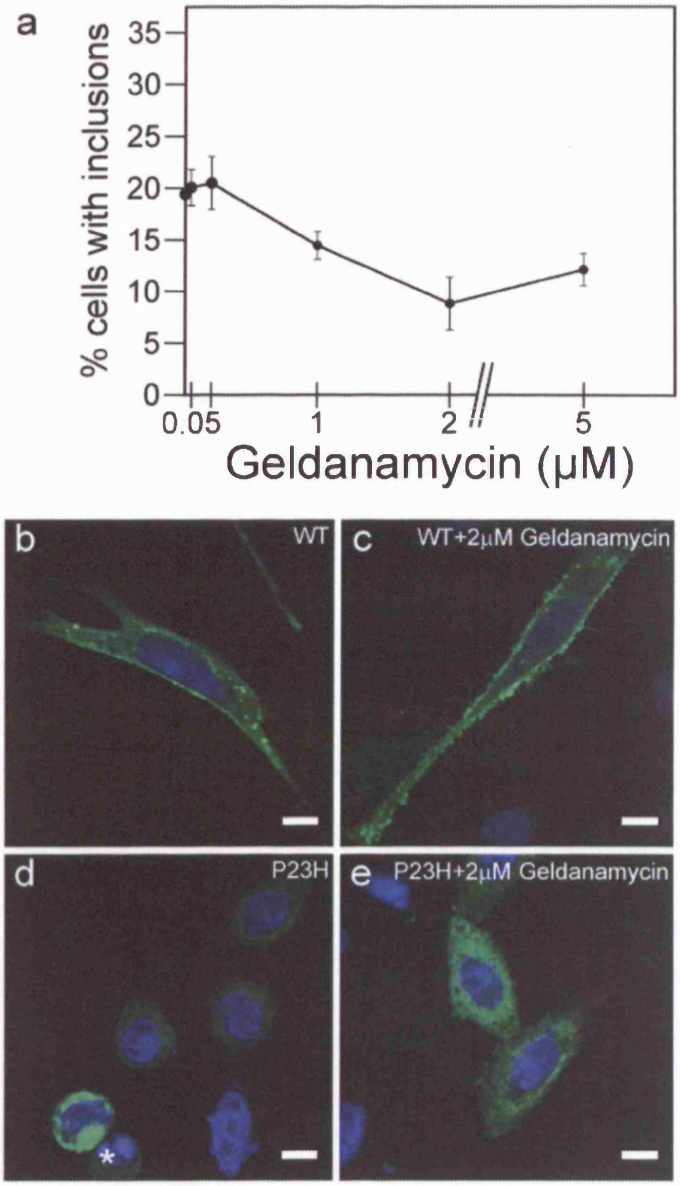

Figure 6.4 The Hsp90 inhibitor geldanamycin reduces inclusion incidence in cells expressing P23H rod opsin.

a) SK-N-SH cells were transfected with P23H-GFP rod opsin and treated with different concentrations of geldanamycin for 24 hours. The most effective concentration was 2 μM geldanamycin which reduced inclusion incidence from 19.40% ± 6.04 in the untreated controls to 8.84% ± 5.11 ($p \leq 0.05$). Error bars represent ± 2SE. b-e) Geldanamycin reduced inclusion incidence but did not promote the translocation of mutant rod opsin to the plasma membrane of the cell. Asterisks highlight inclusions. Scale bar = 10 μm.

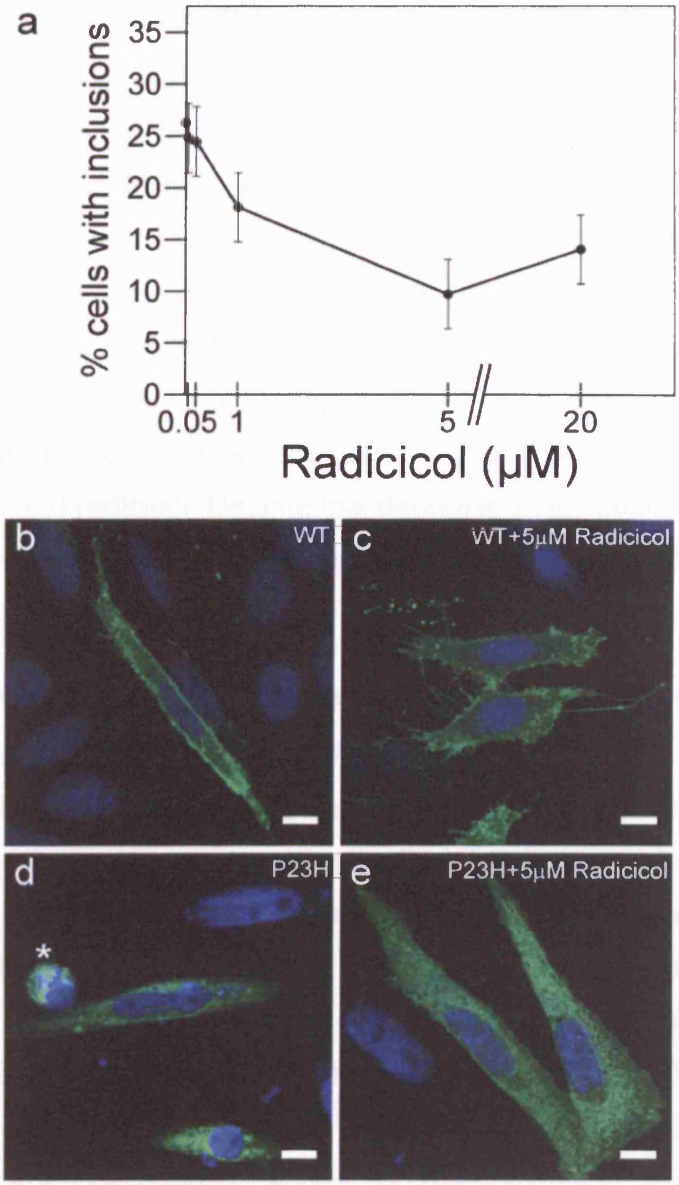

Figure 6.5 The Hsp90 inhibitor radicicol reduces inclusion incidence in cells expressing P23H rod opsin.

a) SK-N-SH cells were transfected with P23H-GFP rod opsin and treated with different concentrations of radicicol for 24 hours. The most effective concentration was 5 μM radicicol which reduced inclusion incidence from 27.19% ± 4.76 in the untreated controls to 10.16 ± 2.68 ($p \leq 0.001$). Error bars represent ± 2SE.

b-e) Radicicol reduced inclusion incidence but did not to promote the translocation of mutant rod opsin to the plasma membrane of the cell. Asterisks highlight inclusions. Scale bar = 10 μm.

6.2.1.5 17-allylamino-17-demethoxygeldanamycin (17-AAG)

17-AAG led to a dose-dependent reduction of inclusion incidence in cells expressing P23H rod opsin (Figure 6.6a). This compound started to have a positive effect on the inclusion incidence at a concentration of 50 nM and had maximal effect at a concentration of 1 μM where it reduced inclusion incidence from 22.20% ± 3.56 in the untreated controls to 6.50% ± 2.09 ($p \leq 0.001$). 17-AAG doses lower than 1 μM 17-AAG had no effect on the cellular morphology of the wild-type protein (Figure 6.6c). In this cell model of rhodopsin RP, 17-AAG appeared to be more effective at reducing inclusion incidence than the other Hsp90 inhibitors used such as geldanamycin and radicicol. Despite this decrease in inclusion incidence 17-AAG did not appear to promote the translocation of P23H rod opsin to the plasma membrane of the cells (Figure 6.6e).

6.2.2 Treatment with HSP inducers and co-inducers fails to promote EndoH resistance in soluble P23H rod opsin species

In order to complement the morphological assessment of the effect of HSP inducers and co-inducers on cells expressing P23H rod opsin, a biochemical characterisation of soluble P23H rod opsin species was carried out. This was achieved by loading 10 μg of soluble cell lysate protein treated with HSP inducers and co-inducers onto a 10% SDS-PAGE gel followed by immunoblotting with 1D4 as described in Chapter 2. Treatment with arimoclomol (Figure 6.7a), geldanamycin (Figure 6.7b) and radicicol (Figure 6.7c) did not increase the levels of soluble P23H protein and did not appear to promote EndoH resistance (arrow) of soluble mutant protein species. Treatment with 17-AAG (Figure 6.7d) appeared to increase the levels of soluble P23H protein although it did not appear to promote EndoH resistance of mature P23H rod opsin species.

6.2.3 Effect of HSP inducers and co-inducers on the total and insoluble rod opsin levels in SK-N-SH cell lysates

The effect of HSP inducers and co-inducers on the levels of WT and P23H rod opsin was assessed by a rod opsin fractionation assay as described in Chapter 2.

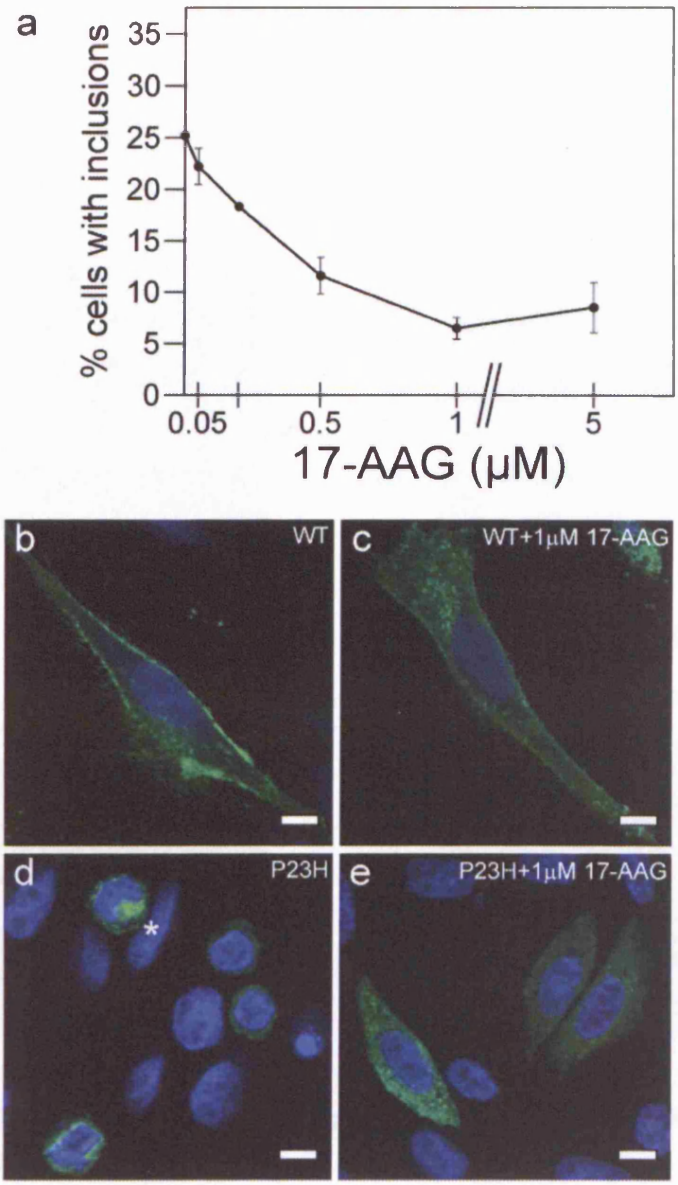

Figure 6.6 17-AAG reduces inclusion incidence in cells expressing P23H rod opsin.

a) SK-N-SH cells were transfected with P23H-GFP rod opsin and treated with different concentrations of 17-AAG for 24 hours. The most effective concentration was 1 μM 17-AAG which reduced inclusion incidence from 22.20% ± 3.56 in the untreated controls to 6.50% ± 2.09 ($p \leq 0.001$). 17-AAG was more effective at reducing inclusion incidence that the other Hsp90 inhibitors used namely geldanamycin and radicicol. Error bars represent ± 2SE. b-e) 17-AAG reduced inclusion incidence but did not promote the translocation of mutant rod opsin to the plasma membrane of the cell. Asterisks highlight inclusions. Scale bar = 10 μm.

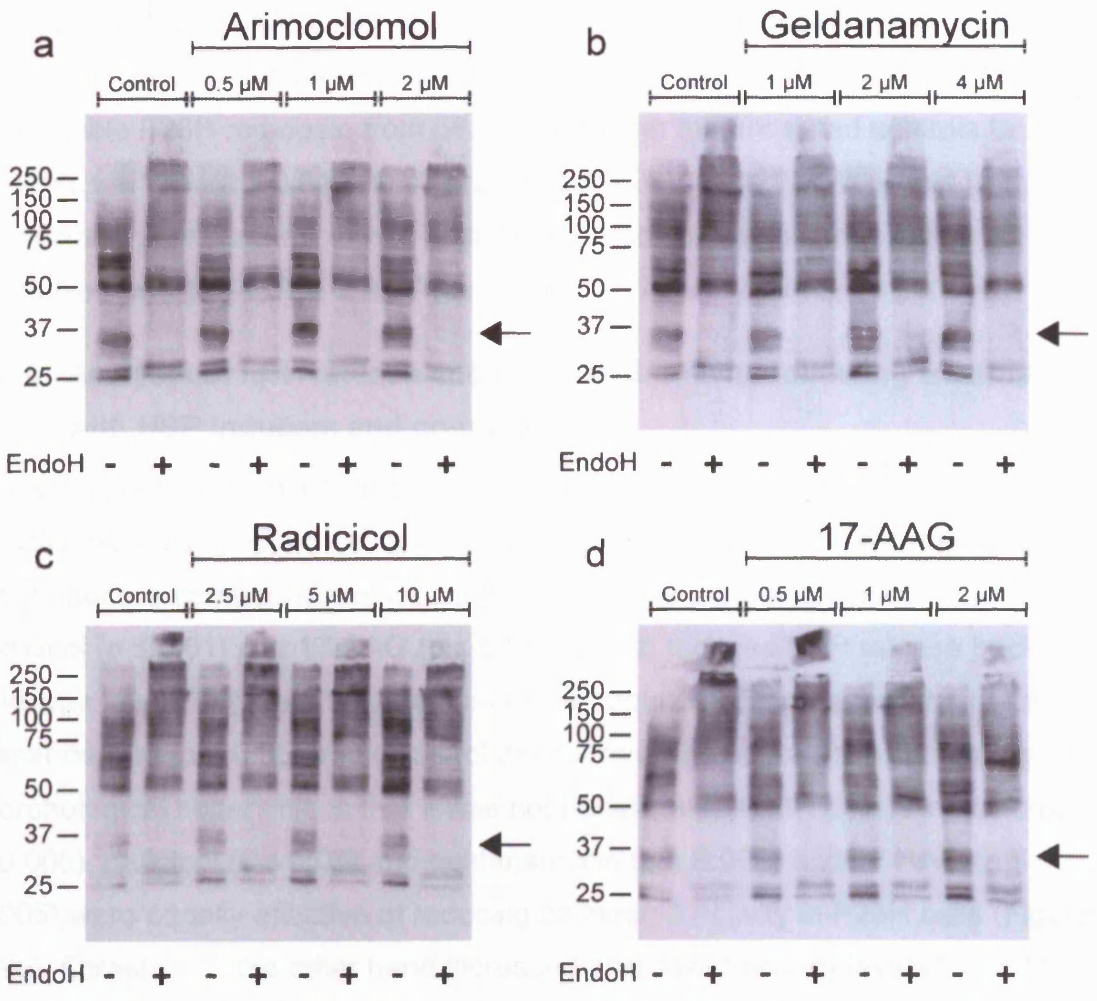

Figure 6.7 HSP inducers and co-inducers fail to promote EndoH resistance of soluble P23H rod opsin species.

SK-N-SH cells expressing untagged P23H rod opsin were treated with arimoclomol (a), geldanamycin (b), radicicol (c) and 17-AAG (d) for 24 hours. Cells were lysed and the soluble fraction was obtained as described in Chapter 3. 10 μg of soluble cell lysate protein were resolved on a 10% SDS-PAGE gel followed by immunoblotting with 1D4. Neither of these compounds promoted mature P23H rod opsin species (arrows). The position of molecular weight markers in kDa are shown on the left.

None of the compounds tested had an effect on the total levels of WT or P23H rod opsin (Figure 6.8a). Arimoclomol, geldanamycin, radicicol and 17-AAG, but not celastrol, had a positive effect in reducing the amount of insoluble rod opsin. 17-AAG, arimoclomol and radicicol were the most efficient and resulted in a reduction of insoluble P23H rod opsin from 58.70% ± 1.58 in the untreated controls to 25.95% ± 1.13% ($p \leq 0.01$), 29.47 ± 2.84 ($p \leq 0.01$), and 29.75% ± 3.44 ($p \leq 0.05$) respectively. Geldanamycin was slightly less efficient reducing the levels of insoluble opsin to 44.07% ± 0.77 ($p \leq 0.001$).

6.2.4 Analysis of LDH release and caspase-3 activity following treatment with HSP inducers and co-inducers

The effect of HSP inducers and co-inducers on LDH release and caspase-3 activity of cells expressing P23H rod opsin was assessed as described in Chapter 2. The most effective compounds at reducing LDH release were arimoclomol ($p \leq 0.01$), radicicol ($p \leq 0.01$) and 17-AAG ($p \leq 0.005$) which reduced LDH release back to wild-type levels (Figure 6.9a). Geldanamycin reduced LDH release albeit to a lesser degree ($p \leq 0.05$) and celastrol did not reduce LDH release confirming initial morphological observations that it was not beneficial to P23H cells. Arimoclomol ($p \leq 0.005$), radicicol ($p \leq 0.05$) and geldanamycin ($p \leq 0.001$) and 17-AAG ($p \leq 0.005$) were equally effective at reducing caspase-3 activity in P23H cells (Figure 6.9b). Celastrol on the other hand increased caspase-3 activity levels by ~20% in agreement with previous morphological observations.

6.2.5 Characterisation of the effect of HSP inducers and co-inducers on the dominant-negative interaction of P23H rod opsin on the wild-type protein

Assessment of the effect of HSP inducers and co-inducers on the dominant-negative mechanism of cell death between the P23H and the wild-type rod opsin was carried out as described in Chapter 2. Treatment with arimoclomol resulted in a decrease in the incidence of inclusions in co-transfected cells containing the wild-type protein (Figure 6.10d-f). Furthermore, arimoclomol resulted in an increase in

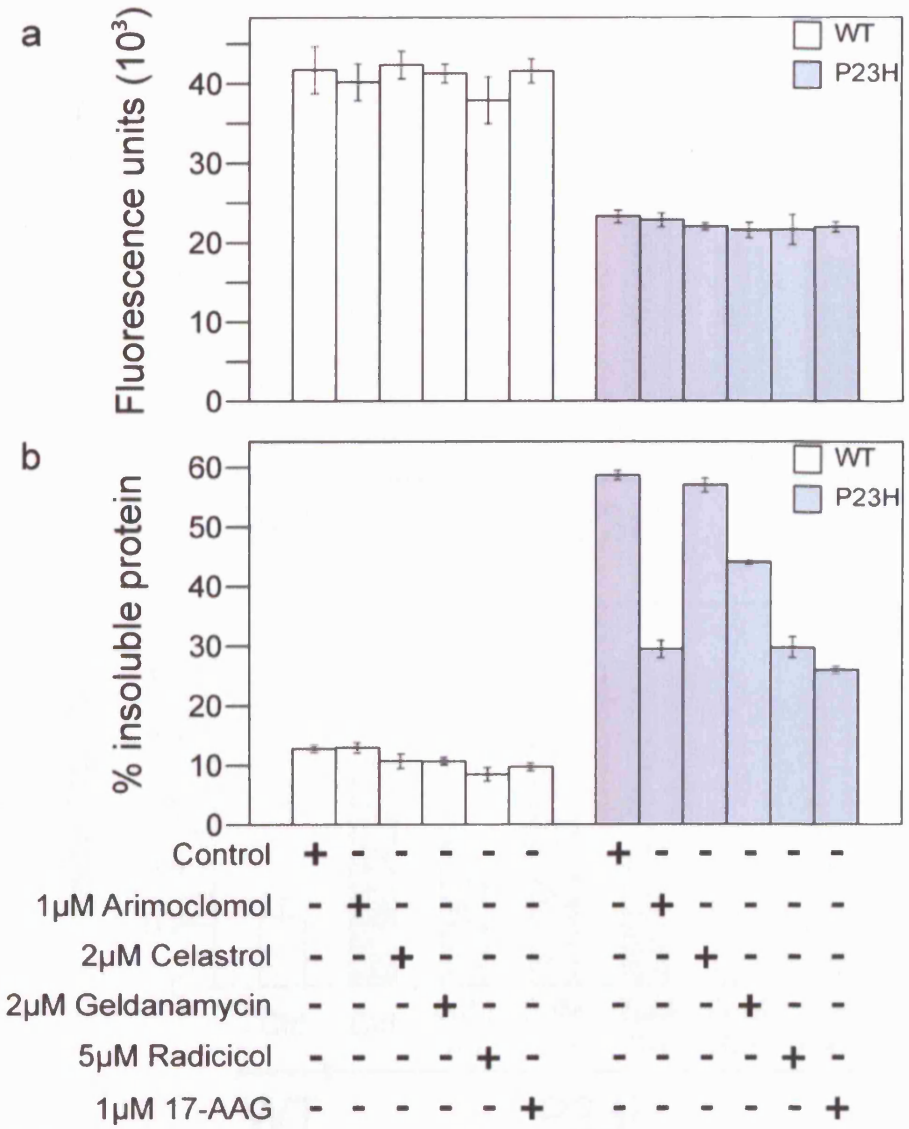

Figure 6.8 Arimoclomol, radicicol, geldanamycin and 17-AAG, but not celastrol, reduce the amount of insoluble P23H rod opsin.

A rod opsin fractionation assay was carried out as described in Chapter 3. SK-N-SH cells expressing WT-GFP or P23H-GFP were treated with HSP inducers and co-inducers as indicated for 24 hours. The concentrations of these compounds were: 1 μM arimoclomol; 2 μM celastrol; 2 μM geldanamycin; 5 μM radicicol and 1 μM 17-AAG . a) HSP inducers and co-inducers had no effect on the total protein levels of WT or P23H rod opsin b) Insoluble WT and P23H rod opsin quantified as percentage of total protein. 17-AAG ($p \leq 0.01$), arimoclomol ($p \leq 0.01$) and radicicol ($p \leq 0.05$) were the most effective at reducing insoluble P23H rod opsin levels. Geldanamycin was less effective ($p \leq 0.001$) and celastrol failed to reduce insoluble P23H levels. Error bars represent ± 2SE.

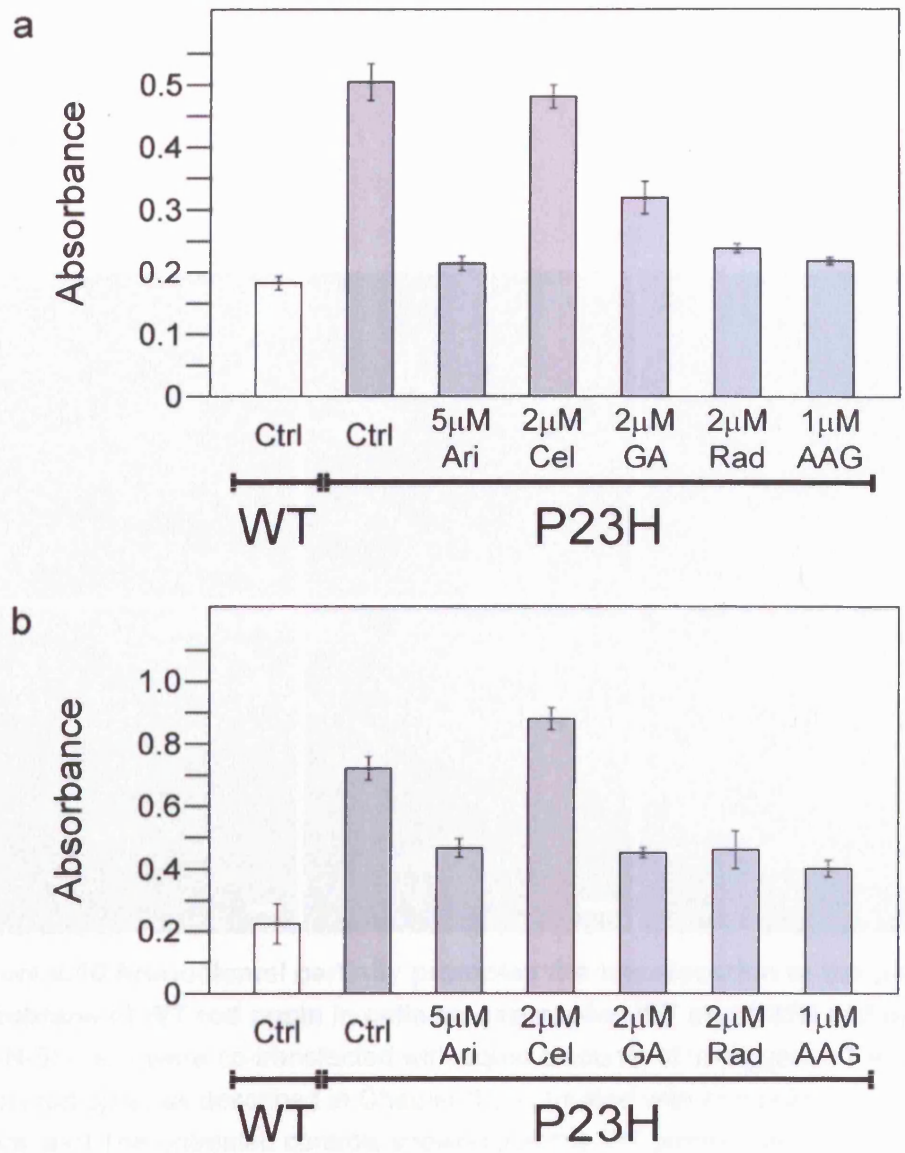

Figure 6.9 Effect of HSP inducers and co-inducers on LDH release and caspase-3 activity in cells expressing P23H rod opsin.

SK-N-SH cells were transfected with WT or P23H rod opsin and treated with HSP inducers and co-inducers for 48h before LDH (a) and caspase-3 activity (b) assays were carried out as described in Chapter 3. Treatment with arimoclomol ($p \leq 0.01$), radicicol ($p \leq 0.01$) and 17-AAG ($p \leq 0.005$) were the most efficient at reducing LDH release in cells expressing P23H rod opsin whereas geldanamycin was less effective ($p \leq 0.05$). Treatment with celastrol failed to reduce LDH release levels. Arimoclomol ($p \leq 0.005$), radicicol ($p \leq 0.05$), geldanamycin ($p \leq 0.001$) and 17-AAG ($p \leq 0.005$) were equally effective at reducing caspase-3 activity levels whereas treatment with celastrol increased caspase-3 activity when compared with the untreated P23H controls. Error bars represent ± 2SE.

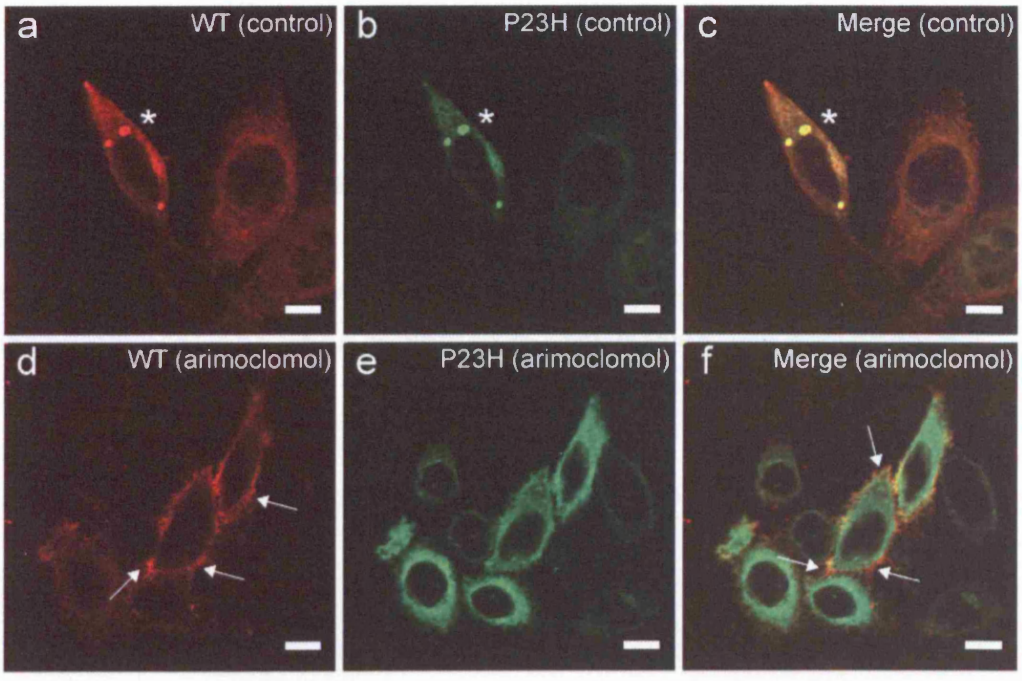

Figure 6.10 Arimoclomol partially promotes the translocation to the plasma membrane of WT rod opsin in cells co-expressing WT and P23H rod opsin. SK-N-SH cells were co-transfected with equal amounts of untagged WT and P23H rod opsin as described in Chapter 3 and treated with arimoclomol for 24 hours. a-c) The untreated controls showed that the WT protein failed to translocate to the plasma membrane of the cells and accumulated with the P23H rod opsin in the ER and in large intracellular inclusions (*). d-f) Treatment with 1 μM arimoclomol ($p \leq 0.001$) partially promoted the translocation of the WT rod opsin to the plasma membrane (arrows). Scale bars = 10 μm.

wild-type rod opsin present on the plasma membrane of co-transfected cells from 3.94% ± 2.00 in the untreated controls to 19.49% ± 6.12 ($p \leq 0.001$) (Figure 6.12). Geldanamycin, radicicol and 17-AAG reduced the incidence of inclusions in co-transfected cells which contained the wild-type protein, whereas celastrol failed to reduce the incidence of these inclusions (not statistically significant) when compared to untreated cells (Figure 6.11; Figure 6.12). The effect of the other HSP inducers on the facilitation of the translocation of the wild-type protein to the plasma membrane of co-transfected cells was less clear. Treatment with radicicol, 17-AAG ($p \leq 0.001$) and geldanamycin ($p \leq 0.05$) resulted in a slight increase on the number of co-transfected cells with the wild-type protein on the plasma membrane (Figure 6.12), however, the wild-type protein on the plasma membrane was less prominent than when compared to cells treated with arimoclomol.

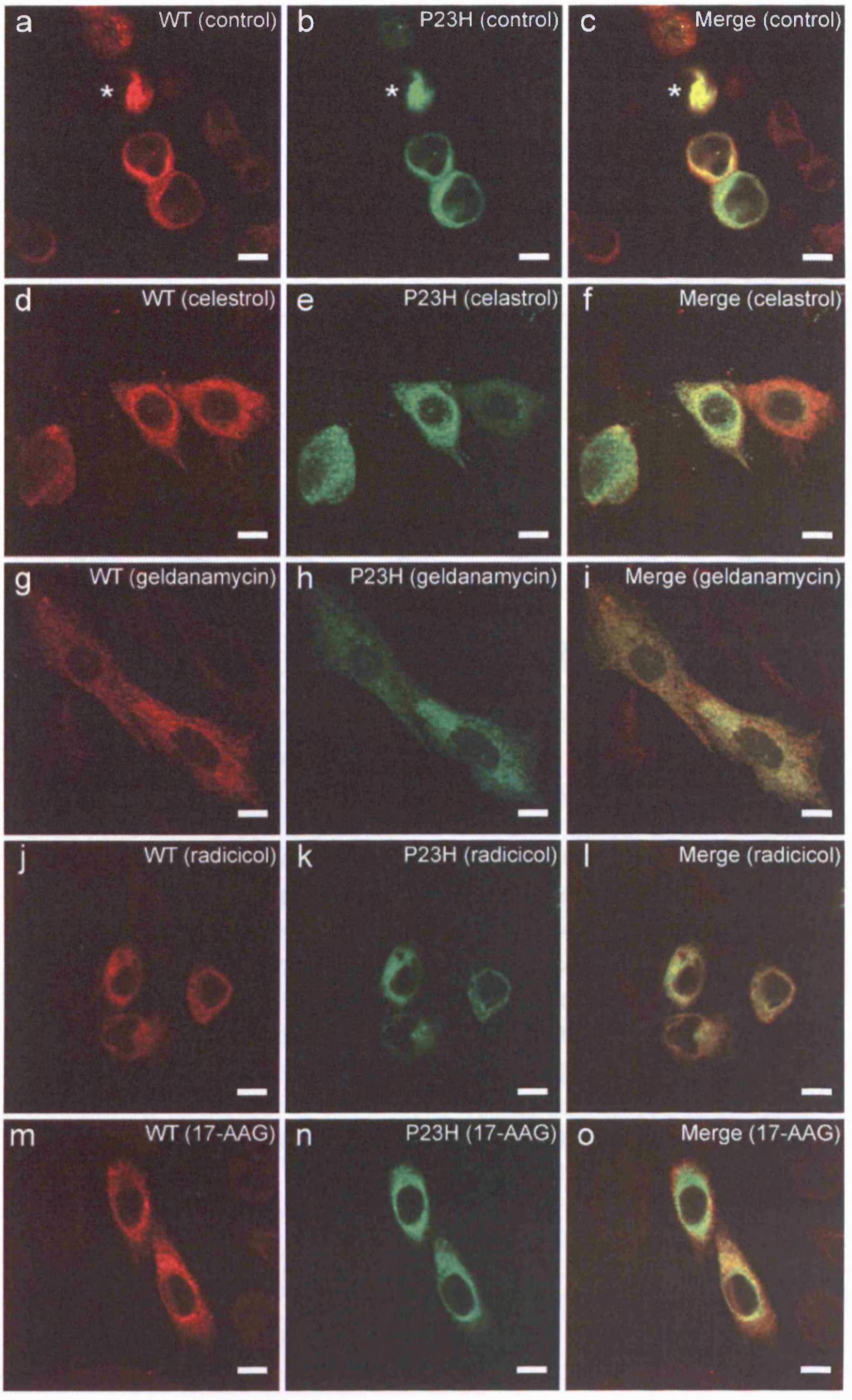
a
WT (control)
b
P23H (control)
c
Merge (control)
d
WT (celestrol)
e
P23H (celastrol)
f
Merge (celastrol)
g
WT (geldanamycin)
h
P23H (geldanamycin)
i
Merge (geldanamycin)
j
WT (radicicol)
k
P23H (radicicol)
l
Merge (radicicol)
m
WT (17-AAG)
n
P23H (17-AAG)
o
Merge (17-AAG)

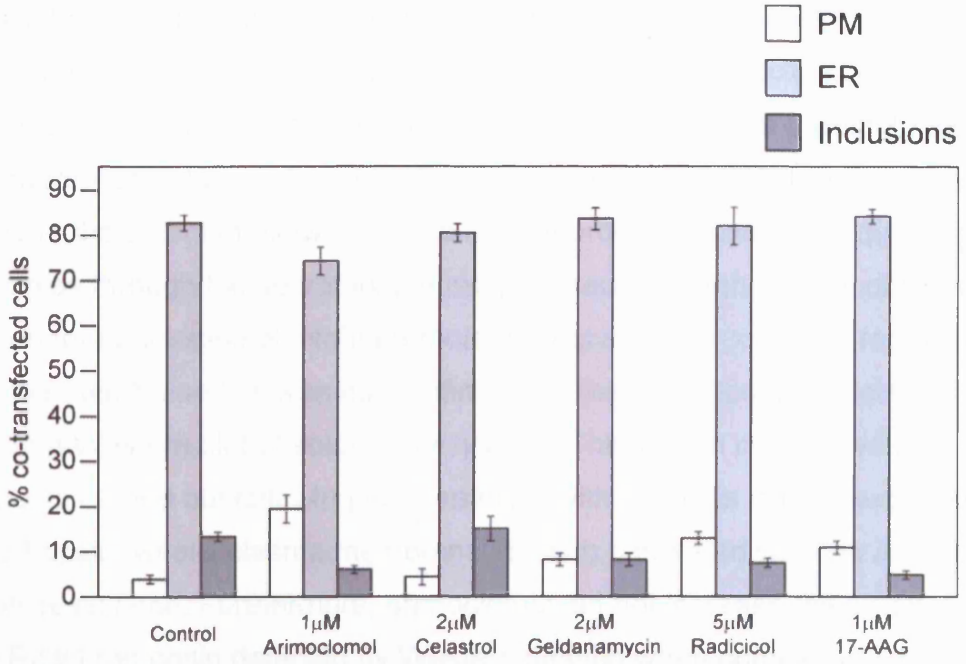

Figure 6.12 Arimoclomol, radicicol, geldanamycin and 17-AAG reduce the inclusion incidence of WT rod opsin in cells co-expressing WT and P23H rod opsin.

SK-N-SH cells were co-transfected with equal amounts of untagged WT and P23H-GFP rod opsin as described in Chapter 3 and treated as indicated for 24 hours with the following doses of HSP inducers and co-inducers: 1 μM arimoclomol, 2 μM celastrol, 2 μM geldanamycin, 5 μM radicicol and 1 μM 17-AAG. The intracellular localisation of WT rod opsin in co-transfected cells was assessed and scored as plasma membrane, ER or inclusions. Arimoclomol reduced the incidence of inclusions containing the WT protein ($p \leq 0.001$) and partially promoted the translocation of WT rod opsin to the plasma membrane of co-transfected cells ($p \leq 0.001$). Error bars represent ± 2SE.

6.3 Discussion

The data presented in this chapter suggest that the hydroxylamine derivative arimoclomol and the Hsp90 inhibitors geldanamycin, radicicol and 17-AAG alleviated the toxic gain of function mechanism of cell death in cells expressing P23H rod opsin. However, none of these compounds with the exception of arimoclomol efficiently promoted the translocation of the mutant protein to the plasma membrane of the cell suggesting that the folding of P23H rod opsin was not improved to the extent of allowing all the mutant protein to evade ER quality control and progress through the secretory pathway. Although morphological observations suggested that arimoclomol might promote the translocation of P23H rod opsin to the plasma membrane this was not confirmed by the detection of EndoH resistant species in a Western blot of soluble cell lysates. This was in contrast with experiments carried out following the treatment with retinoids in cells expressing P23H rod opsin, where plasma membrane staining correlated with the appearance of EndoH resistance. Furthermore, arimoclomol did not increase the amount of soluble P23H rod opsin detected by Western blotting when compared to the untreated controls, as was observed with retinoids. There might be several possibilities for the absence of EndoH resistance in arimoclomol-treated cells. Firstly, the levels of P23H rod opsin that exit the ER to the Golgi and reach the plasma membrane following treatment with arimoclomol might be below the threshold for detection by 1D4 but not by immunocytochemistry as treatment with arimoclomol of cells expressing untagged P23H rod opsin promoted the translocation of the mutant protein to the plasma membrane. Secondly, a greater level of P23H opsin species, independent of drug treatment, appeared to be retained in the stacking gel following digestion with EndoH (Figure 5.7) when compared to undigested cell lysates.

In order to address this apparent discrepancy non-permeabilised SK-N-SH cells expressing P23H-GFP were incubated with the N-terminal-specific 4D2 rhodopsin antibody (a kind gift from Professor Robert Molday, UBC). The rationale for this

approach was that a 4D2 signal would only be detected if P23H rod opsin was present in the plasma membrane and the 4D2 N-terminus epitope was located extracellularly. However, when this experiment was carried out 4D2 also stained the intracellular inclusions preventing the elucidation of the staining pattern following treatment with arimoclomol. These observations suggested membrane leakage and correlate with the LDH assay where the disruption of the plasma membrane in P23H cells resulted in increased LDH release levels indicating a detrimental effect of P23H rod opsin on cell viability.

In the case of the Hsp90 inhibitors geldanamycin, radicicol and 17-AAG the inability to detect EndoH resistant species correlated with the morphological observations, where despite reducing inclusion incidence these compounds did not appear to promote the translocation of the mutant protein to the plasma membrane. Furthermore, geldanamycin and radicicol did not increase the levels of soluble P23H rod opsin whereas 17-AAG appeared to slightly increase the levels of soluble mutant protein.

The rod opsin fractionation assay carried out in P23H cells following treatment with arimoclomol, geldanamycin, radicicol and 17-AAG reduced insoluble mutant opsin while having no effect on the total levels of protein. Previously published data suggested that 17-AAG induced the degradation of misfolded mutant AR (Solit *et al.*, 2002). It would be interesting to assess if the inhibition of the proteasome would result in increased inclusion incidence/insoluble protein following treatment of P23H cells with 17-AAG. This should elucidate whether 17-AAG reduces inclusion incidence/insoluble protein by preventing aggregation of P23H rod opsin or by increasing the degradation of misfolded mutant protein.

The reduced levels of insoluble P23H rod opsin and the maintenance of the total levels of mutant protein following treatment with HSP inducers and co-inducers suggested that soluble P23H levels had increased. However, this was not observed in a Western blot of soluble P23H rod opsin species with the exception of

17-AAG. This phenomenon was also present following treatment with chemical chaperones where the rod opsin fractionation assay suggested an increase in soluble P23H rod opsin which was not observed in a Western blot detecting soluble P23H species.

Arimoclomol, radicicol, 17-AAG, and to a lesser extent geldanamycin, reduced LDH release confirming that these compounds alleviated the gain of function mechanism induced by P23H rod opsin. Arimoclomol, radicicol and 17-AAG reduced LDH release back to wild-type protein levels and were more effective than chemical chaperones and equally as effective as retinoids. Arimoclomol, geldanamycin, radicicol and 17-AAG were equally effective at reducing caspase-3 activity in cells expressing P23H rod opsin. As with chemical chaperones caspase-3 activity was reduced to intermediate levels between those of the wild-type and P23H controls. These compounds were less effective than retinoids as the treatment with 9-*cis*-retinal and 11-*cis*-retinal reduced caspase-3 activity back to wild-type levels.

Westerheide and colleagues (2004) have suggested that the maximal induction of the inducible Hsp70 promoter by celastrol occurred at a concentration of 7 μM with an Ec_{50} of 3 μM. In the cell model for rhodopsin RP presented in this study concentrations ranging from 0.1 μM to 5 μM failed to elicit positive effects on cells expressing P23H despite a marginal reduction in inclusion incidence. It would be interesting to assess the toxicity in cells expressing P23H rod opsin following treatment with celastrol was due to a long incubation with the compound. However, this was not likely to be the case as Westerheide and colleagues (2004) incubated cells with celastrol for 24 hours prior to the assessment of Hsp70 induction.

Arimoclomol appeared to have a mild effect on the dominant-negative effect of P23H rod opsin on the wild-type protein by reducing the recruitment of the wild-type protein to inclusions and by partially promoting the translocation of wild-type protein to the plasma membrane of co-transfected cells, however, this was less

evident that the effects seen following treatment with retinoids. Geldanamycin, radicicol and 17-AAG reduced the incidence of inclusions containing wild-type rod opsin in co-transfected cells and that might account for a partial alleviation of the dominant-negative phenotype. However, as with chemical chaperones there was no evidence that these compounds promoted the folding of P23H rod opsin and consequently suppressed the dominant-negative effect of the P23H rod opsin on the wild-type protein, as demonstrated by the inability of the wild-type rod opsin to exit the ER and re-establish its normal translocation through the secretory pathway in co-transfected cells. This correlated with the inability to promote P23H folding as assessed by the absence of EndoH resistant species.

When COS-1 cells were treated with geldanamycin it resulted in the activation of the heat shock response and prevented the aggregation of a Huntington's disease exon 1 protein with a polyglutamine stretch in the pathological range (Sittler *et al.*, 2001). It was proposed that the effect of geldanamycin on the HD exon 1 aggregation was a direct consequence of the activation of Hsp40, Hsp70 and Hsp90 causing an increased expression of these proteins. These chaperones associated with the mutant HD exon 1 protein and prevented its aggregation into fibrillar structures. Furthermore, these authors demonstrated Hsp90 itself did not appear to be directly involved in the inhibition of mutant HD exon 1 aggregation. Therefore, it appeared that a direct interaction between Hsp90 and the HD exon 1 protein was not necessary for the suppression of aggregation *in vivo* and the key event was the geldanamycin induced dissociation of HSF-Hsp90 complexes. However, Dickey and colleagues (2007) reported that inhibition of Hsp90 led to decreases in p-tau levels, primary pathologic component of Alzheimer's disease, independent of HSF1 activation. A critical mediator of this mechanism appeared to be carboxy terminus of Hsp70-interacting protein (CHIP), a tau ubiquitin ligase. Cochaperones were also involved in Hsp90-mediated removal of p-tau, while those of the mature Hsp90 refolding complex prevented this effect (Dickey *et al.*, 2007).

Geldanamycin however has limitations as a drug candidate in protein-folding disorders due to its poor stability and hepatotoxicity (Supko *et al.*, 1995). This led to the search for synthetic analogues with higher potency and lower toxicity. For example, geldanamycin binds to full-length dimeric Hsp90 with a K_d = 1.2 μM while radicicol has shown significantly higher affinity with a K_d = 19 nM and both compounds bind to intact dimeric yeast Hsp90 with stoichiometries of approximately one antibiotic molecule per Hsp90 monomer (Roe *et al.*, 1999). These data raise important questions in relation to the cellular model for rhodopsin RP as the most effective concentrations for geldanamycin and radicicol were 2 μM and 5 μM respectively, in stark contrast with their K_d values. This might be due to optimal concentrations being determined based on two factors: reduction of inclusion incidence and absence of toxicity. Radicicol while having higher affinity was shown to be far less toxic than geldanamycin at equivalent concentrations (Sano, 2001) and this might account for the higher concentration of radicicol required for maximum effect in cells expressing P23H rod opsin.

Pharmacological interventions with compounds that cause the induction of HSPs have a great therapeutic potential in protein misfolding diseases. This is particularly the case as the late onset of neurodegenerative misfolding diseases may be triggered by an imbalance between the cellular chaperone machinery and the amount of misfolded protein species. This study has identified arimoclomol and three inducers of HSPs such as geldanamycin, radicicol and 17-AAG as potential pharmacological candidates for patients with Class II rhodopsin RP as they were able to alleviate the gain of function mechanisms induced by P23H rod opsin.

Chapter 7: Other compounds and combination of treatments

The data presented in this chapter relates to a variety of other compounds used on the cell model of rhodopsin RP. They include rapamycin an inhibitor of the mammalian target of rapamycin (mTOR); salubrinal an inhibitor of eukaryotic translation initiation factor 2 subunit α (eIF2α) dephosphorylation; the anti-oxidant resveratrol; the deglucosidase inhibitors 1-Deoxynojirimycin (1-DNJ) and N-butyldeoxynojirimycin (NB-DNJ). Furthermore, this chapter also includes preliminary data on treatments combining more than one compound such as 9-*cis*-retinal and chemical chaperones, or a combination of chemical chaperones.

7.1 Autophagy inducers

7.1.1 Introduction

The major pathways for protein and organelle degradation in eukaryotic cells are cytosolic turnover by the proteasome and autophagy. The induction of autophagy can be achieved by inhibiting the mammalian target of rapamycin (mTOR) which negatively regulates autophagy (Ravikumar *et al.*, 2002). mTOR is a well-conserved 289 kDa phosphatidylinositol 3-kinase (PI 3-kinase)-related kinase (PIKK) which is an integrator of various extracellular and intracellular signals including growth factors, nutrients, energy, and stress (Tsang *et al.*, 2007). Rapamycin is a macrolide that is produced by the bacterium *Streptomyces hygroscopicus* and was the first compound identified which acted as an inhibitor of mTOR. Rapamycin includes two separate moieties namely the TOR-binding and the FKBP12-binding regions. In order to be biologically active it forms a tertiary complex with mTOR and FKBP12 (Sabers *et al.*, 1995).

Treatment with rapamycin protected against neurodegeneration whereas the rapamycin analogue CCI-779 improved the performance in behavioural tasks and decreased the levels of inclusions in a mouse model of Huntington's disease

(Ravikumar *et al.*, 2004). More recently rapamycin was shown to enhance the autophagic clearance of a variety of other misfolding proteins and to reduce toxicity in *Drosophila* expressing wild-type or mutant forms of tau (Berger *et al.*, 2006) suggesting a possible wider application for this therapeutic approach.

The autophagy clearance induced by rapamycin on autophagy substrates such as mutant huntingtin and mutant α-synuclein transfected into COS-7 cells was further enhanced when trehalose was used in conjunction with rapamycin (Sarkar *et al.*, 2007). In addition trehalose had autophagic inducing properties *per se* leading to the suggestion that trehalose might have dual protective properties in this model both as an inducer of autophagy and as a chemical chaperone which protected the cells against pro-apoptotic insults via the mitochondrial pathway (Sarkar *et al.*, 2007).

The results obtained in these studies suggested that the induction of autophagy by use of rapamycin could be beneficial in a cell model of rhodopsin RP where the P23H protein misfolded, was retained in the ER and accumulated in intracellular inclusions.

7.1.2 Results

7.1.2.1 Rapamycin reduces inclusion incidence in cells expressing P23H rod opsin and this is enhanced by trehalose

7.1.2.1.1 *Rapamycin*

Treatment with different concentrations of rapamycin resulted in a dose-dependent reduction of inclusion incidence in cells expressing P23H rod opsin (Figure 7.1.1). The most effective concentration of rapamycin at reducing inclusion incidence was 1 μM which resulted in a decrease in inclusion incidence from 24.26% ± 4.52 in the untreated controls to 10.15% ± 3.11 ($p \leq 0.005$). Rapamycin had no effect on cells expressing the wild-type protein at concentrations lower than 1 μM (Figure 7.1.1c).

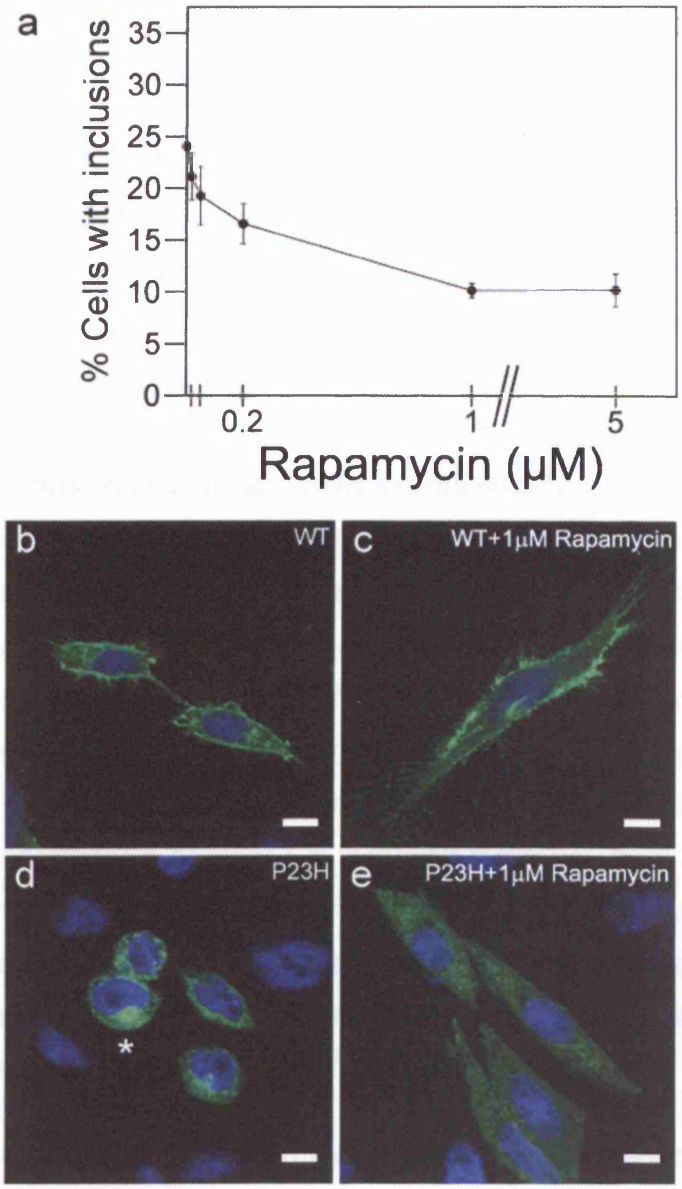

Figure 7.1.1 Rapamycin reduces inclusion incidence in cells expressing P23H rod opsin.

a) SK-N-SH cells expressing P23H-GFP rod opsin were treated with various concentrations of rapamycin for 24 hours. The most effective concentration was 1 μM rapamycin which reduced inclusion incidence from 24.26 ± 4.52 in the untreated controls to 10.15 ± 3.11 ($p \leq 0.005$). Error bars represent ± 2SE.
b-e) Treatment with rapamycin reduced inclusion incidencebut did not promote the translocation of mutant rod opsin to the plasma membrane of the cells. Asterisks highlight inclusions. Scale bar = 10 μm.

Despite the reduction on inclusion incidence rapamycin did not appear to promote the translocation of P23H rod opsin to the plasma membrane (Figure 7.1.1e).

7.1.2.1.2 *Rapamycin + Trehalose*

The rationale for the combination of trehalose to rapamycin in a treatment was based on data from Sarkar and colleagues (2007) where treatment with both drugs exerted an additive effect on the clearance of aggregate-prone proteins and on the data presented in Chapter 5 where trehalose had a positive effect on the gain of function mechanism induced by P23H rod opsin. The effect of rapamycin plus trehalose on the inclusion incidence in cells expressing P23H rod opsin is shown in Figure 7.1.2. The concentrations of rapamycin and trehalose were based on the concentrations used while assessing the effect of each individual compound on the inclusion incidence in P23H cells (shown in Figure 7.1.1 and Figure 5.5 respectively). The most effective concentrations were 5 μM rapamycin (which was not more effective than 1 μM rapamycin in the absence of trehalose) and 100 mM trehalose (which was not more effective than 50 mM trehalose in the absence of rapamycin) and resulted in a decrease in inclusion incidence from 22.93% ± 5.64 in the untreated controls to 6.81% ± 2.00 ($p \leq 0.005$). The most effective concentrations determined here were higher when used in conjunction than when used separately and this may be mainly due to the cumulative protective effect of these drugs when used together.

7.1.2.2 Rapamycin reduces the amount of insoluble rod opsin in P23H-transfected cells and this is enhanced by the presence of trehalose

A rod opsin fractionation assay of cells expressing the WT or P23H protein and treated with 1 μM rapamycin or 5 μM rapamycin plus 100 mM trehalose is shown in Figure 7.1.3. Treatment with rapamycin or rapamycin plus trehalose had no effect on the total levels of WT or P23H rod opsin (Figure 7.1.3a). The percentage of insoluble P23H rod opsin was reduced by treatment with rapamycin from 60.56% ± 2.72 in the untreated controls to 38.73 ± 5.47 ($p \leq 0.01$) whereas rapamycin plus trehalose was more efficient, reducing the percentage of insoluble mutant protein

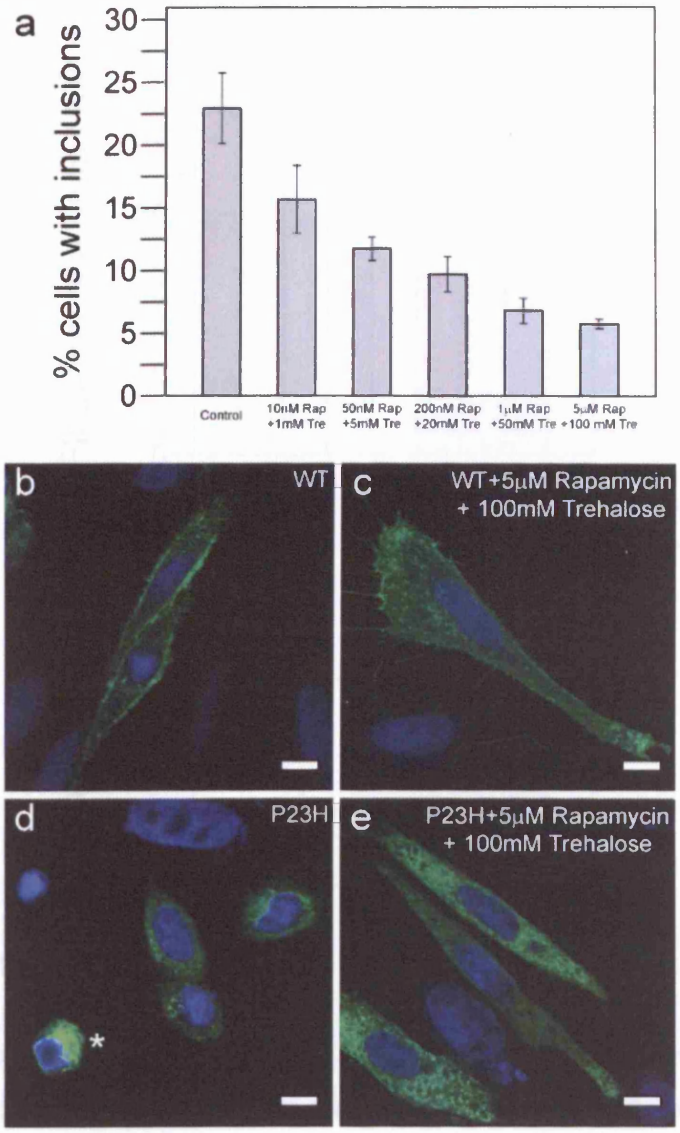

Figure 7.1.2 Trehalose enhances the reduction of inclusion incidence by rapamycin in cells expressing P23H rod opsin.

a) SK-N-SH cells expressing P23H-GFP rod opsin were treated with various concentrations of rapamycin (Rap) and trehalose (Tre) for 24 hours. The most effective concentration was 5 μM rapamycin + 100 mM trehalose which reduced inclusion incidence from 22.93 ± 5.64 in the untreated controls to 6.81 ± 2.00 ($p \leq 0.005$). Error bars represent ± 2SE. b-e) Despite enhancing the reduction of inclusion incidence the combined treatment of P23H cells with rapamycin and trehalose did not promote the translocation of mutant rod opsin to the plasma membrane of the cells. Asterisks highlight inclusions. Scale bar = 10 μm.

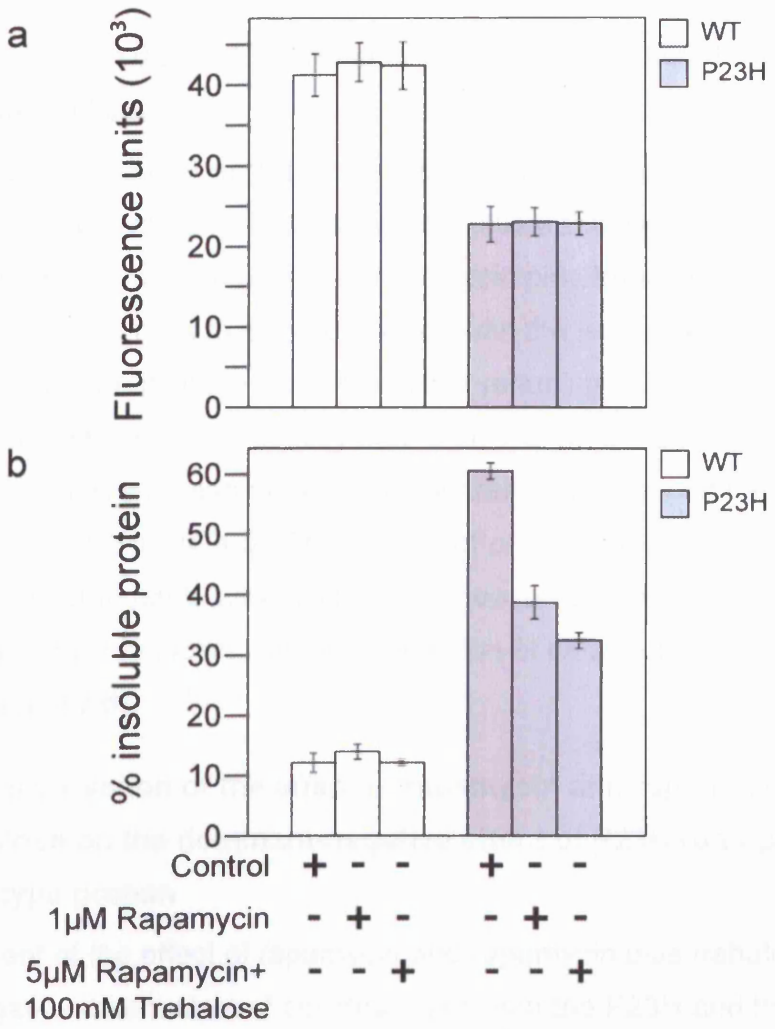

Figure 7.1.3 Rapamycin reduces the amount of insoluble P23H rod opsin and this reduction is increased by optimal concentrations of rapamycin plus trehalose.

A rod opsin fractionation assay was carried out as described in Chapter 3. SK-N-SH cells expressing WT-GFP or P23H-GFP were treated with 1 μM rapamycin or 5 μM rapamycin + 100 mM trehalose. a) The amount of total WT and P23H rod opsin in cells treated with tapamycin and rapamycin + trehalose. b) Quantification of insoluble P23H rod opsin as percentage of total protein. Rapamycin ($p \leq 0.01$) and rapamycin + trehalose ($p \leq 0.05$) reduced the percentage of insoluble P23H rod opsin. Error bars represent ± 2SE.

to 32.44% ± 2.56 ($p \leq 0.005$) ($p \leq 0.05$) (Figure 7.1.3b).

7.1.2.3 Rapamycin reduces LDH release and caspase-3 activity in P23H-transfected cells

LDH release and caspase-3 activity were measured in cells expressing P23H rod opsin and treated with rapamycin or rapamycin plus trehalose as described in Chapter 3. Treatment with rapamycin or rapamycin plus trehalose reduced LDH release levels in P23H cells to those observed with the wild-type protein (Figure 7.1.4a). These treatments were also effective at reducing caspase-3 activity. Rapamycin reduced caspase-3 activity from 0.80 ± 0.18 in the untreated controls to 0.56 ± 0.05 ($p \leq 0.01$) whereas rapamycin plus trehalose reduced caspase-3 activity to 0.51 ± 0.02 ($p \leq 0.005$). The degree of protection against caspase-3 activity by these compounds was similar to that observed with chemical chaperones and HSP inducers, with the exception of celastrol, but was less than that seen with retinoids.

7.1.2.4 Characterisation of the effect of rapamycin and rapamycin plus trehalose on the dominant-negative effect of P23H rod opsin on the wild-type protein

The assessment of the effect of rapamycin and rapamycin plus trehalose on the dominant-negative mechanism of cell death between the P23H and the wild-type rod opsin was carried out by co-transfecting cells with equal amounts of WT and P23H rod opsin as described in Chapter 2 . Treatment with 1 µM rapamycin ($p \leq 0.005$) and 5 µM rapamycin plus 100 mM trehalose ($p \leq 0.001$) reduced the incidence of inclusions in co-transfected cells which contained the wild-type protein (Figure 7.1.5). Furthermore, rapamycin ($p \leq 0.05$) and rapamycin plus trehalose ($p \leq 0.005$) resulted in a very small increase in the percentage of co-transfected cells apparently showing plasma membrane staining (Figure 7.1.5). However, the vast majority of cells showed co-localisation of wild-type and P23H rod opsin in the ER suggesting that these compounds largely failed to alleviate the effect of the mutant rod opsin on the wild-type protein (Figure 7.1.6).

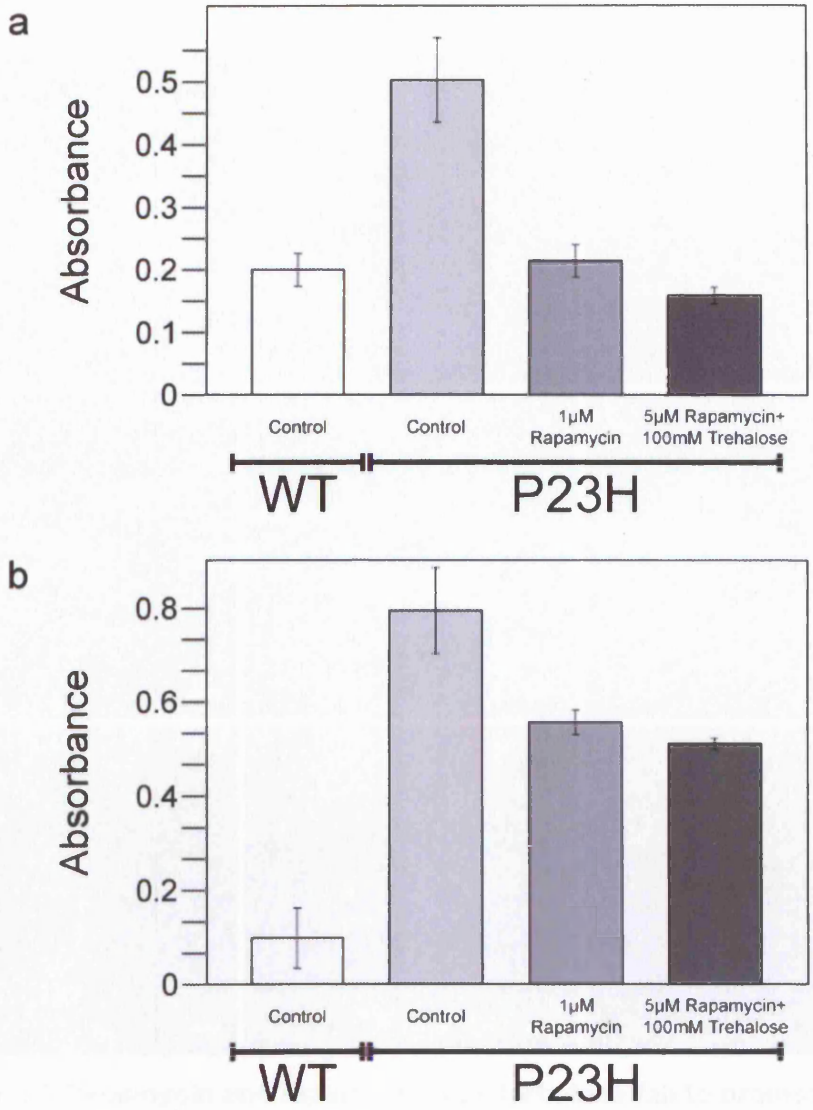

Figure 7.1.4 Rapamycin reduces LDH release and caspase-3 activity in cells expressing P23H rod opsin and trehalose enhances these effects.
SK-N-SH cells expressing WT or P23H rod opsin were treated with 1 μM rapamycin or 5 μM rapamycin + 100 mM trehalose as described for 48h before LDH (a) and caspase-3 activity (b) assays were carried out as described in Chapter 3. LDH release decreased following treatment with rapamycin ($p \leq 0.01$) and rapamycin + trehalose ($p \leq 0.001$). Caspase-3 activity was reduced by treatment with rapamycin ($p \leq 0.01$) and rapamycin + trelalose ($p \leq 0.005$). Error bars represent ± 2SE.

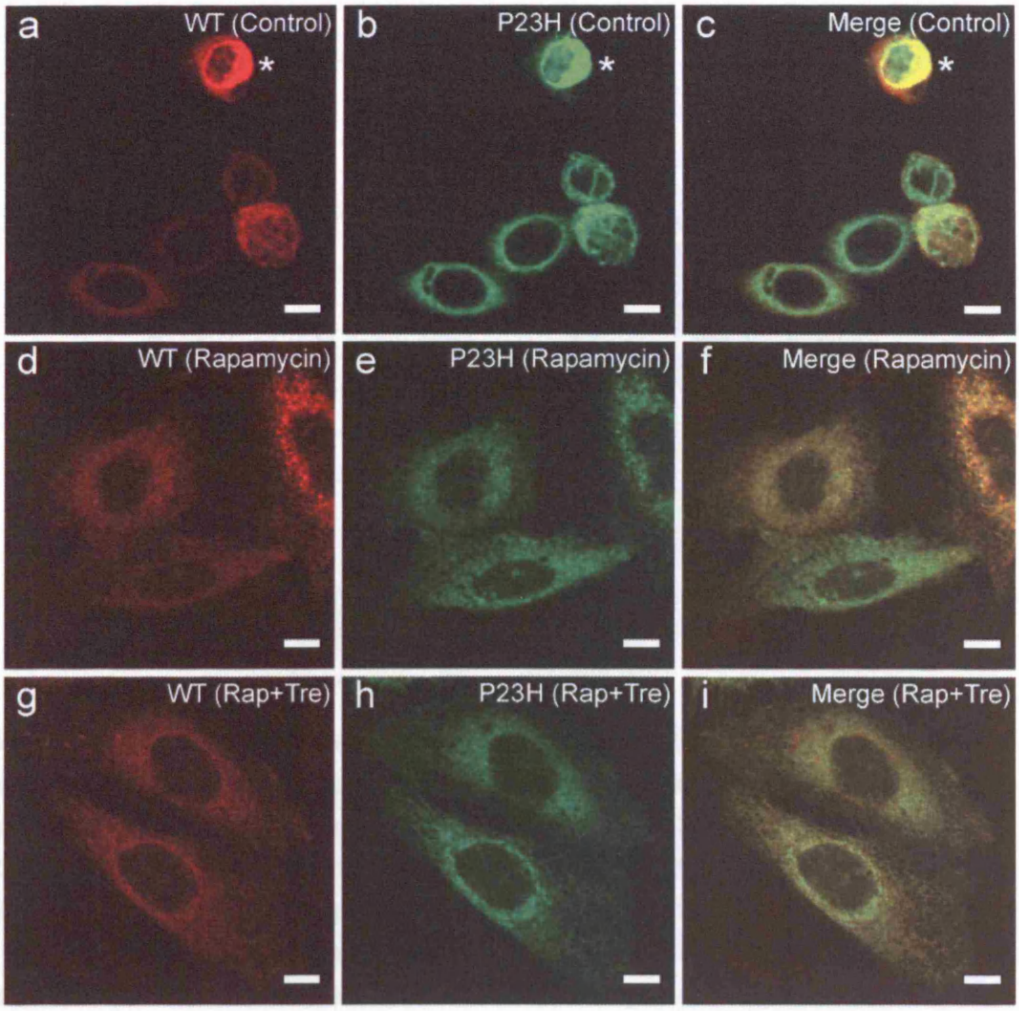

Figure 7.1.5 Rapamycin and rapamycin plus trehalose fail to promote the translocation of WT rod opsin to the plasma membrane in cells co-expressing WT and P23H rod opsin.

SK-N-SH cells were co-transfected with equal amounts of untagged WT and P23H-GFP rod opsin and treated with 1 μM rapamycin or 5 μM rapamycin plus 100 mM trehalose (Rap+Tre) as described for 24 hours. In the untreated controls (a-c) the WT protein failed to translocate to the plasma membrane of the cells and accumulated with the P23H rod opsin in large intracellular inclusions (*). Treatment with rapamycin (d-f) and rapamycin plus trehalose (g-i) reduced WT inclusion incidence in cells co-expressing WT and P23H rod opsin. Scale bars = 10 μm.

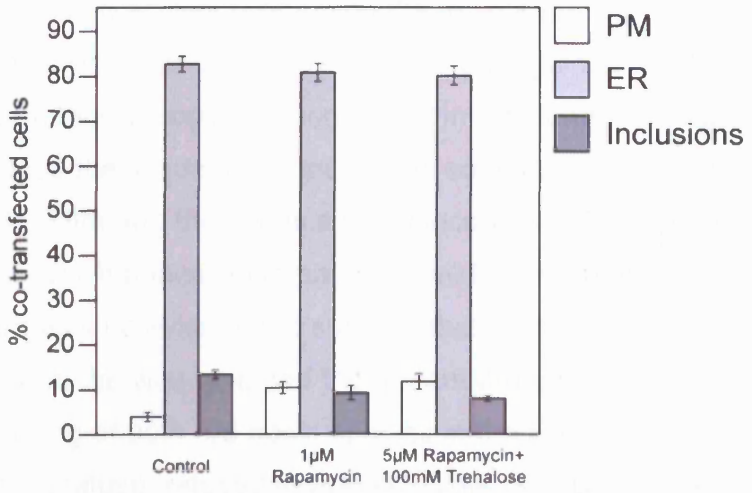

Figure 7.1.6 Rapamycin and rapamycin plus trehalose reduce the inclusion incidence and slightly increase the translocation to the plasma membrane of WT rod opsin in cells co-expressing WT and P23H rod opsin.
SK-N-SH cells were co-transfected with equal amounts of untagged WT and P23H-GFP rod opsin and treated with 1 μM rapamycin and 5 μM rapamycin plus 100 mM trehalose as indicated for 24 hours. The localisation of WT rod opsin in co-transfected cells was assessed and scored as plasma membrane, ER or inclusions. Rapamycin ($p \leq 0.05$) and rapamycin plus trehalose ($p \leq 0.005$) reduced the incidence of inclusions containing the WT protein. In addition, treatment with rapamycin ($p \leq 0.005$) and rapamycin plus trehalose ($p \leq 0.001$) resulted in a slight increase in the percentage of co-transfected cells containing WT rod opsin in the plasma membrane. Error bars ± 2SE.

7.1.3 Discussion

The data presented here suggest that rapamycin was effective in reducing inclusion incidence in cells expressing the P23H mutant rod opsin. However, rapamycin did not appear to promote the translocation of P23H rod opsin to the plasma membrane. Furthermore, rapamycin protected P23H cells against LDH release and caspase-3 activity suggesting that by preventing the P23H rod opsin accumulation in intracellular inclusions it alleviated a gain of function mechanism induced by the mutant rod opsin. When tested in the dominant-negative context rapamycin reduced the incidence of inclusions containing wild-type rod opsin in co-transfected cells. Although there was a small increase in the percentage of co-transfected cells which appeared to have the wild-type protein in the plasma membrane there was no evidence to suggest that rapamycin suppressed the interaction between the wild-type and the mutant protein as the vast majority of the cells had co-staining of both rod opsin species in the ER. Treatment with rapamycin plus trehalose reduced inclusion incidence, LDH release and caspase-3 activity further than rapamycin alone but did not appear to suppress the dominant-negative effect of the P23H rod opsin on the wild-type protein. Inclusion incidence and caspase-3 activity following treatment with rapamycin plus trehalose were similar to those observed with 50 mM trehalose, however, rapamycin plus trehalose conferred P23H cells greater protection against LDH release than trehalose alone. These data suggested that the combination of these compounds might have a positive cumulative effect on protecting cells the gain of function mechanism induced by the P23H protein.

The data suggest that treatment with rapamycin or rapamycin plus trehalose could be beneficial in a range of diseases including ADRP which caused by toxic gain of function mutations which cause protein misfolding. Although these compounds were previously found to have positive effects on cell and animal models of Huntington's disease by inducing autophagy (Berger *et al.*, 2006; Sarkar *et al.*, 2007) we have not yet confirmed if this is the mechanism of action by which

rapamycin exerted its positive effects in this model of rhodopsin RP. This could be assessed, for example, by transfecting cells with wild-type and P23H rod opsin and treating them with rapamycin in the presence of an autophagy inhibitor such as 3-methyl adenine (3-MA).

Kaushal (2007), however, suggested that upon incubation with rapamycin, the levels of P23H rod opsin were reduced more rapidly than in untreated controls while no observable changes in the amounts of wild-type rod opsin was seen. Furthermore, the autophagy specific marker proteins, Atg7, Atg8 (LC3), and LAMP-1, which associate with autophagic vacuoles, co-localised with P23H rod opsin suggesting that autophagy might be directly responsible for the clearance of mutant protein (Kaushal, 2007). Furthermore, this author suggested that neither the unfolded protein response nor the heat shock response were induced upon rapamycin-associated degradation of P23H opsin.

7.2 Preliminary data on additional pharmacological agents

7.2.1 Salubrinal

Salubrinal, whose molecular structure is shown in Figure 7.2.1a, was identified in a screen for pharmacological agents that protected the rat pheochromocytoma cell line PC12 from ER stress-induced apoptosis (Boyce *et al.*, 2005). This study also reported that salubrinal engaged the translational control branch of the UPR by inducing eIF2α phosphorylation without inducing the transcription-dependent component of the UPR. EIF2α phosphorylation has been suggested to be cytoprotective during ER stress as an induced recessive mutation in the gene encoding the ER stress-activated eIF2α kinase abolished the phosphorylation of eIF2α in response to accumulation of misfolded proteins in the ER which resulted in abnormally elevated protein synthesis and higher levels of ER stress (Harding *et al.*, 2000). It was therefore important to test if salubrinal could protect cells expressing P23H rod opsin against the gain of function mechanism induced by the mutant protein.

SK-N-SH cells expressing wild-type and P23H rod opsin were treated with 25 μM, 50 μM and 75 μM salubrinal for 24 hours. These concentrations of salubrinal increased the incidence of inclusions in cells expressing P23H rod opsin from 26.00% ± 1.816 in the untreated controls to 36.97% ± 7.92 ($p \leq 0.001$), 43.24% ± 6.97 ($p \leq 0.001$) and 43.56% ± 6.78 ($p \leq 0.001$) respectively (Figure 7.2.1).

Boyce *et al* (2005) identified a small-molecule inhibitor of eIF2a dephosphorylation, salubrinal, which specifically inhibits the PP1-GADD34 phosphatase activity, resulting in sustained eIF2a phosphorylation. Although the mechanism of salubrinal inhibition is not clear, salubrinal might reduce the effective function of the PP1-GADD34 complex in the cell either by direct binding or through yet-to-be-determined indirect signaling pathways (Boyce *et al.*, 2005). Although eIF2α phosphorylation has been suggested to be cytoprotective during ER stress there

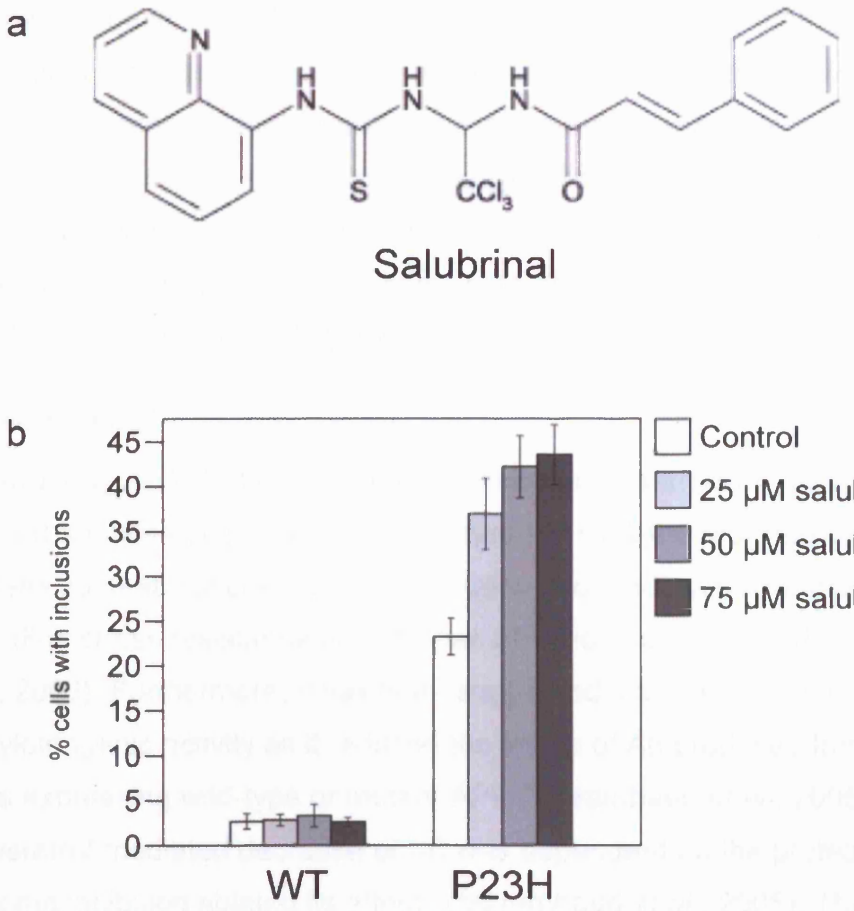

Figure 7.2.1 Salubrinal increases inclusion incidence in cells expressing P23H rod opsin.

a) Representation of the molecular structure of salubrinal. b) SK-N-SH cells were transfected with WT-GFP and P23H-GFP as described in Chapter 3 and treated with different concentrations of salubrinal for 24 hours. 25 μM salubrinal ($p \leq 0.001$), 50 μM salubrinal ($p \leq 0.001$) and 75 μM salubrinal ($p \leq 0.001$). Error bars represent ± 2SE.

are several properties of salubrinal which might account for the increase in inclusion observed in P23H cells. A downside of salubrinal pharmacological treatments is that the global inactivation of the eIF2 complex might have unanticipated effects on cellular and tissue demands for many other regulatory and housekeeping proteins. Furthermore, the administration of salubrinal is also likely to affect the response of folding pathways in tissues not meant to be targeted for correction. Currently, it is poorly understood just how long or at what levels sustained inactivation of the eIF2 complex would be beneficial although it was observed that recovery from PERK-stimulated phosphorylation of eIF2a is essential for a successful UPR (Novoa *et al.*, 2003).

7.2.2 Resveratrol

Resveratrol (Figure 7.2.2) is a polyphenol which is present in abundance in red grapes and red wine and was found to prevent or slow the progression of a variety of diseases such as cancer, ischaemic injuries and cardiovascular disease as well as extending stress resistance and lifespan of various organisms (Baur and Sinclair, 2006). Furthermore, it has been suggested that resveratrol had a potent anti-amyloidogenic activity as it reduced the levels of Aβ produced from different cell lines expressing wild-type or mutant APP (Marambaud *et al.*, 2005). Moreover the resveratrol-mediated decrease of Aβ was dependent on the proteasome as proteasome inhibition ablated its effects (Marambaud *et al.*, 2005). These results suggested resveratrol could be a potential candidate in a cell model of rhodopsin RP where an increased proteasome function could reduce the mechanisms of cell death induced by P23H rod opsin. SK-N-SH cells expressing wild-type and P23H rod opsin were treated with various concentrations of resveratrol for 24 hours prior to quantification of inclusion incidence (Figure 7.2.2). The concentration of resveratrol which elicited the largest reduction in inclusion incidence in P23H cells was 5 μM which reduced inclusion incidence from 25.90% ± 2.33 in the untreated controls to 15.18% ± 2.55 ($p \leq 0.005$).

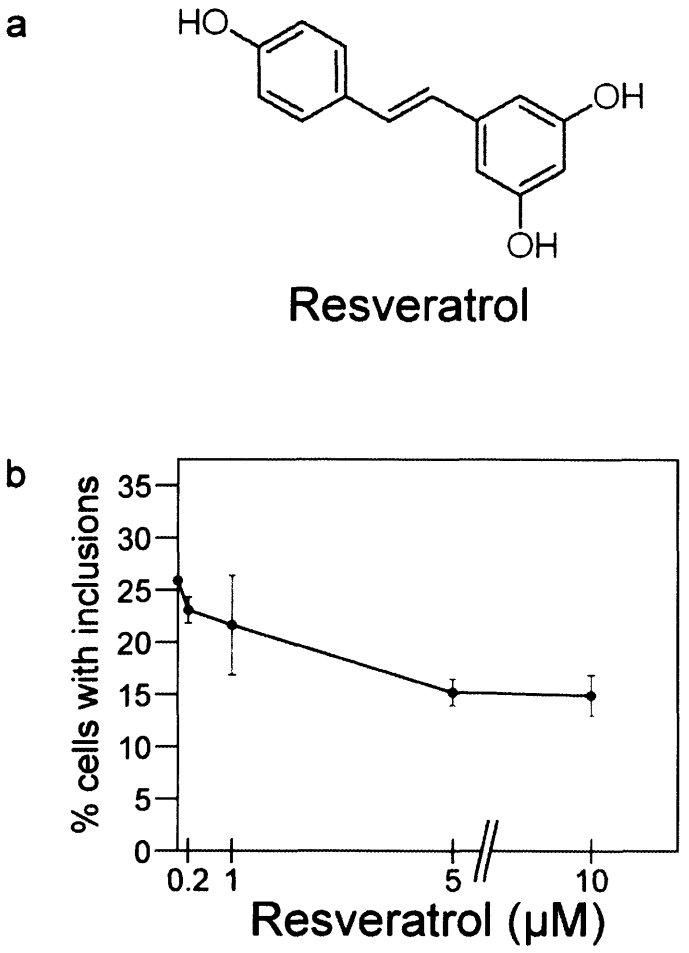

Figure 7.2.2 Resveratrol reduces inclusion incidence in cells expressing P23H rod opsin.

a) Representation of the molecular structure of resveratrol. b) SK-N-SH cells expressing P23H-GFP rod opsin were treated with different concentrations of resveratrol for 24 hours. The most effective concentration was 5 μM resveratrol which reduced inclusion incidence from 25.90% ± 2.33 in the untreated controls to 15.18% ± 2.55 ($p \leq 0.005$). Error bars represent ± 2SE.

Resveratrol was identified as a potent activator of the human sirtuin SIRT1 *in vitro* and of the yeast homologue Sir2 *in vivo*, a mechanism that may extend life span in yeast (Howitz *et al.*, 2003). Furthermore, resveratrol and SIRT1 activation have recently been linked to neuroprotective pathways in models of axonal degeneration (Araki *et al.*, 2004) and of neuronal dysfunctions caused by mutant polyglutamines (Parker *et al.*, 2005). It would therefore be interesting to assess if the same neuroprotective mechanisms apply to P23H cells and if these are related to the decrease in inclusion incidence observed in P23H cells.

7.2.3 Glucosidase inhibitors: 1-Deoxynojirimycin (1-DNJ) and N-butyldeoxynojirimycin (NB-DNJ)

It has recently been suggested that functional ΔF508 CFTR could be rescued by the use of the glucosidase inhibitor N-butyldeoxynojirimycin (NB-DNJ) in human and mice epithelial cells (Norez *et al.*, 2006). Furthermore NB-DNJ prevented the ΔF508 CFTR/calnexin interaction suggesting that the inhibition of deglucosylation of nascent proteins might be the molecular mechanism of action of this compound. Because different protein misfolding diseases might share common mechanisms for mutant protein recognition by calnexin and consequent retention in the ER, glucosidase inhibitors might be pharmacological candidates for a variety of these diseases including ADRP. SK-N-SH cells expressing WT and P23H rod opsin were treated with the glucosidade inhibitors 1-deoxynojirimycin (1-DNJ) (Figure 7.2.3a) and NB-DNJ (Figure 7.24a) for 24 hours. 10 μM 1-DNJ ($p \leq 0.001$), 20 μM 1-DNJ ($p \leq 0.005$), 50 μM 1-DNJ ($p \leq 0.05$) decreased inclusion incidence in cells expressing P23H rod opsin. 10 μM NB-DNJ ($p \leq 0.001$), 20 NB-DNJ ($p \leq 0.005$) and 50 μM NB-DNJ ($p \leq 0.05$) also reduced inclusion incidence in P23H cells. However, neither of these compounds appeared to promote the translocation of the P23H rod opsin to the plasma membrane, in contrast to the functional rescue observed in ΔF508 CFTR (Norez *et al*, 2006).

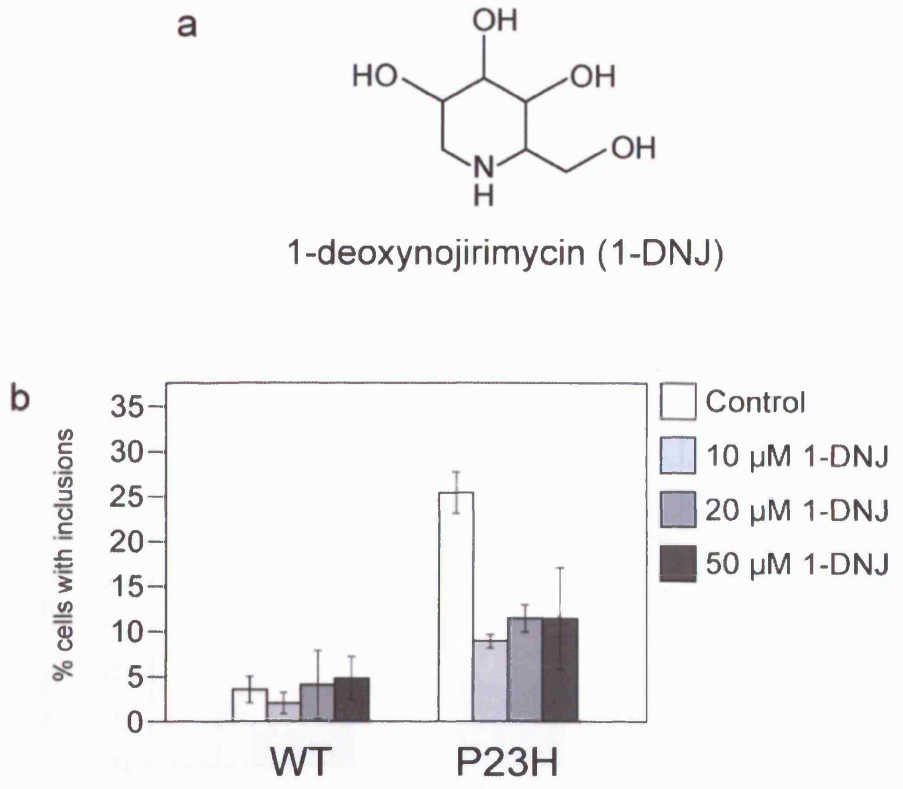

Figure 7.2.3 1-deoxynojirimycin (1-DNJ) decreases inclusion incidence in cells expressing P23H rod opsin.

a) Representation of the molecular structure of 1-DNJ. b) SK-N-SH cells expressing WT-GFP or P23H-GFP were treated with different concentrations of 1-DNJ, as described, for 24 hours. 10 μM 1-DNJ ($p \leq 0.001$), 20 μM 1-DNJ ($p \leq 0.005$) and 50 μM 1-DNJ ($p \leq 0.05$) reduced inclusion incidence in P23H cells. Error bars represent ± 2SE.

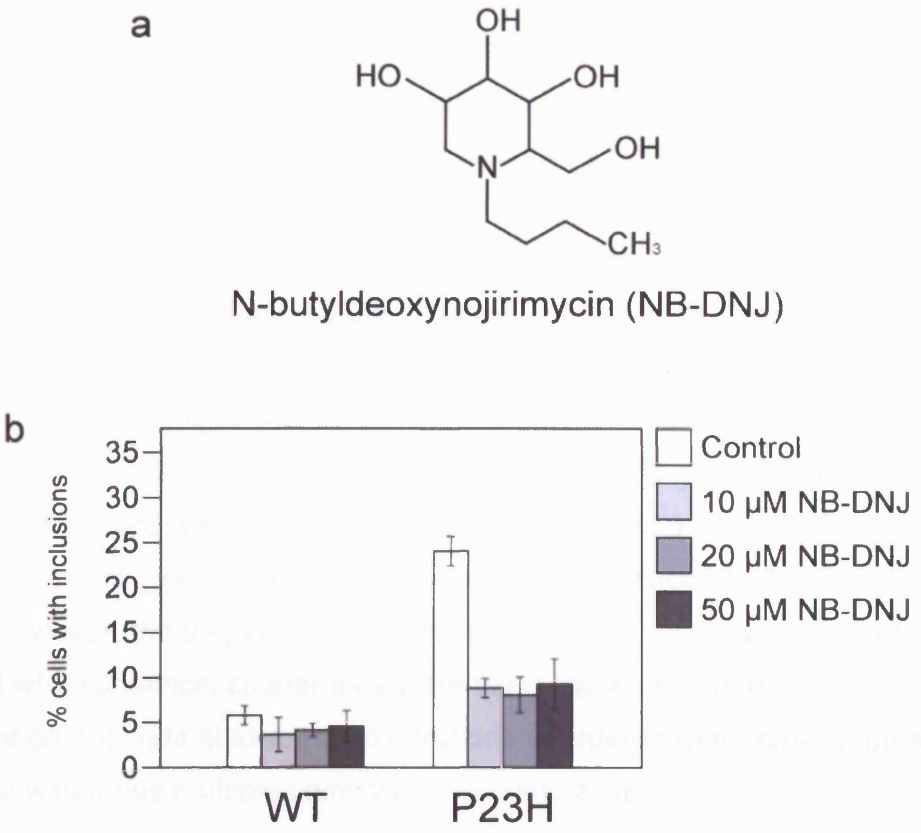

Figure 7.2.4 N-butyldeoxynojirimycin (NB-DNJ) reduces inclusion incidence in cells expressing P23H rod opsin.

a) Representation of the molecular structure of NB-DNJ. b) SK-N-SH cells expressing WT-GFP or P23H-GFP were treated with different concentrations of NB-DNJ, as described, for 24 hours. 10 μM NB-DNJ ($p \leq 0.001$), 20 μM NB-DNJ ($p \leq 0.005$) and 50 μM NB-DNJ ($p \leq 0.05$) reduced inclusion incidence in P23H cells. Error bars represent ± 2SE.

7.3 Multiple compounds used in conjunction

7.3.1 Retinoids and chemical chaperones

Following the positive results obtained with retinoids and chemical chaperones in reducing the gain of function mechanism induced by P23H rod opsin in the cell model for rhodopsin RP, treatment combining these two groups of compounds was attempted in order to assess if their effects could be cumulative. SK-N-SH cells expressing WT, P23H and K296E rod opsin were treated with 9-*cis*-retinal and chemical chaperones for 24 hours prior to the assessment of inclusion incidence (Figure 7.3.1). Treatment with 10 µM 9-*cis*-retinal reduced inclusion incidence in cells expressing P23H rod opsin from 24.12% ± 7.00 in the untreated controls to 12.41% ± 1.67. Treatment with 10 µM 9-*cis*-retinal and 0.25% DMSO reduced inclusion incidence further in P23H cells to 5.93% ± 1.50 ($p \leq 0.001$). A similar result was observed when cells were treated with 10 µM 9-*cis*-retinal and 5 mM TMAO as the inclusion incidence in P23H cells was reduced to 6.14% ± 1.74 ($p \leq 0.001$). However, the degree of inclusion incidence reduction was similar to that obtained when chemical chaperones were used alone. It is therefore necessary to test these compounds at lower concentrations in order to determine whether the treatment with these multiple compounds is cumulative.

Treatment with 10 µM 9-*cis*-retinal failed to reduce inclusion incidence in cells expressing K296E rod opsin as it has previously been described in this study. Treatment with 10 µM 9-*cis*-retinal and 0.25% DMSO reduced inclusion incidence in K296E cells from 13.75% ± 5.60 in the untreated controls to 7.08% ± 4.5 ($p \leq 0.01$). Treatment with 10 µM 9-*cis*-retinal and 5 mM TMAO also reduced inclusion incidence to 7.95% ± 1.28 ($p \leq 0.05$). Both these decreases in inclusion incidence were similar to those obtained when chemical chaperones were used alone (Figure 5.8).

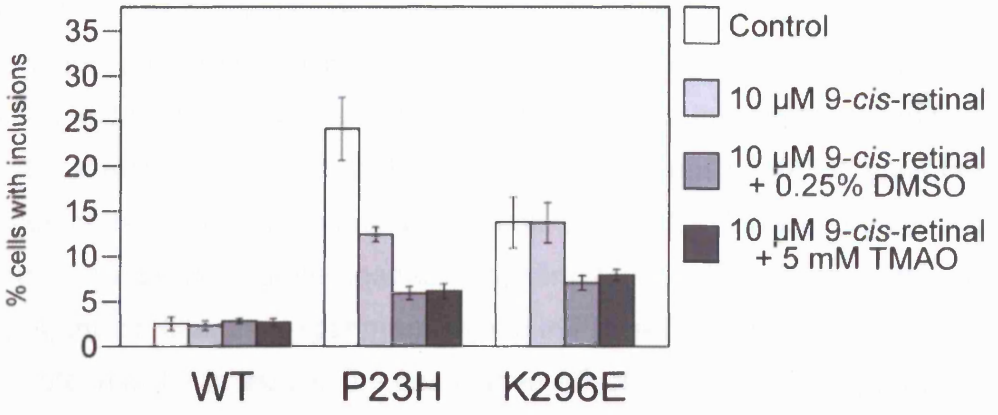

Figure 7.3.1 Chemical chaperones enhance the effects of 9-*cis*-retinal on inclusion incidence in cells expressing P23H rod opsin.
The inclusion incidence in SK-N-SH cells expressing WT-GFP, P23H-GFP and K296E-GFP rod opsin was assessed following treatment with 10 µM 9-*cis*-retinal, 10 µM 9-*cis* retinal + 0.25% DMSO and 10 µM 9-*cis* retinal + 5 mM TMAO, as described, for 24 hours. DMSO ($p \leq 0.001$) and TMAO ($p \leq 0.001$) enhanced the reduction in inclusion incidence caused by 9-*cis*-retinal in P23H cells. DMSO ($p \leq 0.01$) and TMAO ($p \leq 0.05$) also reduced inclusion incidence in K296E cells. Error bars represent ± 2SE.

7.3.2 Multiple chemical chaperones

In order to assess if chemical chaperones had a cumulative effect in protecting cells against the gain of function mechanism induced by the mutant protein, SK-N-SH cells expressing P23H rod opsin were treated with 0.25% DMSO, 5 mM TMAO or 0.25% DMSO plus 5 mM TMAO for 24 hours prior to the quantification of inclusion incidence (Figure 7.3.2). DMSO and TMAO when used alone reduced inclusion incidence from 24.40% ± 2.00 in the untreated controls to 6.21% ± 0.51 and 6.00 ±1.04 as previously described. The combination of DMSO and TMAO led to an enhanced decrease in inclusion incidence resulting in the presence on inclusions in 3.80% ± 1.74 ($p \leq 0.001$) of the cells. Although these preliminary data suggest that treatment with multiple chemical chaperones might increase the protection of cells against the gain of function mechanism induced by the P23H rod opsin further experiments are needed to confirm these initial observations. In hindsight, the preliminary experiment shown in Figure 7.3.2 might not be the most appropriate in order to assess the cumulative effect of chemical chaperones in the inclusion incidence of P23H cells, as it used optimal concentrations of DMSO and TMAO which by themselves lead to large reductions in inclusion incidence. It might be more appropriate for DMSO and TMAO to be used at lower concentrations, which are less effective at reducing inclusion incidence, so that the cumulative effect of these compounds on P23H rod opsin inclusion incidence might become more evident when compared to the effect of each drug alone.

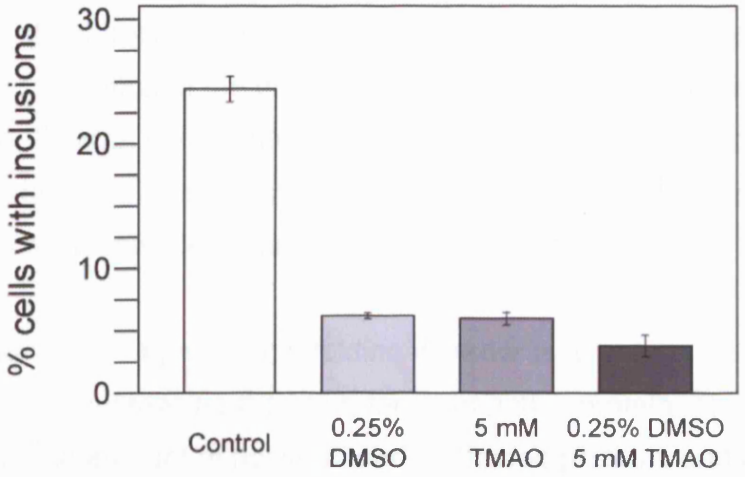

Figure 7.3.2 Treatment of cells expressing P23H rod opsin with DMSO and TMAO enhances the decrease in inclusion incidence observed when these compounds are used alone.

SK-N-SH cells expressing P23H rod opsin were treated with 0.25% DMSO, 5mM TMAO or 0.25% DMSO + 5 mM TMAO as described for 24 hours. DMSO and TMAO reduce the incidence of inclusions from 24.40% ± 2.00 in the untreated controls to 6.21% ± 0.51 and 6.00 ± 1.04 respectively. Treatment with DMSO and TMAO reduced inclusion incidence to 3.80 ± 1.74 ($p \leq 0.001$). Error bars represent ± 2SE.

Chapter 8: General Discussion

For a protein to be functionally active it must attain a correct three-dimensional structure until the protein is turned over to degradation mechanisms. This balance between formation and maintenance of the active conformation is vital to the cell and any disturbances in the amino acid sequence by inherited mutations or acquired amino acid modifications may compromise either the folding or the conformational structural maintenance leading to the disruption of cellular function, aggregation and inhibition of the proteasome which was implicated in neurotoxicity (Hooper, 2003). Several therapeutic strategies have been developed for protein misfolding disorders with the objective of re-establish the balance between the disease protein synthesis, degradation and functional activity.

A potential treatment of a protein misfolding disorder is to enhance the folding of mutant proteins and increasing the abundance of active protein. This would result in a decrease of the amount of accumulated misfolded proteins and alleviate the pathogenic mechanisms of cell death. A different strategy involves the reduction of the misfolding cellular load by promoting the desegregation of accumulated misfolded proteins. One could suggest that there might be an adverse effect of dissolving intracellular inclusions which might be protecting the cell against toxic oligomeric misfolded proteins. However, the number of vital cellular components including molecular chaperones which might be released into the cell are likely to overcome this potential adverse effect. Furthermore, this might confer susceptibility to degradation and therefore suppression of cell death caused by the accumulated misfolded monomers and oligomers. Finally, a strategy in inherited disorders might be to decrease or inhibit the expression of the mutant protein. This could be achieved by repairing the gene defect by targeted gene correction. Alternatively, in the case of a dominant-negative mechanism of cell death the suppression of the mutant protein must be carried out while leaving the wild-type protein at heterozygous expression levels.

Additional considerations when developing a potential therapeutic strategy for rhodopsin RP involves the fact that RP is a chronic disease which leads to blindness, not death. Consequently, any compound must have relatively low side-effects and be well tolerated for a long period of time. In addition, compounds must be able to cross the blood-retinal barrier or being able to be administered as eye drops. In this study, using a cellular model of rhodopsin RP, several of these therapeutic strategies were pursued by using a variety of pharmacological agents whose effects are summarised in Table 8.1.

The retinoids 9-*cis*-retinal and 11-*cis*-retinal, acted as pharmacological chaperones for rod opsin, reduced inclusion incidence and promoted the folding of the P23H rod opsin. The potential use of these compounds in ADRP patients is questionable, however, as they lost their efficacy when bleached and one could not envisage patients being injected with these compounds in the dark. This problem was circumvented by administering vitamin A in RP patients (Berson *et al.*, 1993). These authors carried out a randomised, controlled and double-marked clinical trial where RP patients receiving 15000 IU/d of vitamin A had, on average, a slower rate of decline of retinal function measured by the ERG than the two groups not receiving this dosage. However, no significant difference occurred for the slow loss of visual field with time between the groups of patients receiving vitamin A or placebo. Prolonged daily consumption of < 25000 IU of vitamin A were considered safe in a clinical trial of adults aged 18-54 with RP (Sibulesky *et al.*, 1999), although other studies reported side-effects such as increased intracranial pressure, hepatomegaly and elevated blood lipids with these doses of vitamin A (Bauernfeind, 1980). In addition to the moderate effects of vitamin A on the decline of retinal function they were highly variable between patients and this compound failed to stop the progression of retinal function decline (Berson *et al.*, 1993). Furthermore, there was no available genotypic information on RP patients in this clinical trial and this might account for the high patient variability observed in this study. Finally, questions raised about the toxicity associated with high doses of vitamin A together with the fact that similar data are yet to be replicated

Compound	Inclusions	EndoH resistance	Insoluble protein	LDH release	Caspase-3 activity	Dominant-negative
9-*cis*-retinal	++	Yes	++	+++	+++	+++
11-*cis*-retinal	++	Yes	++	+++	+++	+++
DMSO	+++	No	++	+++	++	+
TMAO	+++	No	++	+++	++	+
4-PBA	+++	No	+	++	++	+
Trehalose	++	No	+	++	++	+
Arimoclomol	+++	No	++	+++	++	++
Celastrol	+	N.A	No effect	No effect	Detrimental	No effect
Geldanamycin	++	No	+	++	++	+
Radicicol	++	No	++	+++	++	+
17-AAG	+++	No	++	+++	++	+
Rapamycin	++	N.D	++	+++	+	+
Rapamycin + Trehalose	+++	N.D	++	+++	+	+

Salubrinal	Detrimental
Resveratrol	++
1-DNJ	+++
NB-DNJ	+++
9-*cis*-retinal + DMSO	+++
9-*cis*-retinal + TMAO	+++
DMSO + TMAO	+++

Table 8.1 Summary of the effects of compounds used in this study on the different parameters of the cellular model of rhodopsin RP.

Positive effects of compounds on the mechanisms of cell death induced by the P23H rod opsin were classified between + and +++ according to the extent to which these effects were reduced. This was assessed by measuring inclusion incidence, insoluble protein determined by the rod opsin fractionation assay, LDH release, caspase-3 activity and suppression of dominant-negative interaction. N.A: Not applicable; N.D: Not done.

suggest that vitamin A might be of marginal benefit, at best, in patients with RP and that this must be weighted with the uncertain risks associated with the long-term exposure to high doses of this compound.

Treatment with retinoids or vitamin A poses another difficulty based on the possibility that in patients with a healthy diet, there might be an adequate supply of 11-*cis*-retinal to the photoreceptors and supplements might not enhance this further. This is not mimicked in this cell model of rhodopsin RP, therefore the results observed in this model might not be possible to replicate *in vivo*. Noorwez and colleagues (2003) have successfully rescued P23H rod opsin with the locked form of retinal, 11-*cis*-7-ring retinal. These authors showed that treatment with 11-*cis*-7-ring retinal increased amounts of the correctly folded P23H protein and is specific as shown by the lack of activity observed with several structural homologs (11-*cis*-9-demethyl-ring retinal and 11-*cis*-6-ring retinal). However, unlike the wild-type rod opsin, purified rescued P23H protein appeared to be in a less compact conformation (Noorwez *et al.*, 2003). Therefore, the identification of other compounds which might be beneficial for RP patients is necessary.

The use of chemical chaperones in the cell model of rhodopsin RP suggested that these compounds alleviated the gain of function mechanism induced by the P23H rod opsin but did not appear to promote the folding of the mutant protein. In addition chemical chaperones, unlike retinoids had a positive effect on the gain of function mechanism induced by the K296E rod opsin.

As the concentrations of chemical chaperones necessary for an effect in cell culture studies of protein misfolding disorders were in the milimolar range is was important to assess if these concentrations could be achieved *in vivo*.

Bai and colleagues (1998) used CD1 mice to assess if the equivalent *in vitro* concentrations of chemical chaperones could be maintained. These authors reported that potentially therapeutic concentrations of TMAO could be sustained in

mice *in vivo*. Single intraperitoneal or subcutaneons doses of TMAO (7 g/kg, 8% solution in water) resulted in serum TMAO greater than 50 mM with a half-life of 18-21 hours. Sustained high serum and tissue TMAO concentration higher than 52 mM for 3 days was achieved by the administration of TMAO (7 g/kg) in water every 8 hours. However, this resulted in the death approximately half of the mice. Although the remaining mice had nearly normal liver, renal, and pancreatic function. A lower dose of TMAO (5 g/kg) given by the subcutaneons route every 8 hours resulted in serum TMAO concentration of 22 mM, a level that was well tolerated by all mice for 72 h. Despite the lower toxicity, a similar therapeutic regime both in terms of quantity and periodicity is not applicable to rhodopsin RP patients.

4-PBA is a low molecular weight fatty acid with FDA approval for clinical use in patients with urea cycle disorders (Burlina *et al.*, 2001) which might suggest that is the most applicable kosmotrope to rhodopsin RP patients. 4-PBA induced CFTR channel function on the plasma membrane of ΔF508-CFTR airway epithelial cells *in vitro* (Rubenstein *et al.*, 1997). In order to assess if 4-PBA could induce epithelial CFTR function in patients homozygous for ΔF508-CFTR a randomized, double-blind and placebo-controlled trial in 18 patients was performed with the maximum approved adult dose of 4-PBA: 19 grams/day (116 mM/day) divided in three oral doses of 6, 6, and 7 grams for 1 week (Rubenstein and Zeitling, 1998). Nasal potential difference (NPD) response patterns and sweat chloride concentrations were determined before and after study drug treatment, and 4-PBA and metabolites were assayed in plasma and urine at the end of drug treatment. Subjects in the 4-PBA group demonstrated small, but statistically significant improvements of the NPD response to perfusion of an isoproterenol/amiloride/chloride-free solution. This measure reflected epithelial CFTR function and was highly discriminatory between patients with and without CF. Subjects who had received 4-PBA did not demonstrate significantly reduced sweat chloride concentrations or alterations in the amiloride-sensitive NPD. Side effects due to drug therapy were minimal and comparable in the two groups.

These data suggest that chemical chaperone concentrations used to alleviate the effects of P23H rod opsin *in vitro* (0.25% DMSO; 5 mM TMAO; 10mM 4-PBA; and 50 mM trehalose) can by sustained *in vivo*. It would be interesting to assess the effect of chemical chaperones on a P23H mouse model of retinal degeneration (Olsson *et al.*, 1992) and investigate if the positive effect of these compounds on the cell model of rhodopsin RP could be replicated *in vivo*.

Treatment with the HSP co-inducer arimoclomol in the cell model of rhodopsin RP alleviated the gain of function mechanism of induced by P23H rod opsin. Furthermore, arimoclomol partially promoted the folding of P23H rod opsin, and wild-type rod opsin, in co-transfected cells. When used in a mouse model of ALS (10 mg/kg intraperitoneally) arimoclomol delayed disease progression and resulted in marked improvement in hind limb muscle function (Kieran *et al.*, 2004). Significantly, a significant delay in ALS disease progression was observed when arimoclomol was administered after the visible onset of disease symptoms. Arimoclomol was well tolerated in a phase I study of healthy volunteers. And a dose ranging, phase II study of arimoclomol in ALS has finished enrollment (http://www.clinicaltrials.gov/ct/show/NCT00244244?order=1). Safety, optimum dose, and pharmacokinetics of arimoclomol, however, are still unknown for patients with ALS.

Treatment of P23H cells with the Hsp90 inhibitors geldanamycin, radicicol and 17-AAG alleviated the gain of function and the dominant-negative mechanism induced by P23H rod opsin. However, these compounds did not appear to promote the folding of P23H or wild-type rod opsin in co-transfected cells respectively. Although it was suggested that the mechanism of action of these compounds on protein misfolding disorders involved the enhanced degradation of the mutant protein (Solit *et al.*, 2002) this did not appear to be the case in this cellular model of rhodopsin RP. It would therefore be interesting to assess if the positive effects of these compounds observed in this study could be replicated *in vivo*. 17-AAG was

examined as a anti-tumour agent in a Phase I clinical trial for paediatric patients with recurrent or refractory neuroblastoma, and a dose of 270 mg/m^2 administered twice weekly for 2 of 3 weeks was well tolerated (Bagatell *et al.*, 2007). The sub-inhibitory doses necessary for an induction of Hsp90 by 17-AAG in a potential rhodopsin RP *in vivo* study (25 mg/kg) should not be associated with toxicity.

Rapamycin protected P23H cells against the gain of function mechanism induced by the mutant protein. It was unclear, however, if these actions were due to an autophagy induction. Rapamycin reduced huntingtin accumulation and cell death in cell models of Huntington's disease and against neurodegeneration in a *Drosophila melanogaster* model of Huntington's disease (Ravikumar *et al.*, 2004). It would be interesting to investigate the effects and the mechanism of action of rapamycin in an *in vivo* in a model of rhodopsin RP. Rapamycin has been approved for clinical trials by the FDA for use at a fixed dose of 2-5 mg/day. However, pharmacokinetic and clinical data showed that rapamycin was a critical-dose drug requiring therapeutic drug monitoring to minimise drug-related toxicities and maximise efficacy (Mahalati and Kahan, 2001) which might not be ideal for the long-term use required by rhodopsin RP patients.

Preliminary data was produced by treating cell expressing P23H rod opsin with salubrinal, resveratrol, 1-DNJ and NB-DNJ. Of these compounds the glycosidase inhibitors 1-DNJ and NB-DNJ appeared to be the most promising as they resulted in a large decrease in inclusion incidence without any observable deleterious effects on cellular morphology. Moreover, a Phase II clinical trial with NB-DNJ was recently completed (http://www.clinicaltrials.gov/ct/show/NCT00002079?order=2).

The initial observations regarding a the use of multiple compounds on the cellular model of rhodopsin RP suggested that 9-cis-retinal plus chemical chaperones and multiple chemical chaperones had a cumulative effect in decreasing inclusion incidence in cells expressing P23H rod opsin. However, more data is required in

order to assess if this positive effect on inclusion incidence is accompanied by cytoprotection and if the suppression of the dominant-negative can be enhanced.

This study has developed and characterised a cell model which can mimic the gain of function and dominant-negative disease mechanisms in rhodopsin RP. This resulted in the creation of a template which could be used for the identification and development of drugs for rhodopsin RP patients. Furthermore, this study has identified compounds which demonstrate the 'proof of principle' that some gain of function and dominant-negative mechanisms of cell death induced by a Class II rod opsin mutation can be manipulated. In would be interesting to establish the efficacy of these pharmacological agents in animal models prior to a potential translation into the clinic.

Chapter 9: References

Abler AS, Chang CJ, Ful J, Tso MO, Lam TT (1996). Photic injury triggers apoptosis of photoreceptor cells. *Res. Commun. Mol. Pathol. Pharmacol.* **92**, 177-189

Ahnelt PK and Kolb H (2000). The mammalian photoreceptor mosaic-adaptive design. *Prog. Retin. Eye Res.* **19**, 711-777

Araki T, Sasaki Y, Milbrandt J (2004). Increased nuclear NAD biosynthesis and SIRT1 activation prevent axonal degeneration. *Science.* **305**, 1010-1013

Anukanth A and Khorana HG (1994). Structure and function in rhodopsin. Requirements of a specific structure for the intradiscal domain. *J. Biol. Chem.* **269**, 19738-19744

Arrasate M, Mitra S, Schweitzer ES, Segal MR, Finkbeiner S (2004). Inclusion body formation reduces levels of mutant huntingtin and the risk of neuronal death. *Nature.* **431**, 805-810

Back JF, Oakenfull D, Smith MB (1979) Increased thermal stability of proteins in the presence of sugars and polyols. *Biochemistry.* **18**, 5191-5196

Bai C, Biwersi J, Verkman AS, Matthay MA (1998). A mouse model to test the in vivo efficacy of chemical chaperones. *J. Pharmacol. Toxicol. Methods.* **40**, 39-45

Bagatell R, Gore L, Egorin MJ, Ho R, Heller G, Boucher N, Zuhowski EG, Whitlock JA, Hunger SP, Narendran A, Katzenstein HM, Arceci RJ, Boklan J, Herzog CE, Whitesell L, Ivy SP, Trippett TM (2007). Phase I pharmacokinetic and pharmacodynamic study of 17-N-allylamino-17-demethoxygeldanamycin in pediatric patients with recurrent or refractory solid tumors: a pediatric oncology

experimental therapeutics investigators consortium study. *Clin. Cancer Res.* **13**, 1783-1788

Bao YP, Cook LJ, O'Donovan D, Uyama E, Rubinsztein DC (2002). Mammalian, yeast, bacterial, and chemical chaperones reduce aggregate formation and death in a cell model of oculopharyngeal muscular dystrophy. *J. Biol. Chem.* **277**, 12263-12269

Barral JM, Broadley SA, Schaffar G, Hartl FU (2004). Roles of molecular chaperones in protein misfolding diseases. *Semin. Cell Dev. Biol.* **15**, 17-29

Baur JA and Sinclair DA (2006). Therapeutic potential of resveratrol: the in vivo evidence. *Nat. Rev. Drug Discov.* **5**, 493-506

Bence NF, Sampat RM, Kopito RR (2001). Impairment of the ubiquitin-proteasome system by protein aggregation. *Science.* **292**, 1552-1555

Berson EL, Rosner B, Sandberg MA, Hayes KC, Nicholson BW, Weigel-DiFranco C, Willett W (1993). A randomized trial of vitamin A and vitamin E supplementation for retinitis pigmentosa. *Arch. Ophthalmol.* **111**, 761-772

Blomhoff R and Blomhoff HK (2006). Overview of retinoid metabolism and function. *J Neurobiol.* **66**, 606-630

Bloomfield SA and Dacheux RF (2001). Rod vision: pathways and processing in the mammalian retina. *Prog. Retin. Eye Res.* **20**, 351-384

Bonapace G, Waheed A, Shah GN, Sly WS (2004). Chemical chaperones protect from effects of apoptosis-inducing mutation in carbonic anhydrase IV identified in retinitis pigmentosa 17. *Proc. Natl. Acad. Sci. U. S. A.* **101**, 12300-12305

Boyce M, Bryant KF, Jousse C, Long K, Harding HP, Scheuner D, Kaufman RJ, Ma D, Coen DM, Ron D, Yuan J (2005). A selective inhibitor of eIF2alpha dephosphorylation protects cells from ER stress. *Science.* **307**, 935-939

Brady OR, Gal AE, Bradley RM, Martensson E, Warshaw AL, Laster L (1967). Enzymatic defect in Fabry's disease: Ceramidetrihexosidase deficiency. *N. Engl. J. Med.* **276**, 1163-1167

Brown CR, Hong-Brown LQ, Biwersi J, Verkman AS, Welch WJ (1996). Chemical chaperones correct the mutant phenotype of the delta F508 cystic fibrosis transmembrane conductance regulator protein. *Cell Stress Chaperones.* **1**, 117-125

Bucciantini M, Calloni G, Chiti F, Formigli L, Nosi D, Dobson CM, Stefani M (2004). Prefibrillar amyloid protein aggregates share common features of cytotoxicity. *J. Biol. Chem.* **279**, 31374-31382

Bunemann M, Hosey MM (1999). G-protein coupled receptor kinases as modulators of G-protein signalling. *J. Physiol.* **517**, 5-23

Bunt-Milam AH, Kalina RE, Pagon RA (1983). Clinical-ultrastructural study of a retinal dystrophy. *Invest. Ophthalmol. Vis. Sci.* **24**, 458-469

Burlina AB, Ogier H, Korall H, Trefz FK (2001). Long-term treatment with sodium phenylbutyrate in ornithine transcarbamylase-deficient patients. *Mol. Genet. Metab.* **72**, 351-355

Burrows JA, Willis LK, Perlmutter DH (2000). Chemical chaperones mediate increased secretion of mutant alpha 1-antitrypsin (alpha 1-AT) Z: A potential pharmacological strategy for prevention of liver injury and emphysema in alpha 1-AT deficiency. *Proc. Natl. Acad. Sci. U. S. A.* **97**, 1796-1801

Chapple JP, Grayson C, Hardcastle AJ, Saliba RS, van der Spuy J, Cheetham ME (2001). Unfolding retinal dystrophies: a role for molecular chaperones? *Trends Mol. Med.* **7,** 414-421

Chapple JP, Cheetham ME (2003). The chaperone environment at the cytoplasmic face of the endoplasmic reticulum can modulate rhodopsin processing and inclusion formation. *J. Biol. Chem.* **278**, 19087-19094

Chen S, Peng GH, Wang X, Smith AC, Grote SK, Sopher BL, La Spada AR (2004). Interference of Crx-dependent transcription by ataxin-7 involves interaction between the glutamine regions and requires the ataxin-7 carboxy-terminal region for nuclear localization. *Hum. Mol. Genet.* **13**, 53-67

Cheng SH, Gregory RJ, Marshall J, Paul S, Souza DW, White GA, O'Riordan CR, Smith AE (1990). Defective intracellular transport and processing of CFTR is the molecular basis of most cystic fibrosis. *Cell.* **63**, 827-834

Corson DW, Cornwall MC, MacNichol EF, Mani V, Crouch RK (1990). Transduction noise induced by 4-hydroxy retinals in rod photoreceptors. *Biophys. J.* **57**, 109-115

Cummings CJ, Mancini MA, Antalffy B, DeFranco DB, Orr HT, Zoghbi HY (1998). Chaperone suppression of aggregation and altered subcellular proteasome localization imply protein misfolding in SCA1. *Nat. Genet.* **19**, 148-154

Cummings CJ, Sun Y, Opal P, Antalffy B, Mestril R, Orr HT, Dillmann WH, Zoghbi HY (2001). Over-expression of inducible HSP70 chaperone suppresses neuropathology and improves motor function in SCA1 mice. *Hum. Mol. Genet.* **10**, 1511-1518

Davidson FF, Loewen PC, Khorana HG (1994). Structure and function in rhodopsin: replacement by alanine of cysteine residues 110 and 187, components of a conserved disulfide bond in rhodopsin, affects the light-activated metarhodopsin II state. *Proc. Natl. Acad. Sci. U. S. A.* **91**, 4029-4033

Denning GM, Anderson MP, Amara JF, Marshall J, Smith AE, Welsh MJ (1992). Processing of mutant cystic fibrosis transmembrane conductance regulator is temperature-sensitive. *Nature.* **358**, 761-764

Deretic D, Williams AH, Ransom N, Morel V, Hargrave PA, Arendt A (2005). Rhodopsin C terminus, the site of mutations causing retinal disease, regulates trafficking by binding to ADP-ribosylation factor 4 (ARF4). *Proc. Natl. Acad. Sci. U. S. A.* **102**, 3301-3306

Doi T, Molday RS, Khorana HG (1990). Role of the intradiscal domain in rhodopsin assembly and function. *Proc. Natl. Acad. Sci. U. S. A.* **87**, 4991-4995

Donovan M and Cotter TG (2002). Caspase-independent photoreceptor apoptosis in vivo and differential expression of apoptotic protease activating factor-1 and caspase-3 during retinal development. *Cell Death Differ.* **9**, 1220-1231

Dryja TP, McGee TL, Hahn LB, Cowley GS, Olsson JE, Reichel E, Sandberg MA, Berson EL (1990). Mutations within the rhodopsin gene in patients with autosomal dominant retinitis pigmentosa. *N. Engl. J. Med.* **323**, 1302-1307

El-Agnaf OM, Jakes R, Curran MD, Middleton D, Ingenito R, Bianchi E, Pessi A, Neill D, Wallace A (1998). Aggregates from mutant and wild-type alpha-synuclein proteins and NAC peptide induce apoptotic cell death in human neuroblastoma cells by formation of beta-sheet and amyloid-like filaments. *FEBS Lett.* **440**, 71-75

Ehrnhoefer DE, Duennwald M, Markovic P, Wacker JL, Engemann S, Roark M, Legleiter J, Marsh JL, Thompson LM, Lindquist S, Muchowski PJ, Wanker EE. Green tea (-)-epigallocatechin-gallate modulates early events in huntingtin misfolding and reduces toxicity in Huntington's disease models. *Hum. Mol. Genet.* **15**, 2743-2751

Fan J, Rohrer B, Moiseyev G, Ma JX, Crouch RK (2003). Isorhodopsin rather than rhodopsin mediates rod function in RPE65 knock-out mice. *Proc. Natl. Acad. Sci. U. S. A.* **100**, 13662-13667

Flannery JG, Farber DB, Bird AC, Bok D (1989). Degenerative changes in a retina affected with autosomal dominant retinitis pigmentosa. *Invest. Ophthalmol. Vis. Sci.* **30**, 191-211

Fliesler SJ, Rapp LM, Hollyfield JG (1984). Photoreceptor-specific degeneration caused by tunicamycin. *Nature*. **311**, 575-577

Franke RR, Sakmar TP, Graham RM, Khorana HG (1992). Structure and function in rhodopsin. Studies of the interaction between the rhodopsin cytoplasmic domain and transducin. *J. Biol. Chem.* **267**, 14767-14774

Frederick JM, Krasnoperova NV, Hoffmann K, Church-Kopish J, Ruther K, Howes K, Lem J, Baehr W (2001). Mutant rhodopsin transgene expression on a null background. *Invest. Ophthalmol. Vis. Sci.* **42**, 826-833

Gao H and Hollyfield JG (1992). Basic fibroblast growth factor (bFGF) immunolocalization in the rodent outer retina demonstrated with an anti-rodent bFGF antibody. *Brain Res.* **585**, 355-360

Grenier C, Bissonnette C, Volkov L, Roucou X (2006). Molecular morphology and toxicity of cytoplasmic prion protein aggregates in neuronal and non-neuronal cells. *J. Neurochem.* **97**, 1456-1466

Harding HP, Zhang Y, Bertolotti A, Zeng H, Ron D (2000). Perk is essential for translational regulation and cell survival during the unfolded protein response. *Mol. Cell.* **5**, 897-904

Hargrave PA (1977). The amino-terminal tryptic peptide of bovine rhodopsin. A glycopeptide containing two sites of oligosaccharide attachment. *Biochim. Biophys. Acta.* **492**, 83-94

Hicks D and Molday RS (1986). Differential immunogold-dextran labeling of bovine and frog rod and cone cells using monoclonal antibodies against bovine rhodopsin. *Exp. Eye Res.* **42**, 55-71

Hooper NM (2003). Could inhibition of the proteasome cause mad cow disease? *Trends Biotechnol.* **21**, 144-145

Howitz KT, Bitterman KJ, Cohen HY, Lamming DW, Lavu S, Wood JG, Zipkin RE, Chung P, Kisielewski A, Zhang LL, Scherer B, Sinclair DA (2003). Small molecule activators of sirtuins extend Saccharomyces cerevisiae lifespan. *Nature.* **425**, 191-196

Humphries MM, Rancourt D, Farrar GJ, Kenna P, Hazel M, Bush RA, Sieving PA, Sheils DM, McNally N, Creighton P, Erven A, Boros A, Gulya K, Capecchi MR, Humphries P (1997). Retinopathy induced in mice by targeted disruption of the rhodopsin gene. *Nat. Genet.* **15,** 216-219

Hwa J, Garriga P, Liu X, Khorana HG (1997). Structure and function in rhodopsin: packing of the helices in the transmembrane domain and folding to a tertiary

structure in the intradiscal domain are coupled. *Proc. Natl. Acad. Sci. U. S. A.* **94**, 10571-10576.

Hwa J, Reeves PJ, Klein-Seetharaman J, Davidson F, Khorana HG (1999). Structure and function in rhodopsin: further elucidation of the role of the intradiscal cysteines, Cys-110, -185, and -187, in rhodopsin folding and function. *Proc. Natl. Acad. Sci. U. S. A.* **96**, 1932-1935

Hwa J, Klein-Seetharaman J, Khorana HG (2001). Structure and function in rhodopsin: Mass spectrometric identification of the abnormal intradiscal disulfide bond in misfolded retinitis pigmentosa mutants. *Proc. Natl. Acad. Sci. U. S. A.* **98**, 4872-4876

Illing ME, Rajan RS, Bence NF, Kopito RR (2002). A rhodopsin mutant linked to autosomal dominant retinitis pigmentosa is prone to aggregate and interacts with the ubiquitin proteasome system. *J. Biol. Chem.* **277**, 34150-34160

Janovick JA, Maya-Nunez G, Conn PM (2002). Rescue of hypogonadotropic hypogonadism-causing and manufactured GnRH receptor mutants by a specific protein-folding template: misrouted proteins as a novel disease etiology and therapeutic target. *J. Clin. Endocrinol. Metab.* **87**, 3255-3262

Jin M, Li S, Moghrabi WN, Sun H, Travis GH (2005). Rpe65 is the retinoid isomerase in bovine retinal pigment epithelium. *Cell.* **122**, 449-459

Kabanarou SA, Holder GE, Fitzke FW, Bird AC, Webster AR (2004). Congenital stationary night blindness and a "Schubert-Bornschein" type electrophysiology in a family with dominant inheritance. *Br. J. Ophthalmol.* **88**, 1018-1022

Kaushal S, Ridge KD, Khorana HG (1994). Structure and function in rhodopsin: the role of asparagine-linked glycosylation. *Proc. Natl. Acad. Sci. U. S. A.* **91**, 4024-4028

Kaushal S and Khorana HG (1994). Structure and function in rhodopsin. 7. Point mutations associated with autosomal dominant retinitis pigmentosa. *Biochemistry.* **33**, 6121–6128

Kaushal S (2007). Effect of rapamycin on the fate of P23H opsin associated with retinitis pigmentosa (an American Ophthalmological Society thesis).*Trans. Am. Ophthalmol. Soc.* **104**, 517-529

Keen TJ, Inglehearn CF, Lester DH, Bashir R, Jay M, Bird AC, Jay B, Bhattacharya SS (1991). Autosomal dominant retinitis pigmentosa: four new mutations in rhodopsin, one of them in the retinal attachment site. *Genomics.* **11**, 199-205

Kiaei M, Kipiani K, Petri S, Chen J, Calingasan NY, Beal MF (2005). Celastrol blocks neuronal cell death and extends life in transgenic mouse model of amyotrophic lateral sclerosis. *Neurodegener. Dis.* **2**, 246-254

Kieran D, Kalmar B, Dick JR, Riddoch-Contreras J, Burnstock G, Greensmith L (2004). Treatment with arimoclomol, a coinducer of heat shock proteins, delays disease progression in ALS mice. *Nat. Med.* **10**, 402-405

Kim S, Nollen EA, Kitagawa K, Bindokas VP, Morimoto RI (2002). Polyglutamine protein aggregates are dynamic. *Nat. Cell Biol.* **4**, 826-831

Kopito RR (2000). Aggresomes, inclusion bodies and protein aggregation. *Trends Cell Biol.* **10**, 524-530

Kubota K, Niinuma Y, Kaneko M, Okuma Y, Sugai M, Omura T, Uesugi M, Uehara T, Hosoi T, Nomura Y (2006). Suppressive effects of 4-phenylbutyrate on the aggregation of Pael receptors and endoplasmic reticulum stress. *J. Neurochem.* **97**, 1259-1268

Kurada P, Tonini TD, Serikaku MA, Piccini JP, O'Tousa JE (1998). Rhodopsin maturation antagonized by dominant rhodopsin mutants. *Vis. Neurosci.* **15**, 693-700

Lem J, Krasnoperova NV, Calvert PD, Kosaras B, Cameron DA, Nicolo M, Makino CL, Sidman RL (1999). Morphological, physiological, and biochemical changes in rhodopsin knockout mice. *Proc. Natl. Acad. Sci. U. S. A.* **96**, 736–741

Li T, Snyder WK, Olsson JE, Dryja TP (1996). Transgenic mice carrying the dominant rhodopsin mutation P347S: evidence for defective vectorial transport of rhodopsin to the outer segments. *Proc. Natl. Acad. Sci. U. S. A.* **93**, 14176-14181

Li T, Sandberg MA, Pawlyk BS, Rosner B, Hayes KC, Dryja TP, Berson EL (1998). Effect of vitamin A supplementation on rhodopsin mutants threonine-17 --> methionine and proline-347 --> serine in transgenic mice and in cell cultures. *Proc. Natl. Acad. Sci. U. S. A.* **95**, 11933-11938

Li ZY, Wong F, Chang JH, Possin DE, Hao Y, Petters RM, Milam AH (1998). Rhodopsin transgenic pigs as a model for human retinitis pigmentosa. *Invest. Ophthalmol. Vis. Sci.* **39**, 808-819

Loo DT, Copani A, Pike CJ, Whittemore ER, Walencewicz AJ, Cotman CW (1993). Apoptosis is induced by beta-amyloid in cultured central nervous system neurons. *Proc. Natl. Acad. Sci. U. S. A.* **90**, 7951-7955

Loo TW, Clarke DM (1997). Correction of defective protein kinesis of human P-glycoprotein mutants by substrates and modulators. *J. Biol. Chem.* **272**, 709-712

Lunkes A and Mandel JL (1998). A cellular model that recapitulates major pathogenic steps of Huntington's disease. *Hum. Mol. Genet.* **7**, 1355-1361

Mahalati K, Kahan BD (2001). Clinical pharmacokinetics of sirolimus. *Clin. Pharmacokinet.* **40**, 573-585

Marambaud P, Zhao H, Davies P (2005). Resveratrol promotes clearance of Alzheimer's disease amyloid-beta peptides. *J. Biol. Chem.* **280**, 37377-37382

May BC, Fafarman AT, Hong SB, Rogers M, Deady LW, Prusiner SB, Cohen FE (2003). Potent inhibition of scrapie prion replication in cultured cells by bis-acridines. *Proc. Natl. Acad. Sci. U. S. A.* **100**, 3416-3421

Mendes HF, van der Spuy J, Chapple JP, Cheetham ME (2005). Mechanisms of cell death in rhodopsin retinitis pigmentosa: implications for therapy. *Trends Mol. Med.* **11**, 177-85

Morello JP, Salahpour A, Laperriere A, Bernier V, Arthus MF, Lonergan M, Petaja-Repo U, Angers S, Morin D, Bichet DG, Bouvier M (2000). Pharmacological chaperones rescue cell-surface expression and function of misfolded V2 vasopressin receptor mutants. *J. Clin. Invest.* **105**, 887-895

Naash ML, Peachey NS, Li ZY, Gryczan CC, Goto Y, Blanks J, Milam AH, Ripps H (1996). Light-induced acceleration of photoreceptor degeneration in transgenic mice expressing mutant rhodopsin. *Invest. Ophthalmol. Vis. Sci.* **37**, 775-782

Nathans J and Hogness DS (1983). Isolation, sequence analysis, and intron-exon arrangement of the gene encoding bovine rhodopsin. *Cell.* **34**, 807-814

Nathans J and Hogness DS (1984). Isolation and nucleotide sequence of the gene encoding human rhodopsin. *Proc. Natl. Acad. Sci. U. S. A.* **81**, 4851-4855

Neidhardt J, Barthelmes D, Farahmand F, Fleischhauer JC, Berger W (2006). Different amino acid substitutions at the same position in rhodopsin lead to distinct phenotypes. *Invest. Ophthalmol. Vis. Sci.* **47**, 1630-1635

Nir I and Papermaster DS (1983). Differential distribution of opsin in the plasma membrane of frog photoreceptors: an immunocytochemical study. *Invest. Ophthalmol. Vis. Sci.* **24**, 868-878

Noorwez SM, Kuksa V, Imanishi Y, Zhu L, Filipek S, Palczewski K, Kaushal S (2003). Pharmacological chaperone-mediated in vivo folding and stabilization of the P23H-opsin mutant associated with autosomal dominant retinitis pigmentosa. *J. Biol. Chem.* **278**, 14442-14450

Noorwez SM, Malhotra R, McDowell JH, Smith KA, Krebs MP, Kaushal S (2004). Retinoids assist the cellular folding of the autosomal dominant retinitis pigmentosa opsin mutant P23H. *J. Biol. Chem.* **279**, 16278-16284

Norez C, Noel S, Wilke M, Bijvelds M, Jorna H, Melin P, DeJonge H, Becq F (2006). Rescue of functional delF508-CFTR channels in cystic fibrosis epithelial cells by the alpha-glucosidase inhibitor miglustat. *FEBS Lett.* **580**, 2081-2086

Novoa I, Zhang Y, Zeng H, Jungreis R, Harding HP, Ron D (2003). Stress-induced gene expression requires programmed recovery from translational repression. *EMBO J.* **22**, 1180-1187

O'Tousa JE (1992). Requirement of N-linked glycosylation site in Drosophila rhodopsin. *Vis. Neurosci.* **8**, 385-390

Olsson JE, Gordon JW, Pawlyk BS, Roof D, Hayes A, Molday RS, Mukai S, Cowley GS, Berson EL, Dryja TP (1992) Transgenic mice with a rhodopsin mutation (Pro23His): a mouse model of autosomal dominant retinitis pigmentosa. *Neuron.* **9**, 815-830

Palczewski K, Hargrave PA, McDowell JH, Ingebritsen TS (1989). The catalytic subunit of phosphatase 2A dephosphorylates phosphoopsin.. *Biochemistry.* **28**, 415-419

Palczewski K, Kumasaka T, Hori T, Behnke CA, Motoshima H, Fox BA, Le Trong I, Teller DC, Okada T, Stenkamp RE, Yamamoto M, Miyano M (2000). Crystal structure of rhodopsin: A G protein-coupled receptor. *Science.* **289**, 739-745

Paleologou KE, Irvine GB, El-Agnaf OM (2005). Alpha-synuclein aggregation in neurodegenerative diseases and its inhibition as a potential therapeutic strategy. *Biochem. Soc. Trans.* **33**, 1106-1110

Park PS, Filipek S, Wells JW, Palczewski K (2004). Oligomerization of G protein-coupled receptors: past, present, and future. *Biochemistry.* **43**, 15643-15656

Parker JA, Arango M, Abderrahmane S, Lambert E, Tourette C, Catoire H, Neri C (2005). Resveratrol rescues mutant polyglutamine cytotoxicity in nematode and mammalian neurons. *Nat. Genet.* **37**, 349-350

Pierce EA (2001). Pathways to photoreceptor cell death in inherited retinal degenerations. *Bioessays.* **23,** 605-618

Powell K and Zeitlin PL (2002). Therapeutic approaches to repair defects in deltaF508 CFTR folding and cellular targeting. *Adv. Drug. Deliv. Rev.* **54**, 1395-1408

Rajan RS and Kopito RR (2005). Suppression of wild-type rhodopsin maturation by mutants linked to autosomal dominant retinitis pigmentosa. *J. Biol. Chem.* **280**, 1284-1291

Rao VR, Cohen GB, Oprian DD (1994). Rhodopsin mutation G90D and a molecular mechanism for congenital night blindness. *Nature.* **367**, 639-642

Ravikumar B, Duden R, Rubinsztein DC (2002). Aggregate-prone proteins with polyglutamine and polyalanine expansions are degraded by autophagy. *Hum. Mol. Genet.* **11**, 1107-1117

Ravikumar B, Vacher C, Berger Z, Davies JE, Luo S, Oroz LG, Scaravilli F, Easton DF, Duden R, O'Kane CJ, Rubinsztein DC (2004). Inhibition of mTOR induces autophagy and reduces toxicity of polyglutamine expansions in fly and mouse models of Huntington disease. *Nat. Genet.* **36**, 585-595

Roe SM, Prodromou C, O'Brien R, Ladbury JE, Piper PW, Pearl LH (1999). Structural basis for inhibition of the Hsp90 molecular chaperone by the antitumor antibiotics radicicol and geldanamycin. *J. Med. Chem.* **42**, 260-266

Rubenstein RC, Egan ME, Zeitlin PL (1997). In vitro pharmacologic restoration of CFTR-mediated chloride transport with sodium 4-phenylbutyrate in cystic fibrosis epithelial cells containing delta F508-CFTR. *J. Clin. Invest.* **100**, 2457-2465

Rubenstein RC, Zeitlin PL (1998). A pilot clinical trial of oral sodium 4-phenylbutyrate (Buphenyl) in deltaF508-homozygous cystic fibrosis patients: partial restoration of nasal epithelial CFTR function. *Am. J. Respir. Crit. Care Med.* **157**, 484-489

Rutkowski DT, Kaufman RJ (2004). A trip to the ER: coping with stress. *Trends Cell Biol.* **14**, 20-28

Sabers CJ, Martin MM, Brunn GJ, Williams JM, Dumont FJ, Wiederrecht G, Abraham RT (1995). Isolation of a protein target of the FKBP12-rapamycin complex in mammalian cells. *J. Biol. Chem.* **270**, 815-822

Saliba RS, Munro PM, Luthert PJ, Cheetham ME (2002). The cellular fate of mutant rhodopsin: quality control, degradation and aggresome formation. *J. Cell Sci.* **115**, 2907-2918

Samardzija M, Wenzel A, Thiersch M, Frigg R, Reme C, Grimm C (2006). Caspase-1 ablation protects photoreceptors in a model of autosomal dominant retinitis pigmentosa. *Invest. Ophthalmol. Vis. Sci.* **47**, 5181-5190

Sano M (2001). Radicicol and geldanamycin prevent neurotoxic effects of anti-cancer drugs on cultured embryonic sensory neurons. *Neuropharmacology.* **40**, 947-953

Sarkar S, Davies JE, Huang Z, Tunnacliffe A, Rubinsztein DC (2007). Trehalose, a novel mTOR-independent autophagy enhancer, accelerates the clearance of mutant huntingtin and alpha-synuclein. *J. Biol. Chem.* **282**, 5641-5652

Saudou F, Finkbeiner S, Devys D, Greenberg ME (1998). Huntingtin acts in the nucleus to induce apoptosis but death does not correlate with the formation of intranuclear inclusions. *Cell.* **95**, 55-66

Scherzinger E, Lurz R, Turmaine M, Mangiarini L, Hollenbach B, Hasenbank R, Bates GP, Davies SW, Lehrach H, Wanker EE (1997). Huntingtin-encoded polyglutamine expansions form amyloid-like protein aggregates in vitro and in vivo. *Cell.* **90**, 549-558

Selkoe DJ (2001). Alzheimer's disease: genes, proteins, and therapy. *Physiol. Rev.* **81**, 741-766

Shichi H and Somers RL (1978). Light-dependent phosphorylation of rhodopsin. Purification and properties of rhodopsin kinase. *J. Biol. Chem.* **253**, 7040-7046

Sibulesky L, Hayes KC, Pronczuk A, Weigel-DiFranco C, Rosner B, Berson EL (1999). Safety of <7500 RE (<25000 IU) vitamin A daily in adults with retinitis pigmentosa. *Am. J. Clin. Nutr.* **69**, 656-663

Singer MA and Lindquist S (1998) Multiple effects of trehalose on protein folding in vitro and in vivo. *Mol Cell.* **1**, 639-648

Sittler A, Lurz R, Lueder G, Priller J, Lehrach H, Hayer-Hartl MK, Hartl FU, Wanker EE (2001). Geldanamycin activates a heat shock response and inhibits huntingtin aggregation in a cell culture model of Huntington's disease. *Hum. Mol. Genet.* **10**, 1307-1315

Solit DB, Zheng FF, Drobnjak M, Munster PN, Higgins B, Verbel D, Heller G, Tong W, Cordon-Cardo C, Agus DB, Scher HI, Rosen N (2002). 17-Allylamino-17-demethoxygeldanamycin induces the degradation of androgen receptor and HER-2/neu and inhibits the growth of prostate cancer xenografts. *Clin. Cancer Res.* **8**, 986-993

Stone J, Maslim J, Valter-Kocsi K, Mervin K, Bowers F, Chu Y, Barnett N, Provis J, Lewis G, Fisher SK, Bisti S, Gargini C, Cervetto L, Merin S, Peer J (1999). Mechanisms of photoreceptor death and survival in mammalian retina. *Prog. Retin. Eye Res.* **18**, 689-735

Sullivan LS, Bowne SJ, Birch DG, Hughbanks-Wheaton D, Heckenlively JR, Lewis RA, Garcia CA, Ruiz RS, Blanton SH, Northrup H, Gire AI, Seaman R, Duzkale H, Spellicy CJ, Zhu J, Shankar SP, Daiger SP (2006). Prevalence of disease-causing mutations in families with autosomal dominant retinitis pigmentosa: a screen of known genes in 200 families. *Invest. Ophthalmol. Vis. Sci.* **47**, 3052-3064

Sung CH, Schneider BG, Agarwal N, Papermaster DS, Nathans J (1991). Functional heterogeneity of mutant rhodopsins responsible for autosomal dominant retinitis pigmentosa. *Proc. Natl. Acad. Sci. U. S. A.* **88**, 8840–8844

Sung CH, Davenport CM, Nathans J (1993). Rhodopsin mutations responsible for autosomal dominant retinitis pigmentosa. Clustering of functional classes along the polypeptide chain. *J. Biol. Chem.* **268**, 26645-26649

Sung CH, Makino C, Baylor D, Nathans J (1994). A rhodopsin gene mutation responsible for autosomal dominant retinitis pigmentosa results in a protein that is defective in localization to the photoreceptor outer segment. *J. Neurosci.* **14**, 5818-5833

Supko JG, Hickman RL, Grever MR, Malspeis L (1995). Preclinical pharmacologic evaluation of geldanamycin as an antitumor agent. *Cancer Chemother. Pharmacol.* **36**, 305-315

Tai AW, Chuang JZ, Bode C, Wolfrum U, Sung CH (1999). Rhodopsin's carboxy-terminal cytoplasmic tail acts as a membrane receptor for cytoplasmic dynein by binding to the dynein light chain Tctex-1. *Cell.* **97**, 877-887

Tam BM and Moritz OL (2006). Characterization of rhodopsin P23H-induced retinal degeneration in a Xenopus laevis model of retinitis pigmentosa. *Invest. Ophthalmol. Vis. Sci.* **47**, 3234-3241

Tamarappoo BK and Verkman AS (1999). Defective aquaporin-2 trafficking in nephrogenic diabetes insipidus and correction by chemical chaperones. *J. Clin. Invest.* **101**, 2257-2267

Tanaka M, Machida Y, Niu S, Ikeda T, Jana NR, Doi H, Kurosawa M, Nekooki M, Nukina N (2004). Trehalose alleviates polyglutamine-mediated pathology in a mouse model of Huntington disease. *Nat. Med.* **10**, 148-154

Tanaka M, Kim YM, Lee G, Junn E, Iwatsubo T, Mouradian MM (2004) Aggresomes formed by alpha-synuclein and synphilin-1 are cytoprotective. *J. Biol. Chem.* **279**, 4625-4631

Tatzelt J, Prusiner SB, Welch WJ (1996). Chemical chaperones interfere with the formation of scrapie prion protein. *EMBO J.* **15**, 6363-6373

Thompson DA and Gal A (2003). Vitamin A metabolism in the retinal pigment epithelium: genes, mutations, and diseases. *Prog. Retin. Eye Res.* **22**, 683-703

Trottier Y, Devys D, Imbert G, Saudou F, An I, Lutz Y, Weber C, Agid Y, Hirsch EC, Mandel JL (1995). Cellular localization of the Huntington's disease protein and discrimination of the normal and mutated form. *Nat. Genet.* **10**, 104-110

Tso MO, Zhang C, Abler AS, Chang CJ, Wong F, Chang GQ, Lam TT (1994). Apoptosis leads to photoreceptor degeneration in inherited retinal dystrophy of RCS rats. *Invest. Ophthalmol. Vis. Sci.* **35**, 2693-2699.

Vilatoba M, Eckstein C, Bilbao G, Smyth CA, Jenkins S, Thompson JA, Eckhoff DE, Contreras JL (2005). Sodium 4-phenylbutyrate protects against liver ischemia reperfusion injury by inhibition of endoplasmic reticulum-stress mediated apoptosis. *Surgery.* **138**, 342-351

Waelter S, Boeddrich A, Lurz R, Scherzinger E, Lueder G, Lehrach H, Wanker EE (2001). Accumulation of mutant huntingtin fragments in aggresome-like inclusion bodies as a result of insufficient protein degradation. *Mol. Biol. Cell.* **12**, 1393-1407

Warrick JM, Chan HY, Gray-Board GL, Chai Y, Paulson HL, Bonini NM (1999). Suppression of polyglutamine-mediated neurodegeneration in Drosophila by the molecular chaperone HSP70. *Nat. Genet.* **23**, 425-428

Waza M, Adachi H, Katsuno M, Minamiyama M, Sang C, Tanaka F, Inukai A, Doyu M, Sobue G (2005). 17-AAG, an Hsp90 inhibitor, ameliorates polyglutamine-mediated motor neuron degeneration. *Nat. Med.* **11**, 1088-1095

Westerheide SD, Bosman JD, Mbadugha BN, Kawahara TL, Matsumoto G, Kim S, Gu W, Devlin JP, Silverman RB, Morimoto RI (2004). Celastrols as inducers of the heat shock response and cytoprotection. J. Biol. Chem. **279**, 56053-56060

White MB, Amos J, Hsu JM, Gerrard B, Finn P, Dean M (1990). A frame-shift mutation in the cystic fibrosis gene. *Nature.* **344**, 665-667

Wilson JH and Wensel TG (2003). The nature of dominant mutations of rhodopsin and implications for gene therapy. *Mol. Neurobiol.* **28**, 149–158

Yam GH, Zuber C, Roth J (2005) A synthetic chaperone corrects the trafficking defect and disease phenotype in a protein misfolding disorder. *FASEB J.* **19**, 12-18

Yang DS, Yip CM, Huang TH, Chakrabartty A, Fraser PE (1999). Manipulating the amyloid-beta aggregation pathway with chemical chaperones. *J. Biol. Chem.* **274**, 32970-32974

Yoshida H, Yoshizawa T, Shibasaki F, Shoji S, Kanazawa I (2002). Chemical chaperones reduce aggregate formation and cell death caused by the truncated

Machado-Joseph disease gene product with an expanded polyglutamine stretch. *Neurobiol. Dis.* **10**, 88-99

Zeiss CJ, Neal J, Johnson EA (2004). Caspase-3 in postnatal retinal development and degeneration. *Invest. Ophthalmol. Vis. Sci.* **45**, 964-970

Zhukovsky EA, Robinson PR, Oprian DD (1991). Transducin activation by rhodopsin without a covalent bond to the 11-cis-retinal chromophore. *Science.* **251**, 558-560

Zuckerman R, Cheasty JE (1986). A 48 kDa protein arrests cGMP phosphodiesterase activation in retinal rod disk membranes. *FEBS Lett.* **207**, 35-41

Chapter 10: Appendix A – Mutations and deletions identified in the rhodopsin gene

Phenotype	Mutation	Basechange	Exon	Reference
ADRP	Thr 4 Lys	ACA-AAA	1	Bunge (1993)
ADRP	Asn 15 Ser	AAT-AAG	1	Kranich (1993)
ADRP	Thr 17 Met	ACG-ATG	1	Sheffield (1991)
ADRP	Val 20 Gly		1	Schuster (2006)
ADRP	Pro 23 Ala	CCC-GCC	1	Oh (2000)
ADRP	Pro 23 His	CCC-CAC	1	Dryja (1990)
ADRP	Pro 23 Leu	CCC-CTC	1	Dryja (1991)
ADRP	Gln 28 His	CAG-CAT	1	Bunge (1993)
ADRP	Leu 40 Arg	CTG-GTG	1	al-Maghtheh (1994)
ADRP	Met 44 Thr	ATG-ACG	1	Reig (1994)
ADRP	Phe 45 Leu	TTT-CTT	1	Sung (1991)
ADRP	Leu 46 Arg	CTG-CGG	1	Rodriguez (1993)
ADRP	Gly 51 Ala	GGC-GCC	1	Macke (1993)
ADRP	Gly 51 Arg	GGC-CGC	1	al-Maghtheh (1993)
ADRP	Gly 51 Val	GGC-GTC	1	Dryja (1991)
ADRP	Pro 53 Arg	CCC-CGC	1	Ingleheam (1992)
ADRP	Thr 58 Arg	ACG-AGG	1	Dryja (1990)
ADRP	Gln 64 ter	CAG-TAG	1	Macke (1993)
ADRP	68-71	12 bp deletion	1	Keen (1994)
ADRP	Val 87 Asp	GTC-GAC	1	Sung (1991)
ADRP	Gly 89 Asp	GGT-GAT	1	Sung (1991)
ADRP	Gly 106 Arg	GGG-AGG	1	Ingleheam (1992)
ADRP	Gly 106 Trp	GGG-TGG	1	Sung (1991)
ADRP	Gly 109 Arg	GGA-AGA	1	Goliath (1998)
ADRP	Cys 110 Phe	TGC-TTC	1	Fuchs (1994)
ADRP	Cys 110 Tyr	TGC-TAC	1	al-Maghtheh (1993)
ADRP	Gly 114 Asp	GGC-GAC	1	Vaithinathan (1994)
ADRP	Gly 114 Val	GGC-GTC	1	Dryja (2000)
ADRP	Leu 125 Arg	CTG-CGG	2	Dryja (1991)
ADRP	Ser 127 Phe	TCC-TTC	2	Souied (1994)

ADRP	Leu 131 Pro	CTG-CCG	2	Fuchs (1994)
ADRP	Arg 135 Gly	CGG-GGG	2	Bunge (1993)
ADRP	Arg 135 Leu	CGG-CTG	2	Andreasson (1992)
ADRP	Arg 135 Pro	CGG-CCG	2	Gal (1997)
ADRP	Arg 135 Trp	CGG-TGG	2	Sung (1991)
ADRP	Tyr 136 ter	TAC-TAA	2	Sanchez (1996)
ADRP	Val 137 Met	GTG-ATG	2	Ayuso (1996)
ADRP	Cys 140 Ser	TGT-TCT	2	Macke (1993)
	Glu 150 Lys	GAG-AAG	2	Kumaraman (1994)
ADRP	Ala 164 Glu	GCG-GAG	2	Vaithinathan (1994)
ADRP	Ala 164 Val	GCG-GTG	2	Fuchs (1994)
ADRP	Cys 167 Arg	TGC-CGC	2	Dryja (1991)
ADRP	Cys 167 Trp	TGC-TGG	2	Preising (1997)
	Pro 170 Arg	CCC-CGC	2	Sohocki (2001)
ADRP	Pro 171 Gln	CCA-CAA	2	Antinolo (1994)
ADRP	Pro 171 Glu	CCA-GAA	2	Rodriguez (1994)
ADRP	Pro 171 Leu	CCA-CTA	2	Dryja (1991)
ADRP	Pro 171 Ser	CCA-TCA	2	Vaithinathan (1994)
ADRP	IVS2-2a-g	A-G	IVS2	Martinez-Gimeno (2000)
	Gly 174 Ser	GGC-AGC		Fujiki (1995)
	Ser 176 Phe			Schuster (2006)
ADRP	Tyr 178 Asn	TAC-AAC	3	Souied (1994)
ADRP	Tyr 178 Cys	TAC-TGC	3	Sung (1991)
ADRP	Pro 180 Ala	CCC-GCC	3	Sohocki (2001)
ADRP	Glu 181 Lys	GAG-AAG	3	Dryja (1991)
ADRP	Gly 182 Ser	GGC-AGC	3	Sheffield (1991)
ADRP	Gln 184 Pro	CAG-CCG	3	Dryja (2000)
	Cys 185 Arg	TGC-CGC	3	Sohocki (2001)
ADRP	Ser 186 Pro	TCG-CCG	3	Dryja (1991)
ADRP	Ser 186 Trp	TCG-TGG	3	Gal (1997)
	Cys 187 Ala		3	Hwa (1999)
ADRP	Cys 187 Tyr	TGT-TAT	3	Richards (1995)
ADRP	Gly 188 Arg	GGA-AGA	3	Dryja (1991)
ADRP	Gly 188 Glu	GGA-GAA	3	Macke (1993)
ADRP	Asp 190 Asn	GAC-AAC	3	Keen (1991)

ADRP	Asp 190 Gly	GAC-GGC	3	Sung (1991)
ADRP	Asp 190 Tyr	GAC-TAC	3	al-Maghtheh (1993)
ADRP	Thr 193 Met	ACG-AUG	3	Cydeciyan (1998)
ADRP	Met 207 Arg	ATG-AGG	3	Farrar (1992)
ADRP	Val 209 Met	ATG-GTG	3	Macke (1993)
ADRP	His 211 Arg	CAC-CGC	3	Macke (1993)
ADRP	His 211 Pro	CAC-GAC	3	Keen (1991)
	Pro 215 Leu		3	Schuster (2006)
ADRP	Pro 215 Thr	CCC-CTC	3	Martinez-Gimeno (2000)
ADRP	Met 216 Arg	ATG-AGG	3	Haim (1996)
ADRP	Met 216 Lys	ATG-AAG	3	al-Maghtheh (1994)
ADRP	Phe 220 Cys	TTT-TGT	3	Bunge (1993)
ADRP	Cys 222 Arg	TGC-CGC	3	Bunge (1993)
	Lys 248 Arg			Kucinskas 1999
ADRP	255 / 256	ATC (I) deletion	4	Inglehearn (1991)
ADRP	264	TGC (C) deletion	4	Vaithinathan (1993)
ADRP	Pro 267 Arg	CCC-CGC	4	Souied (1994)
ADRP	Pro 267 Leu	CCC-CTC	4	Sheffield (1991)
ADRP	Ser 270 Arg	AGC-AGA	4	Sohocki (2001)
ADRP	Thr 289 Pro	ACC-CCC	4	Martinez-Gimeno (2000)
	Lys 296 Asn	AAG-AAT		Sohocki (2001)
ADRP	Lys 296 Glu	AAG-GAG	4	Keen (1991)
ADRP	Lys 296 Met	AAG-ATG	4	Sullivan (1993)
ADRP	Ser 297 Arg	AGC-AGA	4	Souied (1994)
ADRP	Gln 312 ter	CAG-TAG	4	Inglehearn (1991)
ADRP	IVS4+1g-t	G-T	IVS4	Macke (1993)
ADRP	314-316	150 bp insertion / 30 bp deletion	IVS4	al-Maghtheh (1994)
ADRP	IVS4-1g-t	G-T	IVS4	Reig (1996)
ADRP	IVS4-1g-a	G-A	IVS4	Bell (1994)
ADRP	5168del9bp		5	al-Maghtheh (1993)
ADRP	Leu 328 Pro	CTG-CCG	5	Gal (1997)
ADRP	332-338	17 bp deletion	5	Rodriguez (1994)
ADRP	998ins4bp	duplication in	5	Bareil (1999)

		rhodopsin gene		
ADRP	340-348	42 bp deletion	5	Restagno (1993)
ADRP	340	1 bp deletion	5	Horn (1992)
ADRP	341-343	8 bp deletion	5	Horn (1992)
ADRP	Glu 341 Lys	GAG-AAG	5	Gal (1997)
ADRP	Glu 341 ter	GAG-TAG	5	Zhao (2001)
ADRP	Thr 342 Met	ACG-ATG	5	Stone (1993)
ADRP	Gln 344 ter	CAG-TAG	5	Sung (1991)
ADRP	Val 345 Leu	GTG-CTG	5	Vaithinathan (1994)
ADRP	Val 345 Met	GTG-ATG	5	Dryja (1991)
ADRP	Ala 346 Pro	GCC-CCC	5	Borrego (1996)
ADRP	Pro 347 Ala	CCG-GCG	5	Macke (1995)
ADRP	Pro 347 Arg	CCG-CGG	5	Gal (1991)
ADRP	Pro 347 Gln	CCG-CAG	5	Vaithinathan (1994)
ADRP	Pro 347 Leu	CCG-CTG	5	Dryja (1990)
ADRP	Pro 347 Ser	CCG-TCG	5	Dryja (1990)
ADRP	Pro 347 Thr	CCG-ACG	5	Sohocki (2001)
ADRP	Ter 349 Glu	TAA-GAA → stop codon abolished and 51 aa added to C-terminus of rhodopsin	5	Bessant (1999)

ARRP	Glu 150 Lys	GAG-AAG	2	Kumaramanickavel (1994)
ARRP	Gly 174 Ser	GGC-AGC	2	Fujiki (1995)
ARRP	Glu 249 ter	GAG-TAG	4	Rosenfeld (1992)
ARRP	Gly 284 Ser	GGT-AGT	4	Ruther (1995)

CSNB	Gly 90 Asp	GGC-GAC	1	Sieving (1995)
CSNB	Gly 90 Val		1	Kabaranou (2004)
CSNB	Thr 94 Ser	ACC-ATC	1	al-Jandal (1999)
CSNB	Ala 292 Glu	GCG-GAG	4	Dryja (1993)

Polymorphism	269g-a	G-A	5'UTR	Dryja (1991)

Polymorphism	Val 104 Ile	GTC-ATC	1	Macke (1993)
Polymorphism	Pro 107 Pro	CCC-CCT	1	Gal (1997)
Polymorphism	-26A/G	A/G	5'UTR	Bareil (1999)
Polymorphism	Gly 120 Gly	GGC-GGT	1	Dryja (1991)
Polymorphism	721c-t	G-A	IVS1	Trujillo (1998)
Polymorphism	(CA)n		IVS1	Weber (1989)
Polymorphism	Thr 160 Thr	ACC-ACA	2	Sung (1991)
Polymorphism	Ala 173 Ala	GCC-GCT	2	Dryja (1991)
Polymorphism	IVS3+4c-t	C-T	IVS3	Dryja (1990)
Polymorphism	IVS3+62c-a	C-A	IVS3	Saga (1993)
Polymorphism	IVS3+106g-a	G-A	IVS3	
Polymorphism	Lys 248 Lys	AAG-AAA	4	al-Maghtheh (1993)
Polymorphism	IVS4-22g-a	G-A	IVS4	Sung (1991)
Polymorphism	Cys 323 Cys	TGC-TGT	5	Trujillo (1998)
Polymorphism	5300g-t	gt-tt	3'UTR	Bell (1994)
Polymorphism	5311c-t	C-T	3'UTR	
Polymorphism	5312g-a	G-A	3'UTR	Ruiz (1997)
Polymorphism	5321c-a	C-A	3'UTR	Dryja (1990)

Retinitis punctata albescens	Arg 135 Trp	CGG-TGG	2	Souied (1996)